AN ABSTRACT OF THE THESIS OF

Viviane Klein for the degree of Doctor of Philosophy in Mathematics presented on May 26, 2011.

Title:

Two–grid *a-priori* and *a-posteriori* Error Analysis for Coupled Elliptic and Parabolic Systems with Applications to Flow and Transport Problems

Abstract approved: _____

Małgorzata Peszyńska

We develop several *a-priori* and *a-posteriori* error estimates for two–grid finite element discretization of coupled elliptic and parabolic systems with a set of parameters $\mathcal{P}$. We present numerical results that verify the convergence order of the numerical schemes predicted by the *a-priori* estimates. We present numerical results that verify the robustness of the estimators developed with respect to the two–grid discretization and with respect to the parameters $\mathcal{P}$. The theoretical and numerical results in this thesis apply to models of many important phenomena in fluid flow and transport in porous media. We demonstrate some applications with numerical simulations.

Two–grid *a-priori* and *a-posteriori* Error Analysis for Coupled Elliptic and Parabolic Systems with Applications to Flow and Transport Problems

by

Viviane Klein

A THESIS

submitted to

Oregon State University

in partial fulfillment of
the requirements for the
degree of

Doctor of Philosophy

Presented May 26, 2011
Commencement June 2011

Doctor of Philosophy thesis of Viviane Klein presented on May 26, 2011.

APPROVED:

Major Professor, representing Mathematics

Chair of the Department of Mathematics

Dean of the Graduate School

I understand that my thesis will become part of the permanent collection of Oregon State University libraries. My signature below authorizes release of my thesis to any reader upon request.

Viviane Klein, Author

ACKNOWLEDGEMENTS

Academic

I would like to thank my advisor Dr. Małgorzata Peszyńska for her patience and guidance over the last 5 years. Dr. Peszyńska, I am very thankful for all your help and disponibility to go over my questions how many times it was necessary. Thank you for pushing me to go further and to help me to "almost" overcome my fear of presenting at conferences.

I would like to acknowledge that this thesis research was partially supported by the grants NSF 0511190 and DOE 98089.

Personal

Eu gostaria de agradecer aos meus pais, Ivonete e Mercedo, a todo o apoio que me deram quando eu decidi seguir carreira como Matemática. Obrigado por me apoiar em todas as minhas decisões mesmo quando eu sabia que vocês não concordavam com elas. Eu sei que vocês sempre fizeram tudo que puderam para me ajudar e sou muito grata por isso.

Agradeço a professora Teresa Tsukazan de Ruiz que sempre me apoiou desde do início dos meus estudos na Matemática. Agradeço ao professor Julio Ruiz Clayessen por me incentivar a vir fazer meu doutorado no exterior e nunca me deixar desanimar. Sem o apoio do professor Julio e todos os seus conselhos ao longos desses 8 anos eu não chegado a esse feito.

Agradeço as minha amigas Bianca, Luzinha, Taís e Tati que fizeram com que o frio e a distância de casa ficassem mais amenos nesses últimos 5 anos.

TABLE OF CONTENTS

TABLE OF CONTENTS (Continued)

Page

TABLE OF CONTENTS (Continued)

Page

TABLE OF CONTENTS (Continued)

Page

TABLE OF CONTENTS (Continued)

Page

LIST OF FIGURES

LIST OF FIGURES (Continued)

Figure Page

LIST OF TABLES

LIST OF TABLES (Continued)

Table Page

1 Introduction

In this thesis we describe how to solve numerically a particular coupled system of partial differential equations, specifically, of so-called *reaction-diffusion* type.

There are several applications of such systems to subsurface fluid flow and transport models. Models similar to the one considered in this thesis occur also in chemical engineering, and medical applications. In this work we only develop the first class of applications. In particular, we are interested in double porosity models of flow in heterogeneous porous media [12, 34, 50], ([47], II.5), and in diffusion in such media. In addition, we consider kinetic and equilibrium models of adsorption [7, 42, 48]. Such models can be used to simulate oil and gas recovery processes in fractured media, and contamination and remediation of contaminated groundwater. General information about reaction-diffusion systems can be found in [7, 51].

Before the models are solved analytically or numerically, one has to study their well-posedness. In general, the coefficients and source-terms in the models are only piecewise smooth and only bounded. This means that the classical solutions to the models may not exist and one has to seek a weaker notion of solutions. In this work we will consider well-posedness of the weak solutions in appropriate Sobolev spaces.

Since, in general, the differential equations in the models cannot be solved analytically, one uses numerical methods to approximate their solutions. There are many choices of numerical methods that can be used: Finite Elements (FEM), Finite Differences (FDM), and Finite Volume (FVM) methods. They each have several advantages and disadvantages. One has to decide which one to use depending on the regularity of the underlying solutions, the intended accuracy of approximations, the geometry of the domain, and on the ease of implementation. In this work we use only the Finite Element method, and, specifically, the conforming Galerkin FEM, which is well suited to deal with approximation of solutions with different properties and regularity. Most importantly, Galerkin FEM is easy to implement for complicated geometry of the domains, allows for high order approximations to smooth solutions, and has a strong mathematical foun-

dation that allow us to analyse and estimate the numerical error, even for non-smooth solutions.

The main idea of the FEM is to approximate the solution of the PDE in a finite dimensional subspace of the original (Sobolev) function space. We cover the domain Ω with a mesh (grid) made of a finite number of elements and then look for an approximate solution in the form of globally continuous piecewise polynomials on that grid [22].

To estimate the approximation error, i.e., the difference between the true solution and the approximate solution, one combines variational methods with interpolation theory. It is possible to prove that, as the number of elements increases, the approximate solutions converge to the true solution. Unfortunately, the magnitude of the error is unknown *a-priori* if the true solution is not known. In order to control the numerical error, we estimate it by a computable quantity called *a-posteriori* error estimator. In some cases it is possible to prove that a given estimator provides upper and lower bounds to the true error. In this thesis we use *residual type* estimators which can be computed easily from the approximate solution, and we prove appropriate bounds for our model systems. An important feature of the *a-posteriori* error estimators is that they provide information about local behavior of the error so that one can refine the mesh locally wherever the error estimator is large. This process is called mesh adaptivity. The theory and practice of residual *a-posteriori* error estimators is well developed for scalar stationary problems, see review in [53]. For systems, the only results available are for adjoint-based estimators for elliptic equations in [2, 3]. Results for scalar parabolic equations are also available, and we follow the idea of residual estimators developed in [15, 56].

In this thesis we are particularly interested in the influence of the coefficients of the system upon its solutions, and in the choice of optimal numerical techniques to approximate them. In particular, in the applications of interest, the coefficients may vary from case to case by orders of magnitude. It is desirable to have numerical methods whose properties do not depend on the particular value of the coefficients, but which at the same time can exploit the special properties of the solutions in order to decrease the complexity of the numerical computations without sacrificing their accuracy. The feature of independence of *a-posteriori* estimators on the magnitude of the coefficients is called *robustness* and was introduced in [55, 54]. In this thesis we develop robust estimators for systems of elliptic and parabolic equations, and prove appropriate lower and upper bounds for the true error. In fact, we are able to show that these results hold

true when some coefficients are set equal to zero and even when, as a result, the system becomes degenerate, i.e., its type changes.

In addition, an important observation is true for the families of solutions of the systems of PDEs. In some applications the components of the solution may have similar qualitative nature but a significantly different variability, which may lead to different orders of convergence for different components of the solution. In such cases it is natural to approximate the smooth component on a coarse grid and the less-smooth component on a fine grid. This multilevel discretization requires certain grid transfer operators so that the coupling term can be defined and the convergence ensured. Clearly, we want to ensure that the estimators we developed satisfy the lower and upper bounds also in this multilevel case, and that they remain robust. This is presented in this thesis.

The plan of the thesis is as follows. In the outline we emphasize the main results and main difficulties.

In Chapter 2 we give an overview of the applications and the models.

In Chapter 3 we present existence and uniqueness results for the studied models. Most results are straightforward extensions of available theory, but we include them here for completeness.

In Chapter 4 we define the numerical formulation of the model problems. We prove *a-priori* and *a-posteriori* error estimates for the numerical approximation of the model problems. These include the results for the elliptic system called E-model, which we published in [30]. The two challenges here are the treatment of the system and the use of different grids for each component of the system. The bounds for the robust *a-posteriori* estimator are presented in Theorem 4.3.4, 4.3.5.

Next we develop results for the *a-posteriori* error estimator for a parabolic coupled system called the LP-model. Partial results were published in [29]. The *a-posteriori* error estimator is robust with respect to the coefficients of the problem and behaves well also for the cases called WR and PP-model, when some of the coefficients are set to be zero. The main result is presented in Theorem 4.5.6.

The theoretical results that we proved are for linear models. However, they can be extended to a semilinear coupled system.

In Chapter 5 we give details on the implementation of the numerical algorithm, and present numerical experiments to confirm the *a-priori* error estimates as well as we verify the robustness of the *a-posteriori* error estimators. We also show some simulation

results for the double-porosity model, the pseudo-parabolic model, and for the linear and nonlinear adsorption models.

For the double-porosity model, we develop additional results which relate the underlying microscopic model to the coupled system. The latter can be understood as the limit of the former as shown in [50]. In particular, we show how to compute the coefficients of the macroscopic problem.

The implementation details in Chapter 5 include careful development of the intergrid operators that are used for multilevel grids.

In Chapter 6 we present the conclusions of our thesis. The Appendix contains the listing of some of the MATLAB codes that we developed for the computations shown in this thesis.

2 Applications

In this thesis we develop tools to improve the numerical simulation of the modelling of phenomena involving fluid in porous media. In this chapter we give a brief introduction to the applications of models considered in this work, namely: double-porosity model, pseudoparabolic model, diffusion-adsorption system and enhanced coalbed methane recovery (ECBM).

From now on, we consider an open bounded convex region $\Omega \subseteq \mathbb{R}^d$, $d = 1, 2, 3$, with Lipschitz boundary $\partial\Omega$. The variable t denotes time. All the applications above can be modelled by the following general parabolic reaction-diffusion system of partial differential equations (PDEs)

$$\lambda_1 \frac{\partial}{\partial t} u(x,t) - \nabla \cdot (a \nabla u(x,t)) + c(\varphi(x, u(x,t)) - v(x,t)) = f(x,t), x \in \Omega, t > 0, \quad (2.1a)$$

$$\lambda_2 \frac{\partial}{\partial t} v(x,t) - \nabla \cdot (b \nabla v(x,t)) + c(v(x,t) - \varphi(x, u(x,t))) = g(x,t), x \in \Omega, t > 0. \quad (2.1b)$$

Here the set of parameters $\mathcal{P} = \{\lambda_1, \lambda_2, a, b, c\}$ are, in general, non-negative bounded functions of x. The meaning of the unknowns u, v and of the parameters depend on the application considered. The function $\varphi : \mathbb{R} \times \mathbb{R} \to \mathbb{R}$ is, in general, Lipschitz continuous in the second variable, u. The system (2.1) is subject to proper initial and boundary conditions. Before going into the applications mentioned above we present a summary of the governing equations for fluid flow and for solute transport in porous media. The equations shown in here are standard and can be found in several textbooks such as [37, 32]. Throughout this thesis we assume isothermal conditions.

2.1 Basic Models

2.1.1 Flow

We consider the case of single phase and single component fluid flow in porous media. The main three equations governing the fluid flow in single component and phase in porous media are the continuity equation (conservation of mass of the fluid), Darcy's

law (conservation of momentum of the fluid) and equation of state. The continuity equation

$$\frac{\partial}{\partial t}(\phi\rho) + \nabla \cdot (\rho\vec{u}) = q, \tag{2.2}$$

states that the fluid mass is conserved in any fixed control volume. Here, ϕ denotes the porosity of the medium, $\vec{u}$ is the fluid velocity and ρ is the density of the fluid. Throughout this thesis, q is called a source and accounts for all the phenomena that add or subtract (in this case the source term is called a sink) mass within the control volume.

The Darcy's law

$$\vec{u} = -\frac{k}{\mu}(\nabla p - \rho g \nabla z), \tag{2.3}$$

gives an empirical relationship between the fluid velocity and the gradient of pressure p. Here, g is the gravity acceleration, k is the permeability of the medium, μ is the viscosity of the fluid and z represents the depth. In this work, we ignore the gravitational effects, thus we use its simplified version

$$\vec{u} = -\frac{k}{\mu}\nabla p. \tag{2.4}$$

The equation of state is given by

$$\rho = \rho_0 e^{\beta(p-p_0)}, \tag{2.5}$$

where β is the fluid compressibility and ρ_0, p_0 are the density and pressure of the fluid at a reference conditions, respectively. From the equation of state it follows that

$$\frac{\partial \rho}{\partial p} = \beta\rho, \tag{2.6}$$

and consequently,

$$\nabla\rho = \frac{\partial \rho}{\partial p}\nabla p = \beta\rho\nabla p. \tag{2.7}$$

Substituting the Darcy's law (2.4) and then the relation (2.7) into the mass conservation equation (5.14) we arrive at equation describing the density of slightly compressible fluid flow through porous media

$$q = \frac{\partial}{\partial t}(\phi\rho) + \nabla \cdot (\rho\vec{v}) = \frac{\partial}{\partial t}(\phi\rho) - \nabla \cdot (\rho\frac{k}{\mu}\nabla p) = \frac{\partial}{\partial t}(\phi\rho) - \nabla \cdot (\frac{k}{\beta\mu}\nabla\rho).$$

For simplicity, for the rest of the thesis, we set $\beta = 1$, $\mu = 1$, so that

$$\frac{\partial}{\partial t}(\phi\rho) - \nabla \cdot (k\nabla\rho) = 0. \tag{2.8}$$

Note that the use of the relation (2.7) allows us to transform the nonlinear PDE (2.8) into the linear PDE (2.9). This substitution is called Kirchhof's transformation.

It should be noticed that the porosity ϕ and the permeability k are both functions of space and time, $\phi = \phi(x,t)$, $k = k(x,t)$. The dependence in the space variable reflects the fact that most reservoirs are heterogeneous. The dependence on time can be due to natural processes such as, swelling, infiltration, formation of fractures, to cite some. In this thesis we consider only the case in which the porous media is rigid, i.e., $\phi := \phi(x)$ and $k := k(x)$, so that equation (2.8) is simplified to

$$\phi\frac{\partial\rho}{\partial t} - \nabla \cdot (k\nabla\rho) = 0. \tag{2.9}$$

The heterogeneity of the medium properties, ϕ and k, leads to two of the applications considered in this thesis, the double-porosity model and the pseudoparabolic model presented in Sections 2.2 and 2.3, respectively.

2.1.2 Mass Transport

Consider the presence of n distinct substances being transported by the fluid flow. For all i, let c_i be the concentration of solute i. The conservation of mass for solute i, is given by

$$\phi\frac{\partial c_i}{\partial t} + \nabla \cdot F_i + \vec{v} \cdot \nabla c_i = q_i, \ \forall i. \tag{2.10}$$

Here q_i is a source for the solute i. The conservation of mass (2.10) is coupled with the flow equation (2.9) through the fluid velocity, $\vec{v}$. In this thesis we consider these two equations separately. For the remainder of this thesis we consider only the case $\vec{v} = \vec{0}$ in the mass transport equation (2.10). This simplification guarantees that the PDE is self-adjoint in the space derivatives. For the remainder of this section we consider the presence of only one type of solute in the fluid.

We can then rewrite the conservation of mass (omitting the subscript for simplicity)

$$\phi \frac{\partial c}{\partial t} + \nabla \cdot F = q. \tag{2.11}$$

The term F is the diffusive flux given by the Fick's law of diffusion,

$$F = -D\nabla c, \tag{2.12}$$

where D is the diffusion coefficient. Substituting the Fick's law (2.12) into the mass conservation equation (2.11) we get the equation for the mass transport of solute in porous media

$$\phi \frac{\partial c}{\partial t} - \nabla \cdot (D\nabla c) = q. \tag{2.13}$$

where, again, ϕ is the porosity of the porous media. Note that the equation that models the fluid flow (2.9) and the one that models the mass transport (2.13) have the same structure.

The equation for transport of solute (2.13) has to be modified in case of phenomena that affect the mass balance. One of these phenomena, adsorption, arises in the other two applications considered in this thesis, the diffusion-adsorption process and the ECBM.

Besides the four applications studied in this thesis, the system of equations (2.1) have other applications such as heat diffusion in heterogeneous media, chemotaxis, chemical reactions in the presence of catalysis. Next we give a brief introduction to the applications studied here.

2.2 Double-porosity models

Suppose the reservoir Ω presents two regions with very distinct porosities and permeabilities. One scenario for this situation is a porous medium composed of alternate layers of two different materials, e.g., clay and sand. Separate Ω, into two disjoint open regions, Ω_1 and Ω_2. Each region represents one of the two different behavior in Ω such that $\overline{\Omega} = \overline{\Omega}_1 \cup \overline{\Omega}_2$ (see Figure 2.1). Denote the interface between the two regions by Γ. In general, Ω_1 is called the *fast* region and Ω_2 the *slow* region. The porosity, $\phi(x)$, and

permeability, $k(x)$, in Ω can be described as

$$\phi(x) = \begin{cases} \phi_1(x), & x \in \Omega_1, \\ \phi_2(x), & x \in \Omega_2. \end{cases} \qquad k(x) = \begin{cases} k_1(x), & x \in \Omega_1, \\ k_2(x), & x \in \Omega_2. \end{cases}$$

Therefore the density ρ of the fluid flow can represented by

$$\rho = \begin{cases} \rho_1, & \text{in } \Omega_1, \\ \rho_2, & \text{in } \Omega_2. \end{cases}$$

The fluid flow in the region Ω is described by equation (2.9). However equation (2.9) is equivalent to the problem written separately in Ω_1 and Ω_2

$$\phi_1 \frac{\partial \rho_1}{\partial t} - \nabla \cdot (k_1 \nabla \rho_1) = 0, \text{ in } \Omega_1, \tag{2.14a}$$

$$\phi_2 \frac{\partial \rho_2}{\partial t} - \nabla \cdot (k_2 \nabla \rho_2) = 0, \text{ in } \Omega_2. \tag{2.14b}$$

The functions ρ_1, ρ_2 have to satisfy the interface conditions

$$\rho_1 = \rho_2, \text{ on } \Gamma, \tag{2.15a}$$

$$k_1 \nabla \rho_1 \cdot \vec{n}_1 = k_2 \nabla \rho_2 \cdot \vec{n}_2, \text{ on } \Gamma, \tag{2.15b}$$

where $\vec{n}_i$ is the outward normal vector to $\partial\Omega_i$, $i = 1, 2$. These conditions assure the continuity of mass and flow across the interface of the two regions. In general, to numerically simulate fluid flow in such reservoirs, a very fine grid is required to represent the several changes in the properties of Ω.

Two alternatives to the model (2.14)-(2.15) are the Barenblatt model [12], and the Warren-Root model [57]. The novelty proposed by [12] in 1960, was to consider two different averaged fluid variables $\tilde{\rho}_1$, $\tilde{\rho}_2$ in a way that both $\tilde{\rho}_1$ and $\tilde{\rho}_2$ are defined at each point of the domain Ω and that the densities in both regions are connected through an exchange term. The fluid flow is then modelled by the following system of coupled

Figure 2.1: Illustration of double-porosity domain

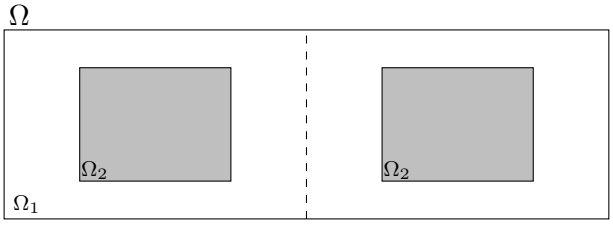

parabolic equations

$$\tilde{\phi}_1 \frac{\partial \tilde{\rho}_1}{\partial t} - \nabla \cdot (\tilde{k}_1 \nabla \tilde{\rho}_1) + c(\tilde{\rho}_1 - \tilde{\rho}_2) = 0, \text{ in } \Omega, \ t > 0, \tag{2.16a}$$

$$\tilde{\phi}_2 \frac{\partial \tilde{\rho}_2}{\partial t} - \nabla \cdot (\tilde{k}_2 \nabla \tilde{\rho}_2) + c(\tilde{\rho}_2 - \tilde{\rho}_1) = 0, \text{ in } \Omega, \ t > 0. \tag{2.16b}$$

Here, c is called the shape factor and $c(\rho_1 - \rho_2)$ is the exchange term between the two regions. The quantities $\tilde{\phi}_1, \tilde{\phi}_2, \tilde{k}_1, \tilde{k}_2$ are averaged functions of the original $\phi(x)$, $k(x)$, in the region Ω, as discussed in Section 2.1.1. The same model was proposed by Rubinstein [41] in 1948 for heat flow in heterogeneous media.

A similar result to the one in [12] was proposed in 1969 by Warren et al. [57]. The difference is that only storage is considered in the region Ω_2. So in this model we set $\tilde{k}_2 = 0$. This model is known as the Warren-Root model. From now on, we drop the superscript $\tilde{}$.

In 1990, Arbogast et al. [6], considered a periodic fractured media problem and used homogenization techniques to derive mathematically a formula for the theoretical models for double-porosity different from those in [12] and [57]. In 2004, Showalter et al. [50], considered a periodic problem with three different regions where the third region separates the other two and is called the exchange region. Applying homogenization theory they arrived at the system of equations (2.16) and presented formulas to calculate the quantities ϕ_1, ϕ_2, k_1, k_2 and c using the geometry of the regions and the properties of the three materials. These formulas and the mathematical model together with its convergence proposed in [50] is implemented and presented in Chapter 5. It is important to stress that these models are only valid for media having a periodic structure.

2.3 Pseudoparabolic Models

A particular case of the double-porosity model (2.16) is a fractured porous media. In this case, the fast region, Ω_1, accounts for the fractures and the slow region, Ω_2, represents the porous media blocks (the matrix). The region Ω_2 is formed by disconnected pieces of porous media, implying $k_2 = 0$, and also the storage term (variation with respect to time) of the fluid in the fractures region Ω_1 is too small in comparison to the other terms and can be disregarded, [12]. The system modelling the fluid flow is then given by

$$-\nabla \cdot (k_1 \nabla \rho_1) + c(\rho_1 - \rho_2) = 0, \text{ in } \Omega, \tag{2.17a}$$

$$\phi_2 \frac{\partial}{\partial t}\rho_2 + c(\rho_2 - \rho_1) = 0, \text{ in } \Omega. \tag{2.17b}$$

The system (2.17) is known as the pseudoparabolic system [49]. Note that by eliminating ρ_2 in the first equation, one arrives at the single nonlinear equation

$$\phi_2 \frac{\partial}{\partial t}\left(\rho_1 - \nabla \cdot \left(\frac{k_1}{c}\nabla \rho_1\right)\right) - \nabla \cdot (k_1 \nabla \rho_1) = 0. \tag{2.18}$$

As c increases, the solution of equation (2.18) tends to the solution of the parabolic equation

$$\phi_2 \frac{\partial \rho_1}{\partial t} - \nabla \cdot (k_1 \nabla \rho_1) = 0. \tag{2.19}$$

A more recent application of the pseudoparabolic system (2.17) is to the modelling of unsaturated flow with dynamic capillary pressure. It this application ρ_1 represents the saturation of the fluid flow and ρ_2 is an auxiliary variable [39]. Another application is heat conduction in heterogeneous media [41].

2.4 Diffusion-Adsorption System

Adsorption is the process where the solute temporarily adheres to the surface of solid in porous media. The solute mass is divided between the amount present in the fluid and the amount adsorbed, a, with reference to the mass of the porous media. The amount adsorbed is proportional to the volume fraction of the porous medium, i.e., $(1 - \phi)$.

Hence, the diffusive transport in presence of adsorption is given by

$$\phi\frac{\partial c}{\partial t} + \frac{\partial a}{\partial t} - \nabla\cdot(D\nabla c) = 0. \tag{2.20}$$

The relationship between the quantities a and c depend on the characteristic of the adsorption process. In general, this relationship can be represented by

$$\frac{\partial a}{\partial t} = \kappa(\varphi(c) - a), \tag{2.21}$$

where κ is the sorption time and φ is called the isotherm curve. Examples of isotherms considered in this thesis are:

1. Linear isotherm :
$$\varphi(c) = \alpha_1 c,\ \alpha_1 > 0, \tag{2.22}$$

2. Langmuir's isotherm:
$$\varphi(c) = \frac{\alpha_2 c}{1+\alpha_3 c},\ \alpha_2, \alpha_3 > 0. \tag{2.23}$$

Examples of other isotherms can be found in [37]. The adsorption process can be in equilibrium or have a kinetic nature.

If the adsorption process is kinetic, the adsorption process is described by equation (2.21). Thus, the diffusion-adsorption process is modelled by the degenerate parabolic system

$$\phi\frac{\partial}{\partial t}c - \nabla\cdot(D\nabla c) + \frac{\partial a}{\partial t} = 0, \tag{2.24a}$$

$$\frac{\partial a}{\partial t} - \kappa(\varphi(c) - a) = 0. \tag{2.24b}$$

Notice that the system (2.24) can be rewritten as the system (2.1).

Another case is when the process is at equilibrium. In this case the adsorption is not modelled by equation (2.21). Instead, the amount adsorbed, a, satisfies the equation

$$a = \varphi(c). \tag{2.25}$$

Substitute the relation 2.25 into the conservation of mass equation (2.20). Then the equilibrium diffusion-adsorption process is modelled by

$$\frac{\partial}{\partial t}(\phi c + \varphi(c)) - \nabla \cdot (D \nabla c) = 0. \tag{2.26}$$

In the diffusion-adsorption application we only consider the case of one species present in the fluid flow. The next application is a multi-component example of diffusion-adsorption.

2.5 Enhanced Coalbed Methane Recovery

Coal reservoirs (coalbeds) contain large amounts of methane adsorbed into the coal surface. The ECBM recovery consists of displacing the methane(CH_4) from the coalbed by carbon dioxide (CO_2) or some other gas(es). When two or more species are competing to adsorb to the surface of a medium, we have the so-called competitive adsorption. In some cases, coal adsorbs two to ten times more CO_2 than CH_4 [45], making the ECBM process favorable.

The general idea of the process is to inject CO_2 into the coalbed, so that the CH_4 desorbs and is recovered while the CO_2 adsorbs replacing the CH_4 in the coal surface, remaining stored. In this thesis we consider the process containing only CH_4 and CO_2; it is usual to also include the gas nitrogen in the mixture. Another simplification is the absence of advection in the process. This is a plausible assumption for the process after the injection wells are shut off.

We are going to consider the so-called dry case model in which the only present phases are the gas phase and the adsorbed phase. Another case is the wet-gas model where three phases are present: the water, the gas and the adsorbed phases. Let us define some notation before introducing the mathematical model.

- Components: CH_4 is denoted by subscript M and CO_2 by D.
- Phases: gas phase is denoted by subscript g and the adsorbed phase by the subscript a.
- Mass fractions: denoted by X, e.g., X_{aM} represents the amount of CH_4 adsorbed to the coal surface.

Since $c_i = X_i \rho_i$, we can rewrite the transport equation (2.20) for component i

$$\phi \rho_{gi} \frac{\partial X_{gi}}{\partial t} + (1-\phi)\rho_{ai} \frac{\partial X_{ai}}{\partial t} - \nabla \cdot (D_i \nabla (\rho_{gi} X_{gi})) = 0, \text{ for } i = M, D. \tag{2.27}$$

In the multi-component case the adsorption process of component i depends on the presence of the other components as well. One way to model this competitive process is through the so-called extended Langmuir

$$\varphi_i(X_{gD}, X_{gM}) = \frac{\beta_i \alpha_i X_{gi}}{1 + \alpha_D X_{gD} + \alpha_M X_{gM}}, \text{ for } i = M, D, \tag{2.28}$$

where β_i, α_i are the Langmuir volume capacity and the Langmuir constant for the component i, respectively. For $i = M, D$, the system of equations describing the ECBM recovery process, with only diffusion, is given by

$$\phi \rho_{gi} \frac{\partial X_{gi}}{\partial t} + (1-\phi)\rho_{ai} \frac{\partial X_{ai}}{\partial t} - \nabla \cdot (D_i \nabla \rho_{gi} X_{gi}) = 0, \tag{2.29a}$$

$$\frac{\partial X_{ai}}{\partial t} - \kappa(\varphi_i(X_{gD}, X_{gM}) - X_{ai}) = 0. \tag{2.29b}$$

In the case of non-equilibrium adsorption we have a system of four PDEs coupled through the extended Langmuir isotherm (2.28). In the case of equilibrium the problem gets reduced to a system of two coupled PDEs.

In this thesis we do not present numerical results for the ECBM application. However we mention this application here, because the results of the *a-posteriori* error estimator developed in this thesis can be applied for the ECBM process. Mathematically, the diffusion-adsorption model can be seen as particular case of the ECBM model with only one component, M or D. We present results for the diffusion-adsorption application. The results for ECBM would be an extension of the results for the diffusion-adsorption application. This extension is part of my future work.

3 Analysis of the models

3.1 Overview

In Chapter 2 we discussed five different physical models. We review them here for convenience, and supplement them with initial and boundary conditions. For simplicity, we consider all models are subject to homogeneous Dirichlet boundary conditions. However, most results can be extended for non-homogeneous Dirichlet conditions or mixed Dirichlet-Neumann conditions. As in Chapter 2, let $\Omega \subseteq \mathbb{R}^d$ be an open bounded convex region, for $d = 1, 2, 3$, with a Lipschitz boundary $\partial\Omega$. For some fixed $T > 0$, let $\Omega_T = \Omega \times (0, T]$.

- LP-model is a particular case of system (2.1) where φ is the linear isotherm (2.22), $\varphi(u) = u$.

$$\lambda_1 \frac{\partial u}{\partial t} - \nabla \cdot (a \nabla u) + c(u - v) = f, \text{ in } \Omega_T, \tag{3.1a}$$

$$\lambda_2 \frac{\partial v}{\partial t} - \nabla \cdot (b \nabla v) + c(v - u) = g, \text{ in } \Omega_T, \tag{3.1b}$$

$$u = 0, \qquad v = 0, \text{ on } \partial\Omega \times [0, T], \tag{3.1c}$$

$$u = u_0, \qquad v = v_0, \text{ in } \Omega \times \{t = 0\}. \tag{3.1d}$$

- E-model is the elliptic system

$$\lambda_1 u(x) - \nabla \cdot (a \nabla u(x)) + c(u(x) - v(x)) = f(x), \text{ in } \Omega, \tag{3.2a}$$

$$\lambda_2 v(x) - \nabla \cdot (b \nabla v(x)) + c(v(x) - u(x))) = g(x), \text{ in } \Omega, \tag{3.2b}$$

$$u = 0, \qquad v = 0, \text{ on } \partial\Omega. \tag{3.2c}$$

  The system (3.2) arises as a discrete time approximation of the system (3.1). To see that, fix a time $t = T_1 > 0$, and approximate the time derivative by a finite

difference. Let $\Delta t > 0$,

$$\frac{\partial u(x,T_1)}{\partial t} \approx \frac{u(x,T_1) - u(x,T_1-\Delta t)}{\Delta t}, \tag{3.3}$$

$$\frac{\partial v(x,T_1)}{\partial t} \approx \frac{v(x,T_1) - v(x,T_1-\Delta t)}{\Delta t}. \tag{3.4}$$

Substitute (3.3)-(3.4) in the system (3.1). After rearranging the terms, we arrive to the stationary system at time $t = T_1$

$$\begin{aligned}
\lambda_1 u(x,T_1) - \nabla\cdot(\bar{a}\nabla u(x,T_1)) + \bar{c}(u(x,T_1) - v(x,T_1)) &= F(x,T_1), \text{ in } \Omega,\\
\lambda_2 v(x,T_1) - \nabla\cdot(\bar{b}\nabla v(x,T_1)) + \bar{c}(v(x,T_1) - u(x,T_1)) &= G(x,T_1), \text{ in } \Omega,\\
u(x,T_1) = 0, \qquad v(x,T_1) &= 0, \text{ on } \partial\Omega.
\end{aligned}$$

where

$$\begin{aligned}
\bar{a} = a\Delta t, \quad & F(x,T_1) = \Delta t f(x,T_1) + \lambda_1 u(x,T_1-\Delta t),\\
\bar{b} = b\Delta t, \quad & G(x,T_1) = \Delta t g(x,T_1) + \lambda_2 v(x,T_1-\Delta t),\\
\bar{c} = c\Delta t. &
\end{aligned}$$

In this way, system (3.2) can be viewed as an approximation of system (3.1).

- WR-model is the degenerate parabolic system. This is a particular case of the LP-model with $b = 0$.

$$\lambda_1\frac{\partial u}{\partial t} - \nabla\cdot(a\nabla u) + c(u-v) = f, \text{ in } \Omega_T, \tag{3.6a}$$

$$\lambda_2\frac{\partial v}{\partial t} + c(v-u) = g, \text{ in } \Omega_T, \tag{3.6b}$$

$$u = 0, \text{ on } \partial\Omega\times[0,T], \tag{3.6c}$$

$$u = u_0, \qquad v = v_0, \text{ in } \Omega\times\{t=0\}. \tag{3.6d}$$

We denote this system as the WR-model regarding the Warren-Root model [57].

- PP-model is the pseudo-parabolic system

$$-\nabla \cdot (a\nabla u) + c(u - v) = f, \text{ in } \Omega_T, \tag{3.7a}$$

$$\lambda_2 \frac{\partial v}{\partial t} + c(v - u) = g, \text{ in } \Omega_T, \tag{3.7b}$$

$$u = 0, \text{ on } \partial\Omega \times [0, T], \tag{3.7c}$$

$$v = v_0, \text{ in } \Omega \times \{t = 0\}. \tag{3.7d}$$

  This is a particular case of the WR-model with $\lambda_1 = 0$, or of the LP-model with $\lambda_1 = b = 0$. However, the structure of the system is very different. Here we couple an ODE with an elliptic PDE, and hence the analysis of the well-posedness is quite different from the WR-model.

- NLP-model is the nonlinear parabolic system (2.1). We repeat the system (2.1) here and add the initial and boundary conditions.

$$\lambda_1 \frac{\partial u}{\partial t} - \nabla \cdot (a\nabla u) + c(\varphi(u) - v) = f, \text{ in } \Omega_T, \tag{3.8a}$$

$$\lambda_2 \frac{\partial v}{\partial t} - \nabla \cdot (b\nabla v) + c(v - \varphi(u)) = g, \text{ in } \Omega_T, \tag{3.8b}$$

$$u = 0, v = 0, \text{ on } \partial\Omega \times [0, T], \tag{3.8c}$$

$$u = u_0, v = v_0, \text{ in } \Omega \times \{t = 0\}. \tag{3.8d}$$

In the remainder of this chapter we discuss the existence and uniqueness of solutions for the models treated in here. Most follows from standard results in the PDE literature, which we review below.

3.2 Existence and uniqueness results for the models

3.2.1 Preliminaries on Sobolev Spaces

We begin by introducing some notation and standard results given in textbooks. We follow closely [1, 26, 47].

For any subset $\omega \subseteq \Omega$, itself an open bounded region, with Lipschitz boundary, $\partial\omega$, consider the Lebesgue spaces $L^p(\omega)$ and denote their norm by $\|\cdot\|_{L^p(\omega)}$. The space $L^2(\omega)$

is equipped with the usual scalar product $(f,\psi)_\omega := (f,\psi)_{L^2(\omega)} = \int_\omega f(x)\psi(x)dx$ and the simplified notation, $\|\cdot\|_\omega$, for its norm is adopted. If $\omega = \Omega$, the subscript ω will be omitted.

Definition 3.2.1. *Let $u, \psi \in L^1_{loc}(\Omega)$, and $\alpha = (\alpha_1, \ldots, \alpha_d)$ be a multi-index. We say that ψ is the weak derivative of u, and denote $\partial^\alpha u = \psi$, if*

$$\int u D^\alpha \phi dx = (-1)^{|\alpha|} \int \psi\phi dx,\ \forall \phi \in C_0^\infty(\Omega),$$

where $|\alpha| = \alpha_1 + \ldots + \alpha_d$.

If it exists, the weak derivative is a linear operator that is uniquely defined. Furthermore, the weak derivative agrees with the classical derivative when the latter exists.

Example 3.2.1. *The weak derivative owes its name to the fact that functions that do not have the classical derivative might have the weak derivative. Let $\Omega = (-1,1)$, and define*

$$h(x) = \begin{cases} x+1, & -1 < x \le 0 \\ -x+1, & 0 \le x < -1 \end{cases}, \quad sgn(x) = \begin{cases} -1, & -1 < x < 0 \\ 1, & 0 \le x < 1 \end{cases}.$$

The function $h(x)$, called the "hat function", is usual in the finite element analysis. Note that $h(x)$ is not differentiable at $x = 0$. However, it is weakly differentiable and $\partial h(x)$ can be identified with $-sgn(x)$, a.e. $x \in \Omega$.

From now on, we adopt the notation D for weak derivative as well. Next we define the Sobolev spaces $W^{m,p}(\Omega)$.

Definition 3.2.2. *If $u \in L^p(\Omega)$ and $D^\alpha u \in L^p(\Omega)$ for all $\alpha \le m$, we then say that $u \in W^{m,p}(\Omega)$ and define the norm in $W^{m,p}(\Omega)$ by*

$$\|u\|_{m,p} = \begin{cases} \left(\sum_{|\alpha|\le m} \|D^\alpha u\|^p_{L^p(\Omega)}\right)^{1/p}, & 1 \le p < \infty, \\ \max_{0\le|\alpha|\le m} \|D^\alpha u\|_{L^\infty(\Omega)}, \end{cases} \tag{3.9}$$

and its semi-norm by

$$|u|_{m,p} = \left(\sum_{|\alpha|=m} \|D^\alpha u\|^p_{L^p(\Omega)} \right)^{1/p}, \ 1 \leq p < \infty. \tag{3.10}$$

To account for Dirichlet boundary conditions, we search for weak solutions of the model problems in the spaces $W_0^{m,p}(\Omega)$ defined below. The reason for that becomes clear after we state the Trace Theorem 3.2.5.

Definition 3.2.3. *Define $W_0^{m,p}(\Omega)$ as the closure of $C_0^\infty(\Omega)$ in $W^{m,p}(\Omega)$.*

Theorem 3.2.4. *The Sobolev spaces are Banach spaces.*

Remark 3.2.1. *Recall that Banach spaces are complete normed spaces.*

The case $p = 2$, is a special case in the sense that $W^{m,2}(\Omega)$ are Hilbert spaces. For that reason, they receive a distinguished notation in the literature. Recall that Hilbert spaces are complete inner product spaces.

Notation. *We denote $H^m(\Omega) := W^{m,2}(\Omega)$ and $H_0^m(\Omega) := W_0^{m,2}(\Omega)$. The usual norms in $H^m(\Omega), H_0^m(\Omega)$ are denoted by $\|\cdot\|_m, |\cdot|_m$, respectively.*

For $u \in W^{1,p}(\Omega)$, u is not necessarily defined pointwise in sets of measure zero. To study PDEs with Dirichlet boundary conditions we need the notion of the value of the function on the boundary of the domain. This notion is given through the trace operator γ.

Theorem 3.2.5 (Trace Theorem)**.** *There exists a bounded linear operator $\gamma : W^{1,p}(\Omega) \to L^p(\partial\Omega)$ such that $\|\gamma u\|_{L^p(\partial\Omega)} \leq C\|u\|_{1,p}$. Moreover, if $u \in C(\overline{\Omega})$, $\gamma u = u|_{\partial\Omega}$.*

The spaces $W_0^{1,p}(\Omega)$ are then characterized by functions $u \in W^{1,p}(\Omega)$ so that $\gamma u \equiv 0$.

Another useful result from Sobolev spaces is the Poincaré-Friedrichs' inequality (Theorem 3, page 265 in [26]).

Lemma 3.2.1 (Poincaré-Friedrichs' Inequality)**.** *Let $u \in W_0^{1,p}(\Omega)$, $1 \leq p \leq \infty$. Then*

$$\|u\|_{L^p(\Omega)} \leq C_{PF}\|\nabla u\|_{L^p(\Omega)}, \tag{3.11}$$

where C_{PF} depend only on p and Ω.

To establish well-posedness of a class of elliptic problems we will use the Lax-Milgram Theorem. Let V be a Hilbert space.

Definition 3.2.6. *The bilinear form $a : V \times V \to \mathbb{R}$ is*

1. *continuous if $\exists C > 0$ such that*

$$a(u, v) \leq C\|u\|_V\|v\|_V, \ \forall u, v \in V,$$

2. *coercive if $\exists \alpha > 0$ such that*

$$a(u, u) \geq \alpha\|u\|_V^2, \ \forall u \in V.$$

Theorem 3.2.7 (Lax-Milgram)**.** *Let $a : V \times V \to \mathbb{R}$ be a bilinear, continuous and coercive mapping. Let $f : V \to \mathbb{R}$ be a bounded linear functional. Then there exists an unique solution $u \in V$ so that*

$$a(u, \phi) = f(\phi), \ \forall \phi \in H.$$

If B is a Banach space, we denote by B' the space of all bounded linear functionals $l : B \to \mathbb{R}$, the dual space. An important space in the study of PDEs is $H_0^1(\Omega)$. Its dual space is denoted by $H^{-1}(\Omega) := (H_0^1(\Omega))'$.

Remark 3.2.2. $H_0^1(\Omega) \subset L^2(\Omega) \subset H^{-1}(\Omega)$.

Along the way we apply the standard inequalities listed below in many instances.

Proposition 3.2.1. *Inequalities:*

1. *Cauchy-Schwarz inequality: let $u, v \in L^2(\Omega)$, then*

$$|(u, v)| \leq \|u\|\|v\|. \tag{3.12}$$

2. *Discrete Cauchy-Schwarz inequality: let $a_i, b_i \in \mathbb{R}$ positive numbers, for every $i = 1, \ldots, n$, then*

$$\sum_{i=1}^{n} a_i b_i \leq \left\{ \sum_{i=1}^{n} a_i^2 \right\}^{1/2} \left\{ \sum_{i=1}^{n} b_i^2 \right\}^{1/2} \tag{3.13}$$

3. *Young's Inequality: let $a, b \in \mathbb{R}$ positive. Then, for any $\epsilon > 0$,*

$$ab \leq \frac{\epsilon}{2}a^2 + \frac{1}{2\epsilon}b^2 \tag{3.14}$$

4. *Hölder Inequality: let $w \in L^p(\Omega), z \in L^q(\Omega)$, where p, q are conjugate exponents, $1 = 1/p + 1/q$, then*

$$|(u, v)| \leq \|u\|_{L^p(\Omega)}\|v\|_{L^q(\Omega)}. \tag{3.15}$$

In order to study the non-stationary models we need the following theory. We use the notation $'$ to denote $\dfrac{\partial}{\partial t}$.

Definition 3.2.8. *Let B be a Banach space, the space $L^p(0, T; B)$ consists of all functions $u : [0, T] \to B$ with*

$$\|u\|_{L^p(0,T;B)} := \left(\int_0^T \|u(t)\|_B^p dt\right)^{1/p}. \tag{3.16}$$

The following is a useful result to establish estimates in Chapter 4.

Proposition 3.2.2. *Let $u \in L^2(0, T; H_0^1(\Omega))$, with $u' \in L^2(0, T; H^{-1}(\Omega))$, then*

1. *$u \in C([0, T], L^2(\Omega))$.*
2. *$\dfrac{1}{2}\dfrac{d}{dt}\|u\|^2 =< u', u >$, a.e. $0 \leq t \leq T$.*

Definition 3.2.9. *We say that V is continuously imbedded in H, and denote this by $V \to H$, if $V \subset H$ and the identity operator I is continuous, i.e., $I : V \to H$, defined via $Ix = x$ is continuous.*

Let V, H be two Hilbert spaces. Consider V is dense subset of H so that $V \to H$.

Definition 3.2.10. *Define the operator $\mathcal{A} : D \to H$ related to the continuous bilinear form $a : V \times V \to \mathbb{R}$ via*

$$a(u, v) = (\mathcal{A}u, v),\ u \in D,\ v \in V.$$

Here D is the set of all functions u on V so that the function $v \mapsto a(u, v)$ is continuous with respect to the H-norm.

Definition 3.2.11. *Let $\mathcal{A} : D \to H$ as above. For $t \in [0, T]$,*

$$\frac{du(t)}{dt} + \mathcal{A}u(t) = f(t), \tag{3.17a}$$

$$u(0) = u_0. \tag{3.17b}$$

This initial boundary value problem is called the Cauchy problem.

Definition 3.2.12. *The operator $\mathcal{A} : D \to H$ is m-accretive if A is positive, i.e., $(\mathcal{A}u, u) \geq 0, \forall u \in D$, and $I + \mathcal{A} : D \to H$ is onto.*

Proposition 3.2.3. *If the bilinear form $a : V \times V \to \mathbb{R}$ satisfies:*

1. *$a(u, u) \geq 0$ for all $u \in V$,*
2. *$\exists \alpha > 0$, so that*

$$a(u, u) + \|u\|_H^2 \geq \alpha \|u\|_V^2.$$

Then $\mathcal{A}$ is m-accretive.

Note that $a(\cdot, \cdot)$ coercive implies that $\mathcal{A}$ is m-accretive.

To establish the well-posedness of the Cauchy problem we use the following application of the Hille-Yosida Theorem, see [47], page 25 and Proposition 2.5 on page 113.

Corollary 3.2.13 (Application of Hille-Yosida Theorem)**.** *Let $\mathcal{A}$ be a m-accretive and self-adjoint operator, $f \in L^2(0, T; H)$ and $u_0 \in V$. Then the Cauchy problem* (3.17) *has a unique solution in $u \in C([0, T], H)$ so that $u(t) \in D(\mathcal{A})$ at a.e. $t \in (0, T)$.*

Below we discuss the weak formulation of the models presented.

3.2.2 E-model

For the purposes of the exposition we adopt the following notation.

Notation.

$$\begin{aligned} V &= H_0^1(\Omega), && (3.18)\\ V' &= H^{-1}(\Omega), && (3.19)\\ V^2 &= V \times V, && (3.20)\\ (V')^2 &= V' \times V', && (3.21)\\ \vec{u} &= (u, v), && (3.22)\\ \vec{\psi} &= (\phi, \psi). && (3.23) \end{aligned}$$

Note that V is a Hilbert space. The norm in V^2 is given by

$$\|\vec{u}\|_{V^2}^2 := |u|_1^2 + |v|_1^2. \tag{3.24}$$

Consider the system (3.2). To get its weak formulation multiply (3.2a), (3.2b) by $\phi, \psi \in V$, respectively. Integrate by parts. The weak form of (3.2) is as follows.

Find $\vec{u} \in V^2$ such that, for all $\vec{\phi} \in V^2$,

$$(\lambda_1 u, \phi) + (a\nabla u, \nabla\phi) + (c(u - v), \phi) = (f, \phi), \tag{3.25a}$$
$$(\lambda_2 v, \psi) + (b\nabla v, \nabla\psi) + (c(v - u), \psi) = (g, \psi). \tag{3.25b}$$

We make the following assumptions in the parameters and data.

Assumptions 3.2.14.

A1. Each function in $\mathcal{P} = \{\lambda_1, \lambda_2, a, b, c\}$ belongs to $L^\infty(\Omega)$.

A2. Each function in $\mathcal{P} = \{\lambda_1, \lambda_2, a, b, c\}$ is bounded below by a positive constant, a.e. $x \in \Omega$

$$\begin{aligned} a(x) \geq a_0 > 0, \quad \lambda_1(x) \geq \lambda_{1,0} > 0,\\ b(x) \geq b_0 > 0, \quad \lambda_2(x) \geq \lambda_{2,0} > 0,\\ c(x) \geq c_0 > 0. \end{aligned}$$

A3. The data $(f, g) \in (V')^2$.

Definition 3.2.15. *Define the form* $A : V^2 \times V^2 \to \mathbb{R}$

$$A(\vec{u}, \vec{\phi}) := (\lambda_1 u, \phi) + (\lambda_2 v, \psi) + (a\nabla u, \nabla\phi) + (b\nabla v, \nabla\psi) + (c(u-v), \phi - \psi). \quad (3.26)$$

Lemma 3.2.2. *A is symmetric, bilinear, continuous, and coercive with respect to the product norm $\|\cdot\|_{V^2}$.*

Proof. The symmetry and bilinearity of $A(\cdot,\cdot)$ are clear. Now, let us prove the continuity of $A(\cdot,\cdot)$. Apply the Cauchy-Schwarz inequality (3.12) to the bilinear form (3.26)

$$\begin{aligned} |A(\vec{u}, \vec{\phi})| &\leq \|\lambda_1^{1/2} u\| \|\lambda_1^{1/2}\phi\| + \|\lambda_2^{1/2} v\| \|\lambda_2^{1/2}\psi\| + \|a^{1/2}\nabla u\| \|a^{1/2}\nabla\phi\| \\ &+ \|b^{1/2}\nabla v\| \|b^{1/2}\nabla\psi\| + \|c^{1/2}(u-v)\| \|c^{1/2}(\phi-\psi)\|. \end{aligned}$$

Now apply the discrete Cauchy-Schwarz inequality

$$\begin{aligned} |A(\vec{u}, \vec{\phi})| &\leq \left\{ \|\lambda_1^{1/2} u\|^2 + \|\lambda_2^{1/2} v\|^2 + \|a^{1/2}\nabla u\|^2 + \|b^{1/2}\nabla v\| + \|c^{1/2}(u-v)\|^2 \right\}^{1/2} \\ &+ \left\{ \|\lambda_1^{1/2}\phi\|^2 + \|\lambda_2^{1/2}\psi\|^2 + \|a^{1/2}\nabla\phi\|^2 + \|b^{1/2}\nabla\psi\|^2 + \|c^{1/2}(\phi-\psi)\| \right\}^{1/2}. \end{aligned}$$

Note that

$$\|c^{1/2}(u-v)\|^2 \leq \|c\|_{L^\infty} (\|u\| + \|v\|)^2 \leq \frac{\|c\|_{L^\infty}}{2} \left(\|u\|^2 + \|v\|^2 \right).$$

Also, by the Poincaré-Friedrichs' inequality in Lemma 3.2.1 and assumption *A1*

$$\|\lambda_1^{1/2} u\|^2 \leq \|\lambda_1\|_{L^\infty} C_{PF}^2 |u|_1^2.$$

Thus

$$|A(\vec{u}, \vec{\phi})| \leq C_A \|\vec{u}\|_{V^2} \|\vec{\phi}\|_{V^2}, \quad (3.27)$$

where

$$C_A = \max\{\|\lambda_1\|_{L^\infty} C_{PF}^2, \|\lambda_2\|_{L^\infty} C_{PF}^2, \|a\|_{L^\infty}, \|b\|_{L^\infty}, \|c\|_{L^\infty} C_{PF}^2\}.$$

Note that the constant $C_A > 0$ independent of u, v, ϕ, ψ.

To prove the coercivity, apply assumption *A2* and the fact that $c(u-v)u+c(v-u)v = c(u-v)^2 \geq 0$.

$$\begin{aligned} A(\vec{u},\vec{u}) &= \|\lambda_1^{1/2}u\|^2 + \|\lambda_2^{1/2}v\|^2 + \|a^{1/2}\nabla u\|^2 + \|b^{1/2}\nabla v\|^2 + \|c^{1/2}(u-v)\|^2 \\ &\geq \|a^{1/2}\nabla u\|^2 + \|b^{1/2}\nabla v\|^2. \end{aligned}$$

Thus

$$A(\vec{u},\vec{u}) \geq \alpha_A \|\vec{u}\|_{V^2}^2, \tag{3.28}$$

where $\alpha_A = \min\{a_0, b_0\}$. We stress that both C_A, α_A depend on $\mathcal{P}$. □

From Lemma 3.2.2 we see that $A(\cdot,\cdot)$ can be used as an inner product on V^2. The associated norm is the energy norm

$$\|\vec{u}\|_e^2 := A(\vec{u},\vec{u}). \tag{3.29}$$

Define a functional $L : V^2 \to \mathbb{R}$ via

$$L(\vec{\phi}) = \langle f, \phi\rangle + \langle g, \psi\rangle, \tag{3.30}$$

where $\langle\cdot,\cdot\rangle$ denotes the standard duality pairing between V and V'. It is standard that L is linear and continuous [26]. The weak formulation of the E-model can be rewritten as follows:

Find $\vec{u} \in V^2$ so that for all $\vec{\phi} \in V^2$

$$A(\vec{u},\vec{\phi}) = L(\vec{\phi}). \tag{3.31}$$

Lemma 3.2.3. *Assume that assumptions A1-A3 holds. The problem* (3.25) *has a unique weak solution $\vec{u} \in V^2$. In addition, if $(f,g) \in L^2(\Omega)\times L^2(\Omega)$, then $\vec{u} \in H^2(\Omega)\times H^2(\Omega)$.*

Proof. By Lemma 3.2.2, we apply the Lax-Milgram Theorem 3.2.7 to conclude the existence of a unique solution for the problem. The extra regularity in $\vec{u}$ follows from the fact that each component solves an elliptic problem with a source term in $L^2(\Omega)$. □

3.2.3 LP-model

Following the same procedure we did for the E-model we arrive at the weak form of the system (3.1)

Find $\vec{u} \in L^2(0,T;V^2)$ *with* $\vec{u'} \in L^2(0,T;(V')^2)$*, such that, for all* $\vec{\phi} \in V^2$*,* $0 \le t \le T$

$$(\lambda_1 u'(t), \phi) + (a\nabla u(t), \nabla\phi) + (c(u(t) - v(t)), \phi) = (f(t), \phi), \tag{3.32a}$$

$$(\lambda_2 v'(t), \psi) + (b\nabla v(t), \nabla\psi) + (c(v(t) - u(t)), \psi) = (g(t), \psi). \tag{3.32b}$$

$$u(0) = u_0 \qquad v(0) = v_0. \tag{3.32c}$$

Remark 3.2.3. *By Proposition 3.2.2,* $\vec{u} \in C([0,T];L^2(\Omega)^2)$*.*

For the LP-model we make the following assumptions.

Assumptions 3.2.16.

B1. Each function in $\mathcal{P} = \{\lambda_1, \lambda_2, a, b, c\}$ *is independent of* t*.*

B2. Assumptions A1 and A2 hold.

B3. The data $(f, g) \in L^2(0,T;L^2(\Omega)) \times L^2(0,T;L^2(\Omega))$*.*

B4. The initial conditions $\vec{u}_0 \in V^2$*.*

Remark 3.2.4. *Note that assumption B1 is consistent with the assumption that the porous medium is rigid in Section 2.1.1.*

Definition 3.2.17. *Define the form* $B : V^2 \times V^2 \to \mathbb{R}$

$$B(\vec{u}, \vec{\phi}) := (a\nabla u, \nabla\phi) + (b\nabla v, \nabla\psi) + (c(u - v), \phi - \psi). \tag{3.33}$$

Remark 3.2.5. *Note that*

$$A(\vec{u}, \vec{\phi}) = B(\vec{u}, \vec{\phi}) + (\lambda_1 u, \phi) + (\lambda_2 v, \psi). \tag{3.34}$$

Lemma 3.2.4. *The form* B *is bilinear, symmetric, continuous, and coercive with respect to the product norm* $\|\cdot\|_{V^2}$*.*

Proof. The proof is analogous for the proof for the form $A(\cdot,\cdot)$ in Lemma 3.2.2. The continuity constant is $C_B = \max\{\|a\|_{L^\infty}, \|b\|_{L^\infty}, \|c\|_{L^\infty} C_{PF}^2\}$, and coercivity constant is $\alpha_B = \alpha_A$. □

From Lemma 3.2.4, $B(\cdot,\cdot)$ defines an inner product on V^2. Next we define the energy norm associated with it

$$\|\vec{u}\|_b^2 := B(\vec{u},\vec{u}). \tag{3.35}$$

With the above notation, the weak problem (3.32) can be rewritten as:

Find $\vec{u} \in L^2(0,T;V^2)$ with $\vec{u'} \in L^2(0,T;(V')^2)$, such that, for all $\vec{\phi} \in V^2$, $0 \le t \le T$

$$(\vec{u'},\vec{\phi}) + B(\vec{u},\vec{\phi}) = L(\vec{\phi}), \forall \vec{\phi} \in V^2, \tag{3.36a}$$

$$\vec{u}(0) = (u_0, v_0). \tag{3.36b}$$

Lemma 3.2.5. *Let assumptions B1-B4 hold. The weak problem* (3.36) *admits a unique solution $\vec{u} \in C([0,T];L^2(\Omega)^2)$.*

Proof. Let $H = L^2(\Omega) \times L^2(\Omega)$, so V^2 is dense and continuously imbedded in H. Define the operator $\mathcal{B} : D \to H$ via the symmetric bilinear form $B(\vec{u},\vec{\phi}) = \left(\mathcal{B}(\vec{u}),\vec{\phi}\right)$,

$$\mathcal{B} = \begin{bmatrix} -a\partial^2 + cI & -cI \\ -cI & -b\partial^2 + cI \end{bmatrix}, \quad D(\mathcal{B}) = \{\vec{u} \in V^2 : \partial^2 \vec{u} \in H\}.$$

Since the form B is coercive, by Proposition 3.2.3, $\mathcal{B}$ is m-accretive and by the application of Hille-Yosida theorem, Corollary 3.2.13, there exists a unique solution $\vec{u} \in C([0;T],H)$ for (3.1) provided that $\vec{u}_0 \in V^2$. □

Another way to prove Lemma 3.2.5 is to apply the Galerkin method. The general idea of the Galerkin method is solve the problem in a subspace $V_m \subset V^2$ generated by m basis functions of V^2. Next step is to let $m \to \infty$ to get a solution in the whole space V^2.

3.2.4 WR-model

The WR-model (3.6) has a degenerate structure in the sense that is an ODE coupled with a parabolic PDE.

Notation. *From now on:*

$$\begin{aligned} W &= H_0^1(\Omega) \times L^2(\Omega), \\ W^2 &= W \times W. \end{aligned}$$

Note that W is a Hilbert space.

Definition 3.2.18. *For $\vec{u} \in W$, we define*

$$\|\vec{u}\|_W^2 := |u|_1^2 + \|v\|^2. \tag{3.37}$$

We define the weak problem which follows from multiplying (3.6a)-(3.6b) by $\phi \in V, \psi \in L^2(\Omega)$, respectively and integrating by parts:

Find $\vec{u} \in L^2(0,T;W)$ with $\vec{u'} \in L^2(0,T;W')$, such that, for all $\vec{\phi} \in W$

$$(\lambda_1 u'(t), \phi) + (a\nabla u(t), \nabla\phi) + (c(u(t) - v(t)), \phi) = (f(t), \phi), \tag{3.38a}$$

$$(\lambda_2 v'(t), \psi) + (c(v(t) - u(t)), \psi) = (g(t), \psi), \tag{3.38b}$$

$$u(0) = u_0 \qquad v(0) = v_0. \tag{3.38c}$$

For the WR-model we make the following assumptions.

Assumptions 3.2.19.

W1. Each function in $\mathcal{P}_{\mathcal{WR}} = \{\lambda_1, \lambda_2, a, c\}$ is independent of t.

W2. Each function in $\mathcal{P}_{WR} = \{\lambda_1, \lambda_2, a, c\}$ belongs to $L^\infty(\Omega)$.

W3. Each function in $\mathcal{P}_{WR} = \{\lambda_1, \lambda_2, a, c\}$ is bounded below by a positive constant, for a.e. $x \in \Omega$

$$\begin{aligned} a(x) \geq a_0 > 0, \quad \lambda_1(x) \geq \lambda_{1,0} > 0, \\ c(x) \geq c_0 > 0, \quad \lambda_2(x) \geq \lambda_{2,0} > 0. \end{aligned}$$

W4. Assumptions B3 and B4 hold.

Definition 3.2.20. *Define the bilinear form* $B_{WR} : W^2 \to \mathbb{R}$ *via*

$$B_{WR}(\vec{u}, \vec{\phi}) := (a\nabla u, \nabla\phi) + (c(u - v), \phi - \psi). \tag{3.39}$$

Lemma 3.2.6. *Assume that assumptions W1-W4 hold. The system* (3.6) *has a unique solution* $\vec{u} \in C([0;T], H)$.

Proof. Let $H = L^2(\Omega) \times L^2(\Omega)$, so W is dense and continuously imbedded in H. Define the operator $\mathcal{W} : D \to H$ via the symmetric bilinear form $B_{WR}(\vec{u}, \vec{\phi}) = \left(\mathcal{W}(\vec{u}), \vec{\phi}\right)$,

$$\mathcal{W} = \begin{bmatrix} -a\partial^2 + cI & -cI \\ -cI & cI \end{bmatrix}, \quad D(\mathcal{W}) = \{\vec{u} \in W : \partial^2 u \in L^2(\Omega)\}.$$

It is easy to see that $B_{WR}(\vec{u}, \vec{u}) \geq 0$ and that for $\alpha_W = \min_{x\in\Omega}\{a_0, 1\}$

$$B_{WR}(\vec{u}, \vec{u}) + \|\vec{u}\|_H^2 \geq \alpha_w \|\vec{u}\|_W^2, \ \forall \vec{u} \in W.$$

Therefore by Proposition 3.2.3, $\mathcal{W}$ is m-accretive and by the application of Hille-Yosida theorem, Corollary 3.2.13, there exists a unique solution $\vec{u} \in C([0;T], H)$ for (3.6) provided that $\vec{u}_0 \in W$. □

3.2.5 PP-model

The weak form of system (3.7) reads:

Find $\vec{u} \in V \times L^2(0,T; L^2(\Omega))$ *with* $v \in L^2(0,T; L^2(\Omega))$*, such that, for all* $\vec{\phi} \in V \times L^2(0,T; L^2(\Omega))$

$$(a\nabla u(t), \nabla\phi) + (c(u(t) - v(t)), \phi) = (f(t), \phi), \tag{3.40a}$$

$$(\lambda_2 v'(t), \psi) + (c(v(t) - u(t)), \psi) = (g(t), \psi), \tag{3.40b}$$

$$v(0) = v_0. \tag{3.40c}$$

The PP-model (3.7) is also a degenerate system. It couples an ODE with an elliptic PDE. In fact, the ODE in the PP-model is the same as the one for the WR-model. We do not

show the well-posedness of (3.40). Instead we rewrite the problem as a pseudo-parabolic problem and state the results found in [18]. Note that from (3.7a)

$$u = \frac{1}{c}\left(\lambda_2 \frac{\partial v}{\partial t} + cv - g\right), \text{ in } \Omega_T. \tag{3.41}$$

Thus, finding the component v gives the component u as well. First, we rewrite (3.7) to put the problem in the framework of [18]. Let $A = -\nabla \cdot (a\nabla)$ and I be the identity operator on V,

$$\lambda_2 \frac{\partial v}{\partial t} + c\left(I - (I + \frac{1}{c}A)^{-1}\right) v = g + (I + \frac{1}{c}A)^{-1} f, \tag{3.42a}$$

$$v(0) = v_0. \tag{3.42b}$$

Next, we apply $(I + \frac{1}{c}A)$ to both sides of (3.42)

$$\lambda_2 \frac{\partial v}{\partial t} + \frac{\lambda_2}{c} A\left(\frac{\partial v}{\partial t}\right) + A(v) = (I + \frac{1}{c}A)g + f, \tag{3.43a}$$

$$v(0) = v_0. \tag{3.43b}$$

The weak formulation of (3.43) is as follows: *Find* $v \in C^1([0,T], V)$ *such that for all* $\psi \in V$

$$(\lambda_2 v', \psi) + \frac{\lambda_2}{c}(a\nabla v', \nabla\psi) + (\nabla v, \nabla\psi) = (I + \frac{1}{c}A)g + f, \psi) \; a.e.t \in (0,T] \tag{3.44a}$$

$$v(0) = v_0. \tag{3.44b}$$

We need the follow assumptions for the existence of a weak solution of (3.44).

Assumptions 3.2.21.

PP1. Each function in $\mathcal{P}_{PP} = \{\lambda_2, a, c\}$ *is independent of* t.

PP2. Each function in $\mathcal{P}_{PP} = \{\lambda_2, a, c\}$ *belongs to* $L^\infty(\Omega)$.

PP3. Each function in $\mathcal{P}_{PP} = \{\lambda_2, a, c\}$ *is bounded below by a positive constant, for a.e.* $x \in \Omega$

$$a(x) \geq a_0 > 0, \quad \lambda_2(x) \geq \lambda_{2,0} > 0$$
$$c(x) \geq c_0 > 0.$$

PP4. $g \in C([0,T], V)$, $f \in C([0,T], L^2(\Omega))$.

PP5. $v_0 \in V$.

We assume that Assumptions 3.2.21 hold. Thus by Theorem 2.3 in [18], the problem (3.44) has a solution $v \in C^1([0,T], V)$. Then with equation (3.41) we can find the component $u \in C^1([0,T], V)$. More results on the well-posedness of such systems can be found in [46, 18, 17].

3.2.6 NLP-model

The weak form of system (3.8) reads: *Find* $\vec{u} \in L^2(0,T;V^2)$ *with* $\vec{u'} \in L^2(0,T;(V')^2)$, *such that, for all* $\vec{\phi} \in V^2$, $0 \leq t \leq T$

$$(\lambda_1 u'(t), \phi) + (a\nabla u(t), \nabla\phi) + (c(\varphi(u(t)) - v(t)), \phi) = (f(t), \phi), \tag{3.45a}$$
$$(\lambda_2 v'(t), \psi) + (b\nabla v(t), \nabla\psi) + (c(v(t) - \varphi(u(t))), \psi) = (g(t), \psi). \tag{3.45b}$$
$$u(0) = u_0 \qquad v(0) = v_0. \tag{3.45c}$$

By Proposition 3.2.2 $\vec{u} \in C([0,T], L^2(\Omega)^2)$.

We define assumptions to guarantee existence and uniqueness of solution for (3.8).

Assumptions 3.2.22.

NL1. Assume that B1-B3 hold.

NL2. $\varphi(0) = 0$.

NL3. φ *is Lipschitz continuous.*

NL4. $u_0, v_0 \in V$.

NL5. φ is monotone increasing.

The following Lemma is immediate.

Lemma 3.2.7. *The Langmuir and linear isotherms, equations* (2.23) *and* (2.22)*, respectively, satisfies the assumptions NL2-NL4.*

To prove the existence and uniqueness of a solution for (3.45) we will apply the Banach Fixed Point Theorem.

Theorem 3.2.23 (Banach Fixed Point Theorem)**.** *Let X be a Banach space and assume $\mathcal{F} : X \to X$ is a non-linear mapping such that for all $u, \tilde{u} \in X$*

$$\|A(u) - A(\tilde{u})\| \leq \gamma \|u - \tilde{u}\|, \tag{3.46}$$

for some constant $\gamma < 1$. That is, suppose that A is a strict contraction. Then A has a unique fixed point.

We also apply the integral form of Gronwall's Lemma.

Lemma 3.2.8 (Gronwall's Lemma - integral form)**.** *Let $\xi(t)$ be a nonnegative, summable function on $[0, T]$ so that a.e. t*

$$\xi(t) \leq C_1 \int_0^t \xi(s) ds + C_2,$$

for some constants $C_1, C_2 \geq 0$. Then a.e. $0 \leq t \leq T$,

$$\xi(t) \leq C_2(1 + C_1 t e^{C_1 t}).$$

Now we have all the tools to prove the following.

Lemma 3.2.9. *Suppose NL1-NL4 hold. Then there exists a unique solution $\vec{u} \in C([0, T], L^2(\Omega)^2)$ for* (3.45)*.*

Proof. This proof is a straightforward adaptation of the proof for a scalar reaction-diffusion problem presented in Example 1, page 499 in [26], we even follow the same notation. Nevertheless the proof is presented here as an exercise.

We apply the Banach Fixed Point Theorem 3.2.23 in the space $X = C([0,T], L^2(\Omega)^2)$ with the norm

$$\|\vec{u}\|_X := \max_{0\le t\le T} \left\{\lambda_1\|u\|^2 + \lambda_2\|v\|\right\}^{1/2}. \tag{3.47}$$

Let the operator A be defined as follows. Given $\vec{u} = (u, v) \in X$, set

$$h(t) := \varphi(u(t)) - v(t),\ 0 \le t \le T. \tag{3.48}$$

With the use of the Nemitskyi operator, φ Lipschitz from $\mathbb{R}$ to $\mathbb{R}$ implies that φ is Lipschitz from L^2 to L^2 (see Proposition in [38], page 169, for functions with linear growth). Following further the example in [26], we see that $h \in L^2(0,T;L^2(\Omega))$. We now rewrite the system (3.8) using the function h for $\vec{w} = (w_1, w_2)$ as follows

$$\lambda_1\frac{\partial w_1}{\partial t} - \nabla\cdot(a\nabla w_1) = f - ch,\ \text{in } \Omega_T, \tag{3.49a}$$

$$\lambda_2\frac{\partial w_2}{\partial t} - \nabla\cdot(b\nabla w_2) = g + ch,\ \text{in } \Omega_T, \tag{3.49b}$$

$$w_1 = 0, w_2 = 0,\ \text{on } \partial\Omega\times[0,T], \tag{3.49c}$$

$$w_1 = u_0, w_2 = v_0,\ \text{in } \Omega\times\{t=0\}. \tag{3.49d}$$

The weak form of (3.49) is given by:

Find $\vec{w} \in L^2(0,T,V^2)$ *with* $\vec{w}' \in L^2(0,T,(V')^2$ *so that for all* $\vec{\phi} \in V^2$

$$(\lambda_1 w_1', \phi) + (a\nabla w_1, \nabla\psi) = (f - ch, \phi), \tag{3.50a}$$

$$(\lambda_2 w_2', \psi) + (b\nabla w_2, \nabla\psi) = (g + ch, \psi), \tag{3.50b}$$

$$w_1 = u_0, w_2 = v_0,\ \text{in } \Omega\times\{t=0\}. \tag{3.50c}$$

Both equations in (3.50) are heat equations with initial data in $L^2(\Omega)$ and right hand side in $L^2(0,T;L^2(\Omega))$. From the theory for linear parabolic PDEs we know that (3.50a) and (3.50b) have a unique weak solution $w_1 \in L^2(0,T,V)$ with $w_1' \in L^2(0,T,V')$ and $w_2 \in L^2(0,T,V)$ with $w_2' \in L^2(0,T,V')$, respectively, provided that Assumptions 3.2.16 hold. Thus (3.50) has a unique solution $\vec{w} \in L^2(0,T,V^2)$ with $\vec{w}' \in L^2(0,T,(V')^2)$.

Define $A : X \to X$ via $A(\vec{u}) = \vec{w}$. We now prove that if T is small enough, A is a strict contraction. Take $\vec{u} = (u_1, u_2), \vec{z} = (z_1, z_2) \in X$ and define $\vec{w}_u = A(\vec{u}), \vec{w}_z = A(\vec{z})$. That is,

$$(\lambda_1 w'_{1,u}, \phi) + (a\nabla w_{1,u}, \nabla\psi) = (f - ch(\vec{u}), \phi), \tag{3.51a}$$
$$(\lambda_2 w'_{2,u}, \psi) + (b\nabla w_{2,u}, \nabla\psi) = (g + ch(\vec{u}), \psi), \tag{3.51b}$$
$$w_{1,u} = u_0, w_{2,u} = v_0, \text{ in } \Omega \times \{t = 0\}. \tag{3.51c}$$

And

$$(\lambda_1 w'_{1,z}, \phi) + (a\nabla w_{1,z}, \nabla\psi) = (f - ch(\vec{z}), \phi), \tag{3.52a}$$
$$(\lambda_2 w'_{2,z}, \psi) + (b\nabla w_{2,z}, \nabla\psi) = (g + ch(\vec{z}), \psi), \tag{3.52b}$$
$$w_{1,z} = u_0, w_{2,z} = v_0, \text{ in } \Omega \times \{t = 0\}. \tag{3.52c}$$

We set $\phi = w_{1,u} - w_{1,z}$, $\psi = w_{2,u} - w_{2,z}$ and subtract equation (3.51a) from (3.52a) and equation (3.51b) from (3.52b)

$$\frac{\lambda_1}{2}\frac{d}{dt}\|w_{1,u} - w_{1,z}\|^2 + a|w_{1,u} - w_{1,z}|_1^2 = (-ch(\vec{u}) + ch(\vec{z}), w_{1,u} - w_{1,z}), \tag{3.53a}$$
$$\frac{\lambda_2}{2}\frac{d}{dt}\|w_{2,u} - w_{2,z}\|^2 + b|w_{2,u} - w_{2,z}|_1^2 = (ch(\vec{u}) - ch(\vec{z}), w_{2,u} - w_{2,z}). \tag{3.53b}$$

Multiplying both equations by 2 both sides and using Young's Inequality (3.14)

$$\begin{aligned}\lambda_1\frac{d}{dt}\|w_{1,u} - w_{1,z}\|^2 + 2a|w_{1,u} - w_{1,z}|_1^2 &\le \frac{1}{\varepsilon}\|h(\vec{u}) - h(\vec{z})\|^2 + \varepsilon\|c(w_{1,u} - w_{1,z})\|^2 \\ &\overset{(3.11)}{\le} \frac{1}{\varepsilon}\|h(\vec{u}) - h(\vec{z})\|^2 + C_{PF}^2\varepsilon|c(w_{1,u} - w_{1,z})|_1^2, \\ \lambda_2\frac{d}{dt}\|w_{2,u} - w_{2,z}\|^2 + 2b|w_{2,u} - w_{2,z}|_1^2 &\le \frac{1}{\varepsilon}\|h(\vec{u}) - ch(\vec{z})\|^2 + \varepsilon\|c(w_{2,u} - w_{2,z})\|^2 \\ &\overset{(3.11)}{\le} \frac{1}{\varepsilon}\|h(\vec{u}) - h(\vec{z})\|^2 + C_{PF}^2\varepsilon|c(w_{2,u} - w_{2,z})|_1^2.\end{aligned}$$

Let $\varepsilon > 0$ sufficiently small to conclude that

$$\begin{aligned}\lambda_1 \frac{d}{dt}\|w_{1,u} - w_{1,z}\|^2 &\leq C\|h(\vec{u}) - h(\vec{z})\|^2,\\ \lambda_2 \frac{d}{dt}\|w_{2,u} - w_{2,z}\|^2 &\leq C\|h(\vec{u}) - ch(\vec{z})\|^2.\end{aligned}$$

Now use that h is Lipschitz,

$$\begin{aligned}\lambda_1 \frac{d}{dt}\|w_{1,u} - w_{1,z}\|^2 &\leq C(\lambda_1,\lambda_2,L)\left(\lambda_1\|(u_1 - z_1)\|^2 + \lambda_2\|u_2 - z_2\|^2\right),\\ \lambda_2 \frac{d}{dt}\|w_{2,u} - w_{2,z}\|^2 &\leq C(\lambda_1,\lambda_2,L)\left(\lambda_1\|(u_1 - z_1)\|^2 + \lambda_2\|u_2 - z_2\|^2\right).\end{aligned}$$

Add both inequalities above and integrate from 0 to s to get to

$$\begin{aligned}\lambda_1\|w_{1,u} - w_{1,z}\|^2(s) + \lambda_2\|w_{2,u} - w_{2,z}\|^2(s) &\leq C(\lambda_1,\lambda_2,L)\int_0^s \left(\lambda_1\|(u_1 - z_1)\|^2\right.\\ &+ \left.\lambda_2\|u_2 - z_2\|^2\right)(t)dt\\ &\leq C(\lambda_1,\lambda_2,L)T\|\vec{u} - \vec{z}\|_X^2,\ 0 \leq s \leq T.\end{aligned}$$

Taking the maximum with respect to s in the left hand side we arrive at

$$\|\vec{w}_u - \vec{w}_z\|_X^2 \leq C(\lambda_1,\lambda_2,L)T\|\vec{u} - \vec{z}\|_X^2.$$

Hence,

$$\|A(\vec{u}) - A(\vec{z})\|_X \leq \left(C(\lambda_1,\lambda_2,L)T\right)^{1/2}\|\vec{u} - \vec{z}\|_X.$$

Thus A is a strict contraction if $\left(C(\lambda_1,\lambda_2,L)T\right)^{1/2} < 1$. Given any $T > 0$, we choose $T_1 > 0$ so that $\left(C(\lambda_1,\lambda_2,L)T_1\right)^{1/2} < 1$. Then by the Banach Fixed Point Theorem 3.2.23 there is a unique solution $\vec{u} \in X$ of (3.45) on $[0, T_1]$. Since $\vec{u}(t) \in V^2$, a.e. $0 \leq t \leq T_1$, we can assume that $\vec{u}(T_1) \in V^2$, we might have to redefine T_1. We can repeat then the construction of the solution in the interval $[T_1, 2T_1]$. After finitely many steps we construct a solution for (3.45) on $[0, T]$.

To show the uniqueness, suppose that $\vec{u}, \vec{z}$ are two solutions of (3.45). Then we have that $\vec{w}_u = \vec{u}, \vec{w}_z = \vec{z}$ in inequality (3.55), so for $0 \leq s \leq T$,

$$\begin{aligned} \lambda_1 \|u_1 - z_1\|^2(s) + \lambda_2 \|u_2 - z_2\|^2(s) &\leq C(\lambda_1, \lambda_2, L) \int_0^s \left(\lambda_1 \|(u_1 - z_1)\|^2 \right. \\ &+ \left. \lambda_2 \|u_2 - z_2\|^2\right)(t) dt. \end{aligned}$$

Using the integral form of the Gronwall's Lemma 3.2.8 with $C_2 = 0$ we see that $\vec{u} = \vec{z}$. $\square$

4 Numerical Analysis

This Chapter presents the theoretical part of the major contributions of this thesis. In Section 4.1 we present an introduction to the Finite Element setting and definitions, with particular attention to the use of multilevel grids. Next, in Section 4.2 we present an introduction to error estimates and estimators. In the remainder of the Chapter we discuss various estimates for the FE solutions to the models E, LP, WR, PP, NLP as listed below.

1. In Section 4.3, we prove *a-priori* and *a-posteriori* error estimates for the E-model (3.25). These results were published in [30].

2. In Section 4.4, we prove *a-priori* error estimates for the NLP-model (3.45).

3. In Section 4.5, we prove *a-posteriori* error estimates for the LP-model (3.32). These results were partially presented in [29]. We also state the *a-priori* error estimates as a particular case of the *a-priori* error estimate for the NLP-model. Note that the NLP-model gets reduced to the LP-model when $\varphi(u) = u$.

4. In Section 4.6, we state the *a-priori* and *a-posteriori* error estimates for the WR-model as Corollaries of the results obtained for the NLP-model in Section 4.4 and the LP-model in Section 4.5, respectively. Note that the WR-model is a particular case of the LP-model with $b = 0$ and of the NLP-model with $b = 0$ and $\varphi(u) = u$.

5. In Section 4.7, we state the *a-priori* and *a-posteriori* error estimates for the PP-model as Corollaries of the results obtained for the WR-model in Section 4.6. Note that the PP-model is a special case of the WR-model with $a = 0$.

6. Finally, in Section 4.8, we postulate *a-posteriori* estimates for the NLP-model. The theoretical work on this is currently in progress. However, we will apply the postulated *a-posteriori* error estimator developed for the LP-model to the cases where $\varphi(u) \approx u$, i.e., the cases where the system is "almost" linear.

7. In Section 4.9 we discuss the dependence of the numerical solution of the LP-model with respect to the parameters $\mathcal{P}$.

4.1 Preliminaries on Multilevel Finite Elements

The finite element method consists of finding a numerical solution in a finite dimensional space that approximates the analytical solution of a given PDE. We apply finite element method to approximate the solution $(u, v) \in V \times V$ of our model systems. First, we discuss a finite dimensional space $V_h \subset V$ constructed as follows.

We denote by $\mathcal{T}_h, h > 0$, a family of partitions of Ω into a finite number of elements. To avoid the presence of curvilinear elements we assume from now on that Ω is a convex polygon. We require that the elements in any partition $\mathcal{T}_h$ satisfy the standard assumptions as in [53]:

- admissibility: any two elements in $\mathcal{T}_h$ are either disjoint, or share a vertex, or share an edge (if d=2, a face, if d=3). This condition assures that the partition has no "hanging" nodes.

- shape-regularity: for any element in $\mathcal{T}_h$ the ratio between the inscribed ball r_T and the circumscribed ball R_T is bounded above by a constant. This condition assures that the inner angles of the elements are bounded below by a constant.

We denote by $\mathcal{E}_h$ the set of all edges in the partition $\mathcal{T}_h$ that are not contained in $\partial\Omega$. For any element $T \in \mathcal{T}_h$ we let $\tilde{\omega}_T$ be the set of all elements that share a vertex or an edge with T and h_T be the diameter of T. We denote by $h = \max_{T\in\mathcal{T}_h} h_T$. For any edge $E \in \mathcal{E}_h$ we define ω_E to be the set of all elements that contain the edge E and we let h_E denote the diameter of the edge E.

Denote by $\mathcal{P}_k(T)$ the space of polynomials of degree k in $\mathbb{R}^d$ and define the space of approximations

$$V_h = \left\{ v_h \in C(\overline{\Omega}) : \forall T \in \mathcal{T}_h, v_h|_T \in \mathcal{P}_k(T),\ v_h|_{\partial\Omega} = 0 \right\}.$$

We actually want to approximate u and v in different finite element spaces. So we seek an approximation $(u_h, v_H) \in V_h \times V_H$ to $(u, v) \in V \times V$. Because of the fact that u and v are approximated in different finite element spaces we call this method multilevel finite element.

Figure 4.1: Illustration of the sets $\tilde{\omega}_T$(left), ω_E(right)

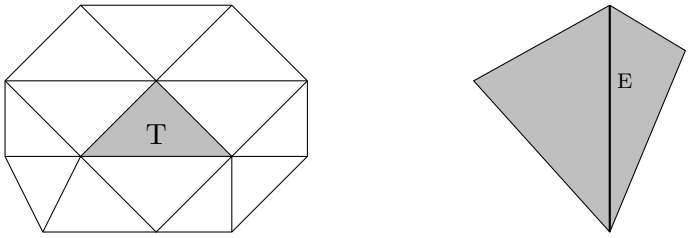

In this thesis we consider the case $V_h \subseteq V$ and $V_H \subseteq V$. Moreover we only consider the case where $V_H \subseteq V_h$. Because the models treated here are coupled we need to define some interpolation/projection operators between the spaces. Various choices for these operators can be made e.g., via inter-grid operators used in multigrid theory or multilevel schemes [27, 20, 59].

Consider now $h \leq H$ and some two partitions $\mathcal{T}_h$, $\mathcal{T}_H$ with the associated spaces V_h, V_H. Denote $\mathcal{H} = \{h, H\}$. Note that $h = H$ does not necessarily mean $\mathcal{T}_h = \mathcal{T}_H$. We seek approximations $(u_h, v_H) \in V_h \times V_H$ to $(u, v) \in V \times V$.

Remark 4.1.1. *If $\mathcal{T}_h \neq \mathcal{T}_H$, we will consider for simplicity only $k = 1$. Our a-posteriori calculations will be carried out however for any k.*

In the analysis below it will be evident that we need to relate the two partitions $\mathcal{T}_h$, $\mathcal{T}_H$ to one another. We say that $\mathcal{T}_h$ is a refinement of $\mathcal{T}_H$, if every element of $\mathcal{T}_h$ intersects the interior of exactly one element in $\mathcal{T}_H$. A general case of unrelated partitions $\mathcal{T}_h$, $\mathcal{T}_H$ could be treated but will not be discussed in this thesis.

Definition 4.1.1. *Let $r \in \mathbb{N}$ be fixed. We call the partition $\mathcal{T}_h$ an r-uniform refinement of $\mathcal{T}_H$ if for every element $K \in \mathcal{T}_H$, the number of $T \in \mathcal{T}_h : T \subseteq K$ equals r.*

Definition 4.1.2. *Let $\Pi : V_H \to V_h$ be the interpolation operator and $\Pi' : V_h \to V_H$ be defined by*

$$(\Pi' \phi_h, \psi_H) := (\phi_h, \Pi \psi_H), \ \forall \psi_H \in V_H, \tag{4.1}$$

That is, Π' is adjoint to Π with respect to the $L^2(\Omega)$ product on V_H. This choice eliminates additional error terms that otherwise would arise in error analysis developed

below. Now let us introduce a partition of the finite element spaces. Note that if $\mathcal{T}_h = \mathcal{T}_H$, then $V_H = V_h$ and Π and Π' both trivially reduce to identity. Another important observation follows.

Lemma 4.1.1. *Let $V_H \subseteq V_h$, we have $\forall \psi_H \in V_H$*

$$\Pi \psi_H = \psi_H, \tag{4.2}$$

$$\Pi' \Pi \psi_H = \psi_H. \tag{4.3}$$

In other words the composition $\Pi' \Pi|_{V_H}$ is the identity operator.

4.2 Overview *a-priori* and *a-posteriori* estimators

Here we give a general overview of error estimates for a general problem. Let X be a Banach space equipped with the norm $\|\cdot\|_*$. Let $\mathcal{Z} : X \times X \times P \to \mathbb{R}$ be a bilinear, continuous and coercive form on X with respect to the norm $\|\cdot\|_*$. Here P represents the set of parameters of the bilinear form. Suppose we want to solve:

Find $u \in X$ such that for all $\phi \in X$

$$\mathcal{Z}(u, \phi, p) =< f, \phi >, \tag{4.4}$$

for $f \in X'$ and $p \in P$.

If we cannot solve problem (4.4) analytically, we want to approximate its solution u by a discrete solution u_h in a finite dimensional subspace $X_h \subset X$ by solving

Find $u_h \in X_h$ such that for all $\phi_h \in X_h$

$$\mathcal{Z}(u_h, \phi_h, p) = (f_h, \phi_h). \tag{4.5}$$

Here f_h is the projection of f into X_h. The subscript h is related with the maximum diameter of the elements of the mesh representing the domain Ω as described in the previous section. We assume that (4.5) can be solved in a computer.

Naturally, we need to quantify how good is the numerical approximation. We choose one of the norms $\|\cdot\|_*$ on X to measure the error $\|u - u_h\|_*$. There are two types of error estimates. The one that uses only *a-priori* knowledge and the one that uses the numerical solution, the *a-posteriori* estimate.

- *A-priori* estimate: controls the error $\|u - u_h\|_*$ by a quantity that is independent of the numerical solution u_h of (4.5). They have the general form:

  Assume that $u \in \mathcal{X} \subset X$ (extra regularity on u), then

  $$\|u - u_h\|_* \leq C(\Omega, p) h^\alpha \|u\|_{**}, \tag{4.6}$$

  where $\|\cdot\|_{**}$ is the norm in $\mathcal{X}$. Here C is a constant that depends on the domain and on the parameters of the problem (4.4). A typical example is $X = H_0^1(\Omega)$ and $\mathcal{X} = H^2(\Omega) \cap H_0^1(\Omega)$.

  The *a-priori* estimate gives the rate of convergence of numerical solution, $O(h^\alpha)$, with respect to the mesh size. It is useful because it guarantees that refining the mesh the numerical solution will converge to the solution of the problem (4.4). However, the *a-priori* estimates have some drawbacks:

  1. Most of the time we cannot guarantee the extra smoothness assumption $u \in \mathcal{X}$.
  2. The right hand side of (4.6) is not computable since we do not know u.
  3. The right hand side of (4.6) gives a global error estimate. It does not give any information about local behaviour of the error.

- *A-posteriori* estimator: controls the error by a quantity that is a function of the mesh, the parameters P, the numerical solution u_h and the data f. *A-posteriori* estimates have the general form:

  $$\|u - u_h\|_* \leq C(\Omega, p) \eta(u_h, f, f_h, p), \tag{4.7}$$

  where

  $$\eta(u_h, f, f_h, p) = \sum_{T \in \mathcal{T}_h} \eta_T(u_h, f, f_h, p). \tag{4.8}$$

  The advantages of the *a-posteriori* estimates besides being computable is the fact that the error is bounded by the sum over all elements in the partition of local estimators η_T (4.8). This "localization" of the *a-posteriori* estimator provides information about where to refine the mesh, i.e., it guides mesh adaptivity. There

are several types of residual estimators [4]. In Table 4.1 we present a summary of some type of estimators. In this thesis we developed explicit residual *a-posteriori* estimators. Below we give a brief description of the explicit residual estimators.

The explicit estimators are computed directly from the numerical solution without the need to solve any additional problems. Define the residual of problem (3.25), $R : X \to X'$, via

$$\begin{aligned} < R(u_h), \phi > &:= < f, \phi > - \mathcal{Z}(u_h, \phi) \\ &= \mathcal{Z}(u - u_h, \phi). \end{aligned} \tag{4.9}$$

Note that the residual R is a function of the approximated solution u_h, the parameters $\mathcal{P}$ and of Ω. Apply the continuity of form $\mathcal{Z}$:

$$| < R(u_h), \phi > | \leq C_{\mathcal{Z}} \|u - u_h\|_* \|\phi\|_*.$$

Now divide by $\|\phi\|_*$ and take the supremum over all $\phi \in X$

$$\|R(u_h)\|_{X'} \leq \overline{C} \|u - u_h\|_*.$$

On the other hand, let $\phi = u - u_h$ in definition (4.9). Apply the coercivity of $\mathcal{Z}$ to see that

$$\begin{aligned} < R(u_h), u - u_h > &= \mathcal{Z}(u - u_h, u - u_h) \\ &\geq \alpha_{\mathcal{Z}} \|u - u_h\|_*^2. \end{aligned}$$

Thus by the definition of dual norms

$$\|R(u_h)\|_{X'} \geq \underline{C} \|u - u_h\|_*.$$

We conclude that the dual norm of residual R is equivalent to norm of the error. It is not usually clear how to compute the norm $\|R(u_h)\|_{X'}$. Instead, we estimate $\|R(u_h)\|_{X'}$ by a computable quantity η called residual estimator so that

$$C^* \eta \leq \|R(u_h)\|_{X'} \leq C_* \eta, \text{ for some constants } C^*, C_*.$$

Therefore,

$$C_*\eta \leq \|u - u_h\|_* \leq C^*\eta.$$

We emphasize that C^*, C_*, η depend on Ω and P.

Definition 4.2.1. *An a-posteriori error estimator η is said to be reliable if, $\exists C^* > 0$ such that*

$$\|u - u_h\|_* \leq C^*\eta,$$

and it is said to be efficient if, $\exists C_* > 0$ such that

$$C_*\eta \leq \|u - u_h\|_*.$$

The reliability of the estimator allow us to control the error. The efficiency of the estimator guarantees that the error and the estimator are of the same order of convergence. The efficiency guarantees that the mesh is not overly refined.

The residual estimators are reliable. Unfortunately, they are not very efficient, i.e., the gap between the estimator and true error can be substantial even for problems with all parameters set equal to one and simple domains [21]. One way used to quantify the quality of an estimator is through its efficiency index Θ.

Definition 4.2.2. *The efficiency index Θ of an estimator is defined as*

$$\Theta := \frac{\eta}{\|u - u_h\|_*}. \tag{4.10}$$

Ideally, one desires that $\Theta \approx 1$ as the mesh size decreases and such estimators are called asymptotically exact. Most estimators, including the residual-type estimator do not have this property. Other families of estimators [53, 21] are much more efficient and even asymptotically exact but can be cumbersome in implementation and computationally expensive. We will not study these but mention the work of [2, 3] on systems.

Aside of efficiency, the additional difficulty with residual estimators is the dependence of the efficiency constants on the parameters of the problem. This is directly related to dependence of the ellipticity, continuity, and equivalence constants on the parameters.

Table 4.1: List of some *a-posteriori* estimators and their properties [4] for elliptic problems

Name	Description	Properties
Explicit residual	estimates the error by the residual of the numerical approximation	easy to implement
Implicit subdomain residual	estimates the error by solving a Dirichlet problem in a neighborhood of a vertex for every vertex in the mesh grid [9]	very expensive to solve the auxiliary problems in such subdomains
Implicit element residual	estimates the error by solving a Dirichlet problem in a neighborhood of each element or by solving a Neumann problem in each element of the mesh [11]	expensive and most the time the Neumann problem does not have a solution
Recovery-based estimator	estimates the error by post-processing the gradient of the numerical solution u_h [60]	easy to implement, asymptotically exact in special meshes, method fails if the approximation u_h is zero in a neighborhood
Hierarchical estimator	estimates the error using a more accurate numerical solution computed in an enhanced space [24, 10]	works for nonlinear problems, hard to implement
Equilibrated residual	estimates the error by solving an auxiliary problem in each element taking into account the inter-element fluxes [31]	can be used in partitions with hanging nodes, very hard to implement

This issue was brought up in [16, 55] and a remedy involving a particular scaling was proposed; we follow these ideas in this thesis.

Definition 4.2.3. *An estimator is said to be robust if* Θ *is independent of the parameters of the problem and of the partition of the domain.*

The robustness of the estimator depend mainly on the choice of the norm. For elliptic linear problems, the choice of the energy norm seems to work well. In this thesis we use the energy norm for all model problems. Below see an example of the norm influence in the robustness of the residual estimator

Example 4.2.1. *Consider the scalar example*

$$\begin{cases} -\epsilon\Delta u + u = 1, & x \in \Omega = (0,1), \\ u = 0, & x \in \partial\Omega, \end{cases}$$

and its FE approximation.

The variational form of the problem is: Find $u \in H_0^1(\Omega)$ so that

$$a_{EX}(u,v) = \int_\Omega v dx,$$

for all $v \in H_0^1(\Omega)$. Here

$$a_{EX}(u,v) = \int_\Omega \epsilon \nabla u \cdot \nabla v + uv dx.$$

The discrete problem is: Find $u_h \in X_h$ so that:

$$a_{EX}(u_h, v_h) = \int_\Omega v_h dx, \quad \forall v_h \in X_h.$$

Here $X_h \subset H_0^1(\Omega)$ is the space of continuous piecewise linear functions with zero value at the boundary

$$X_h = \{v_h \in C^0(\Omega); \forall K \in \mathcal{T}_h, v_{h|K} \in \mathbb{P}_1, v_h = 0 \text{ on } \partial\Omega\}.$$

We are going to compare the error and the explicit residual estimator using the usual H^1-norm

$$\|u\|_1^2 = \int_\Omega (\nabla u)^2 + u^2 dx,$$

and the energy norm

$$\|u\|_e^2 = a_{EX}(u,u) = \int_\Omega \epsilon(\nabla u)^2 + u^2 dx.$$

We now define the estimators η_1, η_e for the H_0^1-norm and energy norm, respectively. The η_1 estimator can be found in textbooks such as [19] and the η_e estimator can be found in [55]. Define the residuals [19]:

$$R_K(u_h) = \epsilon \Delta u_h - u_h + f, \qquad R_e(u_h) = [\epsilon \partial_n u_h]_e.$$

For the η_e estimator we need to define the scaling constants:

$$\gamma = 2\epsilon^{-1/4}, \qquad \beta = \min\{h_K \epsilon^{-1/2}, 1\}.$$

Define the estimators:

$$\begin{aligned}
\eta_1 &= \left\{ \sum_{K \in \tau_h} \left[h_K^2 \|R_K\|_{0,K}^2 + \frac{1}{2} \sum_{e \subset \partial K} h_e \|R_e\|_{0,e}^2 \right] \right\}^{1/2}, \\
\eta_e &= \left\{ \sum_{K \in \tau_h} \left[\beta^2 \|R_K\|_{0,K}^2 + \beta \sum_{e \subset \partial K} \gamma^2 \|R_e\|_{0,e}^2 \right] \right\}^{1/2}.
\end{aligned}$$

We have that

$$\begin{aligned}
\|u - u_h\|_1 &\leq c(\epsilon)\eta_1, \\
\|u - u_h\|_e &\leq c\eta_e.
\end{aligned}$$

Table 4.2: Comparison of efficiency indices for two different choices of estimators in Example 4.2.1

ϵ	Θ_1	Θ_e
10^{-4}	4.85×10^{-4}	7.63
10^{-2}	4.90×10^{-2}	7.73
1	4.90	7.74
10^{2}	4.90×10^{2}	7.74
10^{4}	4.90×10^{4}	7.74
10^{6}	4.90×10^{6}	7.74

Let us fix a uniform partition of $\Omega = (0, 1)$ with 2560 elements. We vary ϵ and test the behavior of the efficiency indices Θ_1, Θ_e for the two cases. Here

$$\Theta_1 = \frac{\eta_1}{\|u - u_h\|_1}, \qquad \Theta_e = \frac{\eta_e}{\|u - u_h\|_e}.$$

We can see in Table 4.2 how the choice of the appropriate norm can lead to a robust estimator. In this case the estimator proposed in [55] for the energy norm of the problem is robust. Meanwhile the usual explicit estimator for the H_0^1-norm varies with the parameter ϵ of the problem.

For convection-diffusion problems, a robust residual *a-posteriori* estimator was proposed in [54]. Later on, with a better norm choice, an alternative *a-posteriori* error estimator was proposed in [44]. In [44] numerical results were presented demonstrating that their choice of norm yielded more robust estimator that in [54]. This illustrates the importance of choosing the right norm.

For semilinear elliptic equations, a residual *a-posteriori* estimator that takes into consideration the error of solving the nonlinear system using Newton's method is presented in [33]. Also for semilinear elliptic (and convective) equations, a robust residual *a-posteriori* estimator was presented in [54]. In both papers, it is assumed that the semilinear function $\varphi(u)$ is differentiable with respect to the u and that the derivatives are bounded.

Up to know we only discussed *a-posteriori* estimators for elliptic problems. Let us consider a time-dependent problem. The error in a time-dependent problem is composed

of the error in the space discretization and in the time discretization. Along this thesis, we use Galerkin finite element method to discretize in space and implicit Euler to discretize in time. Another approach, used in [25] is to apply Galerkin finite elements continuous in space, discontinuous in time and to compute the *a-posteriori* error estimator by solving an adjoint problem. The same approach as ours can be found in [40, 56, 15] for the scalar linear and quasi-linear heat equation. Here we follow closely [15] and extend the results presented there for a coupled parabolic system with a robust and multilevel estimator.

Now we return to our model problems. The main goal in this thesis is to develop *a-posteriori* residual error estimates for the models so that the estimator is robust and multilevel. From Example 4.2.1 we see what we mean by a robust estimator. Our goal is to construct such an estimator for our model problems by extending the ideas presented in [55]. By multilevel we understand that the unknowns of the model problems (u, v) are approximated by (u_h, v_H) in distinct finite dimensional spaces V_h, V_H. The following example gives a motivation for using multilevel approximation:

Example 4.2.2. *Let $\Omega = (0, 1)$. Consider the LP-model with homogeneous Dirichlet boundary conditions and $\mathcal{P} = \{0.08, 0.7, 0.85, 0.2, 3\}$. Suppose the exact solution is $\vec{u} = (e^{-t}\sin(4\pi x), e^{-2t}(x^2 - x))$. The final time is $T = 2 \times 10^{-3}$. We want the error in the energy norm of the model, $\mathcal{E}_{lp} := [[(u, v) - (u_{h\tau}, v_{H\tau}]](T)$, to be less than a fixed tolerance $\tau = 5 \times 10^{-4}$. The energy norm is defined in* (4.115)*. Denote by RT the run time of the computation in seconds. The results can be seen in Table 4.3 and in Figure 4.2.*

Note that the multilevel approach took 1050 elements while the one-level approach needed 2000 elements to achieve the desired tolerance.

In this Chapter we define residual-type error estimators for the models E and LP and prove the global upper and some lower bounds. The lower bounds, due to the presence of coupling terms, work only if $\mathcal{H}$ are small enough. See Theorem 4.3.5 for a qualification of $\mathcal{H}$ "small enough".

We begin the exposition with the E-model. The reason for that is that, as seen in Section 3.1, after discretization in time, the LP-model gets reduced to a system of E-models. Thus some results we will obtain for the E-model will be useful for the LP-model. Next we present a-priori estimates for the NLP-model and adapt it to the LP, WR, and PP models. To finalize we present the a-posteriori results for the LP-model and adapt it for the WR, PP, and NLP models.

Table 4.3: Comparison of run time and number of elements needed to achieve error below a given tolerance τ using the one-level and the multilevel approaches for Example 4.2.2. The first column in each approach denotes the number of elements in the partition $\mathcal{T}_h$ and $\mathcal{T}_H$, respectively.

One-Level			Multilevel		
$V_h \times V_h$	$\mathcal{E}_{lp}$ (10^{-4})	RT	$V_h \times V_H$	$\mathcal{E}_{lp}$ (10^{-4})	RT
125×125	33.66	7.83	125×25	33.76	6.31
250×250	16.82	16.38	250×25	17.02	12.37
500×500	8.41	36.34	500×25	8.81	24.88
1000×1000	4.21	84.10	1000×50	4.28	52.48
2000×2000	2.12	214.73	2000×100	2.14	114.70
2000 elements			1050 elements		

Figure 4.2: Comparison of run time for one-level and multilevel for Example 4.2.2

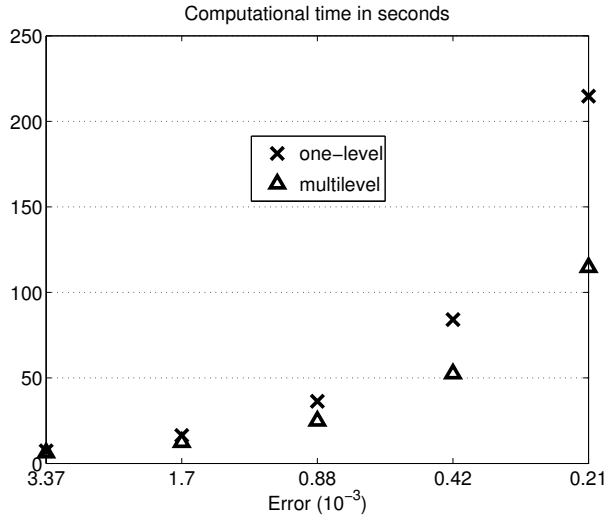

4.3 E-model

Here we first develop estimators for both components of the system (3.25) and later an additional estimator for the error in one component only. We follow standard techniques for residual estimators [53] which for scalar diffusion problems and the error in energy norm involves the following steps. First rewrite the energy norm of the error $(u-u_h, v-v_H)$ using Galerkin orthogonality (4.16) with an auxiliary function $(z_h, w_H) \in V_h \times V_H$, and localize the error by integrating by parts over each element $T \in \mathcal{T}_h$, $K \in \mathcal{T}_H$. Thereby the error terms per element and per element boundary are identified; this follows from integration by parts elementwise. The integration by parts will contain terms with $\Delta u_h|_T, \Delta v_H|_K$. Note that for $k = 1$, both these terms vanish. To keep the calculations general we will keep them in the equations.

The proof of the upper bound is lengthy but not very complicated as it extends the standard techniques to a system, and involves handling the coupling terms. The lower bound is more delicate to obtain; we develop a global lower bound which is valid for fine enough $\mathcal{H}$, and a local lower bound in $\mathcal{T}_H$. Finally, we develop a bound for the error in one component only.

The discrete form of (3.25) reads:

Find $(u_h, v_H) \in V_h \times V_H$ *such that, for all* $(\phi_h, \psi_H) \in V_h \times V_H$,

$$(\lambda_1 u_h, \phi_h) + (a\nabla u_h, \nabla \phi_h) + (c(u_h - \Pi v_H), \phi_h) = (f, \phi_h), \tag{4.11a}$$

$$(\lambda_2 v_H, \psi_H) + (b\nabla v_H, \nabla \psi_H) + (c(\Pi'\Pi v_H - \Pi' u_h), \psi_H) = (g, \psi_H). \tag{4.11b}$$

We assume that Assumptions 3.2.14 hold.

Define the bilinear form

$$\begin{aligned} \tilde{A}((u_h, v_H), (\phi_h, \psi_H)) \;&:=\; (\lambda_1 u_h, \phi_h) + (\lambda_2, v_H \psi_H) + (a\nabla u_h, \cdot \nabla \phi_h) \\ &+\; (b\nabla v_H, \cdot \nabla \psi_H) + (c(u_h - \Pi v_H), \phi_h) + \left(c(\Pi'\Pi v_H - \Pi' u_h), \psi_H\right). \end{aligned} \tag{4.12}$$

Note that $\tilde{A}(\cdot,\cdot)$ is a restriction of $A(\cdot,\cdot)$ to $V_h \times V_H$. It follows from Lemma 3.2.2 that $\tilde{A}(\cdot,\cdot)$ is continuous and coercive on $V_h \times V_H$. Now we rewrite the weak form (4.11) as:

Find $(u_h, v_H) \in V_h \times V_H$ *so that, for all* $(\phi_h, \psi_H) \in V_h \times V_H$

$$\tilde{A}((u_h, v_H), (\phi_h, \psi_H)) = L((\phi_h, \psi_H)),\ \forall (\phi_h, \psi_H) \in V_h \times V_H. \tag{4.13}$$

The problem (4.13) is square and finite dimensional. By Lemma 3.2.3 and the fact that $\tilde{A} = A|_{V_h \times V_H}$ it is easy to see that its solution exists and is unique.

4.3.1 *A-priori* error estimates for the E-model

The error estimates are with respect to the energy norm defined in (3.29)

$$\|\vec{u}\|_e^2 := \|\lambda_1^{1/2} u\|^2 + \|\lambda_2^{1/2} v\|^2 + \|a^{1/2}\nabla u\|^2 + \|b^{1/2}\nabla v\|^2 + \|c^{1/2}(u-v)\|^2.$$

Remark 4.3.1. *The norms $\|\cdot\|_{V^2}, \|\cdot\|_e$ are equivalent and the equivalence constants depend on $\mathcal{P}$.*

For the error analysis of (4.13) we first develop the counterpart of Galerkin orthogonality. Thanks to our definition of Π, Π', the calculations follows smoothly without additional consistency errors.

Notation. *To simplify the exposition, let*

$$e_{u,h} := u - u_h, \tag{4.14}$$

$$e_{v,H} := v - v_H. \tag{4.15}$$

Let $\phi = \phi_h$ and $\psi = \psi_H$ in (3.31) and subtract it from (4.13) to get

$$\begin{aligned} 0 &= A((u,\phi_h),(v,\psi_H)) - \tilde{A}((u_h,\phi_h),(v_H,\psi_H)) \\ &= A((u,\phi_h),(v,\psi_H)) - A((u_h,\phi_h),(v_H,\psi_H)) \\ &- \int_\Omega c(v_H - \Pi v_H)\phi_h - \int_\Omega c(u_h - \Pi' u_h)\psi_H \\ &= A((e_{u,h},\phi_h),(e_{v,H},\psi_H)) - \int_\Omega c(v_H - \Pi v_H)\phi_h + \int_\Omega c(u_h - \Pi' u_h)\psi_H. \end{aligned}$$

Now, if $\mathcal{T}_h$ is a refinement of $\mathcal{T}_H$, then by Lemma 4.1.1 the last two terms vanish and we obtain the Galerkin orthogonality

$$A((e_{u,h},\phi_h),(e_{v,H},\psi_H)) = 0, \;\; \forall (\phi_h,\psi_H) \in V_h \times V_H. \tag{4.16}$$

This is a basic step in proving convergence of the scheme in the energy norm $\|\cdot\|_e$ and of the subsequent a-posteriori estimates.

Theorem 4.3.1. *Assume that the solution $\vec{u} \in V^2$ of the problem (3.25) satisfies $\vec{u} \in \big(H^2(\Omega) \cap H_0^1(\Omega)\big) \times \big(H^2(\Omega) \cap H_0^1(\Omega)\big)$. Assume also that $\mathcal{T}_h$ is a refinement of $\mathcal{T}_H$, $k = 1$, and let $(u_h, v_H) \in V_h \times V_H$ be the two-level solution of the discrete problem (4.11). Then there exist constants κ_1, κ_2 independent of $\mathcal{H}$ and of u, v, such that*

$$\|(u - u_h, v - v_H)\|_e \leq \kappa_1 h \|u\|_2 + \kappa_2 H \|v\|_2. \tag{4.17}$$

Proof. Consider the following calculation, similar to the derivation of Céa's lemma in the scalar case [22, 19]. For an arbitrary $(z_h, w_H) \in V_h \times V_H$ it follows by (4.16) that

$$\begin{aligned} \|(e_{u,h}, e_{v,H})\|_e^2 &= A((e_{u,h}, e_{u,h}), (e_{v,H}, e_{v,H})) \\ &= A((e_{u,h}, e_{u,h}), (e_{v,H}, e_{v,H})) + A(e_{u,h}, u_h - z_h), (e_{v,H}, v_H - w_H)) \\ &= A((e_{u,h}, u - z_h), (e_{v,H}, v - w_H)). \end{aligned}$$

We bound this last term from above and from below using, respectively, continuity and coercivity of $A(\cdot, \cdot)$ in the energy norm. Dividing both sides of the resulting inequality by $\|(e_{u,h}, e_{v,H})\|_e$ yields the standard estimate. Now, since z_h, w_H are arbitrary, we take the infimum to get

$$\|(e_{u,h}, e_{v,H})\|_e \leq C \inf_{(z_h, w_H) \in V_h \times V_H} \|(u - z_h, v - w_H)\|_e, \tag{4.18}$$

where C is a ratio of continuity and coercivity constants. To get the desired convergence estimates, we select the test functions to be the piecewise linear interpolations $(z_h, w_H) = (I_h u, I_H v)$ of the respective components of the analytical solution and set $z = u - I_h u$ and $w = v - I_H v$. Now we have

$$\begin{aligned} \|(e_{u,h}, e_{v,H})\|_e &\leq C \|(z, w)\|_e \\ &= C \left[\int_\Omega (\lambda_1 z^2 + \lambda_2 w^2) + \int_\Omega (a(\nabla z)^2 + b(\nabla w)^2) + \int_\Omega c(z - w)^2 \right] \\ &\leq C \left[\int_\Omega ((\lambda_1 + 2c) z^2 + (\lambda_2 + 2c) w^2) + \int_\Omega (a(\nabla z)^2 + b(\nabla w)^2) \right] \\ &\leq C \left[\max\{a, \lambda_1 + 2c\} \|z\|_1^2 + \max\{b, \lambda_2 + 2c\} \|w\|_1^2 \right] \end{aligned}$$

The interpolation theory [22, 19] lets us bound the interpolation error $\xi - I_h\xi$ for a smooth enough ξ. For $k = 1$ we have as follows

$$\|\xi - I_h\xi\|_m \leq \tilde{c}h^{2-m}|\xi|_{t,\Omega} \quad \text{for} \quad \xi \in H^t(\Omega), \quad 0 \leq m \leq 2.$$

Applying this bound to z and w we get

$$\begin{aligned} \|(e_{u,h}, e_{v,H})\|_e^2 &\leq \max\{a, \lambda_1 + 2c\}\|u - I_h u\|_1^2 + \max\{b, \lambda_2 + 2c\}\|v - I_H v\|_1^2 \\ &\leq C\max\{a, \lambda_1 + 2c\}\tilde{c}^2h^2|u|_2^2 + C\max\{b, \lambda_2 + 2c)\}\tilde{c}^2H^2|v|_2^2. \end{aligned}$$

Taking square root of both sides completes the proof. □

This a-priori result shows the structure of the error. First, if $\mathcal{T}_h = \mathcal{T}_H$, then the error converges with the rate $O(h)$, and an easy extension can be formulated for $k > 1$. If $\mathcal{T}_h \neq \mathcal{T}_H$, then the error in (4.17) is dominated asymptotically by the $O(H)$ terms, at least for $\mathcal{P} = \mathbf{1}^5$. For general $\mathcal{P}$ the individual contributions to the error depend on $\mathcal{P}$. The magnitude of each of the contributions depends on $\mathcal{P}$ and on the variability of u, v. Thus H and h could be adapted to take advantage of this potential disparity.

For example, if $c = O(1)$ is moderate, and $a >> 1$ very large but $b << 1$ very small, one can find $\mathcal{T}_H$ for the component v so that the total error does not increase substantially. Note that with $H > h$ the total number of unknowns decreases. We would proceed similarly if $b = O(1)$ but $|v|_2$ is very small. Conversely, if the error on some coarse grid used for both components is too large for our needs, then one could refine only the grid for the strongly varying component, for example u, for which $|u|_2$ is large. See Section (some examples) for relevant examples.

To guide the adaptive choice of h, H, i.e., of $\mathcal{T}_h, \mathcal{T}_H$, we need the a-posteriori error analysis provided in the next Section.

4.3.2 *A-posteriori* error estimates for the E-model

To develop the *a-posteriori* estimates we make the stronger assumptions than Assumptions 3.2.14 for the parameters and data.

Assumptions 4.3.2.

DA1. Each function in $\mathcal{P} = \{\lambda_1, \lambda_2, a, b, c\}$ *is a positive constant.*

DA2. The data $(f, g) \in L^2(\Omega) \times L^2(\Omega)$.

Our initial goal was to assume that each function in $\mathcal{P} = \{\lambda_1, \lambda_2, a, b, c\}$ to be piecewise constant and to extend the results presented in [16]. The problem treated in [16] is the Poisson problem that do not include zero order terms of the unknowns. The presence of the zero order terms on the system for the E-model complicates the extensions and the results for the extension are not presented here. Besides that, we do apply our *a-posteriori* estimates for piecewise constant parameters with success, as is shown in Chapter 5.

4.3.2.1 Residual calculations

Let $Q_h : V \to V_h, Q_H : V \mapsto V_H$ be some maps to be made precise later. Using (4.16)

$$\begin{aligned} \|(e_{u,h}, e_{v,H})\|_e^2 &= A((e_{u,h}, e_{v,H}), (e_{u,h}, e_{v,H})) \\ &= A((e_{u,h}, e_{v,H}), (e_{u,h} - Q_h e_{u,h}, e_{v,H} - Q_H e_{v,H})). \end{aligned}$$

Now we follow the standard procedure for residual calculations. We rewrite the last term $A((e_{u,h}, e_{v,H}), (\phi, \psi))$ with $\phi = e_{u,h} - Q_h e_{u,h}$, $\psi = e_{v,H} - Q_H e_{v,H}$, replacing $\int_\Omega$ by $\sum_T \int_T$, taking advantage of (3.25a)-(3.25b) and the continuity of u, v, ψ, ϕ across each edge and integrating by parts on each element T. As before, our calculations work for a general $k \geq 1$. We obtain

$$
\begin{aligned}
A((e_{u,h}, e_{v,H}), (\phi, \psi)) &= \sum_T \Big\{ \int_T (\lambda_1 e_{u,h}\phi + \lambda_2 e_{v,H}\psi + (c(e_{u,h} - e_{v,H})(\phi - \psi)) \\
&\quad - \int_T (a\Delta e_{u,h}\phi + b\Delta e_{v,H}\psi) + \int_{\partial T} (a\partial_n e_{u,h}\phi + b\partial_n e_{v,H}\psi) \Big\} \\
&= \sum_T \int_T (\lambda_1 u\phi + \lambda_2 v\psi + c(u - v)(\phi - \psi) - a\Delta u\phi - b\Delta v\psi \\
&\quad - \sum_T \int_T (\lambda_1 u_h\phi + \lambda_2 v_H\psi + c(u_h - v_H)(\phi - \psi) \\
&\quad - a\Delta u_h\phi - b\Delta v_H\psi) \\
&\quad + \sum_E \int_E ([a\partial_n(u - u_h)]\phi + [b\partial_n(v - v_H)]\psi) \\
&= \sum_T \int_T (f\phi + g\psi) \\
&\quad + \sum_T \int_T [-\lambda_1 u_h\phi - \lambda_2 v_H\psi - c(u_h - v_H)(\phi - \psi) \\
&\quad + \sum_E \int_E ([a\partial_n u_h]\phi + [b\partial_n v_H]\psi \Big] .
\end{aligned}
$$

Combining the terms we get

$$
\begin{aligned}
\|(e_{u,h}, e_{v,H})\|_e^2 &= \sum_{T \in \mathcal{T}_h} (R^*_{T,u}, e_{u,h} - Q_h e_{u,h})_T + \sum_{E \in \mathcal{E}_h} (R_{E,u}, e_{u,h} - Q_h e_{u,h})_E \qquad (4.19) \\
&\quad + \sum_{K \in \mathcal{T}_H} (R^*_{K,v}, e_{v,H} - Q_H e_{v,H})_K + \sum_{F \in \mathcal{E}_H} (R_{F,v}, e_{v,H} - Q_H e_{v,H})_F,
\end{aligned}
$$

where we have used the element and edge residual terms defined as follows

$$\begin{aligned}
R^*_{T,u} &:= f - \lambda_1 u_h + a\Delta u_h - c(u_h - v_H) \\
&= f - f_h + \overbrace{f_h - \lambda_1 u_h + a\Delta u_h - c(u_h - v_H)}^{R_{T,u}}, \\
R^*_{K,v} &:= g - \lambda_2 v_H + b\Delta v_H - c(v_H - u_h) \\
&= g - g_H + \overbrace{g_H - \lambda_2 v_H + b\Delta v_H - c(v_H - u_h)}^{R_{K,v}} \\
R_{E,u} &:= [a\partial_n u_h]_E, \\
R_{F,v} &:= [b\partial_n v_H]_F,
\end{aligned}$$

and where f_h, g_H are the L_2-projections of f, g onto V_h, V_H respectively.

Now we estimate the terms in (4.19) by Cauchy-Schwarz inequality to obtain

$$\begin{aligned}
\|(e_{u,h}, e_{v,H})\|_e^2 \;\leq\; & \sum_{T\in\mathcal{T}_h} \|R^*_{T,u}\|_T \|e_{u,h} - Q_h e_{u,h}\|_T + \sum_{E\subset\mathcal{E}_h} \|R_{E,u}\|_E \|e_{u,h} - Q_h e_{u,h}\|_E \\
& + \sum_{K\in\mathcal{T}_H} \|R^*_{K,v}\|_{0,K} \|e_{v,H} - Q_H e_{v,H}\|_K \\
& + \sum_{F\subset\mathcal{E}_H} \|R_{F,v}\|_F \|e_{v,H} - Q_H e_{v,H}\|_F. \qquad (4.20)
\end{aligned}$$

Consider $e_{u,h} - Q_h e_{u,h}$. The idea is to bound the terms $e_{u,h} - Q_h e_{u,h}$ from above by the terms involving the energy norm of $e_{u,h}$, without requiring more smoothness than that $e_{u,h} \in V$; then the estimate for $\|(e_{u,h}, e_{v,H})\|_e$ will follow.

Such estimates are available for various quasi-interpolators [23, 53]. We use the definition and properties of Q_h as modified by Verfürth [53] and quote two basic relevant interpolation estimates which work in any $T \in \mathcal{T}_h$ and any $E \in \mathcal{E}_h$.

The first result ([55], Lemma 3.1) states;

Lemma 4.3.1. *For any $w \in H^k(\tilde{\omega}_T), 0 \leq k \leq 1$*

$$\|\nabla^l (w - Q_h w)\|_T \leq C h_T^{k-l} \|\nabla^k w\|_{\tilde{\omega}_T} \; 0 \leq l \leq k \leq 1, \qquad (4.21)$$

where the constant C is independent of h, w.

This inequality is due to Clément [23].

Next, we quote ([54], Lemma 3.1) to estimate the edge terms.

Lemma 4.3.2. *Let $E \in \mathcal{E}_h$ and let T be an element in $\mathcal{T}_h$ which has E as an edge. The following trace inequality holds for all $w \in H^1(T)$*

$$\|w\|_E \leq c_3 \left(h_T^{-1/2} \|w\|_T + \|w\|_T^{1/2} \|\nabla w\|_T^{1/2} \right), \tag{4.22}$$

where c_3 is a constant independent of w, h_T.

4.3.2.2 Interpolation and scaling techniques

To derive the estimates in the energy norm we find that they involve various equivalence constants dependent on $\mathcal{P}$ between $\|\cdot\|_{V^2}, \|\cdot\|_e$. To prevent the estimates from blowing up when the parameters of the problem change, we define certain scaling factors following [55, 54, 43].

Define for all $T \in \mathcal{T}_h$ and all $K \in \mathcal{T}_H$

$$\begin{aligned}
\theta_{u,T} &:= \min\{h_T a^{-1/2}, \lambda_1^{-1/2}\}, && (4.23)\\
\theta_{v,K} &:= \min\{H_K b^{-1/2}, \lambda_2^{-1/2}\}, && (4.24)\\
\gamma_{u,E} &:= a^{-1/4} \theta_{u,E}^{1/2}, && (4.25)\\
\gamma_{v,F} &:= b^{-1/4} \theta_{v,F}^{1/2}. && (4.26)
\end{aligned}$$

Let $T \in \mathcal{T}_h$ and $K \in \mathcal{T}_H$. Clearly $e_{u,h} \in H^1(\tilde{\omega}_T)$ and $e_{v,H} \in H^1(\tilde{\omega}_K)$. By (4.21)

$$\begin{aligned}
\|e_{u,h} - Q_h e_{u,h}\|_T &\leq C\lambda_1^{-1/2} \|\lambda_1 e_{u,h}\|_{\tilde{\omega}_T} \\
&\leq C\lambda_1^{-1/2} \left\{ \int_{\tilde{\omega}_T} a(\nabla e_{u,h})^2 + \lambda_1 e_{u,h}^2 \right\}^{1/2}, \\
\|e_{u,h} - Q_h e_{u,h}\|_T &\leq C h_T a^{-1/2} \left\{ \int_{\tilde{\omega}_T} a(\nabla e_{u,h})^2 + \lambda_1 e_{u,h}^2 \right\}^{1/2}.
\end{aligned}$$

We combine these and (4.23) to get

$$\|e_{u,h} - Q_h e_{u,h}\|_T \leq C \min\left\{ \lambda_1^{-1/2}, h_T a^{-1/2} \right\} \left\{ \int_{\tilde{\omega}_T} a(\nabla e_{u,h})^2 + \lambda_1 e_{u,h}^2 \right\}^{1/2}. \tag{4.27}$$

Similar calculations can be done for $e_{v,H}$, and it follows that we have

$$\|e_{u,h} - Q_h e_{u,h}\|_T \leq c_1 \theta_{u,T} \left\{ \int_{\tilde{\omega}_T} a(\nabla e_{u,h})^2 + \lambda_1 e_{u,h}^2 \right\}^{1/2}, \tag{4.28}$$

$$\|e_{v,H} - Q_H e_{v,H}\|_K \leq c_2 \theta_{v,K} \left\{ \int_{\tilde{\omega}_K} b(\nabla e_{v,H})^2 + \lambda_2 e_{v,H}^2 \right\}^{1/2}, \tag{4.29}$$

where c_1, c_2 are independent of $\mathcal{P}, \mathcal{H}$.

On the edges the calculations are a bit longer. Apply (4.22) to $w = e_{u,h} - Q_h e_{u,h}$

$$\begin{aligned} \|e_{u,h} - Q_h e_{u,h}\|_E \leq\ & c_3 \Big(h_T^{-1/2} \|e_{u,h} - Q_h e_{u,h}\|_T \\ & + \|e_{u,h} - Q_h e_{u,h}\|_T^{1/2} \|\nabla (e_{u,h} - Q_h e_{u,h})\|_T^{1/2} \Big). \end{aligned}$$

Next, apply (4.21) to get

$$\|\nabla (e_{u,h} - Q_h e_{u,h})\|_T^{1/2} \leq a^{-1/4} \|a^{1/2} \nabla e_{u,h}\|_{\tilde{\omega}_T}^{1/2} \leq a^{-1/4} \left\{ \int_{\tilde{\omega}_T} a(\nabla e_{u,h})^2 + \lambda_1 e_{u,h}^2 \right\}^{1/4}.$$

Using (4.28) and noticing $h_T^{-1/2} \theta_{u,T}^{1/2} + a^{-1/4} \leq 2a^{-1/4}$ we get

$$\begin{aligned} \|e_{u,h} - Q_h e_{u,h}\|_E \leq c_4 \Bigg(& h_T^{-1/2} \theta_{u,T} \left\{ \int_{\tilde{\omega}_T} a(\nabla e_{u,h})^2 + \lambda_1 e_{u,h}^2 \right\}^{1/2} \\ & + \theta_{u,T}^{1/2} a^{-1/4} \left\{ \int_{\tilde{\omega}_T} a(\nabla e_{u,h})^2 + \lambda_1 e_{u,h}^2 \right\}^{1/2} \Bigg), \end{aligned}$$

and conclude

$$\|e_{u,h} - Q_h e_{u,h}\|_E \leq c_4 \gamma_{u,E} \left\{ \int_{\tilde{\omega}_T} a(\nabla e_{u,h})^2 + \lambda_1 e_{u,h}^2 \right\}^{1/2}. \tag{4.30}$$

Similar estimates follow for the edges $F \in \mathcal{E}_H$

$$\|e_{v,H} - Q_H e_{v,H}\|_F \leq c_5 \gamma_{v,F} \left\{ \int_{\tilde{\omega}_K} b(\nabla e_{v,H})^2 + \lambda_2 e_{v,H}^2 \right\}^{1/2}, \tag{4.31}$$

where c_4, c_5 are independent of $\mathcal{P}, \mathcal{H}$.

4.3.2.3 Upper bound

Now we define the local component error estimators

$$\eta_{u,T} := \theta_{u,T}^2 \|R_{T,u}\|_T^2 + \frac{1}{2} \sum_{E \subset \partial T} \gamma_{u,T}^2 \|R_{E,u}\|_E^2, \tag{4.32}$$

$$\eta_{v,K} := \theta_{v,K}^2 \|R_{K,v}\|_K^2 + \frac{1}{2} \sum_{F \subset \partial K} \gamma_{v,K}^2 \|R_{F,v}\|_F^2, \tag{4.33}$$

and the global error estimator for the error in both variables (u, v)

$$\eta_e := \left\{ \sum_{T \in \mathcal{T}_h} \eta_{u,T} + \sum_{K \in \mathcal{T}_H} \eta_{v,K} \right\}^{1/2}. \tag{4.34}$$

Remark 4.3.2. *For $d = 1$, let z_h, z_H be the set of internal nodes of $\mathcal{T}_h, \mathcal{T}_H$, respectively. Then*

$$\eta_{u,T} := \theta_{u,T}^2 \|R_{T,u}\|_T^2 + \sum_{z \in z_h} \gamma_{u,T}^2 [u_h'(z)]^2, \tag{4.35}$$

$$\eta_{v,K} := \theta_{v,K}^2 \|R_{K,v}\|_K^2 + \sum_{z \in z_H} \gamma_{v,K}^2 [v_H'(z)]^2, \tag{4.36}$$

where $[u_h'(z)] := \lim_{\varepsilon \to 0} u_h'(z + \varepsilon) - u_h'(z - \varepsilon)$ is the jump of the derivatives along the nodes of the mesh.

We recognize the two parts of each local component error estimator (4.32), (4.33) as the terms which arise on the right hand side of (4.20). They are multiplied by factors which have been estimated in (4.69)–(4.72). Taking all these into account along with an additional application of the discrete Cauchy-Schwarz inequality yields finally our main result on the upper bound.

Definition 4.3.3. *We denote*

$$\mathcal{E}_e := \|(e_{u,h}, e_{v,H})\|_e. \tag{4.37}$$

Theorem 4.3.4. *Let the assumptions of Theorem 4.3.1 hold and in particular, let (u, v) be the unique solution of (3.25) and (u_h, v_H) be the unique solution of (4.11). The*

following upper bound holds

$$\mathcal{E}_e \leq C^* \eta_e + \left\{ \sum_{T \in \mathcal{T}_h} \theta_{u,T}^2 \|f - f_h\|_{0,T}^2 + \sum_{K \in \mathcal{T}_H} \theta_{v,K}^2 \|g - g_H\|_{0,T}^2 \right\}^{1/2},$$

where C^* does not depend on $\mathcal{H}$, $\mathcal{P}$, or u, v.

In [2, 3], an asymptotically exact *a-posteriori* error estimator for a coupled elliptic system was developed. However this estimator is of the element residual type that estimates the error by solving an auxiliary problem in the neighborhood of each element in the grid (see Table 4.1). This method is more computationally expensive that the explicit residual estimator we present in this thesis. Besides that, the multilevel grid and robustness of the estimator were not taken into account in the results presented in [2, 3].

4.3.2.4 Lower bound

In this section we want to establish the global lower bound i.e. $C_* \eta_e \leq \mathcal{E}_e$, and some appropriate local counterpart, with some constant C_* independent of $\mathcal{H}, \mathcal{P}, u, v$. Due to the coupling terms in our system this is not possible without additional assumptions.

To establish the result, we proceed using the standard approach of bubble functions [53]. Let $T \in \mathcal{T}_h$ be fixed and denote by $\mathcal{N}_T$ the set of its vertices. For $x \in \mathcal{N}_T$ denote by λ_x the nodal basis function from V_h associated with the point x. Define the element bubble $\Psi_T = \Gamma_T \prod_{x \in \mathcal{N}_T} \lambda_x$ where the constant Γ_T is chosen so that Ψ_T equals 1 at the barycenter of T. Now let $E \in \mathcal{E}_h$ and denote by $\mathcal{N}_E$ the set of all vertices of the edge E and define the edge bubble function $\Psi_E = \Gamma_E \prod_{x \in \mathcal{N}_e} \lambda_x$ where the constant Γ_E is chosen so that Ψ_E equals 1 at the barycenter of E.

The element and edge bubbles have the following properties shown in ([55], Lemma 3.3), with generic constants depending only on the shape of the elements; these constants are different from those in Section 4.3.2.3. Let $T \in \mathcal{T}_h, E \in \mathcal{E}_h$ and let $w \in \mathcal{P}_1(T)$,

$\sigma \in \mathcal{P}_1(E)$ be arbitrary. We have

$$\begin{aligned} \|\Psi_T\|_\infty &\leq 1, && (4.38)\\ c_1\|w\|_T^2 &\leq (w, \Psi_T w)_T, && (4.39)\\ \|\nabla\Psi_T w\|_T &\leq c_2 h_T^{-1}\|w\|_T, && (4.40)\\ c_3\|\sigma\|_E^2 &\leq (\sigma, \Psi_E\sigma)_E && (4.41)\\ \|\nabla\Psi_E\sigma\|_T &\leq c_4 h_E^{-1/2}\|\sigma\|_E, && (4.42)\\ \|\Psi_E\sigma\|_{\omega_E} &\leq c_5 h_E^{1/2}\|\sigma\|_E. && (4.43) \end{aligned}$$

Now we fix an element T, define $\rho_T := \Psi_T R_{T,u}$, and estimate $R_{T,u}$ from above in the goal to isolate the coupling terms and to get the bounds in terms of the energy norm of the error.

$$\begin{aligned} \|R_{T,u}\|_{0,T}^2 &= \|(f_h + \nabla(a\nabla u_h) - (\lambda_1 + c)u_h + cv_H)\|_{0,T}^2 && (4.44)\\ &\overset{(4.40)}{\leq} c_1^{-2}\int_T (f_h + a\Delta u_h - (\lambda_1 + c)u_h + cv_H)\rho_T \\ &= c_1^{-2}\left[\int_T (f_h + a\Delta u_h - (\lambda_1 + c)u_h + cv_H)\rho_T + \int_T f\rho_T - \int_T f\rho_T\right]. \end{aligned}$$

Next we integrate by parts over T, use the strong form of (2.1a), i.e., $f = \lambda_1 u - a\Delta u + c(u - v)$, and the fact that $\rho_T|_{\partial T} \equiv 0$ to see from (4.44) that

$$\begin{aligned} \|R_{T,u}\|_T^2 &= c_1^{-2}\left[\int_T (a\nabla(u - u_h)\cdot\nabla\rho_T \right. && (4.45)\\ &\qquad \left. + [(\lambda_1 + c)(u - u_h) - c(v - v_H)]\,\rho_T + \int_T (f_h - f)\rho_T\right] \end{aligned}$$

Now we estimate both integrals using Cauchy-Schwarz inequality. For the second integral in (4.45) we have, using (4.38) and Cauchy-Schwarz again

$$\int_T (f_h - f)\rho_T \leq \|f_h - f\|_{0,T}\|\rho_T\|_{0,T} \leq \|f_h - f\|_{0,T}\|R_{T,u}\|_{0,T}. \tag{4.46}$$

The bounds for the first integral in (4.45) involve $\int_T (c(u-u_h)-c(v-v_H))\rho_T = \int_T \frac{c}{2}(e_{u,h}-e_{v,H})2\rho_T$ leading to, by a multiple application of Cauchy-Schwarz to the upper bound

for that term, to the expression

$$\left\{\int_T (a(\nabla e_{u,h})^2 + \lambda_1 e_{u,h}^2 + \frac{c}{2}(e_{u,h} - e_{v,H})^2\right\}^{1/2} \left\{\int_T a(\nabla \rho_T)^2 + (\lambda_1 + 2c)\rho_T^2\right\}^{1/2}.$$

To estimate the second term in this expression from above by a multiple of $\|R_{T,u}\|_{0,T}$, we first observe that by (4.23)

$$h_T^{-2} a + \lambda_1 \leq 2\max\{a h_T^{-2}, \lambda_1\} = \theta_{u,T}^{-2}. \tag{4.47}$$

Next, applying (4.40), (4.38), followed by (4.47) we estimate

$$\begin{aligned}
\left\{\int_T a(\nabla \rho_T)^2 + (\lambda_1 + 2c)\rho_T^2\right\}^{1/2} &\leq a^{1/2}\|\nabla \rho_T\|_T + (\lambda_1 + 2c)^{1/2}\|\rho_T\|_T \\
&\leq a^{1/2} c_2 h_T^{-1}\|R_{T,u}\|_T + (\lambda_1 + 2c)^{1/2}\|R_{T,u}\|_T \\
&\leq \bar{c}_2(2\max\{a^{1/2}h_T^{-1}, \lambda_1^{1/2}\} + (2c)^{1/2})\|R_{T,u}\|_T \\
&\leq \bar{c}_2(\theta_{u,T}^{-1} + c^{1/2})\|R_{T,u}\|_T.
\end{aligned}$$

Here $\bar{c}_2 = \max\{c_2, 1\}$. Now we combine the estimates following (4.45) to get, upon dividing by $\|R_{T,u}\|_T$

$$\begin{aligned}
\|R_{T,u}\|_T \leq\ & c_1^{-2}\left[\bar{c}_2(\theta_{u,T}^{-1} + c^{1/2})\left\{\int_T a(\nabla e_{u,h})^2 + \lambda_1 (e_{u,h})^2 + \frac{c}{2}(e_{u,h} - e_{v,H})^2\right\}^{1/2}\right. \\
&\left. + \|f_h - f\|_{0,T}\right]. \qquad (4.48)
\end{aligned}$$

Multiplying both sides by $\bar{\theta}_{u,T} := (\theta_{u,T}^{-1} + c^{1/2})^{-1}$ we finally obtain

$$\begin{aligned}
\bar{\theta}_{u,T}\|R_{T,u}\|_{0,T} \leq\ & c_1^{-2}\left[\bar{c}_2\left\{\int_T a(\nabla e_{u,h})^2 + \lambda_1 (e_{u,h})^2 + \frac{c}{2}(e_{u,h} - e_{v,H})^2\right\}^{1/2}\right. \\
&\left. + \bar{\theta}_{u,T}\|f_h - f\|_{0,T}\right].
\end{aligned}$$

Next we estimate the edge residuals. Consider an arbitrary edge $E \in \mathcal{E}_h$ and denote by T_1, T_2 the two elements that it separates. Let $\rho_E := \beta \Psi_E [a\partial_n u_h]_E = \beta \Psi_E R_{E,u}$ with some scaling factor $0 < \beta \leq 1$ to be determined later as in [55]. We will estimate

$\|R_{E,u}\|_{0,E}$ from above using steps similar to those above: adding and subtracting terms and integrating by parts over $T_1 \cup T_2$ and taking advantage of (2.1a) and of the bubbles ω_E vanishing conveniently at all edges of $T_1 \cup T_2$ other than E, and estimating by Cauchy-Schwarz inequality

$$\begin{aligned}
\|R_{E,u}\|_{0,E}^2 &= \|[a\partial_n u_h]_E\|_{0,E}^2 \le c_3^{-2} \int_E [a\partial_n u_h]_E \rho_E \\
&= c_3^{-2} \left[\int_{T_1\cup T_2} a\Delta u_h \rho_E + \int_{T_1\cup T_2} a\nabla u_h \nabla \rho_E + \int_{T_1\cup T_2} f\rho_E - \int_{T_1\cup T_2} f\rho_E \right] \\
&\overset{(2.1a)}{=} c_3^{-2} \left[\int_{T_1\cup T_2} (f + a\Delta u_h)\rho_E - \int_{T_1\cup T_2} a\nabla e_{u,h}\nabla\rho_E + (\lambda_1 u + c(u-v))\rho_E \right] \\
&= c_3^{-2} \left[\int_{T_1\cup T_2} (f_h + a\Delta u_h - \lambda_1 u_h + c(u_h - v_H))\,\rho_E + \int_{T_1\cup T_2} (f - f_h)\rho_E \right. \\
&- \left. \int_{T_1\cup T_2} a\nabla e_{u,h}\nabla\rho_E + (\lambda_1 e_{u,h} + c(e_{u,h} - e_{v,H})\rho_E \right] \\
&\le c_3^{-2} \sum_{i=1}^{2} [\ \|R_{T,u}\|_{0,T_i}\|\rho_E\|_{0,T_i} + \|(f-f_h)\|_{0,T_i}\|\rho_E\|_{0,T_i} \\
&+ \left\{ \int_{T_i} a(\nabla e_{u,h})^2 + \lambda_1 e_{u,h}^2 + \frac{c}{2}(e_{u,h} - e_{v,H})^2 \right\}^{1/2} \\
&\quad \left\{ \int_{T_i} a(\nabla\rho_E)^2 + (\lambda_1 + 2c)\rho_E \right\}^{1/2} \Bigg] .
\end{aligned}$$

In the last inequality we need to bound $\|\rho_E\|_{0,Ti}$ and $\left\{\int_{T_i} a(\nabla\rho_E)^2 + (\lambda_1+2c)\rho_E\right\}^{1/2}$ in terms of the edge residuals. We have

$$\|\rho_E\|_{0,Ti} = \|\beta\Psi_E R_{E,u}\|_{0,T_i} \le c_5 \beta h_E^{1/2} \|R_{E,u}\|_{0,E}.$$

Also, by (4.42) and (4.43)

$$\left\{ \int_{T_i} a(\nabla\rho_E)^2 + (\lambda_1+2c)\rho_E \right\}^{1/2} \le 2\max\{c_4, c_5\}\beta(h_E^{-1/2}\theta_{u,E}^{-1} + h_E^{1/2}c^{1/2})\|R_{E,u}\|_{0,E}$$

To remove the dependence of the constants on the right hand side on h_E, we define $\beta := \min\{1, h_E^{-1/2} a^{1/4} \lambda_1^{-1/4}\}$. Now we see $a^{-1/2} h_E \beta^2 = \theta_{u,E}^2$ and further

$$\begin{aligned} \beta h_E^{1/2} \theta_{u,E}^{-1} &= \gamma_{u,E}^{-1}, \\ \beta h_E^{1/2} &= \gamma_{u,E} a^{1/2}. \end{aligned}$$

We obtain therefore

$$\begin{aligned} \|\rho_E\|_{0,Ti} &\leq c_5 \gamma_{u,E} a^{1/2} \|R_{E,u}\|_E, \\ \left\{ \int_{T_i} a(\nabla \rho_E)^2 + (\lambda_1 + 2c)\rho_E \right\}^{1/2} &\leq c_6 (\gamma_{u,E}^{-1} + \gamma_{u,E} a^{1/2} c^{1/2}) \|R_{E,u}\|_E, \end{aligned}$$

where $c_6 = 2\max\{c_4, c_5\}$. Using the above estimates we get from (4.49), upon dividing by $\|R_{E,u}\|_E$

$$\begin{aligned} \|R_{E,u}\|_E &\leq c_3^{-2} \sum_{i=1}^{2} \Big[c_5 \gamma_{u,E} a^{1/2} \left(\|R_{T,u}\|_{0,T_i} + \|f - f_h\|_{T_i} \right) \\ &+ c_6 \left(\gamma_{u,E}^{-1} + \gamma_{u,E} a^{1/2} c^{1/2} \right) \left\{ \int_{T_i} a(\nabla e_{u,h})^2 + \lambda_1 e_{u,h}^2 + \frac{c}{2} (e_{u,h} - e_{v,H})^2 \right\}^{1/2} \Big]. \end{aligned}$$

Substituting (4.48) in the bound above and with (4.23)-(4.24) we arrive at

$$\begin{aligned} \|R_{E,u}\|_E &\leq C \sum_{i=1}^{2} \Big[\gamma_{u,E} a^{1/2} \|f - f_h\|_{T_i} \\ &+ \left(\gamma_{u,E}^{-1} + \gamma_{u,E} a^{1/2} c^{1/2} \right) \left\{ \int_{T_i} a(\nabla e_{u,h})^2 + \lambda_1 e_{u,h}^2 + \frac{c}{2} (e_{u,h} - e_{v,H})^2 \right\}^{1/2} \Big]. \end{aligned}$$

Equivalently, with $\bar{\gamma}_{u,E} := \left(\gamma_{u,E}^{-1} + \gamma_{u,E} a^{1/2} c^{1/2} \right)^{-1}$ we have

$$\begin{aligned} \bar{\gamma}_{u,E} \|R_{E,u}\|_{0,E} &\leq C \sum_{i=1}^{2} \Big[\gamma_{u,E} a^{1/2} \bar{\gamma}_{u,E} \|f - f_h\|_{0,T_i} \\ &+ \left\{ \int_{T_i} a(\nabla e_{u,h})^2 + \lambda_1 e_{u,h}^2 + \frac{c}{2} (e_{u,h} - e_{v,H})^2 \right\}^{1/2} \Big]. \end{aligned} \tag{4.49}$$

One can now prove similar lower bounds for the second component of the system in terms of $\|R_{F,v}\|_{0,F}$ and $\|R_{K,v}\|_{0,K_i}$, and b en lieu of a, and λ_2 instead of λ_1. Upon adding the u and v components and by combining $\int_{T_i} a(\nabla e_{u,h})^2 + \lambda_1 e_{u,h}^2 + \frac{c}{2}(e_{u,h} - e_{v,H})^2$ with $\int_{T_i} b(\nabla e_{v,H})^2 + \lambda_2 e_{v,H}^2 + \frac{c}{2}(e_{u,h} - e_{v,H})^2$, we recover on the right hand-sides of (4.48) and (4.49) the error $\mathcal{E}_e$. On the left hand side we combine the element and edge residuals corresponding to u and v. This seems superficially like a straightforward procedure leading to the bounds of the type proven in [55].

Unfortunately, due to the presence of the coupling terms, the scaling in the residuals such as in (4.48), (4.49) involves the factors $\bar{\theta}_{u,T}$ and $\bar{\gamma}_{u,E}$ instead of $\theta_{u,T}$ and $\gamma_{u,E}$, respectively. Since these scaling constants are dependent on additional parameters as well as on the grid discretization, we cannot obtain the "usual" lower bounds. However, under additional assumptions the lower bounds can be established.

The main idea to get the lower bound robust in parameters of the problems and mesh discretization is to find a lower bound for $\bar{\theta}_{u,T}$ and $\bar{\gamma}_{u,E}$ in terms of $\theta_{u,T}$ and $\gamma_{u,E}$. These can be established in various ways. Below we show that if h, H are small enough, there is a lower bound for a-posteriori estimates.

Theorem 4.3.5. *Let the assumptions of Theorem 4.3.1 hold. Assume also that*

$$h \leq \sqrt{a}\min\{\lambda_1^{-1/2}, c^{-1/2}\}, \tag{4.50}$$

$$H \leq \sqrt{b}\min\{\lambda_2^{-1/2}, c^{-1/2}\}. \tag{4.51}$$

Then there is a constant C_* such that

$$C_*\eta_e \leq \|(u-u_h, v-v_H)\|_e + \left\{\sum_{T\in\mathcal{T}_h} \theta_{u,T}^2\|f-f_h\|_{0,T}^2 + \sum_{K\in\mathcal{T}_H} \theta_{v,K}^2\|g-g_H\|_{0,T}^2\right\}^{1/2}.$$

Proof. We note that by (4.50) we have from (4.23)

$$\theta_{u,T}\sqrt{c} = \frac{h_T}{\sqrt{a}}\sqrt{c} \leq 1. \tag{4.52}$$

Next, from (4.25) we see that by (4.52) we have

$$\gamma_{u,E} = a^{-1/4}\sqrt{\theta_{u,E}} = \frac{\sqrt{h_E}}{\sqrt{a}}. \tag{4.53}$$

Thus

$$\bar{\theta}_{u,T} := (\theta_{u,T}^{-1} + c^{1/2})^{-1} = \frac{\theta_{u,T}}{1+\theta_{u,T}\sqrt{c}} \geq \frac{\theta_{u,T}}{2}, \tag{4.54}$$

if only $\theta_{u,T}\sqrt{c} \leq 1$ which follows from (4.52). Similarly, we obtain that

$$\bar{\gamma}_{u,E} = (\gamma_{u,E}^{-1} + \gamma_{u,E}a^{1/2}c^{1/2})^{-1} = \frac{\gamma_{u,E}}{1+\gamma_{u,E}^2\sqrt{ac}} \geq \frac{\gamma_{u,E}}{2}, \tag{4.55}$$

as long as $\gamma_{u,E}^2\sqrt{ac} \leq 1$ which in turn is guaranteed by (4.53).

Analogous estimates hold for the v component as a consequence of (4.51)

$$\theta_{v,K} \geq \bar{\theta}_{v,K} \geq \frac{\theta_{v,K}}{2}, \tag{4.56}$$

$$\gamma_{v,F} \geq \bar{\gamma}_{v,F} \geq \frac{\gamma_{v,F}}{2}. \tag{4.57}$$

The rest of the proof is straightforward. We collect (4.48), (4.49), apply (4.54) and (4.55) to see that

$$\begin{aligned} \theta_{u,T}\|R_{T,u}\|_{0,T} \quad &\leq \quad C\,[\theta_{u,T}\|f_h - f\|_{0,T} \\ &\quad + \left\{\int_T (a(\nabla e_{u,h})^2 + \lambda_1 e_{u,h}^2 + \frac{c}{2}(e_{u,h} - e_{v,H})^2\right\}^{1/2}\Bigg], \end{aligned} \tag{4.58}$$

$$\begin{aligned} \gamma_{u,E}\|R_{E,u}\|_{0,E} \quad &\leq \quad C\sum_{i=1}^{2}\,[\theta_{u,E}\|f - f_h\|_{0,T_i} \\ &\quad + 2\left\{\int_{T_i} a(\nabla e_{u,h})^2 + \lambda_1 e_{u,h}^2 + \frac{c}{2}(e_{u,h} - e_{v,H})^2\right\}^{1/2}\Bigg]. \end{aligned} \tag{4.59}$$

We repeat the same steps to estimate $\|R_{K,v}\|_{0,T}, \|R_{E,v}\|_{0,E}$ and obtain

$$\begin{aligned}\theta_{v,K}\|R_{K,v}\|_{0,K} &\leq C\,[\theta_{v,K}\|g-g_H\|_{0,K} \\ &\quad + \left\{\int_K (b(\nabla e_{v,H})^2 + \lambda_2 e_{v,H}^2 + \frac{c}{2}(e_{u,h}-e_{v,H})^2\right\}^{1/2}\Bigg], \end{aligned} \tag{4.60}$$

$$\begin{aligned}\gamma_{v,F}\|R_{F,v}\|_{0,F} &\leq C\sum_{i=1}^{2}[\theta_{v,F}\|g-g_H\|_{0,K_i} \\ &\quad + 2\left\{\int_{K_i} b(\nabla e_{v,H})^2 + \lambda_2 e_{v,H}^2 + \frac{c}{2}(e_{u,h}-e_{v,H})^2\right\}^{1/2}\Bigg]. \end{aligned} \tag{4.61}$$

Adding these equations and summing over all elements T and all elements K completes the proof of the global lower bound. The constant $C_* := \max\{\tilde{c}_2, \frac{c_5\tilde{c}_2+c_6}{c_3^2}\}$, where $\tilde{c}_2 := \frac{\max\{c_2,1\}}{c_1^2}$ is independent of $\mathcal{P}$ and $\mathcal{H}$. □

The bound in Theorem 4.3.5 is a global lower bound. We would like also to prove some local lower bounds which are typically obtained for scalar equations. Define $\omega_T := \cup\{\omega_E : E \subset \partial T\}$. The local lower bound follows by adding the terms similar to those in (4.58)-(4.59) over all edges E of the element T which in turn requires adding the contributions from ω_T. The lower bound involves on the right hand side the energy norm restricted to the neighborhood ω_T of T.

On multilevel grids, in order to obtain a local lower bound between the error and estimator over an element T, we must be able to combine on the left hand side the contributions from all edges of T and over all edges of K. On the right hand-side a recombination in terms of energy norm is only possible if the summation over all elements $T : T \subset K$ and over all corresponding edges E, F is done, see Corollary 4.3.6. However, no result for a lower bound local to T is available.

Corollary 4.3.6. *Let $\mathcal{T}_H \ni K = \bigcup_{i=1}^n T_i$ where $T_i \in \mathcal{T}_h$ and assume* (4.50), (4.51) *hold. Then the following local lower bound holds*

$$\begin{aligned}\left\{\eta_{v,K} + \frac{1}{n}\sum_{i=1}^{n}\eta_{u,T_i}\right\}^{1/2} \quad &\leq \quad \|(u-u_h, v-v_H)\|_{e,\omega_K} \\ &\quad + \left\{\frac{1}{n}\sum_{i=1}^{n}\sum_{T_i'\in\omega_{T_i}}\theta_{u,T_i'}^2\|f-f_h\|_{0,T_i'}^2\right. \\ &\quad \left. + \sum_{K'\in\omega_K}\theta_{v,K'}^2\|g-g_H\|_{0,K'}^2\right\}^{1/2}.\end{aligned}$$

Proof. To shorten the exposition let $A_p := a(\nabla e_{u,h})^2 + \lambda_1 e_{u,h}^2 + \frac{c}{2}(e_{u,h}-e_{v,H})^2$ and $B_p := b(\nabla e_{v,H})^2 + \lambda_2 e_{v,H}^2 + \frac{c}{2}(e_{u,h}-e_{v,H})^2$.

The equation (4.59) can be written as:

$$\gamma_{u,E}\|R_{E,u}\|_{0,E} \quad \leq \quad C\left[\left\{\int_{\omega_E} A_p\right\}^{1/2} + \sum_{T'\in\omega_E}\theta_{u,E}\|f-f_h\|_{0,T'}\right]. \tag{4.62}$$

Adding the square of (4.58) and (4.62), and using (4.32) we have

$$\eta_{u,T} \leq C\left[\int_T A_p + \theta_{u,T}^2\|f_h-f\|_{0,T}^2 + \frac{1}{2}\sum_{E\subset\partial T}\left(\int_{\omega_E} A_p + \sum_{T'\in\omega_E}\theta_{u,E}^2\|f-f_h\|_{0,T'}^2\right)\right].$$

Note that $\sum_{E\subset\partial T}\int_{\omega_E} w \leq s\int_{\omega_T} w$ for any positive-valued w, where s is the number of sides of T. Also $\sum_{E\subset\partial T}\sum_{T'\in\omega_E} w = \sum_{T'\in\omega_T} w$ for any w. Thus

$$\eta_{u,T} \leq C\left[\int_{\omega_T} A_p + \sum_{T'\in\omega_T}\theta_{u,T'}^2\|f_h-f\|_{0,T'}^2\right]. \tag{4.63}$$

Similarly,

$$\eta_{v,K} \leq C\left[\int_{\omega_K} B_p + \sum_{K'\in\omega_K}\theta_{v,K'}^2\|g_H-g\|_{0,K'}^2\right]. \tag{4.64}$$

Let $K = \bigcup_{i=1}^{n} T_i$. Note that $\omega_K \supset \bigcup_{i=1}^{n} \omega_{T_i}$. Then

$$\begin{aligned}
\sum_{i=1}^{n} \eta_{u,T_i} &\leq C \sum_{i=1}^{n} \left[\int_{\omega_{T_i}} A_p + \sum_{T_i' \in \omega_{T_i}} \theta_{u,T_i'}^2 \|f_h - f\|_{0,T_i'}^2 \right] \\
&\leq C \left[n \int_{\bigcup_{i=1}^{n} \omega_{T_i}} A_p + \sum_{i=1}^{n} \sum_{T_i' \in \omega_{T_i}} \theta_{u,T_i'}^2 \|f_h - f\|_{0,T_i'}^2 \right] \\
&\leq C \left[n \int_{\omega_K} A_p + \sum_{i=1}^{n} \sum_{T_i' \in \omega_{T_i}} \theta_{u,T_i'}^2 \|f_h - f\|_{0,T_i'}^2 \right].
\end{aligned}$$

Thus

$$\begin{aligned}
\eta_{v,K} + \frac{1}{n} \sum_{i=1}^{n} \eta_{u,T_i} \leq C \Bigg[& \int_{\omega_K} A_p + B_p \\
& + \frac{1}{n} \sum_{i=1}^{n} \sum_{T_i' \in \omega_{T_i}} \theta_{u,T_i'}^2 \|f_h - f\|_{0,T_i'}^2 + \sum_{K' \in \omega_K} \theta_{v,K'}^2 \|g_H - g\|_{0,K'}^2 \Bigg],
\end{aligned}$$

which completes the proof. □

4.3.2.5 Upper bound for the error in only one of the unknowns

In some instances it may be known *a-priori* that one of the unknowns is smoother than the other and that its numerical approximation has a smaller error associated with it. In such a case, we can use a multilevel grid. For the purposes of grid adaptation, it is also useful to estimate the error only in the variable that contributes the bulk fraction of the error. For example, if v is smoother than u, then it is natural to use a multilevel grid with $H >> h$, and define an estimate for the error in u only.

Throughout this section we will assume that there is a constant $0 < \alpha \ll 1$ such that $c\alpha < 1$ and

$$\|e_{v,H}\|_{0,T} < \alpha \|e_{u,h}\|_{0,T}, \qquad \forall T \in \mathcal{T}_h. \tag{4.65}$$

We will consider the form on $V \times V$

$$a(u,\phi) = \int_\Omega (\lambda_1 + c)u\phi + a\nabla u \cdot \nabla\phi,$$

and the norm $\|u\|_*^2 := a(u,u)$ on V. With these we prove the following result, which resembles the scalar estimates in [55] for $a = 1$.

Theorem 4.3.7. *Let u, u_h, v, v_H be as in Theorem 4.3.1. and suppose that* (4.65) *holds. Then*

$$\mathcal{E}^* := \|e_{u,h}\|_* \leq \bar{C}\eta^*, \tag{4.66}$$

where $\bar{C} := (1 - c\alpha)^{-1} \max\{c_1, c_4\}$ and

$$\eta^* := \left\{ \sum_{T\in\mathcal{T}_h} (\theta^*_{u,T})^2 \|R^*_{T,u}\|^2_{0,T} + \tfrac{1}{2} \sum_{E\subset\partial T} (\gamma^*_{u,E})^2 \|R_{E,u}\|^2_{0,E} \right\}^{1/2} \tag{4.67}$$

with

$$\begin{aligned} \theta^*_{u,T} &:= \min\{h_S a^{-1/2}, (\lambda_1 + c)^{-1/2}\} \quad \forall S \in \mathcal{T}_h \cup \mathcal{E}_h, \\ \gamma^*_{u,E} &:= a^{-1/4} (\theta^*_{u,E})^{1/2}. \end{aligned}$$

Proof. Subtracting the first component of (4.11a) from the respective one of (3.25a) with $\phi = \phi_h$ we get

$$a(e_{u,h}, \phi_h) = \int_\Omega c(v - \lambda v_H)\phi_h \overset{(4.2)}{=} \int_\Omega c e_{v,H}\phi_h. \tag{4.68}$$

By letting $\phi_h = I_h e_{u,h}$ in (4.68) we get

$$\begin{aligned} \|e_{u,h}\|_*^2 &= a(e_{u,h}, e_{u,h}) \overset{(4.68)}{=} a(e_{u,h}, e_{u,h}) - a(e_{u,h}, I_h e_{u,h}) + (c e_{v,H}, I_h e_{u,h}) \\ &= a(e_{u,h}, e_{u,h} - I_h e_{u,h}) + (c e_{v,H}, I_h e_{u,h}). \end{aligned}$$

Now we integrate by parts, use (3.25a), and add and subtract $c(v_H, e_{u,h})$ in the second identity to get

$$\begin{aligned}\|e_{u,h}\|_*^2 &= \sum_{T\in\mathcal{T}_h}(f-(\lambda_1+c)u_h+\nabla(a\nabla u_h)+cv, e_{u,h}-I_he_{u,h})_T+(ce_{v,H}, I_he_{u,h})\\ &\quad+\sum_{E\subset\mathcal{E}_h}([a\partial_n u_h], e_{u,h}-I_he_{u,h})_E\\ &= \sum_{T\in\mathcal{T}_h}(R^*_{T,u}, e_{u,h}-I_he_{u,h})_T+(ce_{v,H}, e_{u,h})+\sum_{E\subset\mathcal{E}_h}(R_{E,u}, e_{u,h}-I_he_{u,h})_E.\end{aligned}$$

Next we estimate the terms in this identity with Cauchy-Schwarz inequality

$$\begin{aligned}\|e_{u,h}\|_*^2 &\le \sum_{T\in\mathcal{T}_h}\|R^*_{T,u}\|_{0,T}\|e_{u,h}-I_he_{u,h}\|_{0,T}+c\|e_{v,H}\|_{0,T}\|e_{u,h}\|_{0,T}\\ &\quad+\sum_{E\subset\mathcal{E}_h}\|R_{E,u}\|_{0,E}\|e_{u,h}-I_he_{u,h}\|_{0,E},\end{aligned}$$

and by (4.65) we obtain

$$(1-c\alpha)\|e_{u,h}\|_*^2\le\sum_{T\in\mathcal{T}_h}\|R^*_{T,u}\|_{0,T}\|e_{u,h}-I_he_{u,h}\|_{0,T}+\sum_{E\subset\mathcal{E}_h}\|R_{E,u}\|_{0,E}\|e_{u,h}-I_he_{u,h}\|_{0,E}.$$

To conclude, we apply (4.28) and (4.30) replacing λ_1 with λ_1+c to get the following estimate

$$\begin{aligned}(1-c\alpha)\|e_{u,h}\|_*^2 &\le \sum_{T\in\mathcal{T}_h}c_1\theta^*_{u,T}\|R^*_{T,u}\|_{0,T}\|e_{u,h}\|_{*,\tilde{\omega}_T}+\sum_{E\subset\mathcal{E}_h}c_4\gamma^*_{u,E}\|R_{E,u}\|_{0,e}\|e_{u,h}\|_{*,\tilde{\omega}_T}\\ &\le \max\{c_1,c_4\}\left[\sum_{T\in\mathcal{T}_h}\theta^*_{u,T}\|R^*_{T,u}\|_{0,T}\|e_{u,h}\|_*\right.\\ &\quad\left.+\sum_{E\subset\mathcal{E}_h}\gamma^*_{u,E}\|R_{E,u}\|_{0,E}\|e_{u,h}\|_*\right].\end{aligned}$$

Dividing both sides by $(1-c\alpha)$ concludes the proof. □

We apply the above estimates to (4.20) and obtain

Lemma 4.3.3. *The following estimates hold*

$$\|e_{u,h} - Q_h e_{u,h}\|_{0,T} \leq c_1 \theta_{u,T} \left\{ \int_{\tilde{\omega}_T} a(\nabla e_{u,h})^2 + \lambda_1 e_{u,h}^2 \right\}^{1/2}, \tag{4.69}$$

$$\|e_{v,H} - Q_H e_{v,H}\|_{0,K} \leq c_2 \theta_{v,K} \left\{ \int_{\tilde{\omega}_K} b(\nabla e_{v,H})^2 + \lambda_2 e_{v,H}^2 \right\}^{1/2}, \tag{4.70}$$

$$\|e_{u,h} - Q_h e_{u,h}\|_{0,E} \leq c_4 \gamma_{u,E} \left\{ \int_{\tilde{\omega}_T} a(\nabla e_{u,h})^2 + \lambda_1 e_{u,h}^2 \right\}^{1/2}, \tag{4.71}$$

$$\|e_{v,H} - Q_H e_{v,H}\|_{0,F} \leq c_5 \gamma_{v,F} \left\{ \int_{\tilde{\omega}_K} b(\nabla e_{v,H})^2 + \lambda_2 e_{v,H}^2 \right\}^{1/2}. \tag{4.72}$$

4.4 NLP-model

Now we present *a-priori* estimates for the NLP-model. Here we discretize the problem first in space. The resulting discrete ODE system is called "continuous in time". We begin by finding an *a-priori* estimate for the one-level approximation (u_h, v_h), then we extend the result found to the multilevel approximation (u_h, v_H) using Lemma 4.1.1. The results presented here are standard for nonlinear parabolic problems. In this Section we follow closely the techniques presented in [52] for scalar problems and extend it to a coupled system.

We mention now the fundamental result in [58] where *a-priori* L^2 error estimates for linear and nonlinear parabolics problems were obtained, and where the use of the Ritz (elliptic) projection (4.78) was first proposed. In [58] the function φ in the semilinear term is Lipschitz continuous. In fact, the results of this section can be seen as a mere extension of the work in [58] to coupled parabolic systems.

For the particular case of $b = 0$, *a-priori* error estimates for the case where φ is not Lipschitz continuous were proved using regularization theory in [13]. Using these results, error estimates for equilibrium diffusion-adsorption process (see equation 2.26) were proved as a limiting case of the NLP-model for c going to infinity in [14].

In this thesis we restrict ourselves to the case which φ is Lipschitz continuous which cover a wide range of applications.

4.4.1 *A-priori* estimation for the continuous in time problem

Let us seek a finite dimensional solution $(u_h, v_h) \in V_h \times V_h$ where $V_h \subset V$. The semi-discrete formulation of the problem will be given by:

Find $(u_h, v_h) \in V_h^2$ *such that for all* $(\xi, \psi) \in V_h^2$

$$(\lambda_1 u_h', \xi) + (a\nabla u_h, \nabla \xi) + c(\varphi(u_h) - v_h, \xi) = (f, \xi) \tag{4.73a}$$

$$(\lambda_2 v_h', \psi) + (b\nabla v_h, \nabla \psi) - c(\varphi(u_h) - v_h, \psi) = (g, \psi) \tag{4.73b}$$

$$(u_h(x,0), \xi) = (u_{0h}, \xi), \qquad (v_h(x,0), \psi) = (v_{0h}, \psi). \tag{4.73c}$$

Represent the solutions by

$$u_h = \sum_{j=1}^{N_h} \alpha_j(t)\omega_j(x), \qquad v_h = \sum_{j=1}^{N_h} \beta_j(t)\omega_j(x),$$

where $\{\omega_j\}_{j=1}^{N_h}$ is the standard basis of piecewise linear functions for V_h. Thus (4.73) may be rewritten as

$$\sum_{j=1}^{N_h} \lambda_1 \alpha_j'(t)(\omega_j, \omega_k) + \sum_{j=1}^{N_h} \alpha_j(t) a(\nabla\omega_j, \nabla\omega_k) + c(\varphi(\sum_{j=1}^{N_h} \alpha_j\omega_j), \omega_k) \tag{4.74a}$$

$$- c\sum_{j=1}^{N_h} \beta_j(\omega_j, \omega_k) = (f, \omega_k), \quad \forall 1 \le k \le N_h,$$

$$\sum_{j=1}^{N_h} \lambda_2 \beta_j(t)'(\omega_j(x), \omega_i) + \sum_{j=1}^{N_h} \beta_j(t) b(\nabla\omega_j, \nabla\omega_i) + c\sum_{j=1}^{N_h} \beta_j(\omega_j, \omega_i) \tag{4.74b}$$

$$- c(\varphi(\sum_{j=1}^{N_h} \alpha_j\omega_j), \omega_i) = (g, \omega_i), \quad \forall 1 \le i \le N_h.$$

Set $\alpha = \alpha(t) = (\alpha_1(t), \alpha_2(t), \ldots, \alpha_{N_h}, \beta_1(t), \beta_2(t), \ldots, \beta_{N_h})^T$.

Let:

$$\begin{aligned} B &= (b_{jk}) \quad \text{where } b_{jk} := (\omega_j, \omega_k), \\ A &= (a_{jk}) \quad \text{where } a_{jk} := (\nabla\omega_j, \nabla\omega_k), \\ F &= ((f,\omega_1),\ldots,(f,\omega_{N_h}),(g,\omega_1),\ldots,(g,\omega_{N_h})), \\ \Phi(\alpha) &= (-\tilde{\varphi}_1(\alpha),\ldots,-\tilde{\varphi}_{N_h}(\alpha),\tilde{\varphi}_1(\alpha),\ldots,\tilde{\varphi}_{N_h}(\alpha))^T \end{aligned}$$

Here $\tilde{\varphi}_j(\alpha) := (\varphi(\sum_{l=1}^{N_h}\alpha_l\omega_l),\omega_j)$. So the system (4.74a)-(4.74b) may also be written in matrix form as

$$\begin{bmatrix} \lambda_1 B & 0 \\ 0 & \lambda_2 B \end{bmatrix} \alpha' + \begin{bmatrix} aA & -cB \\ cB & bA \end{bmatrix} \alpha = F + c\Phi(\alpha). \tag{4.75}$$

We assume that there exists a unique solution for (4.75).

We define a continuous and a discrete norm energy norm for the model problem.

Definition 4.4.1. *For any $(u,v) \in V^2$ define:*

$$|||(u,v)|||^2_{nlp}(t) := \lambda_1\|u(t)\|^2 + \lambda_2\|v(t)\|^2 + \int_0^t \left(a|u(s)|_1^2 + b|v(s)|_1^2\right) ds, \tag{4.76}$$

$$|||(u,v)|||^2_{dnlp}(t_n) := \lambda_1\|u(t_n)\|^2 + \lambda_2\|v(t_n)\|^2 + \tau_n \sum_{m=1}^{n} a|u(t_m)|_1^2 + b|v(t_m)|_1^2 \tag{4.77}$$

Along this Section we shall use the following lemma in its differential form [26], the integral form is given by Lemma 3.2.8.

Lemma 4.4.1 (Gronwall's Lemma)**.** *Let $\beta \in \mathbb{R}$, $\chi \in C^1([0,T],\mathbb{R})$ and $f \in C^0([0,T],\mathbb{R})$ such that $\chi'(t) \le \beta\chi + f$. Then*

$$\chi(t) \le e^{\beta t}\chi(0) + \int_0^t e^{\beta(t-\tau)} f(t) d\tau$$

In order to compute the norm of the difference $(u_h - u)$ we will use the triangle inequality

$$\|u_h - u\|_* \le \|u_h - \tilde{u}\|_* + \|\tilde{u} - u\|_*.$$

Definition 4.4.2. *Define the Ritz-elliptic projection $\tilde{u}$ into V_h via*

$$(\nabla(\tilde{u}-u),\nabla\chi)=0 \qquad \forall\chi\in V_h. \tag{4.78}$$

We will use the following lemma from [52] to prove the *a-priori* estimate for the fully-discrete problem.

Lemma 4.4.2. *Assume that $u,u',u''\in V$. Then for any $t\in[0,T]$*

$$\|\nabla\tilde{u}''(t)\|\le C(u).$$

Using (4.78) into the weak form of the NLP system (3.45) leads us to

$$(\lambda_1\tilde{u}',\xi)+a(\nabla\tilde{u},\nabla\xi)+c(\varphi(u)-v,\xi)=(f,\xi)+(\lambda_1(\tilde{u}_t-u'),\xi), \tag{4.79a}$$
$$(\lambda_2\tilde{v}',\psi)+b(\nabla\tilde{v},\nabla\psi)-c(\varphi(u)-v,\psi)=(g,\psi)+(\lambda_1(\tilde{v}'-v'),\psi). \tag{4.79b}$$

Subtracting the above equation from equation (4.73)

$$(\lambda_1(u_h-\tilde{u})',\xi)+a(\nabla(u_h-\tilde{u}),\nabla\xi)+c((\varphi(u_h)-\varphi(u))-(v_h-v),\xi)=(\lambda_1(u-\tilde{u})',\xi), \tag{4.80a}$$
$$(\lambda_2(v_h-\tilde{v})',\psi)+b(\nabla(v_h-\tilde{v}),\nabla\psi)-c((\varphi(u_h)-\varphi(u))-(v_h-v),\psi)=(\lambda_2(v-\tilde{v})',\psi). \tag{4.80b}$$

Use as test functions $\xi=u_h-\tilde{u}$ and $\psi=v_h-\tilde{v}$.

$$\begin{aligned}
\lambda_1((u_h-\tilde{u})',u_h-\tilde{u}) &= -a|u_h-\tilde{u}|_1^2-c((\varphi(u_h)-\varphi(u))-(v_h-v),u_h-\tilde{u})\\
&\quad +(\lambda_1(u-\tilde{u})',u_h-\tilde{u}),\\
\lambda_2((v_h-\tilde{v})',v_h-\tilde{v}) &= -b|v_h-\tilde{v}|_1^2+c((\varphi(u_h)-\varphi(u))-(v_h-v),v_h-\tilde{v})\\
&\quad +(\lambda_2(v-\tilde{v})',v_h-\tilde{v}).
\end{aligned}$$

Adding the two equations above and using the Proposition 3.2.2

$$\begin{aligned}\frac{1}{2}\frac{d}{dt}\left[\lambda_1\|u_h-\tilde{u}\|^2+\lambda_2\|v_h-\tilde{v}\|^2\right] &\leq -a|u_h-\tilde{u}|_1^2-b|v_h-\tilde{v}|_1^2 \\ &- c(\varphi(u_h)-\varphi(u)-v_h-v,u_h-\tilde{u}-v_h-\tilde{v}) \\ &+ (\lambda_1(u-\tilde{u})',u_h-\tilde{u})+(\lambda_2(v-\tilde{v})',v_h-\tilde{v}).\end{aligned} \tag{4.81}$$

Let φ be Lipschitz with Lipchitz constant L. Apply Cauchy-Schwarz and the Lipschitz assumption to equation (4.81)

$$\begin{aligned}\frac{1}{2}\frac{d}{dt}\left[\lambda_1\|u_h-\tilde{u}\|^2+\lambda_2\|v_h-\tilde{v}\|^2\right] &\leq -a|u_h-\tilde{u}|_1^2-b|v_h-\tilde{v}|_1^2 \\ &+ L\|u_h-u\|(\|u_h-\tilde{u}\|+\|v_h-\tilde{v}\|) \\ &+ \|v_h-v\|(\|u_h-\tilde{u}\|+\|v_h-\tilde{v}\|) \\ &+ \lambda_1\|(u-\tilde{u})'\|\|u_h-\tilde{u}\|+\lambda_2\|(v-\tilde{v})'\|\|v_h-\tilde{v}\|.\end{aligned} \tag{4.82}$$

Use the inequality $ab\leq\frac{1}{2}[\epsilon a^2+\frac{1}{\epsilon}b^2]$,

$$\begin{aligned}\frac{1}{2}\frac{d}{dt}\left[\lambda_1\|u_h-\tilde{u}\|^2+\lambda_2\|v_h-\tilde{v}\|^2\right] &\leq -a|u_h-\tilde{u}|_1^2-b|v_h-\tilde{v}|_1^2 \\ &+ \frac{L}{2}\left[2\|u_h-u\|^2+\|u_h-\tilde{u}\|^2+\|v_h-\tilde{v}\|^2\right] \\ &+ \frac{1}{2}\left[2\|v_h-v\|^2+\|v_h-\tilde{v}\|^2+\|u_h-\tilde{u}\|^2\right] \\ &+ \frac{\lambda_1}{2}\left[\|(u-\tilde{u})'\|^2+\|u_h-\tilde{u}\|^2\right] \\ &+ \frac{\lambda_2}{2}\left[\|(v-\tilde{v})'\|^2+\|v_h-\tilde{v}\|^2\right].\end{aligned} \tag{4.83}$$

Use the triangle inequality to assure that all terms in the equation above are differences containing $\tilde{u}$ or $\tilde{v}$,

$$\begin{aligned}\frac{1}{2}\frac{d}{dt}\left[\lambda_1\|u_h-\tilde{u}\|^2+\lambda_2\|v_h-\tilde{v}\|^2\right] &\leq -a|u_h-\tilde{u}|_1^2-b|v_h-\tilde{v}|_1^2 \\ &+ \frac{C_1}{2}\|u_h-\tilde{u}\|^2+\frac{C_2}{2}\|v_h-\tilde{v}\|^2 \\ &+ L\|u-\tilde{u}\|^2+\|v-\tilde{v}\|^2 \\ &+ \frac{\lambda_1}{2}\|(u-\tilde{u})'\|^2+\frac{\lambda_2}{2}\|(v-\tilde{v})'\|^2.\end{aligned} \tag{4.84}$$

Here,

$$C_1 = 2\left(L + 2 + \frac{\lambda_1}{2}\right), \tag{4.85}$$

$$C_2 = 2\left(3 + \frac{\lambda_2}{2}\right). \tag{4.86}$$

Thus, using that a, b are positive, $-a \leq -\frac{a}{2}$,

$$\begin{aligned} \frac{d}{dt}\left[\lambda_1\|u_h - \tilde{u}\|^2 + \lambda_2\|v_h - \tilde{v}\|^2\right] &\leq -a|u_h - \tilde{u}|_1^2 - b|v_h - \tilde{v}|_1^2 \\ &+ C_1\|u_h - \tilde{u}\|^2 + C_2\|v_h - \tilde{v}\|^2 \\ &+ 2L\|u - \tilde{u}\|^2 + 2\|v - \tilde{v}\|^2 \\ &+ \lambda_1\|(u - \tilde{u})'\|^2 + \lambda_2\|(v - \tilde{v})'\|^2. \end{aligned} \tag{4.87}$$

Apply Gronwall's lemma 4.4.1 with $\beta := \max\{C_1, C_2\}$ and $\chi := \lambda_1\|u_h - \tilde{u}\|^2 + \lambda_2\|v_h - \tilde{v}\|^2$. Also use that $-e^{\beta t} \leq -1$ to get

$$\begin{aligned} \lambda_1\|u_h - \tilde{u}\|^2 + \lambda_2\|v_h - \tilde{v}\|^2 &\leq e^{\beta t}\left[\lambda_1\|u_h - \tilde{u}\|^2(0) + \lambda_2\|v_h - \tilde{v}\|^2(0)\right] \\ &- a|u_h - \tilde{u}|_L^2(0, T; H_0^1(\Omega))^2 - b|v_h - \tilde{v}|_L^2(0, T; H_0^1(\Omega))^2 \\ &+ e^{\beta t}\left[2L\|u - \tilde{u}\|^2_{L^2(0,T;L^2(\Omega))} + \lambda_1\|(u - \tilde{u})'\|^2_{L^2(0,T;L^2(\Omega))}\right] \\ &+ e^{\beta t}\left[2\|v - \tilde{v}\|^2_{L^2(0,T;L^2(\Omega))} + \lambda_2\|(v - \tilde{v})'\|^2_{L^2(0,T;L^2(\Omega))}\right]. \end{aligned}$$

Next we need estimates for $\|(u - \tilde{u})'\|,\ \|u - \tilde{u}\|$. Assume that the following holds ([52], page 4): Given a family $\{V_h\}$ of finite-dimensional subspaces of H_0^1 such that, for some integer $r \geq 2$ and small h,

$$\inf_{\xi \in S_h}\{\|z - \xi\| + h\|\nabla(z - \xi)\|\} \leq C_3 h^s \|z\|_s,\ 1 \leq s \leq r \tag{4.88}$$

when $z \in H^s \cap H_0^1$. The number r is referred to as the order of accuracy of the family $\{V_h\}$. The following result is from ([52], page 8).

Lemma 4.4.3. *Assume that* (4.88) *holds. Then, with* $\tilde{u}$ *defined by* (4.78) *we have*

$$\|\tilde{u} - u\| + h\|\nabla(\tilde{u} - u)\| \leq C_3 h^s \|u\|_s, \textit{for}\ \ u \in H^s \cap H_0^1,\ 1 \leq s \leq r.$$

In particular,

$$\|\nabla(\tilde{u}-u)\| \leq C_3 h\|u\|_2, \tag{4.89}$$

$$\|\tilde{u}-u\| \leq C_3 h^2\|u\|_2. \tag{4.90}$$

We also need estimates for $\|(\tilde{u}-u)_t\|$, for simplicity, let $\rho_t := (\tilde{u}-u)'$. For that we shall use a duality argument (see [52], pages 233-234). We start with the interpolation result: define the interpolator operator $I_h : H^r \cap H_0^1 \to V_h$ such that

$$\|I_h z - z\| + h\|\nabla(I_h z - z)\| \leq C_4 h^s \|z\|_s, \;\; 1 \leq s \leq r. \tag{4.91}$$

for all $z \in H^r$.

Let us solve a dual problem for $\xi \in L^2(\Omega)$:

$$-\nabla\cdot(\nabla\psi) = \xi \quad \text{in } \Omega,\ \psi = 0 \quad \text{on } \partial\Omega. \tag{4.92}$$

The weak formulation of (4.92) is given by :

$$(\nabla\psi, \nabla\chi) = (\xi, \chi), \tag{4.93}$$

for all $\chi \in H_0^1(\Omega)$. Note that since $\|\psi\| \leq C_{PF}\|\nabla\psi\|$ for $\psi \in H_0^1(\Omega)$, (Poincaré-Friedrichs inequality (3.11))

$$\|\nabla\psi\|^2 = (\nabla\psi, \nabla\psi) \overset{(4.93)}{=} (\xi, \psi) \leq \|\xi\|\|\psi\| \leq C_{PF}\|\xi\|\|\nabla\psi\|,$$

which implies that $\|\nabla\psi\| \leq C_{PF}\|\xi\|$ and $\|\psi\| \leq C_{PF}^2\|\xi\|$.

Using $\chi = \rho_t$ as a test function and equation (4.78)

$$(\rho_t, \xi) = (\nabla\rho_t, \nabla\psi) = (\nabla\rho_t, \nabla(\psi - I_h\psi)).$$

Thus,

$$|(\rho_t, \xi)| \leq \|\nabla\rho_t\|\|\nabla(\psi - I_h\psi)\| \overset{(4.91)}{\leq} C_4 h\|\nabla\rho_t\|\|\psi\| \leq C_4 h\|\nabla\rho_t\|\|\xi\|. \tag{4.94}$$

Now we need to estimate $\|\nabla\rho_t\|$. Recall that by definition $(\nabla\rho_t, \nabla\chi) = 0$ for all $\chi \in V_h$.

$$\begin{aligned}\|\nabla\rho_t\|^2 &= (\nabla\rho_t, \nabla\rho_t) = (\nabla\rho_t, \nabla(u' - I_h u') + \underbrace{(\nabla\rho_t, \nabla(\tilde{u}' - I_h u'))}_{=0} \\ &\leq \|\nabla\rho_t\|\|\nabla(u' - I_h u')\| \leq C_5 h\|\nabla\rho_t\|\|u'\|_2.\end{aligned}$$

That is, $\|\nabla\rho_t\| \leq C_5 h\|u'\|_2$. Plugging this into equation (4.94) we arrive at

$$\|(u - \tilde{u})'\| \leq C_5 h^2\|u'\|_2. \tag{4.95}$$

To finalize the semi-discrete *a-priori* estimation we notice that:

$$\|u_h - \tilde{u}\|(0) = \|u_{0h} - \tilde{u}(0)\| \leq \|u_{0h} - u_0\| + \|u_0 - \tilde{u}(0)\| \leq \|u_{0h} - u_0\| + C_6 h^2\|u_0\|.$$

We have proved the following estimate for the Ritz projection (4.78)

Proposition 4.4.1. *Let (u_h, v_h) be the solution of the problem (4.73) and $\tilde{u}, \tilde{v}$ be defined via (4.78). Assume that $(u, v), (u', v') \in L^2(0, T; H^2(\Omega)) \times L^2(0, T; H^2(\Omega))$. Then, for any $t, 0 \leq t \leq T$,*

$$\begin{aligned}\|(\tilde{u} - u_h, \tilde{v} - v_h)\|^2_{nlp}(t) &\leq e^{\beta t}\left[2LC_3^2 h^4\|u\|^2_{L^2(0,T;H^2(\Omega))} + \lambda_1 C_5^2 h^4\|v'\|^2_{L^2(0,T;H^2(\Omega))}\right] \\ &+ e^{\beta t}\left[2C_3^2 h^4\|v\|^2_{L^2(0,T;H^2(\Omega))} + \lambda_1 C_5^2 h^4\|v'\|^2_{L^2(0,T;H^2(\Omega))}\right] \\ &+ 2e^{\beta t}\left[\lambda_1\|u_{0h} - u_0\|^2 + \lambda_1 C_6^2 h^4\|u_0\|^2\right. \\ &+ \left.\lambda_2\|v_{0h} - v_0\|^2 + \lambda_2 C_6^2 h^4\|v_0\|^2\right].\end{aligned} \tag{4.96}$$

Now, to get the error estimate for the error in $u - u_h$, $v - v_h$ we note that by applying the triangle inequality

$$\|(u - u_h, v - v_h)\|^2_{nlp}(t) \leq 2\|(\tilde{u} - u_h, \tilde{v} - v_h)\|^2_{nlp}(t) + 2\|(u - \tilde{u}, v - \tilde{v})\|^2_{nlp}(t).$$

Using (4.96), (4.89), (4.90),

$$\begin{aligned}
\|(u-u_h, v-v_h)\|^2_{nlp}(t) &\leq 2\Big\{2e^{\beta t}\left[\lambda_1\|u_{0h}-u_0\|^2+\lambda_1 C_6^2 h^4\|u_0\|^2\right)\\
&+ \lambda_2\|v_{0h}-v_0\|^2+\lambda_2 C_6^2 h^4\|v_0\|^2\big]\\
&+ e^{\beta t}\left[2LC_3^2h^4\|u\|^2_{L^2(0,T;H^2(\Omega))}+\lambda_2 C_5^2 h^4\|u'\|^2_{L^2(0,T;H^2(\Omega))}\right]\\
&+ e^{\beta t}\left[2C_3^2h^4\|v\|^2_{L^2(0,T;H^2(\Omega))}+\lambda_1 C_5^2 h^4\|v'\|^2_{L^2(0,T;H^2(\Omega))}\right]\Big\}\\
&+ 2\left[\lambda_1 C_3^2h^4\|u\|^2_2(t)+\lambda_2 C_3^2h^4\|v\|^2_2(t)\right]\\
&+ 2\left[aC_3^2h^2\|u\|^2_2+bC_3^2h^2\|v\|^2_2\right].
\end{aligned}$$

We have shown the following.

Theorem 4.4.3. *Suppose that the assumptions of Proposition 4.4.1 hold. Also assume that* (4.88) *holds. If* (u,v) *is the solution of* (3.45) *and* (u_h,v_h) *is the solution of* (4.73)*, then, the following estimate holds:*

$$\begin{aligned}
\|(u-u_h, v-v_h)\|_{nlp}(t)^2 &\leq C_*(u,v,u_0,v_0,\mathcal{P})h^2+C^*(u,v,u_0,v_0,\mathcal{P})h^4 \quad (4.97)\\
&+ 4e^{\beta t}\left[\lambda_1\|u_{0h}-u_0\|^2+\lambda_2\|v_{0h}-v_0\|^2\right].
\end{aligned}$$

Here

$$\begin{aligned}
C^* &:= 4e^{\beta t}\{\, C_6^2\left[\lambda_1\|u_0\|^2+\lambda_2\|v_0\|^2\right]+C_3^2\left[L\|u\|^2_{L^2(0,T;H^2(\Omega))}+\|v\|^2_{L^2(0,T;H^2(\Omega))}\right]\\
&+ C_5^2\left[\lambda_1\|u'\|^2_{L^2(0,T;H^2(\Omega))}+\lambda_2\|v'\|^2_{L^2(0,T;H^2(\Omega))}\right]+2C_3^2\left[\lambda_1\|u\|^2_2+\lambda_2\|v\|^2_2\right]\,\},\\
C_* &:= C_3^2\left[a\|u\|^2_2+b\|v\|^2_2\right].
\end{aligned}$$

4.4.2 *A-priori* estimate for the fully-discrete problem

Notation. *From now on we will adopt the following notation:*

$$\begin{aligned}
u^n &:= u(t_n),\\
\tau_n &:= t_{n+1}-t_n,\\
\partial^n u &:= \frac{u(t_{n+1})-u(t_n)}{\tau_n},\\
\Delta_n(\tilde{u}) &:= \partial^n\tilde{u}-\tilde{u}^n_t.
\end{aligned}$$

Now we consider the backward Euler discretization of equation (4.73). The fully-discrete problem reads:

For $n, 1 \leq n \leq N-1$, *find* $(u_h^{n+1}, v_h^{n+1}) \in V^2$ *such that* $\forall (\xi, \psi) \in V^2$

$$(\lambda_1 \partial^n u_{h,t}, \xi) + a(\nabla u_h^{n+1}, \nabla \xi) + c(\varphi(u_h^{n+1}) - v_h^{n+1}, \xi) = (f^{n+1}, \xi), \tag{4.98a}$$

$$(\lambda_2 \partial^n v_{h,t}, \psi) + b(\nabla v_h^{n+1}, \nabla \psi) - c(\varphi(u_h^{n+1}) - v_h^{n+1}, \psi) = (g^{n+1}, \psi). \tag{4.98b}$$

To derive error estimates, we subtract the system of equations (4.79) from the system (4.98)

$$\begin{gathered}(\lambda_1(\partial^n(u_h - \tilde{u}), \xi) + (\lambda_2 \partial^n(v_h - \tilde{v}), \psi) + a(\nabla(u_h^{n+1} - \tilde{u}^{n+1}), \nabla \xi) \\ + b(\nabla(v_h^{n+1} - \tilde{v}^{n+1}), \nabla \psi) + c((\varphi(u_h^n) - \varphi(u^n)) - (v_h^n - v^n), \xi - \psi) = \\ (\lambda_1(u^n - \tilde{u}^n)', \xi) + (\lambda_2(v^n - \tilde{v}^n)', \xi) - \lambda_1(\Delta_n(\tilde{u}), \xi) - \lambda_2(\Delta_n(\tilde{v}), \psi).\end{gathered}$$

Multiply it all by τ_n and use as test functions $\xi = u_h^{n+1} - \tilde{u}^{n+1}$ and $\psi = v_h^{n+1} - \tilde{v}^{n+1}$

$$\begin{gathered}\lambda_1 \|u_h^{n+1} - \tilde{u}^{n+1}\|^2 + \lambda_2 \|v_h^{n+1} - \tilde{v}^{n+1}\|^2 + \tau_n \left[a|u_h^{n+1} - \tilde{u}^{n+1}|_1^2 + b|v_h^{n+1} - \tilde{v}^{n+1}|_1^2\right] = \\ -c\tau_n((\varphi(u_h^n) - \varphi(u^n)) - (v_h^n - v^n), u_h^{n+1} - \tilde{u}^{n+1} - (v_h^{n+1} - \tilde{v}^{n+1})) \\ +\lambda_1(u_h^n - \tilde{u}^n, u_h^{n+1} - \tilde{u}^{n+1}) + \lambda_2(v_h^n - \tilde{v}^n, v_h^{n+1} - \tilde{v}^{n+1}) \\ +\tau_n \left[(\lambda_1(u^n - \tilde{u}^n)', u_h^{n+1} - \tilde{u}^{n+1}) + (\lambda_2(v^n - \tilde{v}^n)', v_h^{n+1} - \tilde{v}^{n+1})\right. \\ \left. -\lambda_1(\Delta_n(\tilde{u}), u_h^{n+1} - \tilde{u}^{n+1}) - \lambda_2(\Delta_n(\tilde{v}), v_h^{n+1} - \tilde{v}^{n+1})\right].\end{gathered}$$

Since

$$\begin{gathered}-c\tau_n((\varphi(u_h^n) - \varphi(u^n)) - (v_h^n - v^n), u_h^{n+1} - \tilde{u}^{n+1} - (v_h^{n+1} - \tilde{v}^{n+1})) = \\ -c\tau_n(\varphi(u_h^{n+1}) - \varphi(u^{n+1}), u_h^{n+1} - \tilde{u}^{n+1}) + c\tau_n(\varphi(u_h^{n+1}) - \varphi(u^{n+1}), v_h^{n+1} - \tilde{v}^{n+1}) \\ +c\tau_n(v_h^{n+1} - v^{n+1}, u_h^{n+1} - \tilde{u}^{n+1}) - c\tau_n(v_h^{n+1} - v^{n+1}, v_h^{n+1} - \tilde{v}^{n+1}),\end{gathered}$$

we get,

$$\begin{aligned}
\lambda_1\|u_h^{n+1}-\tilde{u}^{n+1}\|^2+\lambda_2\|v_h^{n+1}-\tilde{v}^{n+1}\|^2+\tau_n\left[a|u_h^{n+1}-\tilde{u}^{n+1}|_1^2+b|v_h^{n+1}-\tilde{v}^{n+1}|_1^2\right]=\\
-c\tau_n((\varphi(u_h^n)-\varphi(u^n))-(v_h^n-v^n),u_h^{n+1}-\tilde{u}^{n+1}-(v_h^{n+1}-\tilde{v}^{n+1}))=\\
-c\tau_n(\varphi(u_h^{n+1})-\varphi(u^{n+1}),u_h^{n+1}-\tilde{u}^{n+1})+c\tau_n(\varphi(u_h^{n+1})-\varphi(u^{n+1}),v_h^{n+1}-\tilde{v}^{n+1})\\
+c\tau_n(v_h^{n+1}-v^{n+1},u_h^{n+1}-\tilde{u}^{n+1})-c\tau_n(v_h^{n+1}-v^{n+1},v_h^{n+1}-\tilde{v}^{n+1})\\
+\lambda_1(u_h^n-\tilde{u}^n,u_h^{n+1}-\tilde{u}^{n+1})+\lambda_2(v_h^n-\tilde{v}^n,v_h^{n+1}-\tilde{v}^{n+1})\\
+\tau_n\left[(\lambda_1(u^n-\tilde{u}^n)',u_h^{n+1}-\tilde{u}^{n+1})+(\lambda_2(v^n-\tilde{v}^n)',v_h^{n+1}-\tilde{v}^{n+1})\right.\\
\left.-\lambda_1(\Delta_n(\tilde{u}),u_h^{n+1}-\tilde{u}^{n+1})-\lambda_2(\Delta_n(\tilde{v}),v_h^{n+1}-\tilde{v}^{n+1})\right]. \quad (4.99)
\end{aligned}$$

As in Section 4.4.1 we present an *a-priori* error estimate using the discrete norm (4.77).

Along this section we shall use the Discrete Gronwall's Lemma, [35]:

Lemma 4.4.4 (Discrete Gronwall's Lemma)**.** *Let $t_0 := 0 < t_1 < \ldots < t_n < \ldots < t_N := T$ be a partition of $[0,T]$ into N subintervals of length τ_n and define*

$$J_\tau := \{t_0, t_1, \ldots, t_N = T\}.$$

Let $\phi(t)$ and $\psi(t)$ be non-negative functions defined on J_τ, the latter being non-decreasing. If

$$\phi(t) \leq \psi(t) + C\tau_n \sum_{\tau=0}^{t-\tau_n} \phi(\tau),\ t \in J_\tau,$$

then

$$\phi(t) \leq e^{Ct}\psi(t).$$

We pursue the *a-priori* estimate for the norm $|||\cdot|||_{dnlp}$ (4.77) for the implicit Euler discretization of the weak problem (3.45). Applying the Cauchy-Schwarz inequality to

equation (4.99) we get

$$\begin{aligned}\lambda_1\|u_h^{n+1}-\tilde{u}^{n+1}\|^2+\lambda_2\|v_h^{n+1}-\tilde{v}^{n+1}\|^2+\tau_n\left[a|u_h^{n+1}-\tilde{u}^{n+1}|_1^2+b|v_h^{n+1}-\tilde{v}^{n+1}|_1^2\right]\leq\\ c\tau_n\left[\|\varphi(u_h^{n+1})-\varphi(u^{n+1})\|\|u_h^{n+1}-\tilde{u}^{n+1}\|+\|\varphi(u_h^{n+1})-\varphi(u^{n+1})\|\|v_h^{n+1}-\tilde{v}^{n+1}\|\right.\\ \left.+\|v_h^{n+1}-v^{n+1}\|\|u_h^{n+1}-\tilde{u}^{n+1}\|+\|v_h^{n+1}-v^{n+1}\|\|v_h^{n+1}-\tilde{v}^{n+1}\|\right]\\ +\lambda_1\|u_h^n-\tilde{u}^n\|\|u_h^{n+1}-\tilde{u}^{n+1}\|+\lambda_2\|v_h^n-\tilde{v}^n\|\|v_h^{n+1}-\tilde{v}^{n+1}\|\\ +\tau_n\left[\lambda_1\|(u^n-\tilde{u}^n)'\|\|u_h^{n+1}-\tilde{u}^{n+1}\|+\lambda_2\|(v^n-\tilde{v}^n)'\|\|v_h^{n+1}-\tilde{v}^{n+1}\|\right.\\ \left.+\lambda_1\|\Delta_n\tilde{u}\|\|u_h^{n+1}-\tilde{u}^{n+1}\|+\lambda_2\|\Delta_n(\tilde{v})\|\|v_h^{n+1}-\tilde{v}^{n+1}\|\right].\end{aligned}$$

Now let us apply the inequality $ab\leq\frac{1}{2}[\epsilon a^2+\frac{1}{\epsilon}b^2]$ and the fact that φ is L-Lipschitz

$$\begin{aligned}\lambda_1\|u_h^{n+1}-\tilde{u}^{n+1}\|^2+\lambda_2\|v_h^{n+1}-\tilde{v}^{n+1}\|^2+\tau_n\left[a|u_h^{n+1}-\tilde{u}^{n+1}|_1^2+b|v_h^{n+1}-\tilde{v}^{n+1}|_1^2\right]\leq\\ \frac{\lambda_1}{2}\left[\|u_h^n-\tilde{u}^n\|^2+\|u_h^{n+1}-\tilde{u}^{n+1}\|^2\right]+\frac{\lambda_2}{2}\left[\|v_h^n-\tilde{v}^n\|^2+\|v_h^{n+1}-\tilde{v}^{n+1}\|^2\right]\\ +\frac{\tau_n\lambda_1}{2}\left[\|(u^n-\tilde{u}^n)'\|^2+2\|u_h^{n+1}-\tilde{u}^{n+1}\|+\|\Delta_n(\tilde{u})\|^2\right]\\ +\frac{\tau_n\lambda_2}{2}\left[\|\Delta_n(\tilde{v})\|^2+2\|v_h^{n+1}-\tilde{v}^{n+1}\|^2+\|(v^n-\tilde{v}^n)'\|^2\right]\\ +\frac{c\tau_nL}{2}\left[2\|u_h^{n+1}-u^{n+1}\|^2+\|u_h^{n+1}-\tilde{u}^{n+1}\|^2+\|v_h^{n+1}-\tilde{v}^{n+1}\|^2\right]\\ +\frac{c\tau_n}{2}\left[\|v_h^{n+1}-\tilde{v}^{n+1}\|^2+\|u_h^{n+1}-\tilde{u}^{n+1}\|^2+2\|v_h^{n+1}-v^{n+1}\|^2\right].\end{aligned}$$

Using that $\|a+b\|^2\leq 2\|a\|^2+2\|b\|^2$ we obtain

$$\begin{aligned}\lambda_1\|u_h^{n+1}-\tilde{u}^{n+1}\|^2+\lambda_2\|v_h^{n+1}-\tilde{v}^{n+1}\|^2+\tau_n\left[a|u_h^{n+1}-\tilde{u}^{n+1}|_1^2+b|v_h^{n+1}-\tilde{v}^{n+1}|_1^2\right]\leq\\ \frac{\lambda_1}{2}\left[\|u_h^n-\tilde{u}^n\|^2+\|u_h^{n+1}-\tilde{u}^{n+1}\|^2\right]+\frac{\lambda_2}{2}\left[\|v_h^n-\tilde{v}^n\|^2+\|v_h^{n+1}-\tilde{v}^{n+1}\|^2\right]\\ +\frac{\tau_n\lambda_1}{2}\left[\|(u^n-\tilde{u}^n)'\|^2+2\|u_h^{n+1}-\tilde{u}^{n+1}\|^2+\|\Delta_n(\tilde{u})\|^2\right]\\ +\frac{\tau_n\lambda_2}{2}\left[\|\Delta_n(\tilde{v})\|^2+2\|v_h^{n+1}-\tilde{v}^{n+1}\|^2+\|(v^n-\tilde{v}^n)'\|^2\right]\\ +\frac{c\tau_nL}{2}\left[4\|u_h^{n+1}-\tilde{u}^{n+1}\|^2+4\|\tilde{u}^{n+1}-u^{n+1}\|^2+\|u_h^{n+1}-\tilde{u}^{n+1}\|^2+\|v_h^{n+1}-\tilde{v}^{n+1}\|^2\right]\\ +\frac{c\tau_n}{2}\left[\|v_h^{n+1}-\tilde{v}^{n+1}\|^2+\|u_h^{n+1}-\tilde{u}^{n+1}\|^2+4\|v_h^{n+1}-\tilde{v}^{n+1}\|^2+4\|\tilde{v}^{n+1}-v^{n+1}\|^2\right].\end{aligned}$$

Thus,

$$\begin{aligned}\frac{\lambda_1}{2}\|u_h^{n+1}-\tilde{u}^{n+1}\|^2+\frac{\lambda_2}{2}\|v_h^{n+1}-\tilde{v}^{n+1}\|^2+\frac{\tau_n}{2}\left[a|u_h^{n+1}-\tilde{u}^{n+1}|_1^2+b|v_h^{n+1}-\tilde{v}^{n+1}|_1^2\right]\leq\\ \frac{\lambda_1}{2}\|u_h^{n}-\tilde{u}^{n}\|^2+\frac{\lambda_2}{2}\|v_h^{n}-\tilde{v}^{n}\|^2+\frac{\tau_n\lambda_1}{2}\left[\|(u^n-\tilde{u}^n)'\|^2+\|\Delta_n(\tilde{u})\|^2\right]\\ +\frac{\tau_n\lambda_2}{2}\left[\|\Delta_n(\tilde{v})\|^2+\|(v^n-\tilde{v}^n)'\|^2\right]\\ +\frac{C_7\tau_n\lambda_1}{2}\|u_h^{n+1}-\tilde{u}^{n+1}\|^2+2c\tau_nL\|\tilde{u}^{n+1}-u^{n+1}\|^2\\ +\frac{C_8\tau_n\lambda_2}{2}\|v_h^{n+1}-\tilde{v}^{n+1}\|^2+2c\tau_n\|\tilde{v}^{n+1}-v^{n+1}\|^2.\end{aligned}$$

Here

$$\begin{aligned}C_7 &:= \frac{2\lambda_1+5cL+c}{\lambda_1},\\ C_8 &:= \frac{2\lambda_2+cL+5c}{\lambda_2}.\end{aligned}$$

Multiply the previous equation by 2 and let $\beta_f=\max\{C_7,C_8\}$ to get

$$\begin{aligned}\lambda_1\|u_h^{n+1}-\tilde{u}^{n+1}\|^2 \quad + \quad & \lambda_2\|v_h^{n+1}-\tilde{v}^{n+1}\|^2+\tau_n\left[a|u_h^{n+1}-\tilde{u}^{n+1}|_1^2+b|v_h^{n+1}-\tilde{v}^{n+1}|_1^2\right]\leq\\ & \lambda_1\|u_h^{n}-\tilde{u}^{n}\|^2+\lambda_2\|v_h^{n}-\tilde{v}^{n}\|^2\\ & +\tau_n\lambda_1\left[\|(u^n-\tilde{u}^n)'\|^2+\|\Delta_n(\tilde{u})\|^2\right]\\ & +\tau_n\lambda_2\left[\|\Delta_n(\tilde{v})\|^2+\|(v^n-\tilde{v}^n)'\|^2\right]\\ & +\tau_n\beta_f\left[\lambda_1\|u_h^{n+1}-\tilde{u}^{n+1}\|^2+\lambda_2\|v_h^{n+1}-\tilde{v}^{n+1}\|^2\right]\\ & +4c\tau_nL\|\tilde{u}^{n+1}-u^{n+1}\|^2+4c\tau_n\|\tilde{v}^{n+1}-v^{n+1}\|^2.\end{aligned}\tag{4.100}$$

Adding the equations (4.100) for $n = 0$ to $N-1$ we get

$$\lambda_1\|u_h^N - \tilde{u}^N\|^2 + \lambda_2\|v_h^N - \tilde{v}^N\|^2 + \tau_n \sum_{n=0}^{N-1} a|u_h^{n+1} - \tilde{u}^{n+1}|_1^2 + b|v_h^{n+1} - \tilde{v}^{n+1}|_1^2 \leq$$
$$\lambda_1\|u_h^0 - \tilde{u}^0\|^2 + \lambda_2\|v_h^0 - \tilde{v}^0\|^2 + \beta_f\tau_n \sum_{n=0}^{N-1} \left[\lambda_1\|u_h^{n+1} - \tilde{u}^{n+1}\|^2 + \lambda_2\|v_h^{n+1} - \tilde{v}^{n+1}\|^2\right]$$
$$+\tau_n \sum_{n=0}^{N-1} \lambda_1 \left[\|(u^n - \tilde{u}^n)'\|^2 + \|\Delta_n(\tilde{u})\|^2\right] + \tau_n \sum_{n=0}^{N-1} \lambda_2 \left[\|\Delta_n(\tilde{v})\|^2 + \|(v^n - \tilde{v}^n)'\|^2\right]$$
$$+\tau_n \sum_{n=0}^{N-1} 4c \left[L\|\tilde{u}^{n+1} - u^{n+1}\|^2 + \|\tilde{v}^{n+1} - v^{n+1}\|^2\right].$$

Apply the discrete Gronwall's Lemma 4.4.4

$$\begin{aligned} |||(u_h^N - \tilde{u}(t_N), v_h^N - \tilde{v}(t_N))|||_{dnlp}^2 &\leq e^{\beta_f t_N}\left\{\lambda_1\|u_h^0 - \tilde{u}^0\|^2 + \lambda_2\|v_h^0 - \tilde{v}^0\|^2\right. \\ &+ \tau_n \sum_{n=0}^{N-1} \lambda_1 \left[\|(u^n - \tilde{u}^n)'\|^2 + \|\Delta_n(\tilde{u})\|^2\right] \\ &+ \tau_n \sum_{n=0}^{N-1} \lambda_2 \left[\|\Delta_n(\tilde{v})\|^2 + \|(v^n - \tilde{v}^n)'\|^2\right] \\ &+ \left.\tau_n \sum_{n=0}^{N-1} 4c \left[L\|\tilde{u}^{n+1} - u^{n+1}\|^2 + \|\tilde{v}^{n+1} - v^{n+1}\|^2\right]\right\}. \end{aligned} \tag{4.101}$$

We now require bounds for $\|\Delta_n(\tilde{u})\|, \|\Delta_n(\tilde{v})\|$.

$$\begin{aligned} \tau_n\Delta_n(\tilde{u}) &= \tilde{u}^{n+1} - \tilde{u}^n - \tau_n\tilde{u}_t^{n+1} = -\int_{t_n}^{t_{n+1}} (s - t_n)\tilde{u}_{tt}(s)dt \\ &\Rightarrow \tau_n\|\Delta_n(\tilde{u})\| \leq \int_{t_n}^{t_{n+1}} |s - t_n|\|\tilde{u}_{tt}\|dt \\ &\Rightarrow \|\Delta_n(\tilde{u})\| \leq \int_{t_n}^{t_{n+1}} \|\tilde{u}_{tt}\|dt. \end{aligned}$$

Applying the Poincaré-Friedrichs inequality and Lemma 4.4.2

$$\|\Delta_n(\tilde{u})\| \leq \int_{t_n}^{t_{n+1}} C_{PF}\|\nabla\tilde{u}''\|ds \leq \tau_n C_{PF} C(u).$$

Adding from $n = 0$ to $N - 1$ and using that $N\tau_n = T$

$$\sum_{n=0}^{N-1} \|\Delta_n(\tilde{u})\|^2 \leq \sum_{n=0}^{N-1} \tau_n^2 C_{PF}^2 C(u)^2 = T\tau_n C_{PF}^2 C(u)^2. \tag{4.102}$$

Similarly to (4.102) we obtain,

$$\sum_{n=0}^{N-1} \|\Delta_n(\tilde{v})\|^2 \leq T\tau_n C_{PF}^2 C(v)^2. \tag{4.103}$$

Gathering these estimates into (4.101) plus the estimates (4.89)-(4.95),

$$\begin{aligned} |||(u_h^N - \tilde{u}^N, v_h^N - \tilde{v}^N)|||_{dnlp}^2 &\leq e^{\beta_f t_N} \left\{ \lambda_1 \|u_h^0 - \tilde{u}^0\|^2 + \lambda_2 \|v_h^0 - \tilde{v}^0\|^2 \right. \\ &+ T\tau_n^2 C_{PF}^2 \left[C(u)^2 + C(v)^2 \right] \\ &+ \tau_n \sum_{n=0}^{N-1} C_5^2 h^4 \left[\lambda_1 \|u'^{n+1}\|_2^2 + \lambda_2 \|v'^{n+1}\|_2^2 \right] \\ &+ \left. \tau_n \sum_{n=0}^{N-1} 4cC_3^2 h^4 \left[L\|u^{n+1}\|_2^2 + \|v^{n+1}\|_2^2 \right] \right\}. \end{aligned} \tag{4.104}$$

Using the triangle inequality

$$\begin{aligned} |||(u_h^N - u^N, v_h^N - v^N)|||_{dnlp}^2 &\leq 2|||(u_h^N - \tilde{u}^N, v_h^N - \tilde{v}^N)|||_{dnlp}^2 \\ &+ 2|||(u^N - \tilde{u}^N, v^N - \tilde{v}^N)|||_{dnlp}^2. \end{aligned}$$

Apply (4.104)

$$\begin{aligned}
|||(u_h^N - u^N, v_h^N - v^N)|||_{dnlp}^2 &\leq 2e^{\beta_f T}\left\{\lambda_1\|u_h^0 - \tilde{u}^0\|^2 + \lambda_2\|v_h^0 - \tilde{v}^0\|^2\right. \\
&+ \tau_n \sum_{n=0}^{N-1} C_5^2 h^4 \left[\lambda_1\|u'^{n+1}\|_2^2 + \lambda_2\|v'^{n+1}\|_2^2\right] \\
&+ T\tau_n^2 C_{PF}^2 \left[C(u)^2 + C(v)^2\right] \\
&+ \left.\tau_n \sum_{n=0}^{N-1} 4cC_3^2 h^4 \left[L\|u^{n+1}\|_2^2 + \|v^{n+1}\|_2^2\right]\right\} \\
&+ 2\left[\lambda_1\|u^N - \tilde{u}^N\|^2 + \lambda_2\|v^N - \tilde{v}^N\|^2\right. \\
&+ \left.\tau_n \sum_{n=0}^{N-1} a|u^{n+1} - \tilde{u}^n|_1^2 + b|v^{n+1} - \tilde{v}^n|_1^2\right].
\end{aligned}$$

Using the estimates (4.89)-(4.90)

$$\begin{aligned}
|||(u_h^N - u^N, v_h^N - v^N)|||_{dnlp}^2 &\leq 2e^{\beta_f T}\left\{\lambda_1\|u_h^0 - \tilde{u}^0\|^2 + \lambda_2\|v_h^0 - \tilde{v}^0\|^2\right. \\
&+ \tau_n \sum_{n=0}^{N-1} C_5^2 h^4 \left[\lambda_1\|u'^{n+1}\|_2^2 + \lambda_2\|v'^{n+1}\|_2^2\right] \\
&+ T\tau_n^2 C_{PF}^2 \left[C(u)^2 + C(v)^2\right] \\
&+ \left.\tau_n \sum_{n=0}^{N-1} 4cC_3^2 h^4 \left[L\|u^{n+1}\|_2^2 + \|v^{n+1}\|_2^2\right]\right\} \\
&+ 2C_3^2 h^4 \left[\lambda_1\|u^N\|_2^2 + \lambda_2\|v^N\|_2^2\right] \\
&+ 2C_3^2\tau_n h^2 \sum_{n=0}^{N-1} \left[a\|u^{n+1}\|_2^2 + b\|v^{n+1}\|_2^2\right].
\end{aligned}$$

Theorem 4.4.4. *Assume that the approximation property* (4.88) *holds. Let* (u, v) *be the solution of* (3.45) *and* $\{(u_h^n, v_h^n)\}_{n=1}^N$ *be the solution of* (4.98)*. Then, if the assumptions 3.2.22 hold, and* $\tilde{u}, \tilde{u}', \tilde{u}'', \tilde{v}, \tilde{v}', \tilde{v}'' \in V$

$$\begin{aligned}
|||(u_h^N - u^N, v_h^N - v^N)|||_{dnlp}^2 &\leq 2e^{\beta_f T}\left\{\lambda_1\|u_h^0 - \tilde{u}^0\|^2 + \lambda_2\|v_h^0 - \tilde{v}^0\|^2\right\} \\
&\quad + C_9 h^2 + C_{10} h^4 + C_{11}\tau_n^2.
\end{aligned}$$

Here

$$\begin{aligned} C_9 &:= 2C_3^2 \max_{n=1:N} \left\{ a\|u^n\|_2^2 + b\|v^n\|_2^2 \right\}, \\ C_{10} &:= 2e^{\beta_f T} C_5^2 \max_{n=1:N} \left\{ \lambda_1 \|u'^N\|_2^2 + \lambda_2 \|v'^N\|_2^2 \right\} \\ &\quad + 8e^{\beta_f T} c C_3^2 \max_{n=1:N} \left\{ L\|u^n\|_2^2 + \|v^n\|_2^2 \right\} + 2C_3^2 \left[\lambda_1 \|u^N\|_2^2 + \lambda_2 \|v^N\|_2^2 \right], \\ C_{11} &:= T C_{PF}^2 \left[C(u)^2 + C(v)^2 \right]. \end{aligned}$$

4.4.3 *A-priori* estimates for the multilevel discretization for the NLP-model

We now extend the results of Theorems 4.4.3 and 4.4.4 to the multilevel discretization of problem (3.45). The difficulty of the multilevel problem consists in the interpolator operators Π, Π'. Due to the choice of interpolators operators made in this thesis, and the fact that $V_H \subset V_h$, Lemma 4.1.1 guarantees that the interpolator operators do not add any extra term to the error analysis. The Lemma 4.1.1 also makes it straightforward to eliminate the operators for the error analysis. We first extend the results for the semi-discrete problem, and next we deal with the fully-discrete problem.

The semi-discrete problem may be written as:

Find $(u_h, v_H) \in V_h \times V_H$*, so that for any* $(\xi, \psi) \in V_h \times V_H$

$$(\lambda_1 u_h', \xi) + a(\nabla u_h, \nabla \xi) + c(\varphi(u_h) - \Pi v_H, \xi) = (f, \xi), \tag{4.105a}$$

$$(\lambda_2 v_H', \psi) + b(\nabla v_H, \nabla \psi) + c(\Pi' \varphi(u_h) - \Pi v_H, -\psi) = (g, \psi), \tag{4.105b}$$

$$(u_h(x,0), \xi) = (u_{0h}, \xi), \qquad (v_H(x,0), \psi) = (v_{0H}, \psi). \tag{4.105c}$$

Subtracting the system (4.79) from the system (4.105)

$$\begin{aligned} &(\lambda_1 (u_h - \tilde{u})', \xi) + (a\nabla(u_h - \tilde{u}), \xi) \qquad (4.106a) \\ &\qquad + c((\varphi(u_h) - \varphi(u)) - (\Pi v_H - v), \xi) = (\lambda_1 (u - \tilde{u})', \xi), \\ &(\lambda_2 (v_h - \tilde{v})', \psi) + (b\nabla(v_h - \tilde{v}), \psi) \qquad (4.106b) \\ &\qquad + c((\Pi' \varphi(u_h) - \varphi(u)) - (v_H - v), -\psi) = (\lambda_2 (v - \tilde{v})', \psi). \end{aligned}$$

Because of Lemma 4.1.1, the system (4.106) gets reduced to a system similar to system (4.80).

$$\begin{aligned}
&(\lambda_1(u_h-\tilde{u})',\xi)+a(\nabla(u_h-\tilde{u}),\nabla\xi) && \text{(4.107a)}\\
&\qquad\qquad +c((\varphi(u_h)-\varphi(u))-(v_H-v),\xi)=(\lambda_1(u-\tilde{u})',\xi),\\
&(\lambda_2(v_H-\tilde{v})',\psi)+b(\nabla(v_H-\tilde{v}),\nabla\psi) && \text{(4.107b)}\\
&\qquad\qquad -c((\varphi(u_h)-\varphi(u))-(v_H-v),\psi)=(\lambda_2(v-\tilde{v})',\psi).
\end{aligned}$$

Therefore we can mimic the steps in Section 4.4.1 and arrive at

Theorem 4.4.5. *Suppose that the assumptions of Proposition 4.4.1 hold. Also assume that* (4.88) *holds. If* (u,v) *is the solution of* (3.45) *and* (u_h,v_H) *is the solution of* (4.105)*, then, the following estimate holds:*

$$\begin{aligned}
\|(u-u_h,v-v_H)\|_{nlp}(t)^2 \;\leq\; & C_{12}h^2+C_{13}h^4+C_{14}H^2+C_{15}H^4 \qquad \text{(4.108)}\\
& +4e^{\beta t}\left[\lambda_1\|u_{0h}-u_0\|^2+\lambda_2\|v_{0H}-v_0\|^2\right].
\end{aligned}$$

Here

$$\begin{aligned}
C_{12} &:= C_3^2 a\|u\|_2^2,\\
C_{13} &:= 4e^{\beta t}\Big\{C_6^2\lambda_2\|v_0\|^2+C_3^2L\|u\|^2_{L^2(0,T;H^2(\Omega))}\\
&\quad + C_5^2\lambda_1\|u'\|^2_{L^2(0,T;H^2(\Omega))}+2C_3^2\lambda_1\|u\|_2^2\Big\},\\
C_{14} &:= C_3^2 b\|v\|_2^2,\\
C_{15} &:= 4e^{\beta t}\Big\{C_6^2\lambda_2\|v_0\|^2+C_3^2\|v\|^2_{L^2(0,T;H^2(\Omega))}+C_5^2\ \lambda_2\|v'\|^2_{L^2(0,T;H^2(\Omega))}+2C_3^2\lambda_2\|v\|_2^2\Big\}.
\end{aligned}$$

Next we consider the fully-discrete problem:
For each n, $0\leq n\leq N$, *find* $(u_h^{n+1},v_H^{n+1})\in V_h\times V_H$ *such that for all* $(\xi,\psi)\in V_h\times V_H$

$$\begin{aligned}
&(\lambda_1\partial^n u_h,\xi)+(a\nabla u_h^{n+1},\nabla\xi)+c(\varphi(u_h^{n+1})-\Pi v_H^{n+1},\xi)=(f^{n+1},\xi), && \text{(4.109a)}\\
&(\lambda_2\partial^n v_H,\psi)+(b\nabla v_H^{n+1},\nabla\psi)+c(\Pi'(\varphi(u_h^{n+1})-\Pi v_H^{n+1}),-\psi)=(g^{n+1},\psi).
\end{aligned}$$

Again because of the properties of Π, Π' (4.2), the problem (4.109) gets reduced to the problem (4.98).

Theorem 4.4.6. *Suppose that the assumptions of Proposition 4.4.4 hold. Let (u, v) be the solution of (3.45) and $\{(u_h^n, v_H^n)\}_{n=1}^N$ be the solution of (4.109), then*

$$\begin{aligned} |||(u_h^N - u^N, v_H^N - v^N)|||_{dnlp}^2 &\leq 2e^{\beta_f T}\left\{\lambda_1\|u_h^0 - \tilde{u}^0\|^2 + \lambda_2\|v_H^0 - \tilde{v}^0\|^2\right\} \\ &+ C_{16}h^2 + C_{17}h^4 + C_{18}H^2 + C_{19}H^4 + C_{20}\tau_n^2. \end{aligned}$$

Here

$$\begin{aligned} C_{16} &:= 2C_3^2 \max_{n=1:N}\left\{a\|u^n\|_2^2\right\}, \\ C_{17} &:= 2e^{\beta_f T}C_5^2 \max_{n=1:N}\left\{\lambda_1\|u'^N\|_2^2\right\} + 8e^{\beta_f T}cC_3^2 \max_{n=1:N}\left\{L\|u^n\|_2^2\right\} + 2C_3^2\lambda_1\|u^N\|_2^2, \\ C_{18} &:= 2C_3^2 \max_{n=1:N}\left\{b\|v^n\|_2^2\right\}, \\ C_{19} &:= 2e^{\beta_f T}C_5^2 \max_{n=1:N}\left\{\lambda_2\|v'^N\|_2^2\right\} + 8e^{\beta_f T}cC_3^2 \max_{n=1:N}\left\{\|v^n\|_2^2\right\} + 2C_3^2\lambda_2\|v^N\|_2^2, \\ C_{20} &:= TC_{PF}^2\left[C(u)^2 + C(v)^2\right]. \end{aligned}$$

4.5 LP model

First, we present *a-priori* error estimates for the LP-model as a particular case of the Theorem 4.4.6. Second, we develop an *a-posteriori* error estimator for the LP-model (3.32). Our work is an extension of [15] for the scalar heat equation to a reaction-diffusion system, and also is an extension of our results in [30], described in Section 4.3, for elliptic systems to a parabolic system. The main challenges in extending [15] is to deal with the coupling term $c(u - v)$, to develop a robust estimator, and to deal the interpolation between the spaces.

We need stronger assumptions than Assumptions 3.2.16 to prove the error estimates.

Assumptions 4.5.1.

DB1. Each function in $\mathcal{P} = \{\lambda_1, \lambda_2, a, b, c\}$ is a positive constant.

DB2. The data $(f, g) \in C([0, T], L^2(\Omega)) \times C([0, T], L^2(\Omega))$.

DB3. The initial data $\vec{u}_0 \in V^2$.

4.5.1 Discrete Models

The LP-problem includes spatial and time derivatives. We discretize the problem in two steps. First we discretize the time derivative using the implicit Euler scheme that is unconditionally stable. We call the resulting system semi-discrete. Later, we discretize the time derivatives using the FEM and arrive at the fully-discrete problem.

4.5.1.1 Semi-discrete problem

In order to describe the time discretization of the system (3.32) we introduce a partition of the interval $[0,T]$ into subintervals $[t_{n-1},t_n]$, $1 \le n \le N$, such that $0 = t_0 < t_1 < \ldots < t_N = T$. We denote by τ_n the length of the interval $[t_{n-1},t_n]$ and by σ_τ the maximum ratio between to consecutive time steps, i.e., $\sigma_\tau := \max_{2\le n\le N} \frac{\tau_n}{\tau_{n-1}}$. For uniform time-stepping, $\sigma_\tau = 1$.

We apply the implicit Euler scheme to get to the semi-discrete problem:

Find a sequence $(u^n, v^n)_{0\le n\le N} \in (L_2(\Omega)\times V^N)\times(L_2(\Omega)\times V^N)$ *such that for* $1 \le n \le N$, *for all* $(\phi,\psi)\in V^2$

$$(\lambda_1 u^n,\phi) + \tau_n\left[(a\nabla u^n,\nabla\phi) + (c(u^n - v^n),\phi)\right] = \tau_n(f^n,\phi) + (\lambda_1 u^{n-1},\phi),\ \text{in } \Omega, \tag{4.110a}$$

$$(\lambda_2 v^n,\psi) + \tau_n\left[(b\nabla v^n,\nabla\psi) + (c(v^n - u^n),\psi)\right] = \tau_n(g^n,\psi) + (\lambda_2 v^{n-1},\psi),\ \text{in } \Omega, \tag{4.110b}$$

$$u(\cdot,0) = u_0 \quad v(\cdot,0) = v_0,\ \text{in } \Omega. \tag{4.110c}$$

Between the nodes in the partition of the time interval $[0,T]$ we extend the semi-discrete solution to be piecewise linear in time via the following definition.

Definition 4.5.2. *For any sequence* $\{z^n\}_{1\le n\le N}$ *define the affine function* z_τ *via*

$$z_\tau(t) = z^n - \frac{t_n - t}{\tau_n}(z^n - z^{n-1}) \quad \textit{for any } t\in[t_{n-1},t_n]. \tag{4.111}$$

4.5.1.2 Fully-discrete problem

In this section we describe the spatial discretization of the semi-discrete problem (4.110).

Find $\{(u_h^n, v_H^n)\}_{0\le n\le N} \in (V_{h,0}, V_{H,0}) \times \prod_{n=1}^{N}(V_{h,n}, V_{H,n})$ *such that for* $1 \le n \le N$, $\forall(\phi_h, \psi_H) \in V_{h,n} \times V_{H,n}$

$$\tau_n^{-1}(\lambda_1(u_h^n - u_h^{n-1}), \phi_h) + (a\nabla u_h^n, \nabla\phi_h) + (c(u_h^n - \Pi v_H^n), \phi_h) = (f^n, \phi_h), \quad (4.112a)$$

$$\tau_n^{-1}(\lambda_2(v_H^n - v_H^{n-1}, \psi_H) + (b\nabla v_H^n, \nabla\psi_H) + (c(v_H^n - \Pi' u_h^n), \psi_H) = (g^n, \psi_H), \quad (4.112b)$$

$$(u_h^0, v_H^0) = \mathcal{I}_h(u_0, v_0) \text{ in } \Omega. \quad (4.112c)$$

Here $\mathcal{I}_h$ denotes an interpolator or projection operator into $(V_{h,0}, V_{H,0})$, $\Pi : V_H \to V_h$ is the interpolation operator. Also, $\Pi' : V_h \to V_H$ is defined in Definition 4.1.2.

We assume that the problem (4.112) has a unique solution $(u_{h,n}, v_{H,n}) \in V_{h,n} \times V_{H,n}$ for $f, g \in C^0(0, T; V')$. This can be shown by following the same steps of Lemma 3.2.5.

4.5.2 *A-priori* estimates for the LP-model

We consider here the NLP-model for $\varphi(u) = u$, thus the Lipschitz constant $L = 1$. We state the *a-priori* estimate as a particular case of Theorem 4.4.6.

Corollary 4.5.3. *Suppose that equation* (4.88) *holds. Let* (u, v) *be the solution of* (3.32) *and* $\{(u_h^n, v_H^n)\}_{n=1}^N$ *be the solution of* (4.112)*, then*

$$\begin{aligned} |||(u_h^N - u^N, v_H^N - v^N)|||_{dnlp}^2 &\le 2e^{\beta_f T}\left\{\lambda_1\|u_h^0 - \tilde{u}^0\|^2 + \lambda_2\|v_H^0 - \tilde{v}^0\|^2\right\} \quad (4.113)\\ &+ C_{21}h^2 + C_{22}h^4 + C_{23}H^2 + C_{24}H^4 + C_{25}\tau_n^2. \end{aligned}$$

Here

$$\begin{aligned} C_{21} &:= 2C_3^2 \max_{n=1:N}\left\{a\|u^n\|_2^2\right\},\\ C_{22} &:= 2e^{\beta_f T}C_5^2 \max_{n=1:N}\left\{\lambda_1\|u'^N\|_2^2\right\} + 8e^{\beta_f T}cC_3^2 \max_{n=1:N}\left\{\|u^n\|_2^2\right\} + 2C_3^2\lambda_1\|u^N\|_2^2,\\ C_{23} &:= 2C_3^2 \max_{n=1:N}\left\{b\|v^n\|_2^2\right\},\\ C_{24} &:= 2e^{\beta_f T}C_5^2 \max_{n=1:N}\left\{\lambda_2\|v'^N\|_2^2\right\} + 8e^{\beta_f T}cC_3^2 \max_{n=1:N}\left\{\|v^n\|_2^2\right\} + 2C_3^2\lambda_2\|v^N\|_2^2,\\ C_{25} &:= TC_{PF}^2\left[C(u)^2 + C(v)^2\right]. \end{aligned}$$

That is, $|||(u_h^N - u^N, v_H^N - v^N)|||_{dnlp} = O(h + H + \max_{n=1:N}\tau_n)$. Next we define the energy norms of the LP-model.

4.5.3 Norms

We begin by defining the two norms that are going to be used in the sequel. We define two energy norms; a continuous and a discrete energy norm. In Lemma 4.5.1, we show that the two norms are equivalent. The same procedure can be found in [15]. We recall the definition of the form $B(\cdot,\cdot)$, equation (3.33)

$$B(\vec{u},\vec{u}) = \|a^{1/2}\nabla u\|^2 + \|b^{1/2}\nabla v\|^2 + \|c^{1/2}(u-v)\|^2.$$

Notation. *To simplify the exposition for any* $\vec{u}$

$$\mathcal{B}(\vec{u}) := B(\vec{u},\vec{u}). \tag{4.114}$$

Also note that for $\vec{u} = (u, v)$*, when necessary for clarity, we might write*

$$\mathcal{B}(\vec{u}) = \mathcal{B}(u, v).$$

Definition 4.5.4. *For any* $\vec{u} \in V^2$

$$[[\vec{u}]]^2(t) = \|\lambda_1^{1/2}u(t)\|^2 + \|\lambda_2^{1/2}v(t)\|^2 + \int_0^t \mathcal{B}(\vec{u}), \tag{4.115}$$

and for any sequence $\{\vec{u}^n\}_{n=1} \in V^n \times V^n$

$$[[\vec{u}^m]]_n^2 = \|\lambda_1^{1/2}u^n\|^2 + \|\lambda_2^{1/2}v^n\|^2 + \sum_{m=1}^{n} \tau_m \mathcal{B}(\vec{u}^m). \tag{4.116}$$

Using the definition (4.111) we can see that

$$\int_{t_{n-1}}^{t_n} \mathcal{B}(\vec{u}_\tau) \geq \frac{\tau_n}{4}\mathcal{B}(\vec{u}^n). \tag{4.117}$$

Now we establish the "equivalence" between the norms (4.115) and (4.116).

Lemma 4.5.1. *For any sequence* $\{\vec{u}_n\}_{0\leq n\leq N} \in (V^{N+1})^2$

$$\frac{1}{4}[[\vec{u}^m]]_n^2 \leq [[\vec{u}_\tau]]^2(t_n) \leq \frac{1}{2}\left(1 + \frac{1}{\sigma_\tau}\right)[[\vec{u}^m]]_n^2 + \frac{\tau_1}{2}\mathcal{B}(\vec{u}_0), \tag{4.118}$$

where B is defined by (3.33).

Proof. The proof follow the same steps as the proof of Lemma 2.1 in [15]. Nevertheless, we present the proof in here for completeness. We want to relate $[[(u_\tau, v_\tau)]]^2(t_n)$ to $[[(u^m, v^m)]]_n^2$. By definition

$$[[(u_\tau, v_\tau)]]^2(t_n) = \|\lambda_1^{1/2} u_\tau(t_n)\|^2 + \|\lambda_2^{1/2} v_\tau(t_n)\|^2 + \int_0^{t_n} \mathcal{B}(\vec{u}_\tau). \tag{4.119}$$

But $u_\tau(t_n) = u^n$ and $v_\tau(t_n) = v^n$, thus

$$[[(u_\tau, v_\tau)]]^2(t_n) = \|\lambda_1^{1/2} u^n\|^2 + \|\lambda_2^{1/2} v^n\|^2 + \int_0^{t_n} \mathcal{B}(\vec{u}_\tau). \tag{4.120}$$

Since

$$[[(u^m, v^m)]]_n^2 = \|\lambda_1^{1/2} u^n\|^2 + \|\lambda_2^{1/2} v^n\|^2 + \sum_{m=1}^{n} \tau_m \mathcal{B}(\vec{u}^m),$$

we are, in fact, left to compare $\int_0^{t_n} \mathcal{B}(\vec{u}_\tau)$ to $\sum_{m=1}^n \tau_m \mathcal{B}(\vec{u}^m)$.

By definition,

$$\int_{t_{m-1}}^{t_m} \mathcal{B}(\vec{u}_\tau) = \int_{t_{m-1}}^{t_m} \|a^{1/2}\nabla u\|^2 + \|b^{1/2}\nabla v\|^2 + \|c^{1/2}(u-v)\|^2.$$

From the first term in the right-hand side of the equation above

$$\begin{aligned}
\int_{t_{m-1}}^{t_m} \|a^{1/2}\nabla u_\tau\|^2 dt \overset{(4.111)}{=} & \; a\int_{t_{m-1}}^{t_m} \|\nabla u^m - \frac{t_m - s}{\tau_m}(\nabla u^m - \nabla u^{m-1})\|^2 dt \\
= & \; a\left[\frac{\tau_m}{3}\left(1 - \frac{t_m - s}{\tau_m}\right)^3\right]_{t_{m-1}}^{t_m} \|\nabla u^m\|^2 \\
+ & \; 2\left(\frac{-1}{2}\frac{(t_m - s)^2}{\tau_m} + \frac{1}{3}\frac{(t_m - s)^3}{\tau_m^2}\right)\Bigg|_{t_{m-1}}^{t_m} < \nabla u^m, \nabla u^{m-1} > \\
+ & \; \frac{\tau_m}{3}\left(\frac{t_m - s}{\tau_m}\right)^3 \|\nabla u^{m-1}\|^2 \Bigg|_{t_{m-1}}^{t_m}.
\end{aligned}$$

Thus,

$$\int_{t_{m-1}}^{t_m} \|a^{1/2}\nabla u_\tau\|^2 dt = \frac{a\tau_m}{3}\left[\|\nabla u^m\|^2 + <\nabla u^m, \nabla u^{m-1}> + \|\nabla u^{m-1}\|^2\right]. \quad (4.121)$$

Applying the inequality $xy \geq -x^2 - \frac{1}{4}y^2$, we get

$$\begin{aligned}\int_{t_{m-1}}^{t_m} \|a^{1/2}\nabla u_\tau\|^2 dt &\geq a\frac{\tau_m}{3}\left[\|\nabla u^m\|^2 - \|\nabla u^{m-1}\|^2 - \frac{1}{4}\|\nabla u^m\|^2 + \|\nabla u^{m-1}\|^2\right] \\ &\geq \frac{\tau_m}{4}\|a^{1/2}\nabla u^m\|^2.\end{aligned}$$

Similarly we get

$$\begin{aligned}\int_{t_{m-1}}^{t_m} \|b^{1/2}\nabla v_\tau\|^2 dt &\geq \frac{\tau_m}{4}\|b^{1/2}\nabla v^m\|^2, \\ \int_{t_{m-1}}^{t_m} \|c^{1/2}(u_\tau - v_\tau)\|^2 dt &\geq \frac{\tau_m}{4}\|c^{1/2}(u^m - v^m)\|^2.\end{aligned}$$

Thus,

$$\int_{t_{m-1}}^{t_m} \mathcal{B}(\vec{u}_\tau) \geq \frac{\tau_m}{4}\mathcal{B}(\vec{u}_m). \quad (4.122)$$

Adding from $m = 1$ to n

$$\int_0^{t_n} \mathcal{B}(\vec{u}_\tau) = \sum_{m=1}^{n}\int_{t_{m-1}}^{t_m} \mathcal{B}(\vec{u}_\tau) \geq \frac{1}{4}\sum_{m=1}^{n}\tau_m\mathcal{B}(\vec{u}^m).$$

Therefore

$$[[(u_\tau, v_\tau)]]^2(t_n) \geq \frac{1}{4}[[(u^m, v^m)]]_n^2.$$

On the other hand, if we apply the inequality $xy \leq \frac{x^2}{2} + \frac{y^2}{2}$ to (4.121) we get

$$\int_{t_{n-1}}^{t_n} \|a^{1/2}\nabla u_\tau\|^2 dt \leq a\frac{\tau_n}{2}\left[\|\nabla u^n\|^2 + \|\nabla u^{n-1}\|^2\right].$$

So,

$$\int_{t_{n-1}}^{t_n} \|a^{1/2}\nabla u_\tau\|^2 dt \leq \frac{\tau_n}{2}\left[\|a^{1/2}\nabla u^n\|^2 + \|a^{1/2}\nabla u^{n-1}\|^2\right].$$

Similarly we have

$$\int_{t_{n-1}}^{t_n} \|b^{1/2}\nabla v_\tau\|^2 dt \leq \frac{\tau_n}{2}\left[\|b^{1/2}\nabla v^n\|^2 + \|b^{1/2}\nabla v^{n-1}\|^2\right],$$

and

$$\int_{t_{n-1}}^{t_n} \|c^{1/2}(u_\tau - v_\tau)\|^2 dt \leq \frac{\tau_n}{2}\left[\|c^{1/2}(u^n - v^n)\|^2 + \|c^{1/2}(u^{n-1} - v^{n-1}\|^2\right].$$

So,

$$\int_{t_{n-1}}^{t_n} \mathcal{B}(\vec{u}_\tau) \leq \frac{\tau_n}{2}\left(\mathcal{B}(\vec{u}^n) + \mathcal{B}(\vec{u}^{n-1})\right)$$

$$\begin{aligned}
\int_0^{t_n} \mathcal{B}(\vec{u}_\tau) &= \sum_{m=1}^{n} \int_{t_{m-1}}^{t_m} \mathcal{B}(\vec{u}_\tau) \\
&\leq \sum_{m=1}^{n} \frac{\tau_m}{2}\left(\mathcal{B}(\vec{u}^m) + \mathcal{B}(\vec{u}^{m-1})\right) \\
&= \sum_{m=1}^{n} \frac{\tau_m}{2}\mathcal{B}(\vec{u}^m) + \sum_{m=1}^{n} \frac{\tau_m}{2}\mathcal{B}(\vec{u}^{m-1}) \\
&= \sum_{m=1}^{n} \frac{\tau_m}{2}\mathcal{B}(\vec{u}^m) + \sum_{m=1}^{n-1} \frac{\tau_{m+1}}{2}\mathcal{B}(\vec{u}^{m-1}) + \frac{\tau_1}{2}\mathcal{B}(\vec{u}_0).
\end{aligned}$$

Note that for any $2 \leq m \leq N$, $\sigma_\tau \geq \frac{\tau_{m+1}}{\tau_m} \Rightarrow \tau_{m+1} \leq \frac{\tau_m}{\sigma_\tau}$, and hence

$$\begin{aligned}
\int_0^{t_n} \mathcal{B}(\vec{u}_\tau) &\leq \sum_{m=1}^{n} \frac{\tau_m}{2}\mathcal{B}(\vec{u}^m) + \sum_{m=1}^{n-1} \frac{\tau_m}{2\sigma_\tau}\mathcal{B}(\vec{u}^{m-1}) + \frac{\tau_1}{2}\mathcal{B}(\vec{u}_0) \\
&= \frac{1}{2}\left(1+\frac{1}{\sigma_\tau}\right)\sum_{m=1}^{n-1} \frac{\tau_m}{2}\mathcal{B}(\vec{u}^m) + \frac{\tau_n}{2}\mathcal{B}(\vec{u}^n) + \frac{\tau_1}{2}\mathcal{B}(\vec{u}_0) \\
&\leq \frac{1}{2}\left(1+\frac{1}{\sigma_\tau}\right)\sum_{m=1}^{n} \frac{\tau_m}{2}\mathcal{B}(\vec{u}_0) + \frac{\tau_1}{2}\mathcal{B}(\vec{u}_0).
\end{aligned}$$

So,

$$[[(u_\tau, v_\tau)]]^2(t_n) \leq \frac{1}{2}\left(1+\frac{1}{\sigma_\tau}\right)[[(u^m, v^m)]]_n^2 + \frac{\tau_1}{2}\mathcal{B}(\vec{u}_0).$$

□

4.5.4 Error indicators

The *a-posteriori* error estimator for the LP-model is composed of two parts. A temporal part, called time error indicator, and a spatial part, called space error indicator. For each n, $1 \leq n \leq N$, we define the time error indicator, T_n:

$$T_n^2 := \frac{\tau_n}{3}\mathcal{B}(u_h^n - u_h^{n-1}, v_H^n - v_H^{n-1}). \tag{4.123}$$

The time error indicator indicates the contribution of the time-stepping in the error.

For each n, $1 \leq n \leq N$, any $T \in \mathcal{T}_{n,h}$ and any $K \in \mathcal{T}_{n,H}$ we define the space error indicators, $\mathcal{S}_{n,T,u}, \mathcal{S}_{n,K,v}$:

$$\mathcal{S}_{n,T,u} := \left(\theta_{lp,u,T}^2 \|R_{T,u}^n\|^2 + \frac{1}{2}\sum_{E\in\mathcal{E}_T} \gamma_{lp,u,E}^2 \|R_{E,u}^n\|^2\right)^{1/2}, \tag{4.124}$$

$$\mathcal{S}_{n,K,v} := \left(\theta_{lp,v,K}^2 \|R_{K,v}^n\|^2 + \frac{1}{2}\sum_{F\in\mathcal{E}_K} \gamma_{lp,v,F}^2 \|R_{F,v}^n\|^2\right)^{1/2}. \tag{4.125}$$

Here

$$
\begin{aligned}
R^n_{T,u} &:= f^n - \lambda_1 \frac{u^n_h - u^{n-1}_h}{\tau_n} + \nabla \cdot (a \nabla u^n_h) - c(u^n_h - v^n_H), && (4.126)\\
R^n_{K,v} &:= g^n - \lambda_2 \frac{v^n_H - v^{n-1}_H}{\tau_n} + \nabla \cdot (b \nabla v^n_H) - c(v^n_H - u^n_h), && (4.127)\\
R^n_{E,u} &:= [a \partial_\nu u^n_h]_E, && (4.128)\\
R^n_{E,v} &:= [b \partial_\nu v^n_H]_F, && (4.129)\\
\theta_{lp,u,S} &:= \min\{h_S a^{-1/2}, \max\{c^{-1/2}, h_S b^{-1/2}\}\}, \quad S \in \mathcal{T}_{n,h} \cup \mathcal{E}_{n,h}, && (4.130)\\
\theta_{lp,v,S} &:= \min\{H_S b^{-1/2}, \max\{c^{-1/2}, H_S a^{-1/2}\}\}, \quad S \in \mathcal{T}_{n,H} \cup \mathcal{E}_{n,H}, && (4.131)\\
\gamma_{lp,u,E} &:= 2h_E^{-1/2} \theta_{lp,u,E}, && (4.132)\\
\gamma_{lp,v,F} &:= 2h_F^{-1/2} \theta_{lp,v,F}, && (4.133)
\end{aligned}
$$

where $[\partial_\nu w]_E$ denotes the jump of the normal derivative of w through the edge E.

Note here the similarity with the scaling constants for error estimator of the E-model (4.23)-(4.26). We also would like to point out that the scaling factors (4.130)-(4.133) are well defined and finite for the case where $a = 0$ or $b = 0$ exclusively. These cases account for the WR and PP models so we can apply to these models the error estimators to be developed in this Section.

Finally, we would like to stress an important difference between the results presented in [15] and our results. In [15], the spatial indicator is non-scaled, in the sense that it does not take into account the parameters of the problem. To be precise, in [15], $\theta_{lp,u,S} = h_S$, $\theta_{lp,v,S} = H_S$, $\gamma_{lp,u,E} = h_E^{1/2}$, $\gamma_{lp,v,F} = h_F^{1/2}$. As illustrated by Example 4.2.1 and discussed in [55], a non-scaled error estimator leads to non-robustness of the estimator. Other difference is that we deal with a system with a multilevel finite element approximation, while only the scalar heat equation (linear and quasilinear) is considered in [15].

4.5.5 Upper Bound

Our goal is to achieve an upper bound as in Theorem 4.3.4 for the E-model to bound above the error

$$[[(u, v) - (u_{h\tau}, v_{H\tau})]](t_n),$$

for $1 \leq n \leq N$. We prove this bound by dividing it in two parts $[[(u,v)-(u_\tau,v_\tau)]](t_m)$ and $[[(u_\tau,v_\tau)-(u_{h\tau},v_{H\tau})]](t_n)$. To bound the first part we bound the error of approximating the weak problem (3.32) by the semi-discrete problem (4.110). The second part bounds the error of approximating the semi-discrete problem (4.110) by the fully-discrete problem (4.112). We follow the same techniques used in [15], the difference in here is that we have a coupled system instead of a scalar problem.

First let us estimate $[[(u,v)-(u_\tau,v_\tau)]](t_m)$. Note that

$$\frac{\partial u_\tau}{\partial t} = \frac{u^m - u^{m-1}}{\tau_n} \quad \text{for any } \ t \in [t_{m-1}, t_m]. \tag{4.134}$$

Let

$$T_1 := (\lambda_1 u'_\tau, \phi) + (a\nabla u_\tau, \nabla\phi) + (c(u_\tau - v_\tau), \phi).$$

Apply (4.134) to T_1

$$\begin{aligned} T_1 &= \tau_n^{-1}\left(\lambda_1(u^m - u^{m-1}), \phi\right) + (a\nabla u_\tau, \nabla\phi) + (c(u_\tau - v_\tau), \phi) \\ &= \underbrace{\tau_n^{-1}\left(\lambda_1(u^m - u^{m-1}), \phi\right) + (a\nabla u^m, \nabla\phi) + (c(u^m - v^m), \phi)}_{\overset{(4.110a)}{=}(f^m,\phi)} \\ &\quad +(a\nabla(u_\tau - u^m), \nabla\phi) + (c((u_\tau - u^m) - (v_\tau - v^m)), \phi) \\ &= (f^m, \phi) + (a\nabla(u_\tau - u^m), \nabla\phi) + (c((u_\tau - u^m) - (v_\tau - v^m)), \phi). \end{aligned} \tag{4.135}$$

Similarly,

$$\begin{aligned} (\lambda_2 v'_\tau, \psi) + (b\nabla v_\tau, \nabla\psi) + (c(u_\tau - v_\tau), -\phi) &= (g^m, \psi) + (b\nabla(v_\tau - v^m), \nabla\psi) \\ &+ (c((u_\tau - u^m) - (v_\tau - v^m)), -\psi). \end{aligned} \tag{4.136}$$

Subtract equations (4.135) and (4.136) from equations (3.25a) and (3.25b), respectively,

$$\begin{aligned} (\lambda_1(u - u_\tau)', \phi) &+ (\lambda_2(v - v_\tau)', \psi) + B((u_\tau - u^m, v_\tau - v^m), (\phi, \psi)) \\ &= (f - f^m, \phi) + (g - g^m, \psi) + B((u_\tau - u^m, v_\tau - v^m), (\phi, \psi)). \end{aligned} \tag{4.137}$$

Now, let $\phi = u - u_\tau$ and $\psi = v - v_\tau$

$$\begin{aligned}(\lambda_1(u-u_\tau)', u-u_\tau) &+ (\lambda_2(v-v_\tau)', v-v_\tau) + \mathcal{B}(u-u_\tau, v-v_\tau) \\ &= (f-f^n, u-u_\tau) + (g-g^n, v-v_\tau) \\ &+ B((u_\tau - u^m, v_\tau - v^m), (u-u_\tau, v-v_\tau)).\end{aligned}$$

Integrate from t_{n-1} to t_n and use the property $(w', w) = \frac{1}{2}\frac{d}{dt}\|w\|^2$

$$\begin{aligned}&\frac{1}{2}\left[\|\lambda_1^{1/2}(u-u_\tau)\|^2(t_n) + \|\lambda_2^{1/2}(v-v_\tau)\|^2(t_m)\right] + \int_{t_{m-1}}^{t_m} \mathcal{B}(u-u_\tau, v-v_\tau) \qquad (4.138)\\ &= \int_{t_{m-1}}^{t_m} RHS + \frac{1}{2}\left[\|\lambda_1^{1/2}(u-u_\tau)\|^2(t_{m-1}) + \|\lambda_2^{1/2}(v-v_\tau)\|^2(t_{m-1})\right].\end{aligned}$$

Here

$$\begin{aligned}RHS &:= (f-f^m, u-u_\tau) + (g-g^m, v-v_\tau) \\ &+ B((u_\tau - u^m, v_\tau - v^m), (u-u_\tau, v-v_\tau)).\end{aligned}$$

Add equation (4.138) for $m = 1$ to n and note that by the definition of u_τ, v_τ, we have $(u-u_\tau)(0) = (v-v_\tau)(0) = 0$, to get

$$\frac{1}{2}[[(u,v) - (u_\tau, v_\tau)]]^2(t_n) \le \sum_{m=1}^{n} \int_{t_{m-1}}^{t_m} RHS.$$

Now let us estimate $\int_{t_{m-1}}^{t_m} RHS$.

$$\begin{aligned}\int_{t_{m-1}}^{t_m} RHS &= \int_{t_{m-1}}^{t_m} \Bigg[\underbrace{(f-f^m, u-u_\tau)}_{:=T_2} + \underbrace{(g-g^m, v-v_\tau)}_{:=T_3} \\ &+ \underbrace{B((u_\tau - u^m, v_\tau - v^m), (u-u_\tau, v-v_\tau))}_{:=T_4} \Bigg] dt.\end{aligned}$$

Next we estimate the terms T_2, T_3, T_4. We start with T_4. Apply the Cauchy-Schwarz inequality (3.12) twice to get

$$|\int_{t_{m-1}}^{t_m} T_4 dt| \leq \left\{\int_{t_{m-1}}^{t_m} \mathcal{B}(u_\tau - u^m, v_\tau - v^m)\right\}^{1/2} \left\{\int_{t_{m-1}}^{t_m} \mathcal{B}(u - u_\tau, v - v_\tau)\right\}^{1/2}.$$

We now are left to estimate the terms $\int_{t_{m-1}}^{t_m} T_2$, $\int_{t_{m-1}}^{t_m} T_3$.

$$\begin{aligned} |\int_{t_{m-1}}^{t_m} T_2 dt| &\overset{(3.12)}{\leq} \left\{\int_{t_{m-1}}^{t_m} \frac{1}{a}\|f - f^m\|^2 dt\right\}^{1/2} \left\{\int_{t_{m-1}}^{t_m} \|a^{1/2}(u - u_\tau)\|^2 dt\right\}^{1/2} \\ &\overset{(3.11)}{\leq} \left\{\int_{t_{m-1}}^{t_m} \frac{C_{PF}^2}{a}\|f - f^m\|^2 dt\right\}^{1/2} \left\{\int_{t_{m-1}}^{t_m} \|a^{1/2}\nabla(u - u_\tau)\|^2 dt\right\}^{1/2}. \end{aligned}$$

On the other hand, using the inequalities (3.12) and (3.11)

$$\begin{aligned} |\int_{t_{m-1}}^{t_m} T_2 dt| &\leq \int_{t_{m-1}}^{t_m} |(f - f^m, (u - u_\tau) - (v - v_\tau))| dt + \int_{t_{m-1}}^{t_m} |(f - f^m, v - v_\tau)| dt \\ &\leq \left\{\int_{t_{m-1}}^{t_m} \frac{1}{c}\|f - f^m\|^2 dt\right\}^{1/2} \left\{\int_{t_{m-1}}^{t_m} \|c^{1/2}((u - u_\tau) - (v - v_\tau)\|^2 dt\right\}^{1/2} \\ &+ \left\{\int_{t_{m-1}}^{t_m} \frac{C_{PF}^2}{b}\|f - f^m\|^2 dt\right\}^{1/2} \left\{\int_{t_{m-1}}^{t_m} \|b^{1/2}\nabla(v - v_\tau)\|^2 dt\right\}^{1/2}. \end{aligned}$$

Combining the two inequalities above we arrive at

$$|\int_{t_{m-1}}^{t_m} T_2 dt| \leq F_c \left\{\int_{t_{m-1}}^{t_m} \|f - f^m\|^2 dt\right\}^{1/2} \left\{\int_{t_{m-1}}^{t_m} \mathcal{B}(u - u_\tau, v - v_\tau)\right\}^{1/2}.$$

Here,

$$F_c := \min\left\{\frac{C_{PF}^2}{a^{1/2}}, \frac{1}{c^{1/2}} + \frac{C_{PF}^2}{b^{1/2}}\right\}. \tag{4.139}$$

Similarly,

$$|\int_{t_{m-1}}^{t_m} T_3 dt| \leq G_c \left\{ \int_{t_{m-1}}^{t_n} \|g - g^m\| dt \right\}^{1/2} \left\{ \int_{t_{m-1}}^{t_m} \mathcal{B}(u - u_\tau, v - v_\tau) \right\}^{1/2}.$$

Here,

$$G_c := \min \left\{ \frac{C_{PF}^2}{b^{1/2}}, \frac{1}{c^{1/2}} + \frac{C_{PF}^2}{a^{1/2}} \right\}. \tag{4.140}$$

To put it all together we define $\mathcal{I}_\tau$ as in [15] as the interpolation operator with values in piecewise constant functions on $[0,T]$, defined as follows: for any function w continuous on $[0,T]$, $\mathcal{I}_\tau w$ is constant on each interval $(t_{n-1}, t_n], 1 \leq n \leq N$, and $\mathcal{I}_\tau w(t_n) = w(t_n)$

$$\begin{aligned}
\sum_{m=1}^{n} \int_{t_{m-1}}^{t_m} RHS &\leq \sum_{m=1}^{n} \left\{ \left[F_c \left\{ \int_{t_{m-1}}^{t_m} \|f - f^m\| dt \right\}^{1/2} + G_c \left\{ \int_{t_{m-1}}^{t_m} \|g - g^m\| dt \right\}^{1/2} \right.\right. \\
&+ \left.\left. \left\{ \int_{t_{m-1}}^{t_m} \mathcal{B}(u_\tau - u^m, v_\tau - v^m) \right\}^{1/2} \right] \left\{ \int_{t_{m-1}}^{t_m} \mathcal{B}(u - u_\tau, v - v_\tau) \right\}^{1/2} \right\} \\
&\leq \left[F_c \left\{ \int_0^{t_n} \|f - \mathcal{I}_\tau f\| dt \right\}^{1/2} + G_c \left\{ \int_0^{t_n} \|g - \mathcal{I}_\tau g\| dt \right\}^{1/2} \right. \\
&+ \left. \left\{ \sum_{m=1}^{n} \int_{t_{m-1}}^{t_m} \mathcal{B}(u_\tau - u^m, v_\tau - v^m) \right\}^{1/2} \right] \left\{ \int_0^{t_n} \mathcal{B}(u - u_\tau, v - v_\tau) \right\}^{1/2}.
\end{aligned}$$

Therefore,

$$\frac{1}{2}[[(u - u_\tau, v - v_\tau)]](t_n) \leq C(f,g) + \left\{ \sum_{m=1}^{n} \int_{t_{m-1}}^{t_m} \mathcal{B}(u_\tau - u^m, v_\tau - v^m) \right\}^{1/2}$$

where

$$C(f,g) = F_c \left\{ \int_0^{t_n} \|f - \mathcal{I}_\tau f\| dt \right\}^{1/2} + G_c \left\{ \int_0^{t_n} \|g - \mathcal{I}_\tau g\| dt \right\}^{1/2}. \tag{4.141}$$

To simplify the left-hand side we use the definition of u_τ for $t \in [t_{n-1}, t_n]$

$$u_\tau - u^n = \frac{t_n - t}{\tau_n}(u^n - u^{n-1}).$$

Let $T_5 := \mathcal{B}(u_\tau - u^m, v_\tau - v^m)$

$$\begin{aligned}
\frac{3}{\tau_m}\int_{t_{m-1}}^{t_m} T_5 dt \quad &= \quad \mathcal{B}(u^m - u^{m-1}, v^m - v^{m-1}) \\
&\leq \quad \mathcal{B}((u^m - u_h^m) - (u^{m-1} - u_h^{m-1}), (v^m - v_H^m) - (v^{m-1} - v_H^{m-1})) \\
&\quad +\mathcal{B}(u_h^m - u_h^{m-1}, v_H^m - v_H^{m-1}) \\
&\overset{(4.122)}{\leq} \quad \frac{4}{\tau_m}\int_{t_{m-1}}^{t_m} \mathcal{B}((u-u_h)_\tau, (v-v_H)_\tau) dt \\
&+ \quad \mathcal{B}(u_h^m - u_h^{m-1}, v_H^m - v_H^{m-1}).
\end{aligned}$$

That is,

$$\int_{t_{m-1}}^{t_m} \mathcal{B}(u_\tau - u^m, v_\tau - v^m) \leq \frac{4}{3}\int_{t_{m-1}}^{t_m} \mathcal{B}((u-u_h)_\tau, (v-v_H)_\tau) dt + T_n^2.$$

Summing it over and taking the square-root we arrive at

$$\begin{aligned}
\left\{\sum_{m=1}^{n}\int_{t_{m-1}}^{t_m} \mathcal{B}(u_\tau - u^m, v_\tau - v^m)\right\}^{1/2} \quad &\leq \quad \left\{\sum_{m=1}^{n} T_n^2\right\}^{1/2} \frac{2}{\sqrt{3}} \\
&+ \quad \underbrace{\left\{\int_0^{t_n} \mathcal{B}((u-u_h)_\tau, (v-v_H)_\tau) dt\right\}^{1/2}}_{\leq [[(u-u_h)_\tau, (v-v_h)_\tau]]}.
\end{aligned}$$

We have proved the following result.

Proposition 4.5.1. *Suppose Assumptions 4.5.1 hold. The following bound for error between the solution (u, v) of (3.32) and the solution $(u^n, v^n)_{0\leq n\leq N}$ of the problem (4.110), for all t_n, $1 \leq n \leq N$:*

$$\frac{1}{2}[[(u - u_\tau, v - v_\tau)]](t_n) \leq C(f, g) + \frac{2}{\sqrt{3}}[[(u-u_h)_\tau, (v-v_H)_\tau]](t_n) + \left\{\sum_{m=1}^{n} T_m^2\right\}^{1/2} \quad (4.142)$$

Now we are left to bound $[[(u_\tau, v_\tau) - (u_{h\tau}, v_{H\tau})]](t_n)$.

4.5.5.1 Bound for $[[(u_\tau, v_\tau) - (u_{h\tau}, v_{H\tau})]](t_n)$

In here we bound the error between the semi-discrete and the fully-discrete problems, $[[(u_\tau, v_\tau) - (u_{h\tau}, v_{H\tau})]](t_n)$. Use $(v_H^n - \Pi v_H^n, \phi_h) = 0$ (see Lemma 4.1.1) in equation (4.112a) to reduce it to

$$(\lambda_1 u_h^n, \phi_h) + \tau_n \left[(a\nabla u_h^n, \nabla\phi_h) + c(u_h^n - v_H^n, \phi_h)\right] = \tau_n(f^n, \phi_h) + (\lambda_1 u_h^{n-1}, \phi_h), \quad (4.143)$$

Let $\phi = \phi_h$, in the semi-discrete equation (4.110a) and subtract it from the fully-discrete equation (4.143) to get

$$\begin{aligned} \lambda_1(u^n - u_h^n, \phi_h) \quad &+ \quad \tau_n \left[(a\nabla(u^n - u_h^n), \nabla\phi_h)\right. \\ &+ \quad \left. c((u^n - u_h^n) - (v^n - v_H^n), \phi_h)\right] = \lambda_1(u^{n-1} - u_h^{n-1}, \phi_h). \end{aligned}$$

Adding and subtracting the appropriate terms we arrive at

$$\begin{aligned} \underbrace{\lambda_1(u^n - u_h^n, \phi) + \tau_n \left[(a\nabla(u^n - u_h^n), \nabla\phi) + (c((u^n - u_h^n) - (v^n - v_H^n)), \phi)\right]}_{:=T_6} \\ = \lambda_1(u^{n-1} - u_h^{n-1}, \phi_h) + \lambda_1(u^n - u_h^n, \phi - \phi_h) \\ + \tau_n \left[(a\nabla(u^n - u_h^n), \nabla(\phi - \phi_h)) + c((u^n - u_h^n) - (v^n - v_H^n), \phi - \phi_h)\right]. \end{aligned}$$

Integrating the right hand side of the equation above by parts,

$$\begin{aligned} T_6 \quad &= \quad \tau_n \sum_{T\in\mathcal{T}_h} \left[\int_T \left(\lambda_1 \frac{u^n - u_h^n - (u^{n-1} - u_h^{n-1})}{\tau_n} - \nabla\cdot(a\nabla(u^n - u_h^n))\right.\right. \\ &+ \quad \left. c((u^n - u_h^n) - (v^n - v_H^n))\right)(\phi - \phi_h) \\ &+ \quad \left.\frac{1}{2}\sum_{e\in\partial T} \int_E [a\partial_\nu u_h^n](\phi - \phi_h)\,\right] + \lambda_1(u^{n-1} - u_h^{n-1}, \phi), \end{aligned}$$

Using the semi-discrete equation (4.110a), the right hand side of the equation above becomes

$$T_6 = \tau_n \sum_{T\in\mathcal{T}_h} \left[\int_T \left(f^n - \lambda_1 \frac{u_h^n - u_h^{n-1}}{\tau_n} + \nabla(a\nabla u_h^n) - c(u_h^n - v_H^n) \right)(\phi - \phi_h) \right. \quad (4.144)$$
$$\left. + \frac{1}{2} \sum_{E\in\partial T} \int_E [a\partial_\nu u_h^n]_E (\phi - \phi_h) \right] + \lambda_1 (u^{n-1} - u_h^{n-1}, \phi),$$

Repeating the same steps for the (4.112b) we arrive at

$$\begin{aligned} \lambda_2(v^n - v_H^n, \psi) &+ \tau_n \left[(b\nabla(v^n - v_H^n), \nabla\psi) - (c((u^n - u_h^n) - (v^n - v_H^n)), \psi) \right] \\ &= \tau_n \sum_{K\in\mathcal{T}_H} \left[\int_K \left(g^n - \lambda_2 \frac{v_H^n - v_H^{n-1}}{\tau_n} + \nabla(b\nabla v_H^n) \right.\right. \\ &- \left.\left. c(v_H^n - u_h^n)\right)(\psi - \psi_H) + \frac{1}{2} \sum_{F\in\partial K} \int_F [b\partial_\nu v_H^n]_F (\psi - \psi_H) \right] \\ &+ \lambda_2(v^{n-1} - v_H^{n-1}, \psi). \end{aligned} \quad (4.145)$$

Using the notation (4.126)-(4.129), we add both equations above and let $\phi = u^n - u_h^n$, $\psi = v^n - v_H^n$ to get to

$$\begin{aligned} \|\lambda_1^{1/2}(u^n - u_h^n)\|^2 &+ \|\lambda_2^{1/2}(v^n - v_H^n)\|^2 + \tau_n \mathcal{B}(u^n - u_h^n, v^n - v_H^n) \\ &\overset{(3.12)}{\leq} \sum_{T\in\mathcal{T}_h} \tau_n \left[\|R_{Tu}^n\|_T \|\phi - \phi_h\|_T + \|R_{Tv}^n\|_T \|\psi - \psi_H\|_T \right. \\ &+ \left. \frac{1}{2} \sum_{E\in\partial T} \|R_{Eu}^n\|_E \|\phi - \phi_h\|_E + \|R_{Ev}^n\|_E \|\psi - \psi_H\|_E \right] \\ &+ \|\lambda_1^{1/2}(u^{n-1} - u_h^{n-1})\| \|\lambda_1^{1/2}(u^n - u_h^n)\| \\ &+ \|\lambda_2^{1/2}(v^{n-1} - v_H^{n-1})\| \|\lambda_2^{1/2}(v^n - v_H^n)\|. \end{aligned}$$

Applying Young's inequality 3.14 in the two last terms and adding the equations for $m = 1$ to n

$$\begin{aligned}\|\lambda_1^{1/2}(u^n - u_h^n)\|^2 + \|\lambda_2^{1/2}(v^n - v_H^n)\|^2 + 2\sum_{m=1}^{n}\tau_m\mathcal{B}(u^m - u_h^m, v^m - v_H^m) \qquad (4.146)\\ \leq 2\sum_{m=1}^{n}\sum_{T\in\mathcal{T}_h}\tau_n\left[\|R_{Tu}^m\|_T\|\phi-\phi_h\|_T + \|R_{Tv}^m\|_T\|\psi-\psi_H\|_T\right.\\ \left. + \frac{1}{2}\sum_{E\in\partial T}\|R_{Eu}^m\|_E\|\phi-\phi_h\|_E + \|R_{Ev}^m\|_E\|\psi-\psi_H\|_E\right]\\ +\|\lambda_1^{1/2}(u^0 - u_h^0)\|^2 + \|\lambda_2^{1/2}(v^0 - v_H^0)\|^2.\end{aligned}$$

Next we need to establish some interpolation results to be able to estimates the terms of the type $\|\phi - \phi_h\|$ in the equation above.

4.5.5.2 Interpolation Results

In here we mimic the same procedures done in Section 4.3.2.2. Recall that $V_H \subseteq V_h$. Let ϕ_h, ψ_h be the interpolator of ϕ, ψ into V_h respectively and ϕ_H, ψ_H be the interpolator of ϕ, ψ into V_H respectively.

$$\begin{aligned}\|\phi-\phi_h\|_T &\leq \|(\phi-\phi_h)-(\psi-\psi_h)\|_T + \|\psi-\psi_h\|_T \overset{(4.21)}{\leq} \|\phi-\psi\|_{\tilde{\omega}_T} + h_T\|\nabla\psi\|_{\tilde{\omega}_T}\\ &= \frac{1}{c^{1/2}}\|c^{1/2}(\phi-\psi)\|_{\tilde{\omega}_T} + \frac{h_T}{b^{1/2}}\|b^{1/2}\nabla\psi\|_{\tilde{\omega}_T}\\ &\leq \max\{\frac{1}{c^{1/2}}, \frac{h_T}{b^{1/2}}\}\left(\|c^{1/2}(\phi-\psi)\|_{\tilde{\omega}_T} + \|b^{1/2}\nabla\psi\|_{\tilde{\omega}_T}\right)\\ &\leq \sqrt{2}\max\{\frac{1}{c^{1/2}}, \frac{h_T}{b^{1/2}}\}\left(\int_{\tilde{\omega}_T} c(\phi-\psi)^2 + b\nabla\psi^2\right)\\ &\leq \sqrt{2}\max\{\frac{1}{c^{1/2}}, \frac{h_T}{b^{1/2}}\}\underbrace{\left(\int_{\tilde{\omega}_T} c(\phi-\psi)^2 + b\nabla\psi^2 + a\nabla\phi^2\right)^{1/2}}_{:=\mathcal{B}_T=\mathcal{B}|_{\tilde{\omega}_T}}.\end{aligned}$$

Also

$$\|\phi-\phi_h\|_T \overset{(4.21)}{\leq} h_T\|\nabla\phi\|_{\tilde{\omega}_T} = \frac{h_T}{a^{1/2}}\|a^{1/2}\nabla\phi\|_{\tilde{\omega}_T} \leq \frac{h_T}{a^{1/2}}\mathcal{B}_T,$$

thus, for $\theta_{lp,u,T} := \min\{\frac{h_T}{a^{1/2}}, \max\{\frac{1}{c^{1/2}}, \frac{h_T}{b^{1/2}}\}\}$

$$\|\phi - \phi_h\|_T \leq \theta_{lp,u,T}\mathcal{B}_T. \tag{4.147}$$

To prove the interpolation estimates in the edges we use Lemma 4.3.2. To apply equation (4.22) we need to estimate $\|\nabla(\phi - \phi_h)\|_T$:

$$\begin{aligned} \|\nabla(\phi - \phi_h)\|_T &\overset{(4.21)}{\leq} \|\nabla\phi\|_{\tilde{\omega}_T} = \frac{h_T}{a^{1/2}h_T}\|a^{1/2}\nabla\phi\|_{\tilde{\omega}_T} \\ &\leq h_T^{-1}\theta_{lp,u,T}\mathcal{B}_T. \end{aligned} \tag{4.148}$$

Estimating (4.22)

$$\begin{aligned} \|\phi - \phi_h\|_E &\leq h_T^{-1/2}\|\phi - \phi_h\|_T + \|\phi - \phi_h\|_T^{1/2}\|\nabla\phi - \phi_h\|^{1/2} \\ &\overset{(4.147)+(4.148)}{\leq} h_T^{-1/2}\theta_{lp,u,T}\mathcal{B}_T + \theta_{lp,u,T}^{1/2}\mathcal{B}_T^{1/2}h_T^{-1/2}\theta_{lp,u,T}^{1/2}\mathcal{B}_T^{1/2} \\ &\leq \underbrace{2h_T^{-1/2}\theta_{lp,u,T}}_{:=\gamma_{lp,u,E}}\mathcal{B}_T. \end{aligned}$$

Similarly we can get the upper bounds to $\|\psi - \psi_H\|_K$ and $\|\psi - \psi_H\|_F$.

We summarize the interpolation bounds that will be used further on:

$$\|\phi - \phi_h\|_T \leq \theta_{lp,u,T}\mathcal{B}_T, \qquad \|\phi - \phi_h\|_E \leq \gamma_{lp,u,T}\mathcal{B}_T, \tag{4.149}$$

$$\|\psi - \psi_H\|_K \leq \theta_{lp,v,K}\mathcal{B}_K, \qquad \|\psi - \psi_h\|_F \leq \gamma_{lp,v,F}\mathcal{B}_K. \tag{4.150}$$

Let us go back to the estimation of $\|\lambda_1^{1/2}(u^n - u_h^n)\|^2 + \|\lambda_2^{1/2}(v^n - v_H^n)\|^2 + \tau_n\mathcal{B}(u^n - u_h^n, v^n - v_H^n)$. Applying the interpolation results above to equation (4.146) and the

Cauchy-Schwarz inequality we have that:

$$
\begin{aligned}
&\underbrace{\|\lambda_1^{1/2}(u^n-u_h^n)\|^2+\|\lambda_2^{1/2}(v^n-v_H^n)\|^2+2\sum_{m=1}^{n}\tau_m\mathcal{B}(u^m-u_h^m,v^m-v_H^m)}_{:=T_7}\\
\overset{(3.12)}{\leq}\;&\sum_{m=1}^{n}\tau_n\sum_{T\in\mathcal{T}_h}\Big[\theta_{lp,u,T}\|R_{T,u}^n\|_T\mathcal{B}_T(u^n-u_h^n,v^n-v_H^n)\\
+\;&\frac{1}{2}\sum_{E\in\partial T}\gamma_{lp,u,E}\|R_{E,u}^n\|_E\mathcal{B}_T(u^n-u_h^n,v^n-v_H^n)\Big]\\
+\;&\tau_n\sum_{K\in\mathcal{T}_H}\Big[\theta_{lp,v,K}\|R_{K,v}^n\|_K\mathcal{B}_K(u^n-u_h^n,v^n-v_H^n)\\
+\;&\frac{1}{2}\sum_{F\in\partial K}\gamma_{lp,u,F}\|R_{F,v}^n\|_F\mathcal{B}_K(u^n-u_h^n,v^n-v_H^n)\Big]\\
+\;&\|\lambda_1^{1/2}(u^0-u_h^0)\|^2+\|\lambda_2^{1/2}(v^0-v_H^0)\|^2.
\end{aligned}
$$

Apply the Cauchy-Schwarz inequality two more times

$$
\begin{aligned}
T_7\;\overset{(3.12)}{\leq}\;&\sum_{m=1}^{n}\tau_n\sum_{T\in\mathcal{T}_h}\underbrace{\left(\theta_{lp,u,T}^2\|R_{T,u}^n\|_T^2+\frac{1}{2}\sum_{E\in\partial T}\gamma_{lp,u,T}^2\|R_{E,u}^n\|_E^2\right)^{1/2}}_{:=\mathcal{S}_{n,T,u}}\mathcal{B}_T\\
+\;&\sum_{m=1}^{n}\tau_n\sum_{K\in\mathcal{T}_H}\underbrace{\left(\theta_{lp,v,T}^2\|R_{K,v}^n\|_K^2+\frac{1}{2}\sum_{F\in\partial K}\gamma_{lp,v,K}^2\|R_{E,v}^n\|_E^2\right)^{1/2}}_{:=\mathcal{S}_{n,K,v}}\mathcal{B}_K\\
+\;&\|\lambda_1^{1/2}(u^0-u_h^0)\|^2+\|\lambda_2^{1/2}(v^0-v_H^0)\|^2\\
\overset{(3.12)}{\leq}\;&\sum_{m=1}^{n}\tau_n\left(\sum_{T\in\mathcal{T}_h}\mathcal{S}_{n,T,u}^2\sum_{K\in\mathcal{T}_H}\mathcal{S}_{n,K,v}^2\right)+\sum_{m=1}^{n}\tau_m\mathcal{B}(u^m-u_h^m,v^m-v_H^m)\\
+\;&\|\lambda_1^{1/2}(u^0-u_h^0)\|^2+\|\lambda_2^{1/2}(v^0-v_H^0)\|^2.
\end{aligned}
$$

Subtracting $\sum_{m=1}^{n}\tau_m\mathcal{B}(u^m-u_h^m,v^m-v_H^m)$ from both sides we arrive at the following result.

Proposition 4.5.2. *Assume that the data $f, g \in C([0,T], L^2(\Omega))$ and that the functions $u_0, v_0 \in V$. Then, the following a-posteriori error bound holds for the error between the solution $(u^n, v^n)_{0\le n\le N}$ of the problem (3.32) and the solution $(u_h^n, v_H^n)_{0\le n\le N}$ of problem (4.112), for all t_n, $1 \le n \le N$:*

$$[[(u-u_h)^m,(v-v_H)^m]]_n^2 \le \sum_{m=1}^{n} \tau_m \left(\sum_{T\in\mathcal{T}_h} \mathcal{S}_{m,T,u}^2 + \sum_{K\in\mathcal{T}_H} \mathcal{S}_{m,K,v}^2 \right) + \|\lambda_1^{1/2}(u^0-u_h^0)\|^2 + \|\lambda_2^{1/2}(v^0-v_H^0)\|^2 \tag{4.151}$$

4.5.5.3 Bound for $[[(u,v)-(u_{h\tau},v_{H\tau})]](t_n)$

Now we can use Propositions 4.5.1 and 4.5.2 to get the estimate for the total error,

$$\begin{aligned}
[[(u,v)-(u_{h\tau},v_{H\tau})]](t_n) &\le [[(u,v)-(u_\tau,v_\tau)]](t_n) + [[(u_\tau,v_\tau)-(u_{h\tau},v_{H\tau})]](t_n) \\
&\overset{(4.142)}{\le} 2C(f,g) + \frac{4}{\sqrt{3}}[[(u_\tau,v_\tau)-(u_{h\tau},v_{H\tau})]](t_n) \\
&+ 2\left\{\sum_{m=1}^{n} T_m^2\right\}^{1/2} + [[(u_\tau,v_\tau)-(u_{h\tau},v_{H\tau})]](t_n) \\
&= 2C(f,g) + \frac{4+\sqrt{3}}{\sqrt{3}}[[(u_\tau,v_\tau)-(u_{h\tau},v_{H\tau})]](t_n) \\
&+ 2\left\{\sum_{m=1}^{n} T_m^2\right\}^{1/2}.
\end{aligned}$$

We apply Lemma 4.5.1 to get

$$\begin{aligned}
[[(u,v)-(u_{h\tau},v_{H\tau})]](t_n) &\leq 2C(f,g)+1\left\{\sum_{m=1}^{n}T_m^2\right\}^{1/2}\\
&+ C_{26}\left[C_{27}[[(u-u_h)^m,(v-v_H)^m]]_n^2+\frac{\tau_1}{2}\mathcal{B}(u^0,v^0)\right]^{1/2}\\
&\overset{(4.151)}{\leq} 2C(f,g)+2\left\{\sum_{m=1}^{n}T_m^2\right\}^{1/2}\\
&+ C_{26}\left[C_{27}\left[\sum_{m=1}^{n}\tau_m\left(\sum_{T\in\mathcal{T}_h}\mathcal{S}_{m,T,u}^2+\sum_{K\in\mathcal{T}_H}\mathcal{S}_{m,K,v}^2\right)\right.\right.\\
&+ \left.\|\lambda_1^{1/2}(u^0-u_h^0)\|^2+\|\lambda_2^{1/2}(v^0-v_H^0)\|^2\right]\\
&+ \left.\frac{\tau_1}{2}\mathcal{B}(u^0,v^0)\right]^{1/2}.
\end{aligned}$$

Here

$$C_{26} := \frac{4+\sqrt{3}}{\sqrt{3}}, \tag{4.152}$$

$$C_{27} := \frac{1}{2}\left(1+\frac{1}{\sigma_\tau}\right). \tag{4.153}$$

We recall the following property of positive numbers x, y,

$$\sqrt{x+y} \leq \sqrt{x}+\sqrt{y}, \tag{4.154}$$

$$\sqrt{x}+\sqrt{y} \leq \sqrt{2}\sqrt{x+y}. \tag{4.155}$$

We can reorganize the last expression arriving at:

$$
\begin{aligned}
[[(u,v)-(u_{h\tau},v_{H\tau})]](t_n) &\overset{(4.154)}{\leq} 2C(f,g)+2\left\{\sum_{m=1}^{n}\eta_m^2\right\}^{1/2} \\
&\quad + C_{26}C_{27}^{1/2}\left\{\sum_{m=1}^{n}\tau_m\left(\sum_{T\in\mathcal{T}_h}\eta_{m,T,u}^2+\sum_{K\in\mathcal{T}_H}\eta_{m,K,v}^2\right)\right\}^{1/2} \\
&\quad + C_{26}C_{27}^{1/2}\|\lambda_1^{1/2}(u^0-u_h^0)\|+C_1C_2^{1/2}\|\lambda_2^{1/2}(v^0-v_H^0)\| \\
&\quad + C_{26}\sqrt{\frac{\tau_1}{2}}\mathcal{B}(u^0,v^0)^{1/2} \\
&\overset{(4.155)}{\leq} \sqrt{2}\left\{4\sum_{m=1}^{n}T_m^2+C_{26}^2C_{27}\sum_{m=1}^{n}\tau_m\left(\sum_{T\in\mathcal{T}_h}\mathcal{S}_{m,T,u}^2+\sum_{K\in\mathcal{T}_H}\mathcal{S}_{m,K,v}^2\right)\right\}^{1/2} \\
&\quad + 2C(f,g)+C_{26}C_{27}^{1/2}\|\lambda_1^{1/2}(u^0-u_h^0)\|+C_{26}C_{27}^{1/2}\|\lambda_2^{1/2}(v^0-v_H^0)\| \\
&\quad + C_{26}\sqrt{\frac{\tau_1}{2}}\mathcal{B}(u^0,v^0)^{1/2}.
\end{aligned}
$$

Define the constants,

$$
C^* := \sqrt{2}\max\left\{2,\frac{4+\sqrt{3}}{\sqrt{6}}\left(1+\frac{1}{\sigma_\tau}\right)^{1/2}\right\}, \tag{4.156}
$$

$$
C_* := \max\left\{2,\frac{4+\sqrt{3}}{\sqrt{6}}\left(1+\frac{1}{\sigma_\tau}\right)^{1/2},\frac{4+\sqrt{3}}{\sqrt{6}}\right\}. \tag{4.157}
$$

We have proved the following.

Definition 4.5.5. *We denote*

$$
\mathcal{E}_{lp}(t_n) := [[(u,v)-(u_{h\tau},v_{H\tau}]](t_n). \tag{4.158}
$$

Theorem 4.5.6. *The following upper bound holds for the a-posteriori estimator holds for the error between the solution* (u,v) *of the system* (3.32) *and the solution* $\{(u_h^n,v_H^n)\}_{0\leq n\leq N}$

of the problem (4.112)*, for all* t_n*,* $1 \le n \le N$*:*

$$\begin{aligned} \mathcal{E}_{lp} &\le C^* \eta_{lp} + C_* \Big(C(f,g) + \|\lambda_1^{1/2}(u^0 - u_h^0)\| \\ &+ \|\lambda_2^{1/2}(v^0 - v_H^0)\| + \sqrt{\tau_1}\mathcal{B}(u^0, v^0)^{1/2} \Big), \end{aligned} \tag{4.159}$$

$$\eta_{lp}^2 := \sum_{m=1}^{n} \left[\tau_m \left(\sum_{T \in \mathcal{T}_h} \mathcal{S}_{m,T,u}^2 + \sum_{K \in \mathcal{T}_H} \mathcal{S}_{m,K,v}^2 \right) + T_m^2 \right]. \tag{4.160}$$

where $C(f,g), C^*, C_*$ *is given by equation* (4.141)*,* (4.156)*, and* (4.157)*, respectively.*

4.5.6 Lower Bound

Here we prove a lower bound for the error indicators. We prove separate bounds for the time indicator T_n and the spatial indicators $\mathcal{S}_{n,T,u}, \mathcal{S}_{n,K,v}$. Due to the presence of the scaling factors we do not prove a lower bound for the estimator η_{lp}. However, its efficiency is guaranteed by the former bounds.

4.5.6.1 Bound for the time indicator T_n

Applying the inequality $(a+b+c)^2 \le 3(a^2+b^2+c^2)$ to the definition of T_n (4.123)

$$\begin{aligned} T_n &\le \sqrt{\tau_n} \big[\mathcal{B}(u^n - u^{n-1}, v^n - v^{n-1}) \\ &+ \mathcal{B}(u^n - u_h^n, v^n - v_H^n) + \mathcal{B}(u^{n-1} - u_h^{n-1}, v^{n-1} - v_H^{n-1}) \big]^{1/2}. \end{aligned}$$

Since

$$\tau_n \mathcal{B}(u^n - u_h^n, v^n - v_H^n) = \int_{t_{n-1}}^{t_n} \mathcal{B}(u^n - u_h^n, v^n - v_H^n) \le [[(u^n - u_h^n, v^n - v_H^n)]]^2(t_n),$$

we have that

$$\begin{aligned} T_n &\le \big\{ \tau_n \mathcal{B}(u^n - u^{n-1}, v^n - v^{n-1}) \\ &+ [[(u^n - u_h^n, v^n - v_H^n)]]^2(t_n) + [[u^{n-1} - u_h^{n-1}, v^{n-1} - v_H^{n-1}]]^2(t_n) \big\}^{1/2} \\ &\le \sqrt{\tau_n}\mathcal{B}(u^n - u^{n-1}, v^n - v^{n-1})^{1/2} \\ &+ [[(u^n - u_h^n, v^n - v_H^n)]](t_n) + [[u^{n-1} - u_h^{n-1}, v^{n-1} - v_H^{n-1}]](t_n). \end{aligned} \tag{4.161}$$

Let $\phi = u^n - u^{n-1}$ and $\psi = v^n - v^{n-1}$ in equation (4.137) and integrate between t_{n-1} and t_n

$$\begin{aligned}\int_{t_{n-1}}^{t_n} [\,(\lambda_1(u-u_\tau)', u^n - u^{n-1}) &+ (\lambda_2(v-v_\tau)', v^n - v^{n-1}) \\ &+ B(u-u_\tau, v-v_\tau), (u^n - u^{n-1}, v^n - v^{n-1}))\big] \\ &= \int_{t_{n-1}}^{t_n} \big[(f - f^n, u^n - u^{n-1}) + (g - g^n, v^n - v^{n-1}) \\ &+ B((u_\tau - u^n, v_\tau - v^n), (u^n - u^{n-1}, v^n - v^{n-1}))\big]\,.\end{aligned}$$

Note that $u_\tau - u^n = \frac{t-t_n}{\tau_n}(u^n - u^{n-1})$. Thus,

$$\begin{aligned}&\int_{t_{n-1}}^{t_n} B((u_\tau - u^n, v_\tau - v^n), (u^n - u^{n-1}, v^n - v^{n-1})) \\ &\quad = \int_{t_{n-1}}^{t_n} \frac{t-t_n}{\tau_n}\mathcal{B}(u^n - u^{n-1}, v^n - v^{n-1}) = -\frac{\tau_n}{2}\mathcal{B}(u^n - u^{n-1}, v^n - v^{n-1}). \quad (4.162)\end{aligned}$$

So we get,

$$\begin{aligned}\int_{t_{n-1}}^{t_n} [\,(\lambda_1(u-u_\tau)', u^n - u^{n-1}) &+ (\lambda_2(v-v_\tau)', v^n - v^{n-1}) \\ &+ B((u_\tau - u^n, v_\tau - v^n), (u^n - u^{n-1}, v^n - v^{n-1}))\big] \\ &= \int_{t_{n-1}}^{t_n} \big[(f - f^n, u^n - u^{n-1}) + (g - g^n, v^n - v^{n-1})\big] \\ &- \frac{\tau_n}{2}\mathcal{B}(u^n - u^{n-1}, v^n - v^{n-1}).\end{aligned}$$

Rearranging the terms

$$\begin{aligned}\frac{\tau_n}{2}\mathcal{B}(u^n - u^{n-1}, v^n - v^{n-1}) &\int_{t_{n-1}}^{t_n} \big[(f - f^n, u^n - u^{n-1}) + (g - g^n, v^n - v^{n-1})\big] \\ &- \int_{t_{n-1}}^{t_n} \big[(\lambda_1(u-u_\tau)', u^n - u^{n-1}) + (\lambda_2(v-v_\tau)', v^n - v^{n-1}) \\ &\qquad + B((u_\tau - u^n, v_\tau - v^n), (u^n - u^{n-1}, v^n - v^{n-1}))\,\big]\,.\end{aligned}$$

Note that if $u_0, v_0 \in H_0^1(\Omega)$

$$
\begin{aligned}
&|\int_{t_{n-1}}^{t_n} (\lambda_1(u-u_\tau)', u^n - u^{n-1})| \\
&\leq \frac{\lambda_1}{a^{1/2}} \|(u-u_\tau)'\|_{L^2(t_{n-1},t_n,H^{-1}(\Omega))} \left\{ \int_{t_{n-1}}^{t_n} \|a^{1/2}\nabla(u^n - u^{n-1})\|^2 \right\}^{1/2} \\
&= \frac{\lambda_1}{a^{1/2}} \|(u-u_\tau)'\|_{L^2(t_{n-1},t_n,H^{-1}(\Omega))} \sqrt{\tau_n} \|a^{1/2}\nabla(u^n - u^{n-1})\|.
\end{aligned}
$$

Using the same calculations as above we conclude that

$$
\begin{aligned}
|\int_{t_{n-1}}^{t_n} \big[(f-f^n, u^n - u^{n-1}) + (g-g^n, v^n - v^{n-1}) \\
+ \big[(\lambda_1(u-u_\tau)', u^n - u^{n-1}) + (\lambda_2(v-v_\tau)', v^n - v^{n-1}) \\
+ B((u_\tau - u^n, v_\tau - v^n), (u^n - u^{n-1}, v^n - v^{n-1}))\big]\big| \\
\leq \sqrt{\frac{\tau_n}{a}} \|f-f^n\|_{L^2(t_{n-1},t_n;H^{-1}(\Omega))} \|a^{1/2}\nabla(u^n - u^{n-1})\| \\
+ \sqrt{\frac{\tau_n}{b}} \|g-g^n\|_{L^2(t_{n-1},t_n;H^{-1}(\Omega))} \|b^{1/2}\nabla(v^n - v^{n-1})\| \\
+ \frac{\lambda_1\sqrt{\tau_n}}{a^{1/2}} \|\partial_t(u-u_\tau)\|_{L^2(t_{n-1},t_n;H^{-1}(\Omega))} \|a^{1/2}\nabla(u^n - u^{n-1})\| \\
+ \frac{\lambda_2\sqrt{\tau_n}}{b^{1/2}} \|\partial_t(v-v_\tau)\|_{L^2(t_{n-1},t_n;H^{-1}(\Omega))} \|b^{1/2}\nabla(v^n - v^{n-1})\| \\
+ \sqrt{\tau_n} \|a^{1/2}\nabla(u-u_\tau)\|_{L^2(t_{n-1},t_n;L^2(\Omega))^d} \|a^{1/2}\nabla(u^n - u^{n-1})\| \\
+ \sqrt{\tau_n} \|b^{1/2}\nabla(v-v_\tau)\|_{L^2(t_{n-1},t_n;L^2(\Omega))^d} \|b^{1/2}\nabla(v^n - v^{n-1})\| \\
+ \sqrt{\tau_n} \|c^{1/2}((u-u_\tau) - (v-v_\tau))\|_{L^2(t_{n-1},t_n;L^2(\Omega))} \|c^{1/2}(u^n - u^{n-1}) - (v^n - v^{n-1}))\|.
\end{aligned}
$$

Using the Cauchy-Schwarz inequality

$$
\begin{aligned}
|\int_{t_{n-1}}^{t_n} \big[(f-f^n, u^n - u^{n-1}) + (g-g^n, v^n - v^{n-1}) + (\lambda_1(u-u_\tau)', u^n - u^{n-1}) \\
+ (\lambda_2(v-v_\tau)', v^n - v^{n-1}) + B((u_\tau - u^n, v_\tau - v^n), (u^n - u^{n-1}, v^n - v^{n-1}))\big]| \\
\leq \sqrt{3\tau_n} C(f, g, u, u_\tau, v, v_\tau)^{1/2} \mathcal{B}(u^n - u^{n-1}, v^n - v^{n-1})^{1/2},
\end{aligned}
$$

where

$$\begin{aligned} C(f,g,u,u_\tau,v,v_\tau) &:= \{\frac{1}{a}\|f-f^n\|^2_{L^2(t_{n-1},t_n;H^{-1}(\Omega))} + \frac{1}{b}\|g-g^n\|^2_{L^2(t_{n-1},t_n;H^{-1}(\Omega))} \\ &+ \frac{\lambda_1^2}{a}\|\partial_t(u-u_\tau)\|^2_{L^2(t_{n-1},t_n;H^{-1}(\Omega))} \\ &+ \frac{\lambda_2^2}{b}\|\partial_t(v-v_\tau)\|^2_{L^2(t_{n-1},t_n;H^{-1}(\Omega))} \\ &+ \|a^{1/2}\nabla(u-u_\tau)\|_{L^2(t_{n-1},t_n;L^2(\Omega))^d} \\ &+ \|b^{1/2}\nabla(v-v_\tau)\|_{L^2(t_{n-1},t_n;L^2(\Omega))^d} \\ &+ \|c^{1/2}((u-u_\tau)-(v-v_\tau))\|_{L^2(t_{n-1},t_n;L^2(\Omega))}\}. \end{aligned} \tag{4.163}$$

Putting it all together

$$\frac{\tau_n}{2}\mathcal{B}(u^n-u^{n-1},v^n-v^{n-1}) \le \sqrt{3}\sqrt{\tau_n}C(f,g,u,u_\tau,v,v_\tau)^{1/2}\mathcal{B}(u^n-u^{n-1},v^n-v^{n-1})^{1/2}$$

and simplifying

$$\sqrt{\tau_n}\mathcal{B}(u^n-u^{n-1},v^n-v^{n-1})^{1/2} \le 2\sqrt{3}C(f,g,u,u_\tau,v,v_\tau)^{1/2}.$$

Substituting in (4.161) we arrive at the following result:

Proposition 4.5.3. *Assume that the data $f,g \in C[0,T],V')$ and that the functions $u_0,v_0 \in V$. The following estimate holds for the indicator T_n defined by* (4.123)*, $1 \le n \le N$:*

$$\begin{aligned} T_n \le\ & 2\sqrt{3}C(f,g,u,u_\tau,v,v_\tau)^{1/2} \\ & + [[(u^n-u_h^n,v^n-v_H^n)]](t_n) + [[u^{n-1}-u_h^{n-1},v^{n-1}-v_H^{n-1}]](tn) \end{aligned} \tag{4.164}$$

where $C(f,g,u,u_\tau,v,v_\tau)$ is defined by (4.163)*.*

4.5.6.2 Bound for the spatial estimators

Recall the definition of

$$\mathcal{S}_{n,T,u} := \left(\theta^2_{lp,u,T} \|R^n_{T,u}\|^2 + \frac{1}{2} \sum_{E \in \mathcal{E}_T} \gamma^2_{lp,u,E} \|R^n_{E,u}\|^2 \right)^{1/2},$$

where

$$\begin{aligned} R^n_{T,u} &:= f^n - \lambda_1 \frac{u^n_h - u^{n-1}_h}{\tau_n} + \nabla \cdot (a \nabla u^n_h) - c(u^n_h - v^n_H), \\ R^n_{E,u} &:= [a \partial_\nu u^n_h]_E, \\ \theta_{lp,u,S} &:= \min\{h_S a^{-1/2}, \max\{c^{-1/2}, h_S b^{-1/2}\}\} \quad S \in \mathcal{T}_{n,h} \cup \mathcal{E}_{n,h}, \\ \gamma_{lp,u,E} &:= 2 h_E^{-1/2} \theta_{lp,u,E}. \end{aligned}$$

We are going to estimate the two parts of the spatial estimator $\mathcal{S}_{n,T,u}$ separately.

4.5.6.3 Estimate in the elements

Fix an element $T \in \mathcal{T}_h$ and let Φ_T be the element bubble function as described in [30]. In equation (4.144), let $\phi_h = 0$ and $\phi = R^n_{T,u} \Phi_T$, so that

$$\begin{aligned} &\lambda_1(u^n - u^n_h, \phi) + \tau_n \left[a(\nabla(u^n - u^n_h), \nabla\phi) + c((u^n - u^n_h) - (v^n - v^n_H), \phi) \right] \qquad (4.165) \\ &= \lambda_1(u^{n-1} - u^{n-1}_h, \phi) + \tau_n \sum_{T \in \mathcal{T}_h} \left[\int_T R^n_{T,u} \phi - (f^n - f^n_h)\phi + \frac{1}{2} \sum_{E \subset \partial T} \int_E R^n_{E,u} \phi ds \right]. \end{aligned}$$

Because of the properties of the bubble function we have that $supp(\phi) \subset T$. Thus the equation above simplifies to

$$\begin{aligned} \lambda_1(u^n - u^n_h, \phi)_T &+ \tau_n \left[a(\nabla(u^n - u^n_h), \nabla\phi)_T + c((u^n - u^n_h) - (v^n - v^n_H), \phi)_T \right] \\ &= \lambda_1(u^{n-1} - u^{n-1}_h, \phi)_T + \tau_n \int_T R^n_{T,u} \phi - (f^n - f^n_h)\phi. \end{aligned}$$

Reorganizing the terms

$$\|R^n_{T,u}\Phi^{1/2}_T\|^2_T = \lambda_1 \left(\frac{(u^n - u^n_h) - (u^{n-1} - u^{n-1}_h)}{\tau_n}, \phi \right)_T + a(\nabla(u^n - u^n_h), \nabla\phi)_T + c((u^n - u^n_h) - (v^n - v^n_H), \phi)_T - (f^n - f^n_h, \phi)_T.$$

The element and edge bubbles have the same properties as in Section 4.3.2.4

$$\begin{aligned} c_1\|R^n_{T,u}\|^2_T &\leq \|R^n_{t,u}\Phi^{1/2}_T\|^2_T \overset{(4.39)}{\leq} \lambda_1 \left\| \frac{(u^n - u^n_h) - (u^{n-1} - u^{n-1}_h)}{\tau_n} \right\|_T \|\phi\|_T \\ &+ a\|\nabla(u^n - u^n_h)\|_T\|\nabla\phi\|_T + c\|(u^n - u^n_h) - (v^n - v^n_H)\|_T\|\phi\|_T \\ &+ \|f^n - f^n_h\|_T\|\phi\|_T \\ &\overset{(3.12)}{\leq} \left(\lambda_1 \left\| \frac{(u^n - u^n_h) - (u^{n-1} - u^{n-1}_h)}{\tau_n} \right\|_T + \|f^n - f^n_h\|_T \right) \|\phi\|_T \\ &+ \left\{ \int_T a\nabla(u^n - u^n_h)^2 + c((u^n - u^n_h) - (v^n - v^n_H))^2 \right\}^{1/2} \\ &\quad \left\{ \int_T a\nabla\phi^2 + c\phi^2 \right\}^{1/2}. \end{aligned}$$

Using the fact that $\Phi_T \leq 1$ everywhere, we notice that

$$\left\{ \int_T a\nabla\phi^2 + c\phi^2 \right\}^{1/2} \overset{(4.154)}{\leq} a^{1/2}\|\nabla\phi\|_T + c^{1/2}\|\phi\|_T \overset{(4.40)}{\leq} (c_2 h_T^{-1} a^{1/2} + c^{1/2})\|R^n_{T,u}\|_T.$$

Recalling the definition (4.23)

$$\theta_{lp,u,T} := \min\{h_T a^{-1/2}, \max\{c^{-1/2}, h_T b^{-1/2}\}\},$$

it is easy to see that

$$\theta^{-1}_{lp,u,T} = \max\{h_T^{-1} a^{1/2}, \min\{c^{1/2}, h_T^{-1} b^{1/2}\}\}.$$

This leads us to make the following assumption about the mesh size:

$$h_T \leq \sqrt{\frac{b}{c}}, \tag{4.166}$$

obtaining then the relation

$$\sqrt{c} \leq \min\{c^{1/2}, h_T^{-1} b^{1/2}\}.$$

Thus

$$\begin{aligned}(c_2 h_T^{-1} a^{1/2} + c^{1/2}) &\leq \max\{c_2, 1\}(h_T^{-1} a^{1/2} + c^{1/2}) \\ &\leq \max\{c_2, 1\}(h_T^{-1} a^{1/2} + \min\{c^{1/2}, h_T^{-1} b^{1/2}\}),\end{aligned}$$

arriving at the estimate

$$(c_2 h_T^{-1} a^{1/2} + c^{1/2}) \leq 2\max\{c_2, 1\}\theta_{lp,u,T}^{-1}. \tag{4.167}$$

Finally, we arrive at the estimate for $\|R_{T,u}^n\|_T$

$$\begin{aligned}c_1\|R_{T,u}^n\|_T &\leq \lambda_1 \left\| \frac{(u^n - u_h^n) - (u^{n-1} - u_h^{n-1})}{\tau_n} \right\|_T + \|f^n - f_h^n\|_T \\ &+ 2\max\{c_2, 1\}\theta_{lp,u,T}^{-1} \left\{ \int_T a\nabla(u^n - u_h^n)^2 + c((u^n - u_h^n) - (v^n - v_H^n))^2 \right\}^{1/2}.\end{aligned} \tag{4.168}$$

Similarly, for any element $K \in \mathcal{T}_H$ and assuming that $H_k \leq \sqrt{\frac{a}{c}}$:

$$\begin{aligned}c_1\|R_{K,v}^n\|_K &\leq \lambda_2 \left\| \frac{(v^n - v_H^n) - (v^{n-1} - v_H^{n-1})}{\tau_n} \right\|_K + \|g^n - g_h^n\|_K \\ &+ 2\max\{c_2, 1\}\theta_{lp,v,K}^{-1} \left\{ \int_K b\nabla(v^n - v_H^n)^2 + c((u^n - u_h^n) - (v^n - v_H^n))^2 \right\}^{1/2}.\end{aligned} \tag{4.169}$$

4.5.6.4 Estimate on the edges

In the edges, let $E \in \mathcal{E}_h$ such that T_1, T_2 are the two elements that contain E. Go back to (4.165) and now let $\phi = R^n_{E,u}\Phi_E$ where Φ_E is the edge bubble function. Recall that $\Phi_E = 0$ at all edges of $T_1 \cup T_2$ other than E and that $supp(\Phi_E) \subset T_1 \cup T_2$.

Then from (4.165) we get

$$\lambda_1 \left(\frac{(u^n - u^n_h) - (u^{n-1} - u^{n-1}_h)}{\tau_n}, \phi \right) + a(\nabla(u^n - u^n_h), \nabla\phi) + c((u^n - u^n_h) - (v^n - v^n_H), \phi)$$
$$= \int_{T_1 \cup T_2} (R^n_{T,u} - (f^n - f^n_h))\phi + \|R^n_{E,u}\Phi_E^{1/2}\|^2_E.$$

Thus using the estimate (4.41) and Cauchy-Schwarz inequality

$$\begin{aligned}
c_3\|R^n_{E,u}\|^2_E &\leq \|R^n_{E,u}\Phi_E^{1/2}\|^2_E \\
&\leq \lambda_1 \left(\frac{(u^n - u^n_h) - (u^{n-1} - u^{n-1}_h)}{\tau_n}, \phi \right) + a(\nabla(u^n - u^n_h), \nabla\phi) \\
&+ c((u^n - u^n_h) - (v^n - v^n_H), \phi) - \int_{T_1 \cup T_2} (R^n_{T,u} - (f^n - f^n_h))\phi \\
&\leq \sum_{i=1}^{2} \left(\lambda_1 \left\| \frac{(u^n - u^n_h) - (u^{n-1} - u^{n-1}_h)}{\tau_n} \right\|_{T_i} \right. \\
&\quad \left. + \|R^n_{T,u}\|_{T_i} + \|f^n - f^n_h\|_{T_i} \right) \|\phi\|_T \\
&\quad + \left\{ \int_{T_i} a\nabla(u^n - u^n_h)^2 + c((u^n - u^n_h) - (v^n - v^n_H))^2 \right\}^{1/2} \\
&\quad + \left\{ \int_{T_i} a\nabla\phi^2 + c\phi^2 \right\}^{1/2}.
\end{aligned}$$

Recalling the definition (4.25)

$$\gamma_{lp,u,E} := 2h_E^{-1/2}\theta_{lp,u,E},$$

we see that

$$\begin{aligned}
\left\{\int_{T_i} a\nabla\phi^2 + c\phi^2\right\}^{1/2} &\leq a^{1/2}\|\nabla\phi\|_T + c^{1/2}\|\phi\|_T \\
&\overset{(4.42)-(4.43)}{\leq} (c_4 h_E^{-1/2} a^{1/2} + c_5 h_E^{1/2} c^{1/2})\|R^n_{E,u}\|_T \\
&\leq \max\{c_4, c_5\} h_E^{1/2}(h_E^{-1}a^{1/2} + c^{1/2})\|R^n_{E,u}\|_T \\
&\overset{(4.167)}{\leq} \max\{c_4, c_5\} h_E^{1/2}\theta^{-1}_{lp,u,E}\|R^n_{E,u}\|_T \\
&= 2\max\{c_4, c_5\}\gamma^{-1}_{lp,u,E}\|R^n_{E,u}\|_T.
\end{aligned}$$

Using (4.43) we conclude that

$$\begin{aligned}
c_3\|R^n_{E,u}\|_E &\leq \sum_{i=1}^{2} c_5 h_E^{1/2}\left(\lambda_1\left\|\frac{(u^n - u_h^n) - (u^{n-1} - u_h^{n-1})}{\tau_n}\right\|_{T_i}\right. \\
&+ \left.\|R^n_{T,u}\|_{T_i} + \|f^n - f_h^n\|_{T_i}\right) \\
&+ 2\max\{c_4, c_5\}\gamma^{-1}_{u,E}\left\{\int_{T_i} a\nabla(u^n - u_h^n)^2 + c((u^n - u_h^n) - (v^n - v_H^n))^2\right\}^{1/2}.
\end{aligned}$$

Now apply (4.168)

$$\begin{aligned}
c_3\|R^n_{E,u}\|_E &\leq \sum_{i=1}^{2} c_5 h_E^{1/2}\left[\lambda_1\left\|\frac{(u^n - u_h^n) - (u^{n-1} - u_h^{n-1})}{\tau_n}\right\|_{T_i}\right. \\
&+ c_1^{-1}\left(\lambda_1\left\|\frac{(u^n - u_h^n) - (u^{n-1} - u_h^{n-1})}{\tau_n}\right\|_{T_i} + \|f^n - f_h^n\|_{T_i}\right. \\
&+ 2\max\{c_2, 1\}\theta^{-1}_{lp,u,T}\left\{\int_T a\nabla(u^n - u_h^n)^2\right. \\
&+ \left.\left. c((u^n - u_h^n) - (v^n - v_H^n))^2\right\}^{1/2}\right) + \|f^n - f_h^n\|_{T_i}] \\
&+ 2\max\{c_4, c_5\}\gamma^{-1}_{u,E}\left\{\int_{T_i} a\nabla(u^n - u_h^n)^2 + c((u^n - u_h^n) - (v^n - v_H^n))^2\right\}^{1/2}.
\end{aligned}$$

Thus

$$
\begin{aligned}
&c_3\|R^n_{E,u}\|_E \leq \\
&\sum_{i=1}^{2}\left\{ c_5 h_E^{1/2}\left((1+c_1^{-1})\lambda_1 \left\| \frac{(u^n-u_h^n)-(u^{n-1}-u_h^{n-1})}{\tau_n}\right\|_{T_i} + (1+c_1^{-1})\|f^n-f_h^n\|_{T_i}\right)\right. \\
&\qquad + 2\left(2c_5\max\{c_2,1\}+\max\{c_4,c_5\}\right)\gamma^{-1}_{lp,u,E} \\
&\qquad\qquad \left.\left\{ \int_{T_i} a\nabla(u^n-u_h^n)^2 + c((u^n-u_h^n)-(v^n-v_H^n))^2\right\}^{1/2}\right\}.
\end{aligned}
$$

Adding over the edges of T we arrive at the following result:

Proposition 4.5.4. *Assume that the data $f, g \in C([0,T], L^2(\Omega))$ and that $u_0, v_0 \in V$. The following estimate holds for the indicator $\mathcal{S}_{n,T,u}$ defined by (4.124), for all $T \in \mathcal{T}_h$, $1 \leq n \leq N$:*

$$
\begin{aligned}
\mathcal{S}_{n,T,u} \quad \leq \quad & \theta^n_{lp,u,T}\tilde{C}_1\left(\lambda_1\left\|\frac{(u^n-u_h^n)-(u^{n-1}-u_h^{n-1})}{\tau_n}\right\|_{\omega_T} + \|f^n-f_h^n\|_{\omega_T}\right) \\
& + \tilde{C}_2\left\{\int_{\omega_T} a\nabla(u^n-u_h^n)^2 + c((u^n-u_h^n)-(v^n-v_H^n))^2\right\}^{1/2}.
\end{aligned} \tag{4.170}
$$

Here

$$
\tilde{C}_1 := c_1^{-1} + c_3^{-1}c_5(1+c_1^{-1}), \tag{4.171}
$$

$$
\tilde{C}_2 := 2(c_1^{-1}+c_3^{-1}c_5)\max\{c_2,1\} + c_3^{-1}\max\{c_4,c_5\}. \tag{4.172}
$$

Similarly we arrive at

Proposition 4.5.5. *Assume that the data $f, g \in C([0,T], L^2(\Omega))$ and that $u_0, v_0 \in V$. The following estimate holds for the indicator $\mathcal{S}_{n,K,v}$ defined by (4.125), for all $K \in \mathcal{T}_H$,*

$1 \leq n \leq N$:

$$\begin{aligned} \mathcal{S}_{n,K,v} &\leq \theta^n_{lp,v,K}\tilde{C}_1 \left(\lambda_2 \left\| \frac{(v^n - v^n_H) - (v^{n-1} - v^{n-1}_H)}{\tau_n} \right\|_{\omega_K} + \|g^n - g^n_H\|_{\omega_K} \right) \\ &\quad + \tilde{C}_2 \left\{ \int_{\omega_K} b\nabla(v^n - v^n_H)^2 + c((u^n - u^n_h) - (v^n - v^n_H))^2 \right\}^{1/2}. \end{aligned} \tag{4.173}$$

The lower bound is not complete, now it would remain to add the estimates (4.164), (4.170), and (4.173) for $n = 1, \ldots, N$. However, due to the choice of the scalar factors and the presence of terms involving the scaling factors multiplying the terms u^n, u^n_h, v^n, v^n_H in the estimates listed above, a usual lower bound cannot be obtained for the whole estimator η_{lp}.

4.6 WR-model

Here we use the results from Sections 4.5, 4.4 to get *a-priori* and *a-posteriori* error estimates for the discretization of the WR-model. The fully-discrete problem for the WR-model is as follows:

For each n, $0 \leq n \leq N$, *find* $(u^{n+1}_h, v^{n+1}_H) \in V_h \times V_H$ *such that for all* $(\xi, \psi) \in V_h \times V_H$

$$(\lambda_1 \partial^n u_h, \xi) + (a\nabla u^{n+1}_h, \nabla\xi) + c(u^{n+1}_h - \Pi v^{n+1}_H, \xi) = (f^{n+1}, \xi), \tag{4.174a}$$

$$(\partial^n v'_H, \psi) + c(\Pi' u^{n+1}_h - v^{n+1}_H, -\psi) = (g^{n+1}, \psi). \tag{4.174b}$$

The *a-priori* estimate is derived with respect to the following norm

Definition 4.6.1. *For any* $(u, v) \in V^2$

$$|||(u,v)|||^2_{wr}(t_n) := \lambda_1 \|u(t_n)\|^2 + \lambda_2 \|v(t_n)\|^2 + \tau_n \sum_{m=0}^{n-1} a|u(t_{m+1})|^2_1. \tag{4.175}$$

This norm is just a particular case of norm (4.77). We can now set $b = 0$ in Theorem 4.4.6 to arrive at the following estimate for the WR-model. Also note that in here, $L = 1$ since $\varphi(u) = u$.

Corollary 4.6.2. *Suppose that equation* (4.88) *holds. Let* (u, v) *be the solution of* (3.38) *and* $\{(u_h^n, v_H^n)\}_{n=1}^N$ *be the solution of* (4.174)*, then*

$$\begin{aligned} |||(u_h^N - u^N, v_H^N - v^N)|||_{wr}^2 &\leq 2e^{\beta_f T}\left\{\lambda_1\|u_h^0 - \tilde{u}^0\|^2 + \lambda_2\|v_H^0 - \tilde{v}^0\|^2\right\} \\ &\quad + C_{28}h^2 + C_{29}h^4 + C_{30}H^4 + C_{31}\tau_n^2. \end{aligned} \tag{4.176}$$

Here

$$\begin{aligned} C_{28} &:= 2C_3^2 \max_{n=1:N}\left\{a\|u^n\|_2^2\right\}, \\ C_{29} &:= 2e^{\beta_f T}C_5^2 \max_{n=1:N}\left\{\lambda_1\|u'^N\|_2^2\right\} + 8e^{\beta_f T}cC_3^2 \max_{n=1:N}\left\{\|u^n\|_2^2\right\} + 2C_3^2\lambda_1\|u^N\|_2^2, \\ C_{30} &:= 2e^{\beta_f T}C_5^2 \max_{n=1:N}\left\{\lambda_2\|v'^N\|_2^2\right\} + 8e^{\beta_f T}cC_3^2 \max_{n=1:N}\left\{\|v^n\|_2^2\right\} + 2C_3^2\lambda_2\|v^N\|_2^2, \\ C_{31} &:= TC_{PF}^2\left[C(u)^2 + C(v)^2\right]. \end{aligned}$$

We comment now on the difference between the order of convergence for the LP-model and the order of convergence of the WR-model. Note that $|||(u_h^N - u^N, v_H^N - v^N)|||_{wr} = O(h + H^2 + \max_{n=1:N}\tau_n)$. For the LP-model the convergence is of order $O(h + H + \max_{n=1:N}\tau_n)$ while for the WR-Model is $O(h + H^2 + \max_{n=1:N}\tau_n)$. Thus for approximating the WR-model we need a much coarser mesh for the V_H space than for the LP-model. This makes clear the importance of multilevel discretization used in this thesis.

To get the *a-posteriori* error estimator we use the results from Section 4.5.

Definition 4.6.3. *For any* $\vec{u} \in V^2$

$$[[\vec{u}]]_{wr}^2(t) = \|\lambda_1^{1/2}u(t)\|^2 + \|\lambda_2^{1/2}v(t)\|^2 + \int_0^t B_{WR}(\vec{u}, \vec{u}). \tag{4.177}$$

Now we have to adapt the error indicators for the WR-model.

4.6.1 Error indicators

For each n, $1 \leq n \leq N$, we define the time error indicator, $T_{n,wr}$:

$$T_{n,wr}^2 := \frac{\tau_n}{3}B_{WR}(u_h^n - u_h^{n-1}, v_H^n - v_H^{n-1}). \tag{4.178}$$

For each n, $1 \le n \le N$, any $T \in \mathcal{T}_{n,h}$ and any $K \in \mathcal{T}_{n,H}$ we define the space error indicators, $\mathcal{S}_{n,T,u,wr}, \mathcal{S}_{n,K,v,wr}$:

$$\mathcal{S}_{n,T,u,wr} := \left(\theta^2_{wr,u,T} \|R^n_{T,u,wr}\|^2 + \frac{1}{2} \sum_{E \in \mathcal{E}_T} \gamma^2_{wr,u,E} \|R^n_{E,u,wr}\|^2 \right)^{1/2}, \quad (4.179)$$

$$\mathcal{S}_{n,K,v,wr} := \left(\theta^2_{wr,v,K} \|R^n_{K,v,wr}\|^2 \right)^{1/2}. \quad (4.180)$$

Here

$$R^n_{T,u,wr} := f^n - \lambda_1 \frac{u^n_h - u^{n-1}_h}{\tau_n} + \nabla \cdot (a \nabla u^n_h) - c(u^n_h - v^n_H), \quad (4.181)$$

$$R^n_{K,v,wr} := g^n - \lambda_2 \frac{v^n_H - v^{n-1}_H}{\tau_n} - c(v^n_H - u^n_h), \quad (4.182)$$

$$R^n_{E,u,wr} := [a \partial_\nu u^n_h]_E, \quad (4.183)$$

$$\theta_{wr,u,S} := h_S a^{-1/2}, \quad S \in \mathcal{T}_{n,h} \cup \mathcal{E}_{n,h}, \quad (4.184)$$

$$\theta_{wr,v,S} := \max\{c^{-1/2}, H_S a^{-1/2}\}, \quad S \in \mathcal{T}_{n,H} \cup \mathcal{E}_{n,H}, \quad (4.185)$$

$$\gamma_{wr,u,E} := 2 h_E^{-1/2} \theta_{wr,u,E}, \quad (4.186)$$

where $[\partial_\nu w]_E$ denotes the jump of the normal derivative of w through the edge E.

Definition 4.6.4. *Denote*

$$\mathcal{E}_{wr}(t_n) := [[(u, v) - (u_{h\tau}, v_{H\tau}]]_{wr}(t_n). \quad (4.187)$$

Corollary 4.6.5. *The following a-posteriori error estimator holds between the solution (u, v) of the system (3.38) and the solution $\{(u^n_h, v^n_H)\}_{0 \le n \le N}$ of the problem (4.174), for all t_n, $1 \le n \le N$:*

$$\mathcal{E}_{wr}(t_n) \le C^* \eta_{wr} + C_* \Big(C(f, g) + \|\lambda_1^{1/2}(u_0 - u_{h,0})\| + \|\lambda_2^{1/2}(v_0 - v_{0,H})\| + \sqrt{\tau_1} B_{WR}(\vec{u}_0, \vec{u}_0)^{1/2} \Big), \quad (4.188)$$

$$\eta^2_{wr} := \sum_{m=1}^{n} \left[\tau_m \left(\sum_{T \in \mathcal{T}_h} \mathcal{S}^2_{m,T,u,wr} + \sum_{K \in \mathcal{T}_H} \mathcal{S}^2_{m,K,v,wr} \right) + T^2_{m,wr} \right], \quad (4.189)$$

where $C(f,g), C^*, C_*$ *are given by equations* (4.141), (4.156), *and* (4.157), *respectively.*

4.7 PP-model

Here we use the results from Section 4.6 with $\lambda_1 = 0$ to get *a-priori* and *a-posteriori* error estimates for the discretization of the PP-model. The fully-discrete problem for the PP-model is:

For each n, $0 \le n \le N$, *find* $(u_h^{n+1}, v_H^{n+1}) \in V_h \times V_H$ *such that for all* $(\xi, \psi) \in V_h \times V_H$

$$(a\nabla u_h^{n+1}, \nabla\xi) + c(u_h^{n+1} - \Pi v_H^{n+1}, \xi) = (f^{n+1}, \xi), \tag{4.190a}$$

$$(\partial^n v_h', \psi) + c(\Pi'(u_h^{n+1} - \Pi v_h^{n+1}), -\psi) = (g^{n+1}, \psi). \tag{4.190b}$$

We get the *a-priori* estimate with respect to the following norm

Definition 4.7.1. *For any* $(u,v) \in V^2$

$$|||(u,v)|||_{pp}^2(t_n) := \lambda_2\|v(t_n)\|^2 + \tau_n \sum_{m=0}^{n-1} a|u(t_{m+1})|_1^2. \tag{4.191}$$

This norm is just a particular case of norm (4.175). We can now set $\lambda_1 = 0$ in Corollary 4.6.2 to arrive at the following estimate for the WR-model.

Corollary 4.7.2. *Suppose that equation* (4.88) *holds. Let* (u,v) *be the solution of* (3.40) *and* $\{(u_h^n, v_H^n)\}_{n=1}^N$ *be the solution of* (4.190), *then*

$$\begin{aligned} |||(u_h^N - u^N, v_H^N - v^N)|||_{wr}^2 &\le 2e^{\beta_f T}\left\{\lambda_2\|v_H^0 - \tilde{v}^0\|^2\right\} \\ &+ C_{32}h^2 + C_{33}h^4 + C_{34}H^4 + C_{35}\tau_n^2. \end{aligned}$$

Here

$$\begin{aligned} C_{32} &:= 2C_3^2 \max_{n=1:N}\left\{a\|u^n\|_2^2\right\}, \\ C_{33} &:= 8e^{\beta_f T}cC_3^2 \max_{n=1:N}\left\{\|u^n\|_2^2\right\}, \\ C_{34} &:= 2e^{\beta_f T}C_5^2 \max_{n=1:N}\left\{\lambda_2\|v'^N\|_2^2\right\} + 8e^{\beta_f T}cC_3^2 \max_{n=1:N}\left\{\|v^n\|_2^2\right\} + 2C_3^2\lambda_2\|v^n\|_2^2, \\ C_{35} &:= TC_{PF}^2\left[C(u)^2 + C(v)^2\right]. \end{aligned}$$

Note that $|||(u_h^N - u^N, v_H^N - v^N)|||_{pp} = O(h + H^2 + \tau_n)$ the same convergence rate we have for the WR-model.

To get the *a-posteriori* error estimator we use the results from Section 4.6 with $\lambda_1 = 0$. Now we have to adapt the error indicators for the WR-model.

4.7.1 Error indicators

For each n, $1 \leq n \leq N$, we define the time error indicator, $T_{n,pp}$:

$$T_{n,pp}^2 := \frac{\tau_n}{3} B_{WR}(u_h^n - u_h^{n-1}, v_H^n - v_H^{n-1}). \tag{4.192}$$

For each n, $1 \leq n \leq N$, any $T \in \mathcal{T}_{n,h}$ and any $K \in \mathcal{T}_{n,H}$ we define the space error indicators, $\mathcal{S}_{n,T,u,pp}, \mathcal{S}_{n,K,v,pp}$:

$$\mathcal{S}_{n,T,u,pp} := \left(\theta_{pp,u,T}^2 \|R_{T,u,pp}^n\|^2 + \frac{1}{2} \sum_{E \in \mathcal{E}_T} \gamma_{wr,u,E}^2 \|R_{E,u,pp}^n\|^2 \right)^{1/2}, \tag{4.193}$$

$$\mathcal{S}_{n,K,v,pp} := \left(\theta_{pp,v,K}^2 \|R_{K,v,pp}^n\|^2 \right)^{1/2}. \tag{4.194}$$

Here

$$R_{T,u,pp}^n := f^n + \nabla \cdot (a \nabla u_h^n) - c(u_h^n - v_H^n), \tag{4.195}$$

$$R_{K,v,pp}^n := g^n - \lambda_2 \frac{v_H^n - v_H^{n-1}}{\tau_n} - c(v_H^n - u_h^n), \tag{4.196}$$

$$R_{E,u}^n := [a \partial_\nu u_h^n]_E, \tag{4.197}$$

$$\theta_{pp,u,S} := h_S a^{-1/2}, \quad S \in \mathcal{T}_{n,h} \cup \mathcal{E}_{n,h}, \tag{4.198}$$

$$\theta_{pp,v,S} := \max\{c^{-1/2}, H_S a^{-1/2}\}, \quad S \in \mathcal{T}_{n,H} \cup \mathcal{E}_{n,H}, \tag{4.199}$$

$$\gamma_{pp,u,E} := 2 h_E^{-1/2} \theta_{pp,u,E}, \tag{4.200}$$

where $[\partial_\nu w]_E$ denotes the jump of the normal derivative of w through the edge E.

Definition 4.7.3. *Denote*

$$\mathcal{E}_{pp}(t_n) := [[(u, v) - (u_{h\tau}, v_{H\tau}]]_{pp}(t_n) \tag{4.201}$$

Corollary 4.7.4. *The following a-posteriori error estimator holds between the solution* (u, v) *of the system* (3.40) *and the solution* $\{(u_h^n, v_H^n)\}_{0\le n\le N}$ *of the problem* (4.190)*, for all* t_n*,* $1 \le n \le N$*:*

$$\begin{aligned}
\mathcal{E}_{pp}(t_n) &\le C^*\eta_{pp} + C_*\Big(C(f,g) + \|\lambda_1^{1/2}(u_0 - u_{h,0})\| && (4.202)\\
&+ \|\lambda_2^{1/2}(v_0 - v_{0,H})\| + \sqrt{\tau_1}B_{WR}(\vec{u}_0,\vec{u}_0)^{1/2}\Big), && (4.203)\\
\eta_{pp}^2 &:= \sum_{m=1}^{n}\left[\tau_m\left(\sum_{T\in\mathcal{T}_h}\mathcal{S}_{m,T,u,pp}^2 + \sum_{K\in\mathcal{T}_H}\mathcal{S}_{m,K,v,pp}^2\right) + T_m^2\right], && (4.204)
\end{aligned}$$

where $C(f,g), C^*, C_*$ *are given by equations* (4.141)*,* (4.156)*, and* (4.157)*, respectively.*

4.8 *A-posteriori* error estimator for the NLP-model

In this Section we consider the particular case where $\varphi(u) \approx u$ and apply the results of Section 4.5 for the NLP-problem to arrive at an upper bound for the error. We only postulate the theoretical result and present no proofs. Numerical experiments are shown in the next Chapter.

We need to modify the residual definitions (4.126)-(4.127) to add the nonlinearity φ. Define the space error indicators, $\mathcal{S}_{n,T,u,nlp}, \mathcal{S}_{n,K,v,nlp}$:

$$\mathcal{S}_{n,T,u,nlp} := \left(\theta_{lp,u,T}^2\|R_{T,u,nlp}^n\|^2 + \frac{1}{2}\sum_{E\in\mathcal{E}_T}\gamma_{lp,u,E}^2\|R_{E,u}^n\|^2\right)^{1/2}, \quad (4.205)$$

$$\mathcal{S}_{n,K,v,nlp} := \left(\theta_{lp,v,K}^2\|R_{K,v,nlp}^n\|^2 + \frac{1}{2}\sum_{F\in\mathcal{E}_K}\gamma_{lp,v,F}^2\|R_{F,v}^n\|^2\right)^{1/2}. \quad (4.206)$$

Here

$$R_{T,u,nlp}^n := f^n - \lambda_1\frac{u_h^n - u_h^{n-1}}{\tau_n} + \nabla\cdot(a\nabla u_h^n) - c(\varphi(u_h^n) - v_H^n), \quad (4.207)$$

$$R_{K,v,nlp}^n := g^n - \lambda_2\frac{v_H^n - v_H^{n-1}}{\tau_n} + \nabla\cdot(b\nabla v_H^n) - c(v_H^n - \varphi(u_h^n)). \quad (4.208)$$

Definition 4.8.1. *Denote*

$$\mathcal{E}_{nlp} := [[\vec{u} - (u_{h\tau}, v_{H\tau}]](t_n). \tag{4.209}$$

The following proposition is not proved.

Proposition 4.8.1. *The following bound for the a-posteriori error estimator holds between the solution* (u, v) *of the system* (3.45) *and the solution* $\{(u_h^n, v_H^n)\}_{0\leq n\leq N}$ *of the problem* (4.109)*, for all* t_n*,* $1 \leq n \leq N$*:*

$$\begin{aligned} \mathcal{E}_{nlp} &\leq C^* \eta_{nlp} + C_* \Big(C(f,g) + \|\lambda_1^{1/2}(u^0 - u_h^0)\| \qquad (4.210) \\ &+ \|\lambda_2^{1/2}(v^0 - v_H^0)\| + \sqrt{\tau_1}\mathcal{B}(u^0, v^0)^{1/2} \Big), \\ \eta_{nlp}^2 &:= \sum_{m=1}^{n} \left[\tau_m \left(\sum_{T\in\mathcal{T}_h} \mathcal{S}_{m,T,u,nlp}^2 + \sum_{K\in\mathcal{T}_H} \mathcal{S}_{m,K,v,nlp}^2 \right) + T_m^2 \right], \qquad (4.211) \end{aligned}$$

where $C(f,g), C^*, C_*$ *are given by equations* (4.141)*,* (4.156)*, and* (4.157)*, respectively.*

4.9 Dependence of the solution on the parameters

In this last section we are interested in the effect that the parameter c has in the numerical solution of the LP-model. Suppose that $\mathcal{P} = \{\lambda_1, \lambda_2, a, b, c\}$ denotes the correct parameters for the LP-model that generates the numerical solution (u_h^n, v_H^n), $n = 1, \ldots, N$, for the problem (4.112). Suppose also a different set of parameters $\tilde{\mathcal{P}} = \{\lambda_1, \lambda_2, a, b, \tilde{c}\}$ that generates the numerical solution $(\tilde{u}_h^n, \tilde{v}_H^n)$, $n = 1, \ldots, N$, for the problem (4.112). The difference between c and $\tilde{c}$ can be due, for example, to measurement or numerical computation errors.

An example where the parameters are computed numerically is shown in Section 5.7, where the parameters of the macro-model model have to be computed from the parameters of the original model.

Let $e^n_{u,c} := u^n_h - \tilde{u}^n_h$ and $e^n_{v,c} := v^n_H - \tilde{v}^n_H$, $n = 1, \ldots, N$. We estimate the error caused by using $\tilde{c}$ instead of c in the norm

$$\|(e_{u,c}, e_{v,c})\|_{**} := \|\lambda_1^{1/2} e^N_{u,c}\|^2 + \|\lambda_2^{1/2} e^N_{v,c}\|^2 + \sum_{n=1}^{N} \tau_n \left[\|a^{1/2} \nabla e^n_{u,c}\| + \|b^{1/2} \nabla e^n_{v,c}\|^2 \right], \tag{4.212}$$

We assume that $\tilde{c}(x) > 0, x \in \Omega$. Subtracting the system (4.112) for $\mathcal{P}$ from the system (4.112) for $\tilde{P}$ we get

$$\begin{aligned}
(\lambda_1 e^n_{u,c}, \phi_h) + \quad & \tau_n \quad \left(a \nabla e^n_{u,c}, \nabla \phi_h) + (\tilde{c}(e^n_{u,c} - \Pi e^n_{v,c}), \phi_h)\right) \\
& = \quad \tau_n((\tilde{c} - c)(u^n_h - \Pi v^n_H), \phi_h) + (\lambda_1 e^{n-1}_{u,c}, \phi_h), \\
(\lambda_2 e^n_{v,c}, \psi_H) + \quad & \tau_n \quad \left(b \nabla e^n_{v,c} \nabla \psi_H) + (\tilde{c}(e^n_{v,c} - \Pi' e^n_{u,c}), \psi_H)\right) \\
& = \quad \tau_n((\tilde{c} - c)(v^n_H - \Pi' u^n_h), \psi_H) + (\lambda_2 e^{n-1}_{v,c}, \psi_H).
\end{aligned}$$

Use Lemma 4.1.1 and let $\phi_h = e^n_{u,c}$ and $\psi_H = e^n_{v,c}$ in the system above. Adding the two resulting equations

$$\begin{aligned}
\|\lambda_1^{1/2} e^n_{u,c}\|^2 + \|\lambda_2^{1/2} e^n_{v,c}\|^2 + \tau_n \left[\|a^{1/2} \nabla e^n_{u,c}\| + \|b^{1/2} \nabla e^n_{v,c}\|^2 + \|\tilde{c}^{1/2}(e^n_{u,c} - e^n_{v,c})\|^2 \right] \\
= \tau_n((\tilde{c} - c)(u^n_h - v^n_H), e^n_{u,c} - e^n_{v,c}) + (\lambda_1 e^{n-1}_{u,c}, e^n_{u,c}) + (\lambda_2 e^{n-1}_{v,c}, e^n_{v,c}) \\
\leq \tau_n((\tilde{c} - c)(u^n_h - v^n_H), e^n_{u,c} - e^n_{v,c}) + \frac{1}{2} \left(\|\lambda_1^{1/2} e^{n-1}_{u,c}\|^2 + \|\lambda_1^{1/2} e^n_{u,c}\|^2 \right) \\
+ \frac{1}{2} \left(\|\lambda_2^{1/2} e^{n-1}_{v,c}\|^2 + \|\lambda_2^{1/2} e^n_{v,c}\|^2 \right).
\end{aligned}$$

Reorganizing the terms

$$\begin{aligned}
\frac{1}{2} \left(\|\lambda_1^{1/2} e^n_{u,c}\|^2 + \|\lambda_2^{1/2} e^n_{v,c}\|^2 \right) + \tau_n \left[\|a^{1/2} \nabla e^n_{u,c}\| + \|b^{1/2} \nabla e^n_{v,c}\|^2 + \|\tilde{c}^{1/2}(e^n_{u,c} - e^n_{v,c})\|^2 \right] \\
= \tau_n((\tilde{c} - c)(u^n_h - v^n_H), e^n_{u,c} - e^n_{v,c}) + (\lambda_1 e^{n-1}_{u,c}, e^n_{u,c}) + (\lambda_2 e^{n-1}_{v,c}, e^n_{v,c}) \\
\leq \tau_n((\tilde{c} - c)(u^n_h - v^n_H), e^n_{u,c} - e^n_{v,c}) + \frac{1}{2} \left(\|\lambda_1^{1/2} e^{n-1}_{u,c}\|^2 + \|\lambda_2^{1/2} e^{n-1}_{v,c}\|^2 \right).
\end{aligned}$$

We need to simplifying the term $\tau_n((\tilde{c}-c)(u_h^n - v_h^n), e_{u,c}^n - e_{v,c}^n)$ to get rid of terms involving $e_{u,c}^n, e_{v,c}^n$ in the right-hand side of the inequality above

$$\begin{aligned}\tau_n((\tilde{c}-c)(u_h^n - v_h^n), e_{u,c}^n - e_{v,c}^n) &= \tau_n\left(\frac{(\tilde{c}-c)}{\sqrt{\tilde{c}}}(u_h^n - v_H^n), \sqrt{\tilde{c}}(e_{u,c}^n - e_{v,c}^n)\right) \\ &\leq \frac{\tau_n}{2}\left(\|\frac{|\tilde{c}-c|}{\sqrt{\tilde{c}}}(u_h^n - v_H^n)\|^2 + \|\tilde{c}^{1/2}(e_{u,c}^n - e_{v,c}^n)\|^2\right).\end{aligned}$$

This leads to

$$\begin{aligned}\|\lambda_1^{1/2} e_{u,c}^n\|^2 + \|\lambda_2^{1/2} e_{v,c}^n\|^2 + \tau_n\left[\|a^{1/2}\nabla e_{u,c}^n\| + \|b^{1/2}\nabla e_{v,c}^n\|^2 + \|\tilde{c}^{1/2}(e_{u,c}^n - e_{v,c}^n)\|^2\right] \\ \leq \|\lambda_1^{1/2} e_{u,c}^{n-1}\|^2 + \|\lambda_2^{1/2} e_{v,c}^{n-1}\|^2 + \tau_n\|\frac{|\tilde{c}-c|}{\sqrt{\tilde{c}}}(u_h^n - v_H^n)\|^2.\end{aligned} \tag{4.213}$$

Recall that $\sum_{n=1}^N \tau_n = T$. Adding the equations (4.213) for $n = 1, \ldots, N$, we obtain

$$\begin{aligned}\|(e_{u,c}, e_{v,c})^N\|_{**}^2 &\leq \tau_n \sum_{n=1}^N \|\frac{|\tilde{c}-c|}{\sqrt{\tilde{c}}}(u_h^n - v_H^n)\|^2 \\ &\leq T \max_{1\leq n\leq N}\left\{\|\frac{|\tilde{c}-c|}{\sqrt{\tilde{c}}}(u_h^n - v_H^n)\|^2\right\}.\end{aligned}$$

Applying Cauchy-Schwarz inequality we arrive at

$$\|(e_{u,c}, e_{v,c})\|_{**}^2 \leq T\int_\Omega \frac{|\tilde{c}-c|^2}{\tilde{c}}dx \max_{1\leq n\leq N}\left\{\|u_h^n - v_H^n\|^2\right\}.$$

Suppose that $\tilde{c}(x) = c(x) + \epsilon$ where ϵ is the "error" in $\tilde{c}$. We have proven the following *a-priori* error estimate

Proposition 4.9.1. *Let (u_h^n, v_H^n), $(\tilde{u}_h^n, \tilde{v}_H^n)$, $n = 1, \ldots, N$, be the solutions of the problem (4.112) for $\mathcal{P}$ and $\tilde{\mathcal{P}}$, respectively. Then the difference between the two set of solutions can be estimate by*

$$\|(e_{u,c}, e_{v,c})\|_{**}^2 \leq T\int_\Omega \frac{\epsilon^2}{c+\epsilon}dx \max_{1\leq n\leq N}\left\{\|u_h^n - v_H^n\|^2\right\}. \tag{4.214}$$

Here $\|(e_{u,c}, e_{v,c})\|_{**}^2$ is given by (4.212).

From the MacLaurin series expansion of $\frac{\epsilon^2}{c+\epsilon}$

$$\frac{\epsilon^2}{c+\epsilon} = \frac{1}{c}\epsilon^2 - \frac{1}{c^2}\epsilon^3 + \frac{1}{c^3}\epsilon^4 + \dots.$$

Thus for $\epsilon \approx 0$,

$$\|(e_{u,c}, e_{v,c})\|_{**} = O\left(||\epsilon||\right).$$

5 Implementation and Numerical Experiments

In this Chapter we explain how the numerical algorithms are implemented and we present numerical examples to illustrate the theoretical results obtained in Chapter 4.

In Section 5.1, we give an overview of finite element implementation. In Section 5.2 we give details on the multilevel grids. In particular, we discuss the interpolation operators, $\Pi : V_H \to V_h$, $\Pi' : V_h \to V_H$. In Section 5.3 we give the details of the discrete formulation of the models. In Sections 5.4–5.6 we present numerical examples to verify the *a-priori* and *a-posteriori* estimates derived for the model problems in Chapter 4. In Section 5.7 we present an application of the double-porosity model obtained via homogenization and compare the numerical results of solving the original problem and solving the homogenized problem. In Section 5.8 we present numerical results to illustrate Proposition 4.9.1. The results estimate the dependence of the numerical solution on $\mathcal{P}$.

5.1 General notes on the implementation of the models

Here we outline how to implement the discrete formulation of the models E, LP, NLP given by (4.11),(4.112), and (4.98), respectively. The implementation of the WR and PP models are just particular cases of the implementation of the LP-model. Most of these steps are common to all finite element implementation. In this thesis the implementation is made in MATLAB. Some codes are shown in the Appendix.

We follow these steps:

STEP 1. Discretization of the domain into finite elements:

In the 1-dimensional case, the elements in the domain are segments. The mesh can be uniform or not. For the 2-dimensional implementation, we use a uniform mesh with right isosceles triangles with directions as shown in Figure 5.1.

STEP 2. Computation of the matrices and right hand sides of the linear and residuals and Jacobians of the nonlinear system:

For the 2-dimensional examples the matrices computations are based in the code presented in [5]. Most of the implementation is standard finite element implemen-

Figure 5.1: Example of mesh in 2-dimensions

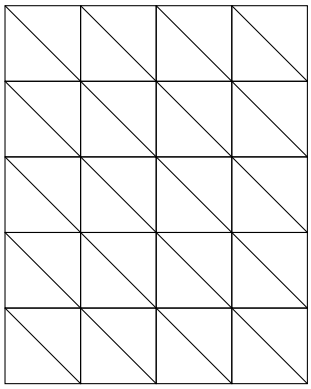

tation. The difference here is the multilevel finite element. Because the systems in the model problems are coupled we need to implement the interpolation operators Π, Π' (4.2). The derivation and implementation of the interpolators is shown in Section 5.2.

STEP 3. Solve the linear and nonlinear algebraic systems.

After the problems are in the algebraic form we implement them in the computer using MATLAB. We solve the systems using the backslash "\" operation in MATLAB. We use the Newton-Raphson method for the nonlinear system [8, 28].

With the discrete solutions of the model problems in hand, the next step is to analyse the convergence of the method, and check the *a-priori* and *a-posteriori* error estimates developed in Chapter 4.

STEP 4. Assess the convergence of the methods and verify the *a-priori* estimates:

We test the methods with model problems for which the analytical solution is known, and compute the errors $\mathcal{E}_e$, $\mathcal{E}_{lp}$ given by (4.37), (4.158). For the NLP-model we compute the error also using $\mathcal{E}_{lp}$ however we call it $\mathcal{E}_{nlp} := \mathcal{E}_{lp}$ for symmetry in the exposition. The errors are computed element-by-element using Gauss integration with 7 points. For the WR-model we compute the particular case of $\mathcal{E}_{lp}$ for $b = 0$ and we denote it by $\mathcal{E}_{wr}$. For the PP-model we compute the particular

cases of $\mathcal{E}_{lp}$ for $\lambda_1 = b = 0$ and we denote it by $\mathcal{E}_{pp}$. We recall here the order of convergence expected from the *a-priori* estimates for uniform time-stepping τ:

$$\begin{aligned} \mathcal{E}_e &= O(h+H) && (5.1)\\ \mathcal{E}_{lp} &= O(h+H+\tau) && (5.2)\\ \mathcal{E}_{wr} &= O(h+H^2+\tau) && (5.3)\\ \mathcal{E}_{pp} &= O(h+H^2+\tau) && (5.4)\\ \mathcal{E}_{nlp} &= O(h+H+\tau) && (5.5) \end{aligned}$$

STEP 5. Test the *a-posteriori* error estimators:

We implement the estimators η_e, η_{lp}, η_{wr}, and η_{nlp} given by equations (4.34), (4.160), (4.189), (4.204), and (4.211), respectively. For model problems we compute the efficiency index Θ and test the robustness of the estimators with respect to the mesh and with respect to the parameters $\mathcal{P}$.

STEP 6. Simulations:

We implement simulations examples and use the *a-posteriori* error estimator to guide adaptivity of the meshes.

5.2 Interpolation between the spaces V_h and V_H

In this Section we address the issue of multilevel grids. We explain the derivation and implementation of the interpolator operators Π, Π'. Let $V_H \subseteq V_h$, $\{\phi_i\}_{i=1}^n$ be a basis for V_h and $\{\psi_i\}_{i=1}^N$ be a basis for V_H. We want to construct the projection operator $\Pi : V_H \to V_h$ such that for any $v \in V_H$

$$(\Pi v, g) = (v, g), \qquad \forall g \in V_h. \tag{5.6}$$

To solve the discrete models we are actually interested in the quantity $(\Pi v, \phi_i),\ i = 1, \ldots, n$. See for example the discrete formulation for the E-model (4.11). Note that by (5.6), $(\Pi v, \phi_i) = (v, \phi_i),\ i = 1, \ldots, n$.

We can write $v = \sum_{k=1}^{N} v_k \psi_k$, so

$$(\Pi v, \phi_i) = (v, \phi_i) = \sum_{k=1}^{N} v_k (\psi_k, \phi_i) := \left(I_H^h \vec{v} \right)_i, \ i = 1, \ldots, n. \tag{5.7}$$

Here $\vec{v} = [v_1, \ldots, v_N]$ and $\left(I_H^h\right)$ is i-th row of the $n \times N$ interpolation matrix given by

$$I_H^h = \begin{bmatrix} (\psi_1, \phi_1) & (\psi_2, \phi_1) & \ldots & (\psi_N, \phi_1) \\ (\psi_1, \phi_2) & \ddots & & \vdots \\ \vdots & & \ddots & \vdots \\ (\psi_1, \phi_n) & \ldots & \ldots & (\psi_N, \phi_n) \end{bmatrix}. \tag{5.8}$$

Due to the fact that $V_H \subseteq V_h$, the projection operator Π defined by (5.6) is an interpolation operator, since it preserves the values of the function in the nodes. For an illustration of the action of Π see Figure 5.2.

5.2.1 Projection Π'

Now we discuss the projection operator $\Pi' : V_h \to V_H$. Let $V_H \subseteq V_h$, $\{\phi_i\}_{i=1}^n$ be a basis for V_h and $\{\psi_i\}_{i=1}^N$ be a basis for V_H. We want to construct the projection operator $\Pi' : V_h \to V_H$ so that for any $u \in V_h$

$$(\Pi' u, g) = (u, g), \qquad \forall g \in V_H. \tag{5.9}$$

We are interested in the quantity $(\Pi' u, \psi_i)$, $i = 1, \ldots, N$. We can write $u = \sum_{k=1}^{n} u_k \phi_k$ and using the definition (5.9).

$$(\Pi u', \psi_i) = (u, \psi_i) = \sum_{k=1}^{n} u_k (\phi_k, \psi_i) = \left((I_H^h)^T \vec{u} \right)_i, \ i = 1, \ldots, N. \tag{5.10}$$

Here $\vec{u} = [u_1, \ldots, u_n]$ and $(I_h^H)^T$ is the transpose of the interpolation matrix (5.8).

Figure 5.2: Projection operator $\Pi : V_H \to V_h$. V_H is generated by the spanning of $\{\psi_i(x)\}_{i=1}^5$ and V_h is generated by the spanning of $\{\phi_i(x)\}_{i=1}^7$. The node i of the mesh is denoted by x_i.

$$v(x) = 1 * \psi_1(x) + 2 * \psi_2(x) + 3 * \psi_3(x) + 2 * \psi_4(x) + 4 * \psi_5(x)$$

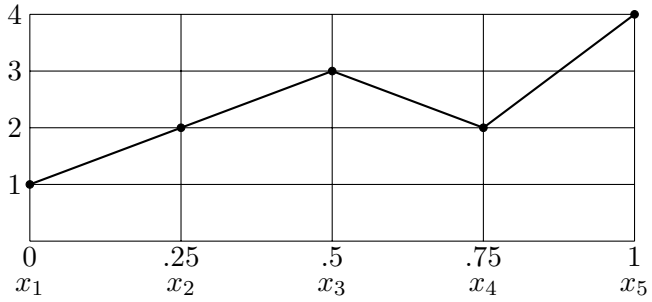

$$\Pi v(x) = \phi_1(x) + 1.4 * \phi_2(x) + 2 * \phi_3(x) + 3 * \phi_4(x) + 2.6 * \phi_5(x) + 2 * \phi_6(x) + 4 * \phi_7(x)$$

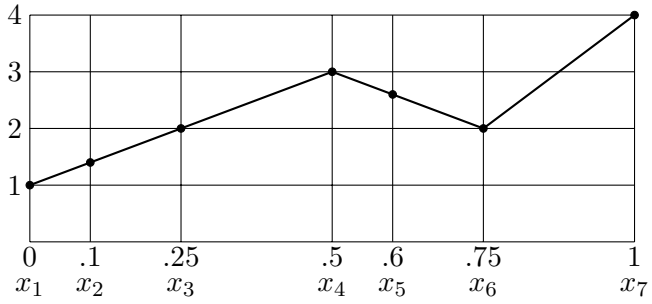

Figure 5.3: Illustration of a uniform refinement in 1D with $r = 2$. Plotted are the basis functions $\psi_1(x)$, $\psi_2(x)$, $\psi_3(x)$ spanning V_h which is based on cells 1 and 2; and basis functions $\phi_1(x)$, $\phi_2(x)$ spanning V_H which is based on element 1. x_1, x_2, x_3 are the nodes of the grid.

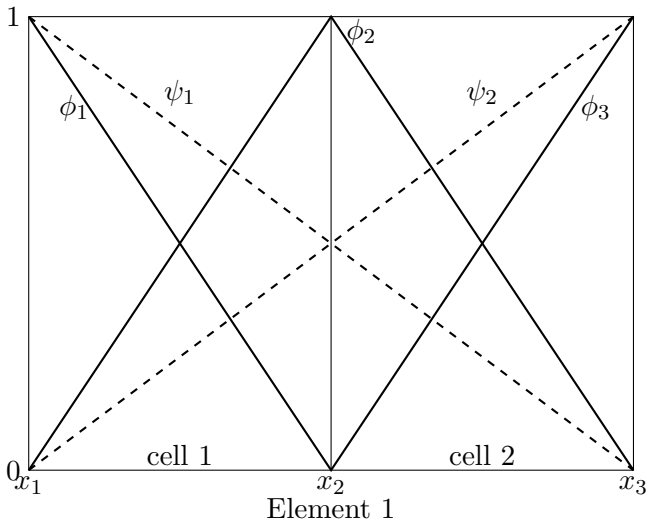

5.2.2 Implementation of I_H^h in 1D

Now we show how to implement the computation of matrix I_H^h. From now on, we denote the elements on the fine mesh $\mathcal{T}_h$ by cells, and the elements of the coarse grid $\mathcal{T}_H$ by elements. We denote by r_i the number of cells in the element i. Note that if the $r_i = r$, $\forall i$, the refinement is uniform, see Definition 4.1.1.

We need to compute the entries (ψ_i, ϕ_j) of the matrix I_H^h (5.8). To compute (ψ_i, ϕ_j), we integrate in the reference element $(-1, 1)$ for each cell. Notice that when we do this, the functions ψ are transformed into functions that depend on the value of r. In Figure 5.3 see an example for $r = 2$. In Figure 5.4 we show the reference element for cell 1, and we illustrate how the functions ψ's and ϕ's are translated to the reference element.

Figure 5.4: Illustration of the basis functions $\phi_1(x)$, $\phi_2(x)$, $\psi_1(x)$, $\psi_2(x)$ transformed from cell 1 to the reference element $(-1, 1)$.

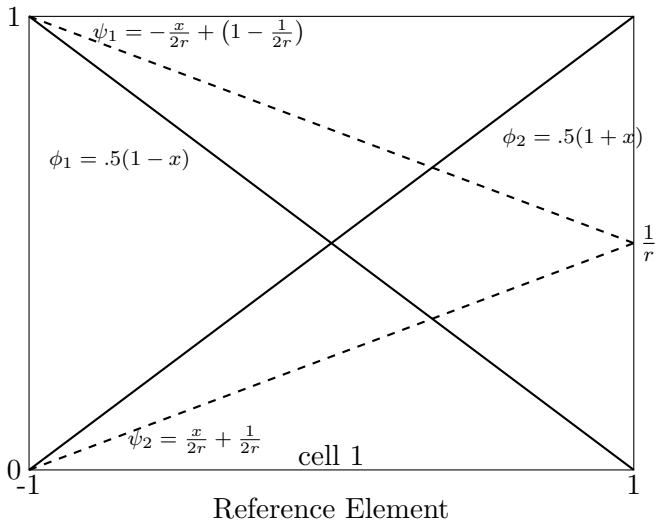

In general for an element with r cells, ψ_1, ψ_2 at the $j - th$ cell is given by :

$$\begin{aligned} \psi_1(x) &= \frac{-x}{2r} + \frac{2r - (2j-1)}{2r}, \\ \psi_2(x) &= \frac{x}{2r} + \frac{(2j-1)}{2r} \end{aligned}$$

where j is a integer with values from 1 to r that informs the location of the cell inside the element.

For every element T of $\mathcal{T}_h$ we do the integration in every cell contained in T.After assembling the matrix for every element, we assemble the matrices for all the elements getting the interpolation matrix I_H^h.

Next we give some simple examples of interpolation matrices.

Example 5.2.1. *Assume that $\mathcal{T}_H$ has one element only, and let $r = 2$, i.e., $\mathcal{T}_h$ has two cells. This is the scenario illustrated in Figure 5.3. In this case the interpolation matrix*

Figure 5.5: Illustration of triangles (elements) in the coarse mesh (full line) and fine mesh (dashed line)

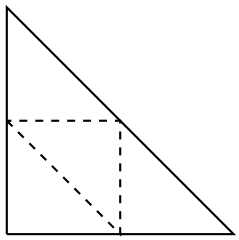

is given by

$$I_H^h = \frac{1}{2}\begin{bmatrix} 5/6 & 1/6 \\ 1 & 1 \\ 1/6 & 5/6 \end{bmatrix}.$$

Next let $r = 4$, i.e., $\mathcal{T}_h$ has four cells. In this case the interpolation matrix is given by

$$I_H^h = \frac{1}{4}\begin{bmatrix} 11/12 & 1/12 \\ 3/2 & 1/2 \\ 1 & 1 \\ 1/2 & 3/2 \\ 1/12 & 11/12 \end{bmatrix}.$$

5.2.3 Implementation of I_H^h in 2D

Here we consider for simplicity only uniform refinements. Let $r = \dfrac{H}{h}$. In each element of the coarse grid $\mathcal{T}_H$ we have r^2 elements of the refined grid $\mathcal{T}_h$, as one can see in Figure 5.5 for the case $r = 2$. As before, we refer to the elements of the fine grid $\mathcal{T}_h$ as cells, and to the elements in the coarse grid $\mathcal{T}_H$ as elements. The reference element in 2D triangulations is the right triangle with vertices at $(0, 0)$, $(1, 0)$, and $(0, 1)$.

The integration to compute the entries (ψ_i, ϕ_j) of the interpolation matrix takes place in each of the cells, then the values are assembled for each element. Each cell is mapped to the reference element with basis functions $\phi_1(x, y) = 1 - x - y$, $\phi_2(x, y) = x$,

Figure 5.6: Illustration of the cell numbering in one element for $r = 2$. The fine mesh $\mathcal{T}_h$ has 8 cells [dashed line], the coarse mesh $\mathcal{T}_h$ has 2 elements [full line]. The first number correspond to the local numbering of the cell inside the element, the second number corresponds to the global numbering of the cell in $\mathcal{T}_h$.

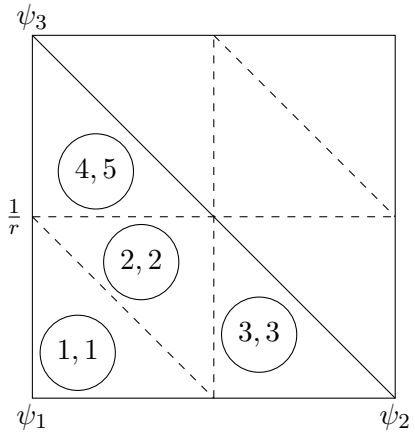

$\phi_3(x, y) = y$. In each element we compute a submatrix of I_H^h of size $3 \times \frac{(r+2)(r+1)}{2}$. $\frac{(r+2)(r+1)}{2}$ is the number of nodes of the refined mesh in one element of the coarse mesh.

Due to the uniformity of the mesh and of the refinement we calculate a relationship between the elements in both meshes. Let $r = 2$ as in Figure 5.6. Each triangle is subdivided into $r^2 = 4$ cells. Note that cell 2 has orientation different from the orientation of triangle that was refined. In this cases we say that the cell 2 is "flipped". It is easy to see that the flipped cells are cells with even global indices in the grid $\mathcal{T}_h$.

One of the challenges in the implementation is to realize how the basis functions of the element place themselves in each cell. This depends on:

- the location of each cell inside the element.
- the orientation of the cell (flipped or not): every element have $\frac{r(r+1)}{2}$ flipped cells.

To keep track of this location, each cell i is identified with a vector $\vec{j}_i = (j_i(1), j_i(2), j_i(3))$. The entry $j_i(k)$ gives information about the k-th basis element ψ_k in the cell i. The $j_i(k)$ are integers from 1 to r for the non-flipped cells and from 1 to r-1 for the flipped cells.

The $j_i(k)$ depends on the position and orientation of the cell. So every cell has its vector $\vec{j}$ that tells us how are we seeing the basis function ψ of the element in it.

Example 5.2.2. *In Figure 5.6, only cell* 2 *is a flipped cell. First let us consider the non-flipped cells. The k-th position of the vector* $\vec{j}_i$ *informs the "distance + 1" of where* $\psi(x,y)_k = 1$ *from the k-th node of cell i. In this way we see that for cell 1:* $\vec{j}_1 = (1,2,2)$ *since* $\psi_1(x,y) = 1$ *at node* 1 *of cell 1,* $\psi_2(x,y) = 1$ *at one "distance" of node* 2 *of cell* 1*, and* $\psi_3(x,y) = 1$ *at one "distance" of node* 3 *of cell* 1*. Similarly we get that*

$$\begin{aligned} \vec{j}_1 &= (1,2,2), \\ \vec{j}_3 &= (2,1,2), \\ \vec{j}_4 &= (2,2,1). \end{aligned}$$

For the flipped cell 2 *we get the vector* $\vec{j}$ *by the "distance"* $(1/r)$ *of where* $\psi_k = 1$ *from the k-th node of cell i. So that* $\vec{j}_2 = (1,1,1)$*. To illustrate better, how the algorithm for generating the vectors* $\vec{j}$ *work we present another example. Consider* $r = 4$*, then we have* $r^2 = 16$ *cells inside every element and* $\frac{r(r+1)}{2} = 6$ *flipped cells. For* $r = 4$*:*

Non-flipped	*Flipped*
$\vec{j}_1 = (1,4,4)$,	$\vec{j}_2 = (1,3,3)$,
$\vec{j}_3 = (2,3,4)$,	$\vec{j}_4 = (2,2,3)$,
$\vec{j}_5 = (3,2,4)$,	$\vec{j}_6 = (3,1,3)$,
$\vec{j}_7 = (4,1,4)$,	$\vec{j}_9 = (2,3,2)$,
$\vec{j}_8 = (2,4,3)$,	$\vec{j}_{11} = (3,2,2)$,
$\vec{j}_{10} = (3,3,3)$,	$\vec{j}_{14} = (3,3,1)$,
$\vec{j}_{12} = (4,2,3)$,	
$\vec{j}_{13} = (3,4,2)$,	
$\vec{j}_{15} = (4,3,2)$,	
$\vec{j}_{16} = (4,4,1)$.	

After some routine computation, one can realize that in each non-flipped cell:

$$\begin{aligned}\psi_1(x,y) &= \frac{r-j(1)+1}{r} - \frac{x}{r} - \frac{y}{r},\\ \psi_2(x,y) &= \frac{r-j(2)}{r} + \frac{x}{r},\\ \psi_3(x,y) &= \frac{r-j(3)}{r} + \frac{y}{r}.\end{aligned}$$

For the flipped cells, the basis functions ψ of the element are:

$$\begin{aligned}\psi_1(x,y) &= \frac{r-j(1)-1}{r} + \frac{x}{r} + \frac{y}{r},\\ \psi_2(x,y) &= \frac{r-j(2)}{r} - \frac{x}{r},\\ \psi_3(x,y) &= \frac{r-j(3)}{r} - \frac{y}{r}.\end{aligned}$$

If the refinement is uniform this has to be done for one element only.

5.2.4 Idea of the algorithm that implements I_H^h

1. Decide if the cell is flipped or not. This is going to be given by the even numbered cells. See the code `elementmatching.m` in the Appendix.

2. Get the cells nodes numbers inside the element. This only had to be done once because we are only considering uniform meshes and uniform refinements in 2D. The code can be easilly extend for non-uniform refinements by just informing the vector r_i where r_i is the number of cells inside the element i of the coarser mesh. See code `assemblingcells.m` in the Appendix.

3. Get the address of the cell $\vec{j}$. See code the `interpolator2D.m` in the Appendix.

4. Get a local interpolation matrix for each cell in an element. See code the `interpolator2D.m` in the Appendix.

5. Assemble the local interpolation matrices into another local interpolation matrix now in the element. See the code `interpolator2D.m` in the Appendix.

6. Assemble the local element interpolation matrices for all elements to get I_H^h. See the codes `interpolator2D.m` and `matching.m` in the Appendix.

5.3 Implementation of the models

In this Section we briefly discuss the implementation of the model problems.

5.3.1 Implementation of the E-Model

Recall the discrete formulation of the E-model, see equation (4.11):

Find $(u_h, v_H) \in V_h \times V_H$ *such that, for all* $(\phi_h, \psi_H) \in V_h \times V_H$,

$$(\lambda_1 u_h, \phi_h) + (a\nabla u_h, \nabla \phi_h) + (c(u_h - \Pi v_H), \phi_h) = (f, \phi_h),$$
$$(\lambda_2 v_H, \psi_H) + (b\nabla v_H, \nabla \psi_H) + (c(v_H - \Pi' u_h), \psi_H) = (g, \psi_H).$$

Let $V_H \subseteq V_h$, $\{\phi_i\}_{i=1}^{N_u}$ be a basis for V_h and $\{\psi_i\}_{i=1}^{N_v}$ be a basis for V_H. Using the basis notation we can write

$$u_h = \sum_{i=1}^{N_u} u_i \phi_i, \qquad v_H = \sum_{i=1}^{N_v} v_i \psi_i.$$

Thus for $j = 1, \ldots, N_u$ and $k = 1, \ldots, N_v$.

$$\sum_{i=1}^{N_u} \lambda_1 u_i(\phi_i, \phi_j) + \sum_{i=1}^{N_u} a u_i(\nabla\phi_i, \nabla\phi_j) + c\sum_{i=1}^{N_u} u_i(\phi_i, \phi_j) - c(\Pi v_H, \phi_i) = (f, \phi_j),$$
$$\sum_{i=1}^{N_v} \lambda_2 v_i(\psi_i, \psi_k) + \sum_{i=1}^{N_v} b v_i(\nabla\psi_i, \nabla\psi_k) + \sum_{i=1}^{N_v} v_i c(\psi_i, \psi_k) - c(\Pi' u_h, \psi_k) = (g, \psi_k).$$

In the matrix form, using (5.7) and (5.10)

$$\lambda_1 M_{V_h} \vec{u}_h + a S_{V_h} \vec{u}_h + c M_{V_h} \vec{u}_h - c I_H^h \vec{v}_H = \vec{f}, j = 1, \ldots, N_u,$$
$$\lambda_2 M_{V_H} \vec{v}_H + b S_{V_H} \vec{v}_H + c M_{V_H} \vec{v}_H - c (I_H^h)^T \vec{u}_h = \vec{g}, k = 1, \ldots, N_v.$$

Here the vectors are defined by

$$\begin{aligned}
\vec{u}_h &= [u_{h,1}, \ldots, u_{h,N_u}], \\
\vec{v}_H &= [v_{H,1}, \ldots, v_{H,N_v}], \\
\vec{f} &= [(f, \phi_1), \ldots, (f, \phi_{N_u})], \\
\vec{g} &= [(g, \psi_1), \ldots, (g, \psi_{N_v})].
\end{aligned}$$

Also M_{V_h} is called the mass matrix and S_{V_h} is called the stiffness matrix and they are given by

$$M_{V_h} = \begin{bmatrix} (\phi_1, \phi_1) & (\phi_2, \phi_1) & \ldots & (\phi_{N_u}, \phi_1) \\ (\phi_1, \phi_2) & \ddots & & \vdots \\ \vdots & & \ddots & \vdots \\ (\phi_1, \phi_{N_u}) & \ldots & \ldots & (\phi_{N_u}, \phi_{N_u}) \end{bmatrix}, \tag{5.14}$$

$$S_{V_h} = \begin{bmatrix} (\nabla\phi_1, \nabla\phi_1) & (\nabla\phi_2, \nabla\phi_1) & \ldots & (\nabla\phi_{N_u}, \nabla\phi_1) \\ (\nabla\phi_1, \nabla\phi_2) & \ddots & & \vdots \\ \vdots & & \ddots & \vdots \\ (\nabla\phi_1, \nabla\phi_{N_u}) & \ldots & \ldots & (\nabla\phi_{N_u}, \nabla\phi_{N_u}) \end{bmatrix}. \tag{5.15}$$

In the implementation we solve the system

$$A_E \vec{U} = b_E, \tag{5.16}$$

using the backslash "\" operation in MATLAB. Here

$$A_E := \begin{bmatrix} (\lambda_1 + c)M_{V_h} + aS_{V_h} & -cI_H^h \\ -c(I_H^h)^T & (\lambda_2 + c)M_{V_H} + aS_{V_H} \end{bmatrix}, \tag{5.17}$$

$$\vec{U} := \begin{bmatrix} \vec{u}_h \\ \vec{v}_H \end{bmatrix}, \tag{5.18}$$

$$b_E := \begin{bmatrix} \vec{f} \\ \vec{g} \end{bmatrix}. \tag{5.19}$$

5.3.2 Implementation of the LP, PP, and WR models

Here we describe the implementation of the LP-model. The implementation of the WR-model and the PP-model, are obtained by setting $b = 0$ and $\lambda_1 = b = 0$ in the LP-model, respectively. Recall the discrete formulation of the LP-model (4.112).

For each n, $1 \le n \le N$, *find* $(u_h, v_H) \in V_h \times V_H$ *such that* $\forall (\phi_h, \psi_H) \in V_h \times V_H$

$$\tau_n^{-1}(\lambda_1(u_h^n - u_h^{n-1}), \phi_h) + (a\nabla u_h^n, \nabla\phi_h) + (c(u_h^n - \Pi v_H^n), \phi_h) = (f^n, \phi_h),$$
$$\tau_n^{-1}(\lambda_2(v_H^n - v_H^{n-1}, \psi_H) + (b\nabla v_H^n, \nabla\psi_H) + (c(v_H^n - \Pi' u_h^n), \psi_H) = (g^n, \psi_H).$$

Let $V_H \subseteq V_h$, $\{\phi_i\}_{i=1}^{N_u}$ be a basis for V_h and $\{\psi_i\}_{i=1}^{N_v}$ be a basis for V_H. Using the bases notation we write

$$u_h^n = \sum_{i=1}^{N_u} u_i^n \phi_i, \qquad v_H^n = \sum_{i=1}^{N_v} v_i^n \psi_i. \tag{5.21}$$

Multiply the system by τ_n and use (5.21). At every time step n we solve

$$\sum_{i=1}^{N_u} \lambda_1 u_i^n(\phi_i, \phi_j) + \tau_n \sum_{i=1}^{N_u} u_i^n \left[(a\nabla\phi_i, \nabla\phi_j) + (c\phi_i, \phi_j)\right] - c(\Pi v_H^n, \phi_j) =$$
$$(f^n + \lambda_1 u_h^{n-1}, \phi_j), j = 1, \ldots, N_u,$$
$$\sum_{i=1}^{N_v} v_i^n \lambda_2(\psi_i, \psi_k) + \tau_n \sum_{i=1}^{N_v} v_i^n \left[(b\nabla\psi_i, \nabla\psi_k) + (c\psi_i, \psi_k)\right] - c(\Pi' u_h^n, \psi_k) =$$
$$(g^n + \lambda_2 v_H^{n-1}, \psi_k), k = 1, \ldots, N_v.$$

We apply (5.7) and (5.10) and write the system in the matrix form,

$$A_{LP}\vec{U} = b_{LP}. \tag{5.23}$$

Here

$$
\begin{aligned}
A_{LP} &:= \begin{bmatrix} (\lambda_1 + c)M_{V_h} + aS_{V_h} & -cI_H^h \\ -c(I_H^h)^T & (\lambda_2 + c)M_{V_H} + bS_{V_H} \end{bmatrix}, \\
\vec{U} &:= \begin{bmatrix} \vec{u}_h^n \\ \vec{v}_H^n \end{bmatrix}, \\
b_{LP} &:= \begin{bmatrix} \vec{f}^n \\ \vec{g}^n \end{bmatrix}.
\end{aligned}
$$

The matrices M_{V_h} and S_{V_h} are the mass and the stiffness matrices given by (5.14), (5.15), respectively. The vectors are defined by

$$
\begin{aligned}
\vec{u}_h^n &= [u_{h,1}^n, \ldots, u_{h,N_u}^n], && (5.24) \\
\vec{v}_H^n &= [v_{H,1}^n, \ldots, v_{H,N_v}^n], && (5.25) \\
\vec{f}^n &= [(f^n + u_h^{n-1}, \phi_1), \ldots, (f^n + u_h^{n-1}, \phi_{N_u})], && (5.26) \\
\vec{g}^n &= [(g^n + v_H^{n-1}, \psi_1), \ldots, (g^n + v_H^{n-1}, \psi_{N_v})]. && (5.27)
\end{aligned}
$$

For every n, $1 \leq n \leq N$ we solve the algebraic system (5.23) using the backslash operator "\" in MATLAB.

5.3.3 Implementation of the NLP-model

Here we discuss the fully-discrete form of the NLP-model, (4.109). For every n, $1 \leq n \leq N$ we need to solve find $(u_h^{n+1}, v_H^{n+1}) \in V_h \times V_H$ such that for all $(\xi, \psi) \in V_h \times V_H$.

$$
\begin{aligned}
(\lambda_1 u_h^n, \xi) + \tau_n \left[(a\nabla u_h^n, \nabla \xi) + c(\varphi(u_h^n) - \Pi v_H^{n+1}, \xi) \right] &= (\tau_n f^n + \lambda_1 u_h^{n-1}, \xi), \\
(\lambda_2 v_H^n, \psi) + \tau_n \left[(b\nabla v_H^n, \nabla \psi) - c(\Pi' \varphi(u_h^n) - v_H^n, \psi) \right] &= (\tau_n g^n + \lambda_2 v_H^{n-1}, \psi).
\end{aligned}
$$

Since this system is nonlinear, we apply the Newton-Raphson's method [8, 28].

Rewrite the problem in the residual form: find $(u_h^{n+1}, v_H^{n+1}) \in V_h \times V_H$ such that for all $(\xi, \psi) \in V_h \times V_H$

$$
A_{NLP}^n(u_h^n, v_H^n, \xi, \phi) = \vec{0}.
$$

Here $A^n_{NLP} = [A^n_1, A^n_2]^T$ where

$$\begin{aligned} A^n_1(u^n_h, v^n_H, \xi, \phi) &= (\lambda_1 u^n_h, \xi) + \tau_n \left[(a\nabla u^n_h, \nabla\xi) + c(\varphi(u^n_h) - \Pi v^{n+1}_H, \xi) \right] \\ &\quad -(\tau_n f^n + \lambda_1 u^{n-1}_h, \xi), \\ A^n_2(u^n_h, v^n_H, \xi, \phi) &= (\lambda_2 v^n_H, \psi) + \tau_n \left[(b\nabla v^n_H, \nabla\psi) - c(\Pi'\varphi(u^n_h) - v^n_H, \psi) \right] \\ &\quad -(\tau_n g^n + \lambda_2 v^{n-1}_H, \psi). \end{aligned}$$

We need to compute the Jacobian DA_{NLP} of the operator. Let $(z_1, z_2) \in V_h \times V_H$

$$DA^n_{NLP}(u^n_h, v^n_H, \xi, \phi; z_1, z_2) = \begin{bmatrix} A^n_{1,u^n_h}(z_1) & A^n_{1,v^n_H}(z_2) \\ A^n_{2,u^n_h}(z_1) & A^n_{2,v^n_H}(z_2) \end{bmatrix}.$$

Here

$$A^n_{1,u^n_h}(z_1) = (\lambda_1 z_1, \xi) + \tau_n \left[(a\nabla z_1, \nabla\xi) + c(\varphi'(u^n_h) z_1, \xi) \right].$$

Note that if φ is the Langmuir isotherm (2.23), we have

$$\varphi'(u^n_h) z_1 = \frac{\beta z_1}{(1 + \alpha u^n_h)^2}.$$

The operators Π, Π' defined by (5.6), (5.9) are clearly linear. Using this linearity we compute

$$\begin{aligned} A^n_{1,v^n_H}(z_2) &= \lim_{\epsilon\to 0} \frac{A^n_1(u^n_h, v^n_H + \epsilon z_2, \xi, \phi) - A^n_1(u^n_h, v^n_H, \xi, \phi)}{\epsilon} = -\tau_n c(\Pi z_2, \xi), \\ A^n_{2,u^n_h}(z_1) &= \lim_{\epsilon\to 0} \frac{A^n_2(u^n_h + \epsilon z_1, v^n_H, \xi, \phi) - A^n_2(u^n_h, v^n_H, \xi, \phi)}{\epsilon} = -c\tau_n(\Pi'\varphi'(u^n_h) z_1, \psi), \\ A^n_{2,v^n_H}(z_2) &= \lim_{\epsilon\to 0} \frac{A^n_2(u^n_h, v^n_H + \epsilon z_2, \xi, \phi) - A^n_2(u^n_h, v^n_H, \xi, \phi)}{\epsilon} \\ &= (\lambda_2 z_2, \psi) + \tau_n \left[(b\nabla z_2, \nabla\psi) + c(z_2, \psi) \right]. \end{aligned}$$

Now for each n, $1 \le n \le N$, we choose some initial guess $(u^{n,0}_h, v^{n,0}_H) \in V_h \times V_H$. At every k-th iteration step, we compute $(z^k_1, z^k_2) = (u^{n,k}_h - u^{n,k-1}_h, v^{n,k}_H - v^{n,k-1}_H) \in V_h \times V_H$

so that for all $(\xi, \psi) \in V_h \times V_H$

$$DA^n_{NLP}(u_h^{n,k}, v_H^{n,k}, \xi, \phi; z_1^k, z_2^k) = A^n_{NLP}(u_h^{n,k-1}, v_H^{n,k-1}, \xi, \phi). \tag{5.29}$$

In here, at every time step we choose as initial guess the solution for the previous time step. We stop this iteration when

$$\|(u_h^{n,k} - u_h^{n,k-1}, v_H^{n,k} - v_H^{n,k-1})\| \leq 10^{-6}.$$

We can now apply the basis notation (5.21) and rewrite the Newton-Raphson's method (5.29) as a linear algebraic system. To that end, note that by definition of Π' via (5.9), for $j = 1, \ldots, N_v$, we have

$$(\Pi'\varphi'(u_h^n)z_1, \psi_j) = (\varphi'(u_h^n)z_1, \psi_j) = \sum_{i=1}^{N_u} z_{1,i}(\varphi'(u_h^n)\phi_i, \psi_j).$$

The matrix $(I_H^h(\varphi(u)))^T$, which is a "weighted" version of the interpolation matrix $(I_H^h)^T$, is defined via

$$I_H^h(\varphi(u)) = \begin{bmatrix} (\varphi'(u)\psi_1, \phi_1) & (\varphi'(u)\psi_2, \phi_1) & \ldots & (\varphi'(u)\psi_{N_v}, \phi_1) \\ (\varphi'(u)\psi_1, \phi_2) & \ddots & & \vdots \\ \vdots & & \ddots & \vdots \\ (\varphi'(u)\psi_1, \phi_{N_u}) & \ldots & \ldots & (\varphi'(u)\psi_{N_v}, \phi_{N_u}) \end{bmatrix}. \tag{5.30}$$

Also let $M_{V_h,\varphi(u)}$ be the "weighted" mass matrix

$$M_{V_h,\varphi'(u)} = \begin{bmatrix} (\varphi'(u)\phi_1, \phi_1) & (\phi_2, \phi_1) & \ldots & (\varphi'(u)\phi_{N_u}, \phi_1) \\ (\varphi'(u)\phi_1, \phi_2) & \ddots & & \vdots \\ \vdots & & \ddots & \vdots \\ (\varphi'(u)\phi_1, \phi_{N_u}) & \ldots & \ldots & (\varphi'(u)\phi_{N_u}, \phi_{N_u}) \end{bmatrix}. \tag{5.31}$$

Therefore the system (5.29) is equivalent to

$$\begin{bmatrix} \lambda_1 M_{V_h} + \tau_n \left[aS_{V_h} + cM_{V_h,\varphi'(u_h^{n,k-1})} \right] & -\tau_n c I_H^h \\ -\tau_n c (I_H^h(\varphi(u_h^{n,k-1}))^T & (\lambda_2 + \tau_n c) M_{V_H} + \tau_n b S_{V_H} \end{bmatrix} \begin{bmatrix} \vec{z}_1^{\,k} \\ \vec{z}_2^{\,k} \end{bmatrix} = \begin{bmatrix} \vec{F}^{n,k} \\ \vec{G}^{n,k} \end{bmatrix}. \tag{5.32}$$

Here the vectors are defined by

$$\begin{aligned} \vec{F}^{n,k} &= (\lambda_1 M_{V_h} + \tau_n a S_{V_h}) \vec{u}_h^{n,k-1} + c\tau_n \left[\varphi_{V_h}(u_h^{n,k-1}) - I_H^h \vec{v}_H^{n,k-1} \right] \\ &\quad -\tau_n \vec{f}^n - \lambda_1 M_{V_h} \vec{u}_h^{n-1}, \\ \vec{G}^{n,k} &= \left[(\lambda_2 + \tau_n c) M_{V_H} + \tau_n b S_{V_H} \right] \vec{v}_H^{n,k-1} - c\tau_n \varphi_{V_H}(v_H^{n,k-1}) \\ &\quad -\tau_n \vec{g}^n - \lambda_2 M_{V_H} \vec{v}_H^{n-1}, \end{aligned}$$

where $\vec{f}^n, \vec{g}^n$ are given by (5.26)-(5.27), and the vector $\varphi_{V_h}(u_h^{n,k-1})$ is given by

$$\begin{aligned} \varphi_{V_h}(u_h^{n,k-1}) &= [(\varphi(u_h^{n,k-1}), \phi_1), \ldots, (\varphi(u_h^{n,k-1}), \phi_{N_u})], \\ \varphi_{V_h}(v_H^{n,k-1}) &= [(\varphi(v_H^{n,k-1}), \psi_1), \ldots, (\varphi(v_H^{n,k-1}), \psi_{N_v})]. \end{aligned}$$

Note that if $V_h = V_H$ then $I_H^h(\varphi(u_h^n)) = I_H^h$ and $M_{V_h,\varphi'(u)} = M_{V_h}$.

5.4 Numerical results for the E-model

In this section we present results for the elliptic system E-model. We do not spend much time on the verification of the *a-priori* results because they are fairly standard. Our focus is to demonstrate the robustness of *a-posteriori* estimators with respect to $\mathcal{P} = (\lambda_1, \lambda_2, a, b, c)$ and to illustrate how the multilevel scheme and error estimation work together.

On multilevel grids, we use grid parameters h and H with the number of elements in $\mathcal{T}_h$ and $\mathcal{T}_H$ denoted, respectively, by n and N. Except in Example 5.4.5 we only consider r-refinements $\mathcal{T}_h$ of $\mathcal{T}_H$. That is, we only consider the case $r = H/h$ where $1 \leq r \in \mathbb{N}$. For $r > 1$ we refer to $\mathcal{T}_h$ as the fine mesh and to $\mathcal{T}_H$ as the coarse mesh.

In each case, we obtain (u_h, v_H) by solving the linear system associated with (4.11), and compute the error $\mathcal{E}_e$ (4.37) using the known analytical solution (u, v). If (u, v)

are not known, then we estimate it from the finest grid possible or by Richardson's extrapolation.

We recall that the efficiency index $\Theta := \frac{\eta_e}{\mathcal{E}_e}$. For various implicit estimators, asymptotically, $\Theta \downarrow 1$. However, for residual estimators $\Theta >> 1$ [21, 44]. For perspective, we show typical values of Θ for scalar and non-scalar model problems below. In this paper our concern is in showing that Θ remains constant or stable for a large range of values in $\mathcal{P}$.

We consider the numerical solution (4.11) to the coupled system (3.25). We demonstrate that the algorithm converges on multilevel grids and that Θ remains essentially constant. The latter is thanks to the appropriate scaling in the definition of the estimator.

5.4.1 Numerical results in 1D

Example 5.4.1. *Let $\Omega = (0,1)$ and $u(x) = x^2\sin(\pi x)$, $v(x) = x - x^3$, be the exact solution of (3.25) with $\mathcal{P} = \mathbf{1}^5$. We compute the corresponding f and g, and solve for the numerical solutions u_h, v_H. We consider here various uniform multilevel grids with $r = 1, 2, 5, 100$. Table 5.1 shows the value of the error and of the error estimate as well as of the efficiency index Θ.*

We see that for any grid level r, the error and the estimator converge linearly with H: the error decreases by $1/2$ when N is halved. This example also shows robustness of the estimator with respect to h and r: Θ remains essentially constant in all Tables. The value $\Theta \approx 7$ is typical for the coupled system in 1-dimensional examples.

Next we discuss the error for a fixed H and varying r, in order to understand the merits of multilevel discretizations. For example we compare the error and the estimator for $N = 160$ i.e. fourth row in the list for each r in Table 5.1. We see that the error decreases quite a bit initially between $r = 1$ and $r = 2$ but that it remains dominated by the $O(H)$ component for large r.

These results illustrate in what instances it makes sense to refine the grid in one component only. In general, the refinement in u-component increases the total number of unknowns from $N+N = 2N$ to $rN+N = (r+1)N$. If useful, this should be accompanied by a proportional decrease in the error by a factor of $(1+r)/2$. In Example 5.4.1 for large r this is not true since for small h the error remains bounded by the $O(H)$ contribution.

Table 5.1: Results for Example 5.4.1

N	$\mathcal{E}_e$	η_e	Θ	N	$\mathcal{E}_e$	η_e	Θ
$r=1$				$r=2$			
20	0.109	0.814	7.46	20	0.0696	0.526	7.56
40	0.0545	0.415	7.61	40	0.0348	0.266	7.62
80	0.0272	0.209	7.68	80	0.0174	0.134	7.70
160	0.0136	0.105	7.71	160	0.00870	0.0672	7.72
320	0.0068	0.0526	7.73	320	0.00435	0.0336	7.73
640	0.00341	0.0264	7.74	640	0.00218	0.0168	7.74
1280	0.00170	0.0132	7.74	1280	0.00109	0.00842	7.74
2560	0.00085	0.0066	7.74	2560	0.000544	0.00421	7.74
5120	0.00042	0.0033	7.74	5120	0.000272	0.00211	7.74
N	$\mathcal{E}_e$	η_e	Θ	N	$\mathcal{E}_e$	η_e	Θ
$r=5$				$r=100$			
20	0.0536	0.404	7.54	20	0.0500	0.376	7.52
40	0.0268	0.205	7.64	40	0.0250	0.191	7.63
80	0.0134	0.103	7.69	80	0.0125	0.0961	7.69
160	0.00670	0.052	7.72	160	0.00625	0.0482	7.72
320	0.00335	0.026	7.73	320	0.00312	0.0242	7.73
640	0.00168	0.013	7.74	640	0.00156	0.0121	7.74
1280	0.000838	0.0065	7.74				
2560	0.000419	0.0032	7.74				
5120	0.000209	0.0016	7.74				

However, for $r = 2$ we have the desired proportional decrease in the error. Here the number of unknowns between $r = 1$ and $r = 2$ increases by a factor of 1.5 while the error decreases by the factor of $0.0136/0.00870 \approx 1.563$.

The computational cost of a multilevel algorithm is obviously case-dependent since the error components depend on u, v, h, H. Example 5.4.1 can be seen as the "worst case scenario", since the components u and v have comparable variability and $\mathcal{P} = \mathbf{1}^5$. However, the usefulness of multilevel grids is evident in other cases to follow, and, in particular, in the next example which is a variation on Example 5.4.1.

Example 5.4.2. *Here we modify Example 5.4.1 and choose a fast oscillating u component $u(x) = x^2 \sin(10\pi x)$. We keep $v(x) = x - x^3$ with $\mathcal{P} = (1, 1, 1, 1, 1)$. Table 5.2 shows the results.*

Table 5.2: Results for Example 5.4.2

n	$\mathcal{E}_e$	η_e	Θ	n	$\mathcal{E}_e$	η_e	Θ
$r=1$				$r=5$			
20	4.4206	30.049	6.7975	20	4.4274	30.094	6.7971
40	2.2704	16.996	7.4860	40	2.2737	17.019	7.4850
80	1.1433	8.7785	7.6780	80	1.1450	8.7904	7.6774
160	0.57269	4.4259	7.7281	160	0.57351	4.4320	7.7278
320	0.28648	2.2176	7.7411	320	0.28688	2.2208	7.7409
640	0.14325	1.1094	7.7446	640	0.14346	1.1110	7.7445
1280	0.071629	0.55480	7.7455	1280	0.071731	0.55559	7.7455
2560	0.035815	0.27741	7.7458	2560	0.035866	0.27781	7.7458
5120	0.017907	0.13871	7.7459	5120	0.017933	0.13891	7.7459

Consider the error in Example 5.4.2 for a fixed h and varying r. For instance, focus on $n = 160$ and the fourth row in each r in Table 5.2. The error remains almost constant between $r = 1$ and $r = 5$ despite the fact that we are coarsening the H grid by a factor of 5. This is because the error is dominated by the $O(h)$ terms for small r. The number of elements between $r = 1$ and $r = 5$ decreases from 320 down to 192, i.e., by the factor of 1.66, while the error increases only by less than one percent since $0.5735/0.5727 \approx 1.0014$.

Next we illustrate other properties of the estimator. First we verify how η_e behaves for a system close to being degenerate.

Example 5.4.3. *Let* $\Omega = (0, 1)$ *and* $u(x) = v(x) = x^2 \sin(\pi x)$ *be the exact solution of* (3.25). *Let* $\mathcal{P} = (1, 1, 1, 10^{-5}, 10)$. *We use* $r = 1, 5, 40$, *see Table 5.3.*

In Example 5.4.3 we demonstrate the robustness of the estimator with respect to H, r, i.e., we show that the estimator converges and that Θ is essentially constant with respect to H and r. This Example also provides yet another motivation for the use of multilevel grids. The error between $r = 1$ and $r = 5$ appears to decrease by the factor $0.0625/0.0015 \approx 4.1$ while the number of unknowns increases by $(1+5)/2 = 3$ (cf. row 4). With $r > 5$ the advantages of multilevel grids deteriorate slowly as r increases because the error in u gets resolved better and it slowly stops dominating the total error. For $r = 40$ we have a decrease of the error by $0.0625/0.00015 \approx 40$ in row 4 but only $0.0499/0.0017 \approx 29$ while the number of unknowns increases by about 20.5. This

Table 5.3: Results for Example 5.4.3 with degenerate $\mathcal{P}$

N	$\mathcal{E}_e$	η_e	Θ
$r=1$			
20	0.049999	0.37583	7.52
40	0.025000	0.19076	7.63
80	0.012500	0.096101	7.68
160	0.0062500	0.048231	7.71
320	0.0031250	0.024161	7.73
640	0.0015625	0.012092	7.73
1280	0.00078125	0.0060487	7.74
2560	0.00039063	0.0030251	7.74
5120	0.00019531	0.0015127	7.74
$r=5$			
20	0.010069	0.077007	7.64
40	0.0050085	0.038615	7.71
80	0.0025013	0.019336	7.73
160	0.0012503	0.0096758	7.74
320	0.00062509	0.0048400	7.74
640	0.00031254	0.0024205	7.74
1280	0.00015627	0.0012103	7.74
2560	7.81×10^{-5}	0.00060520	7.74
5120	3.91×10^{-5}	0.00030261	7.74

N	$\mathcal{E}_e$	η_e	Θ
$r=40$			
20	0.0017252	0.0098209	5.69
40	0.00069009	0.0048530	7.03
80	0.00032240	0.0024250	7.52
160	0.00015841	0.0012146	7.67
320	7.89×10^{-5}	0.00060995	7.73
640	3.94×10^{-5}	0.00030498	7.74
1280	1.97×10^{-5}	0.00015249	7.74

suggests that $r = 40$ is close to the final value of r beyond which no decrease of the error can happen.

Now we demonstrate the robustness of the estimator with respect to $\mathcal{P}$.

Example 5.4.4. *Here we have $\Omega = (0,1)$ and f, g as in Example 5.4.1. We now vary the coefficients in $\mathcal{P}$. Since an analytical solution is not easily obtained for such a problem, we approximate $(u, v) \approx (u_*, v_*)$ where the latter is obtained on a grid with $n_* = 5210$ elements. We fix the grid and set $N = 160$ elements. and let the various coefficients in $\mathcal{P}$ vary, one at a time, by several orders of magnitude. In Table 5.4 we show the variation of the efficiency index Θ with respect to $\mathcal{P}$ and r.*

We observe in Table 5.4 that the ratio Θ is essentially constant i.e. the estimator η_e is quite robust with respect to r and c, λ_1. It is also stable with respect to a, b. However, for $a, b \downarrow 0$ the efficiency index Θ varies, even though it changes only by a factor less

Table 5.4: Efficiency index Θ in Example 5.4.4. Each row corresponds to a different value of a parameter from $\mathcal{P}$ as indicated while other parameters are kept fixed with value 1. Each column corresponds to the different r

a \ r	1	2	4	16
10^{10}	7.76	7.75	7.76	7.72
10^{5}	7.76	7.75	7.76	7.72
1	7.76	7.82	7.92	7.73
10^{-5}	3.06	5.59	6.89	8.08
10^{-10}	1.42	1.63	1.48	2.26

b \ r	1	2	4	16
10^{10}	7.76	7.89	8.67	8.94
10^{5}	7.76	7.89	8.67	8.94
1	7.76	7.82	7.92	7.73
10^{-5}	3.19	3.11	3.10	3.06
10^{-10}	1.53	1.53	1.42	1.43

c \ r	1	2	4	16
10^{10}	7.76	6.94	6.24	5.67
10^{5}	7.76	7.61	7.60	7.51
1	7.76	7.82	7.92	7.73
10^{-5}	7.76	7.82	7.92	7.74
10^{-10}	7.76	7.82	7.92	7.74

λ_1 \ r	1	2	4	16
10^{10}	7.76	7.75	7.76	7.72
10^{5}	7.69	7.74	7.76	7.72
1	7.76	7.82	7.92	7.73
10^{-5}	7.76	7.82	7.92	7.74
10^{-10}	7.76	7.82	7.92	7.74

than 4 when a, b change by a factor of 10^{10}. This variability could be eliminated for a small enough H, h.

5.4.2 Adaptivity example

Next we consider application of the multilevel estimator to grid adaptivity.

Remark 5.4.1. *Various adaptive strategies based on a-posteriori error estimates can be defined. For the needs of the subsequent example, we use the following strategy one. In each step we mark for refinement those elements $T' \in \mathcal{T}_h$ for which the local estimator*

$$\eta_{T',u} > 0.5 \max_{T} \eta_{T,u}.$$

Analogously we mark the elements $K \in \mathcal{T}_H$. The actual choice of new grid elements honors the requirement that $\mathcal{T}_h$ be a refinement of $\mathcal{T}_H$.

As an alternative strategy we refine those $T' \in \mathcal{T}_h$ for which

$$\eta_{T',u} > 0.5 \min(\max_{T} \eta_{T,u}, \max_{K} \eta_{K,v}),$$

Figure 5.7: Solutions u, v in Example 5.4.5. Left: plot over $(0,1)$. Right: zoomed in boundary layer for u, v with an additional boundary layer for u.

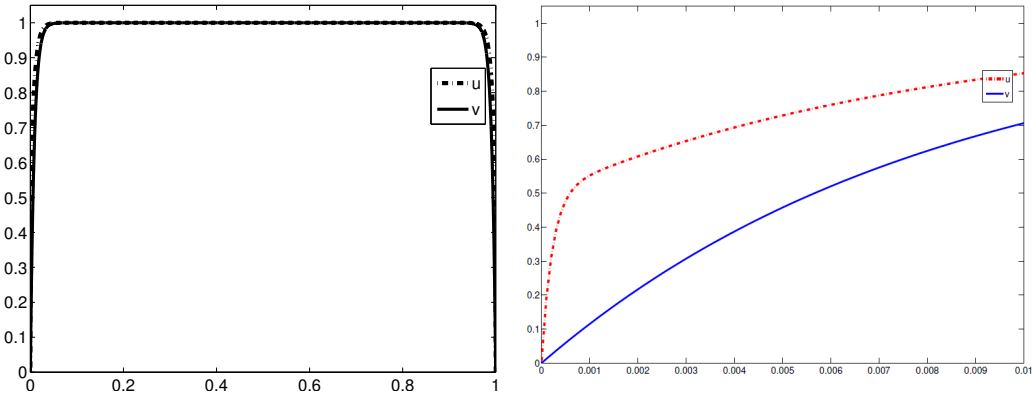

with a natural K-analogue. These two strategies can frequently mark the same elements, but sometimes the alternative method leads to a faster decrease in $\mathcal{E}_e$ than the original.

Example 5.4.5. *Let $\mathcal{P} = (1, 1, a, b, 1)$ and $\Omega = (0,1)$, $f = g \equiv 1$. This example is from ([36], Example 1) where it is shown that both u, v have both boundary layers of width $O(b^{1/2} \ln b)$, and that u has an extra layer of width $O(a^{1/2} \ln a)$. Let $a = 10^{-7}$, $b = 10^{-4}$. The solution is shown in Figure 5.7.*

Starting from a uniform grid $\mathcal{T}_h^0 = \mathcal{T}_H^0$ with $h = 0.2$ and $n = N = 5$, we use our a-posteriori estimator η_e to guide the appropriate grid refinement in the boundary layer as in Remark 5.4.1. We show details of the first few steps of this strategy, referring only to the boundary layer on the left hand side; the other side follows by symmetry. Table 5.5 summarizes the quantitative information and Figures 5.8 and 5.9 illustrate its effects.

1. *After we compute the solution (u_h, v_H) and the local error estimator for $\mathcal{T}_h^0 = \mathcal{T}_H^0$ we find that we need to refine the grid in the intervals $[0, 0.2]$ for both u and v components, according to both strategies in Remark 5.4.1. We denote this grid by $\mathcal{T}_h^1 = \mathcal{T}_H^1$.*

2. *Compute the solution and the local error estimator for $\mathcal{T}_h^1 = \mathcal{T}_H^1$, here $n = N = 43$. We find that we need to refine the elements in $[0, 0.1]$ for u components and in $[0, 0.1]$, $[0.1, 0.2]$ for v component. The marking is the same for both strategies. We denote the resulting grid by $\mathcal{T}_h^2, \mathcal{T}_H^2$. Note that $\mathcal{T}_h^2 \neq \mathcal{T}_H^2$.*

Table 5.5: Refinement at each step (recall symmetry of the domain)

	1^{st} Step	2^{nd} Step	3^{rd} Step
$\max \eta_{u,T}$	0.2318	0.0518	0.0178
$\max \eta_{v,K}$	0.2315	0.1087	0.0444
η_e	0.4818	0.2120	0.140
# of elements	5 + 5 =10	43+43 = 86	79 + 61 = 140

3. *Compute the solution and the local error estimator for* $\mathcal{T}_h^2, \mathcal{T}_H^2$. *Here we have* $n = 79, N = 61$. *Using the original component-based strategy, we find that we need to refine in the interval* $[0, 0.001]$ *for* u *and in* $[0.02, 0.03]$ *for* v *component. The alternative strategy marks* $[0, 0.001]$ *for* u *and* $[0.01, 0.02], [0.02, 0.03]$ *for* v.

4. *Continue ...*

Analysing this last Example we see that the a-posteriori error estimators suggest after Step 2 that a multilevel rather than identical grid should be used for the two components. In order to refine separately the u- and v- grids, we need an ability to estimate the error in each component separately and at best locally.

5.4.3 Numerical results for error in only one of the variables

Our next example shows the application of the error estimate in one variable only.

Example 5.4.6. *Let* $\Omega = (0, 1)$ *and* $u(x) = x^2 \sin(10\pi x)$, $v(x) = x - x^2$ *be the exact solution of* (2.1a)–(2.1b) *with* $\mathcal{P} = (1, 1, 10^{-3}, 1, 100)$. *We note that* $c = 100$ *indicates a rather strong coupling in the system. We use* $N = 320$ *and let* r *vary. Table 5.6 shows the application of the global system estimator and of the one for* u*-variable only.*

Studying the first row of Table 5.6 and comparing $\mathcal{E}_e$ with $\mathcal{E}^*$ and η_e with η^* we notice that that they are close, i.e., error is dominated by the error in u. It is important to notice that since both estimators are robust in r, we can use the estimators instead of the error information as a tool to determine the dominating component. To decrease that component of the error, we refine the mesh on which u is computed. This helps to decrease the error significantly while making the total number of unknowns grow by a factor smaller than $2r$ between each grid steps. However, in row 6 the errors and the

Figure 5.8: Illustration of adaptive steps from Example 5.4.5: plot of solution (u_h, v_H). Top: solution in step 1. Bottom: solution step 2.

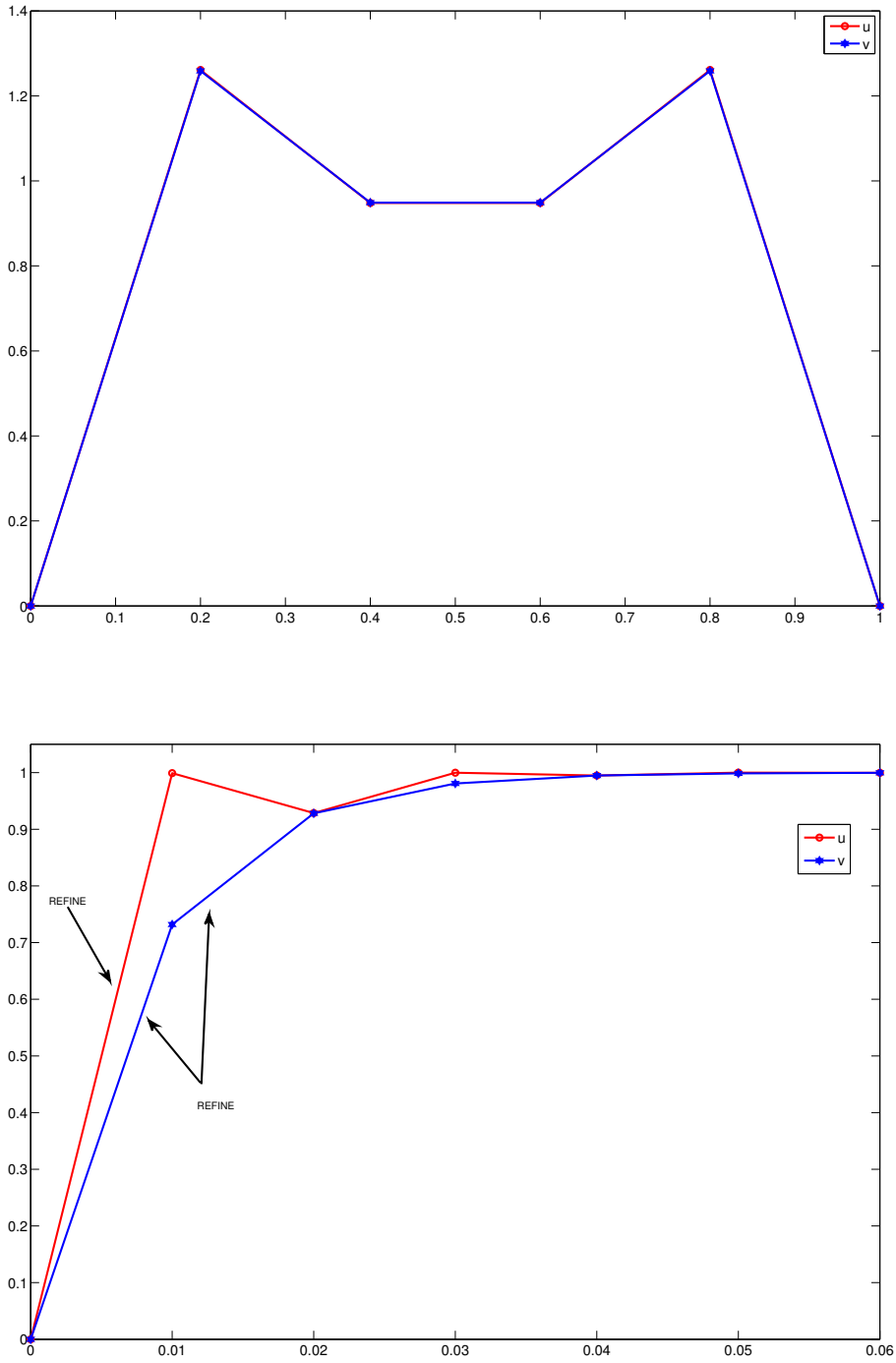

Figure 5.9: Illustration of adaptive steps from Example 5.4.5: plot of solution (u_h, v_H). Top: step 3 with original strategy. Bottom: step 3 with alternative strategy. Zoom is indicated by the range of x.

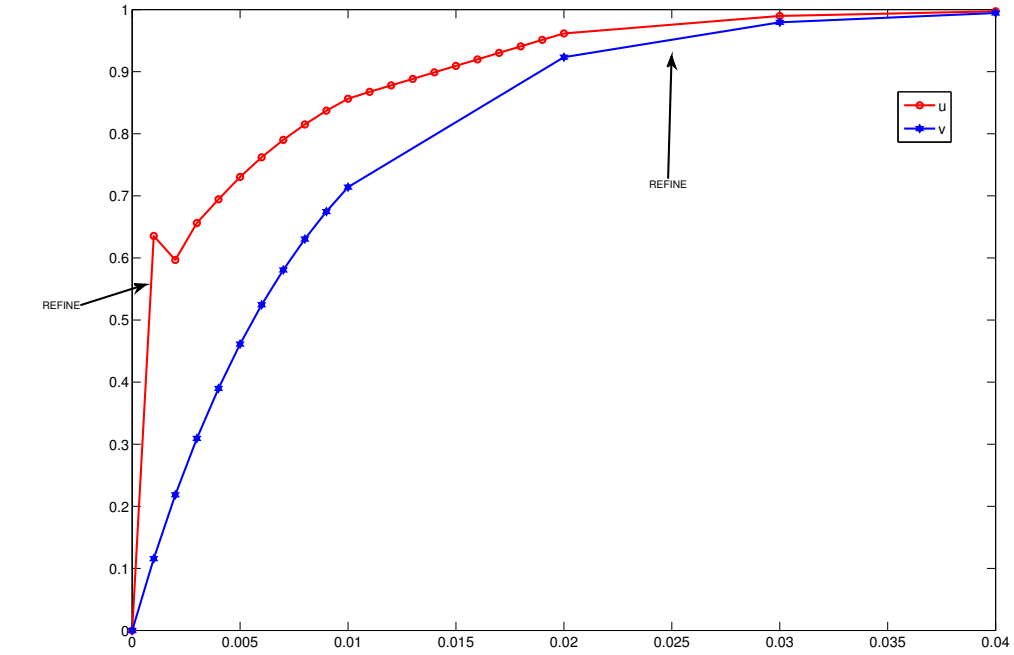

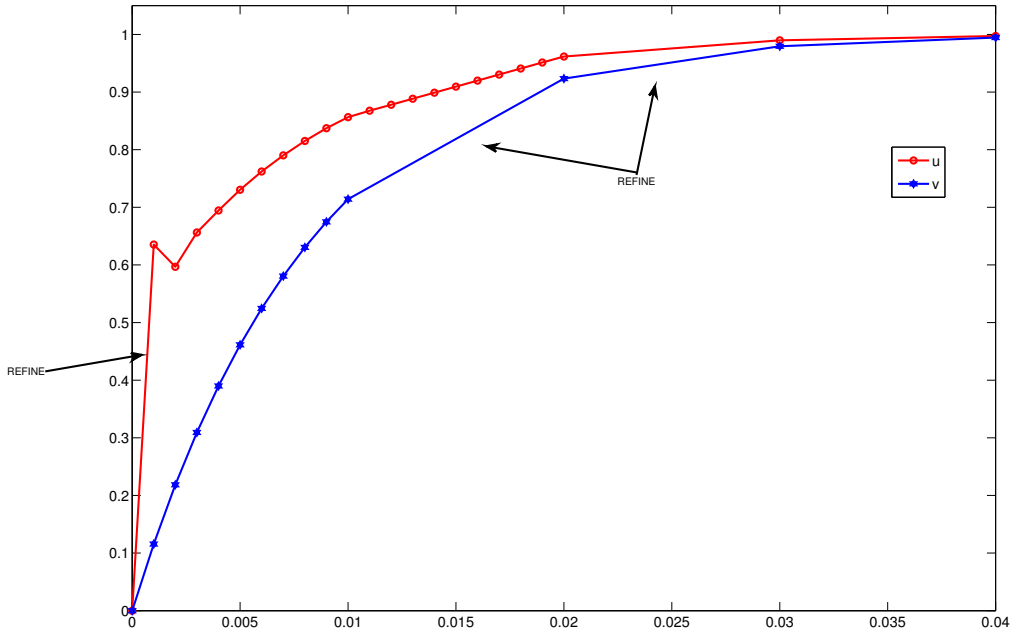

Table 5.6: Robustness and use of estimator in one variable only in Example 5.4.6. Shown on the left are the error, estimate, and efficiency index corresponding to the usual estimator (4.34). On the right we show the corresponding values for the quantities computed in the u variable only (4.67) and in particular η^* and $\mathcal{E}^* := \|u - u_h\|_*$, and $\Theta^* := \frac{\eta^*}{\mathcal{E}^*}$

rN	η_e	$\mathcal{E}_e$	Θ	rN	η^*	$\mathcal{E}^*$	$\eta^*/\mathcal{E}^*$
320	0.071569	0.0093135	7.6844	320	0.070195	0.0091370	7.6825
640	0.037764	0.0048850	7.7305	640	0.035090	0.0045396	7.7296
1280	0.022419	0.0028967	7.7396	1280	0.017544	0.0022662	7.7416
2560	0.016486	0.0021303	7.7387	2560	0.0087722	0.0011327	7.7443
5120	0.014631	0.0018910	7.7371	5120	0.0043861	0.00056644	7.7433
10240	0.014129	0.0018263	7.7365	10240	0.0021931	0.00028347	7.7365

estimators vary already by a factor of ≈ 6 that is, we have decreased the dominating component of the error.

As for computational complexity, we see that the error decreases by a factor of almost 2 between the first row and the second while the number of unknowns increased by a factor of $3/2 = 1.5$. Without multilevel grids, we would have to refine grid in u, v simultaneously, i.e., double the total number of unknowns. We conclude that multilevel grids are quite useful in this example.

In summary, Example 5.4.6 is a nice illustration of applicability of the estimator in one variable only. It is associated by design with the strongly varying component, i.e., the u component.

Next we consider a few examples in $d = 2$ dimensions.

5.4.4 Numerical results in 2D

Example 5.4.7. *Use as exact solution to* (3.25) *the functions* $u(x, y) = \sin(2\pi x)(y^2 - y)$, $v(x, y) = (x^2 - x)(y^2 - x)$. *Let* $\Omega = (0, 1)^2$. *The coefficients are set to be* $\mathcal{P} = (1, 1, 1, 10^{-3}, 10)$. *We calculate the corresponding* f, g. *Next, we solve for* (u_h, v_H) *and consider the rate of convergence of the energy error and of the estimator. We use* $N = rn$ *for* $r = 1, 4$. *In Table 5.7 we can see that* Θ *changes a little with* N *but not much with* r.

Example 5.4.8. *Now we vary* $\mathcal{P}$ *in Example 5.4.7. Since the analytical solution for general* $\mathcal{P}$ *is not easy to find, we use Richardson extrapolation with* $n_* = 131072$ *elements to*

Table 5.7: Convergence of the error and estimator for Example 5.4.7, $N = n$ that is $r = 1$ (left) and $N = 4n$ or $r = 4$ (right)

$\frac{1}{h}$	$\mathcal{E}_e$	η_e	Θ
16	0.13244	1.6367	12.358
32	0.066409	0.83876	12.630
64	0.033228	0.42340	12.742
128	0.016617	0.21255	12.791

$\frac{1}{h}$	$\mathcal{E}_e$	η_e	Θ
4	0.13966	1.6731	11.979
8	0.067145	0.84301	12.555
16	0.033321	0.42397	12.724
32	0.016632	0.21265	12.786

Table 5.8: Efficiency index Θ for Example 5.4.8

a \ λ_2	10^{-10}	10^{-5}	1	10^5	10^{10}
10^{-10}	3.8324	3.8324	3.7714	1.3563	1.3563
10^{-5}	4.5796	4.5796	4.5117	1.8375	1.8375
1	12.237	12.237	12.231	12.076	12.076
10^5	13.839	13.839	13.839	12.025	12.076
10^{10}	13.840	13.840	13.839	2.2928	12.039

approximate the true error. We are interested in the behavior of Θ *for* $\mathcal{P} = (1, \lambda_2, a, 1, 10)$ *when* a *and* λ_2 *decrease; this example is relevant to a steady-state pseudo-parabolic system [39]. The solution* u_h, v_H *is computed with* $n = 8192, N = 2048$ *elements. The results are presented in Table 5.8.*

Our last example shows the application of the global error estimate to adapt the grid uniformly in the goal to satisfy a prescribed tolerance. Specifically, we want to ensure

$$\|(e_u, e_v)\|_e \leq \tau \tag{5.33}$$

for a given τ. This follows of course if we ensure $\eta_e \leq \tau$.

Example 5.4.9. *We consider* $\mathcal{P} = (0.1, 1, 1, 10^{-3}, 10)$ *and* $\Omega = (0, 1)^2$ *in* (3.25). *The analytical solution is given by* $u(x, y) = \sin(2\pi x)(y^2 - y)$, $v(x, y) = (x^2 - x)(y^2 - y)$.

To satisfy (5.33) *with* $\tau = 0.02$ *we can use either* $\mathcal{T}_h = \mathcal{T}_H$ *and* $h = H = 1/128$ *with a total* $16641 + 16641 = 33282$ *nodes. On the other hand, to satisfy the same tolerance with multilevel mesh it suffices to have* $h = 1/128$, $H = 1/16$, $r = 8$ *and* $16641 + 289 = 16930$ *nodes.*

For $\tau = 0.05$, we find that $4225 + 4225 = 8450$ nodes are necessary while $4225 + 81$ nodes of multilevel mesh will suffice. Here $h = 1/64 = 0.015625$, and $H = 1/8 = 0.0125$, so $r = H/h = 8$.

5.4.5 Numerical results for piecewise constant coefficients

In the two examples below we consider the following setting:

- $\Omega = (0, 1)$.
- $f \equiv 1$ and $g \equiv 0$.
- Homogeneous Dirichlet boundary conditions.
- $\mathcal{P} = \{1, 1, a(x, q), 10\}$.

The parameter $a(x, q)$ is given by

$$a(x,q) = \begin{cases} 1, & x \in (0, 0.2) \cup (0.3, 0.5) \cup (0.7, 0.8) \cup (0.9, 1), \\ q, & \text{otherwise.} \end{cases}$$

Here q is a positive constant. Note that if $q = 1$, then $a \equiv 1$. Figure 5.10 illustrates $a(x, q)$.

We vary the parameter q and analyse the robustness of the estimator η_e. To compute the efficiency index Θ we use as the true solution the solution approximated in a mesh with 8000 elements and use this solution to approximate the true error $\mathcal{E}_e$.

Example 5.4.10. *Let $q = 10^{-3}$. We test the error convergence and the robustness of the estimator for:*

- *h^{-1} = 500, 1000, 2000.*
- *r = 1, 2, 5, 10.*

In Table 5.9 we observe that the efficiency Θ remains close to the value 7.7 despite the fact that a is piecewise constant.

Example 5.4.11. *Fix $h^{-1} = 2000$. We verify the robustness of the estimator η_e for:*

- $r = 1, 2, 5, 10$.

Figure 5.10: Illustration of the piecewise constant parameter $a(x, q)$

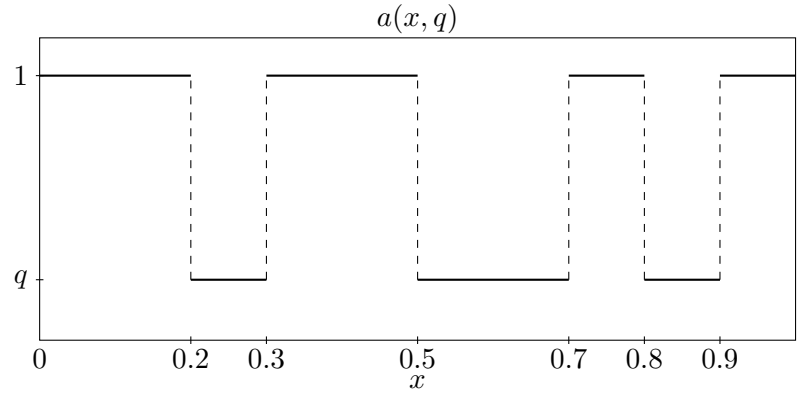

Table 5.9: Example 5.4.10: Robustness of the estimator for the E-model with $\mathcal{P} = \{1, 1, a(x, 10^{-3}), 1, 10\}$.

	$r = 1$			$r = 2$		
h^{-1}	$\mathcal{E}_e$	η_e	Θ	$\mathcal{E}_e$	η_e	Θ
500	0.0021545	0.015812	7.3390	0.0022479	0.016566	7.3695
1000	0.00098153	0.0081987	8.3530	0.0010323	0.0085637	8.2958
2000	0.00049239	0.0041781	8.4854	0.00051766	0.0043574	8.4175
	$r = 5$			$r = 10$		
h^{-1}	$\mathcal{E}_e$	η_e	Θ	$\mathcal{E}_e$	η_e	Θ
500	0.0028460	0.021086	7.4090	0.0045935	0.032313	7.0345
1000	0.0013387	0.010775	8.0495	0.0021298	0.016378	7.6902
2000	0.00066880	0.0054494	8.1480	0.0010476	0.0082400	7.8659

Table 5.10: Example 5.4.11: Efficiency index Θ_r for different values of q and r.

q	Θ_1	Θ_2	Θ_5	Θ_{10}
1	8.6501	8.3646	7.9388	7.8013
10^{-2}	8.6036	8.4139	8.0071	7.8217
10^{-4}	8.1298	8.1165	8.0148	7.6365
10^{-6}	5.8863	5.8891	5.8500	5.6569

- $q = 1, 10^{-2}, 10^{-4}, 10^{-6}$.

In Table 5.10 we observe that the estimator is essentially robust with respect to r and to the parameter $a(x, q)$.

5.5 Numerical results for the LP, WR, and PP models

In this Section we show examples of the application of the *a-posteriori* error estimators η_{lp}, η_{wr}, η_{pp} for the LP, WR, and PP models, respectively. We verify the robustness of the estimators with respect to the multilevel scheme and with respect to the parameters $\mathcal{P} = (\lambda_1, \lambda_2, a, b, c)$. For all the examples we use uniform time stepping, i.e., $\tau_n = \tau$, $\forall n$.

We begin by showing a simulation example that illustrates the effect of the parameters $\mathcal{P}$ in the behavior of the solution. Figure 5.11 illustrates the effect of $\mathcal{P}$ on the solutions.

Example 5.5.1. *We use homogeneous initial and boundary conditions and $g \equiv 0$ and f a point source at $x = 1/3$. In Figure 5.11, we plot the solutions and the spatial estimators for $\mathcal{P} = \{1, 1, 1, 1, 10\}$ and $\mathcal{P} = \{1, 1, 1, 0, 10\}$ at the times $t = 0.002, 0.3$.*

Notice in Figure 5.11 the difference in scales and in qualitative behavior of u, v for different $\mathcal{P}$. In particular, the error in v is always small at the initial time steps but when $b = 0$ it may dominate the global error long after u is smooth.

Next, we verify the *a-priori* error estimate given in Corollary 4.5.3. Based on the a-priori error estimate we know that the error is $O(h + H + \tau)$. So we refine h, H and τ at the same rate. We also verify the robustness of the *a-posteriori* estimator η_{lp} from Theorem 4.5.6 with respect to the h and τ and the ratio $r = H/h$.

Example 5.5.2. *Let $\Omega = (0, 1)$ and $(e^{-t}\sin(4\pi x), -e^{-2t}(x^2 - x))$ be the exact solution of 3.32. We are going to test the estimator for:*

Figure 5.11: Example 5.5.1: behavior of solutions u, v to LP-model and of spatial error indicators $[\partial_\nu u], [\partial_\nu v]$ for different $\mathcal{P}$.

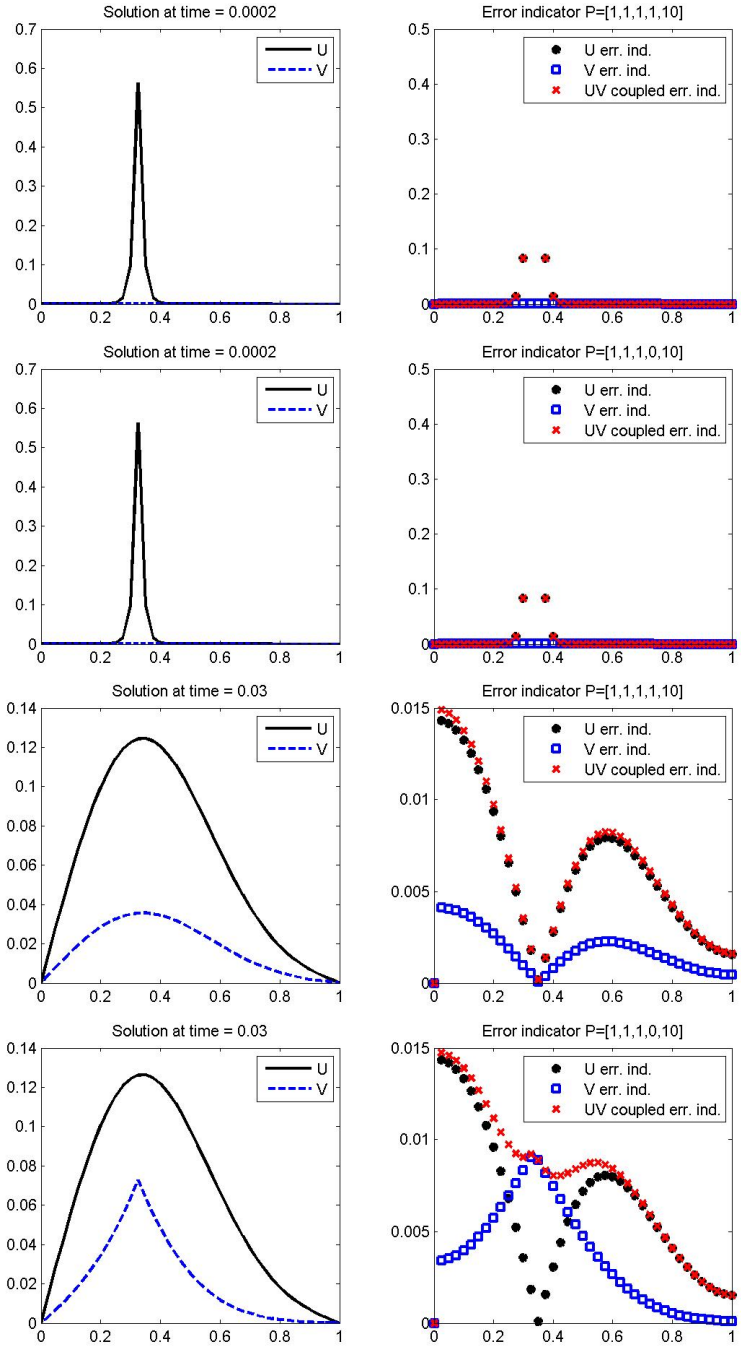

Table 5.11: Example 5.5.2: Robustness of the estimator for the LP-model with $\mathcal{P} = 1^5$, $T = 0.1$, $\tau = h$. The numerical experiment convergence order is $O(h^\alpha)$. From theory, we expect $\alpha = 1$.

	$r = 1$				$r = 2$			
h^{-1}	$\mathcal{E}_{lp}$	α	η_{lp}	Θ	$\mathcal{E}_{lp}$	α	η_{lp}	Θ
100	0.097818	-	0.74751	7.6418	0.097860	-	0.74783	7.6418
200	0.049037	0.9962	0.37498	7.6470	0.049057	0.9963	0.37514	7.6471
400	0.024549	0.9982	0.18776	7.6483	0.024560	0.9981	0.18784	7.6484
800	0.012282	0.9991	0.093944	7.6487	0.012288	0.9991	0.093985	7.6488
	$r = 4$				$r = 10$			
h^{-1}	$\mathcal{E}_{lp}$	α	η_{lp}	Θ	$\mathcal{E}_{lp}$	α	η_{lp}	Θ
100	0.098024	-	0.74907	7.6417	0.099179	-	0.75728	7.6355
200	0.049140	0.9962	0.37578	7.6472	0.049718	0.9963	0.38012	7.6454
400	0.024601	0.9982	0.18817	7.6486	0.024891	0.9981	0.19039	7.6489
800	0.012308	0.9991	0.094148	7.6491	0.012454	0.9990	0.095275	7.6504

- *LP-model:* $\mathcal{P} = 1^5$.
- $h^{-1} = 100, 200, 400, 800$.
- $r = 1, 2, 4, 10$.

The time step is kept $\tau = h$ *and the errors are all analysed at* $T = 0.1$. *In Tables 5.11,* $\mathcal{E}_{lp}$ *and* η_{lp} *is given by* (4.158) *and* (4.160)*, respectively.*

In Table 5.11 we show the results of theses experiments. As expected from Corollary 4.5.3, $\mathcal{E}_{lp}$ decays by a factor of 2 as we decrease h by a factor of 2. In this Example the use of a multilevel mesh is beneficial due to the nature of the solutions. The u component changes more in the spatial direction while the changes in the v component are not as drastic.

Next verify the robustness of the estimators η_{wr}, η_{pp}, presented in Corollaries 4.6.5 and 4.7.4, with respect to the h and τ and the ratio $r = H/h$ for the WR-model and PP-model. We also confirm the *a-priori* error estimates given by Corollaries 4.6.2 and 4.7.2, respectively. For both models, WR and PP, the order of convergence of error is $O(h + H^2 + \tau)$. So if we refine H by a factor of s, we refine h and τ by a factor of s^2.

Table 5.12: Example 5.5.3: Robustness of the estimator for the WR-model with $\mathcal{P} = \{1, 1, 1, 0, 1\}$, $T = 0.1$, $\tau = h$. The numerical experiment convergence order is $O(h^\alpha)$. From theory, we expect $\alpha = 1$.

h^{-1}	H^{-1}	r	$\mathcal{E}_{wr}$	α	η_{wr}	Θ
20	20	1	0.48200	-	3.6523	7.5774
80	40	2	0.12121	0.9958	0.93748	7.7344
320	80	4	0.030324	0.9995	0.23484	7.7443
1280	160	8	0.0075821	0.9999	0.058723	7.7449

Example 5.5.3. *Let $\Omega = (0, 1)$ and $(e^{-t}\sin(4\pi x), -e^{-2t}(x^2 - x))$ be the exact solution of 3.38 and 3.40. We test the estimator for:*

- *WR-model: $\mathcal{P} = \{1, 1, 1, 0, 1\}$.*
- *PP-model : $\mathcal{P} = \{0, 1, 1, 0, 1\}$.*
- *$h^{-1} = 20, 80, 320, 1280$.*
- *$H^{-1} = 20, 40, 80, 160$.*

The time step is kept $\tau = h$ and the errors are all analysed at $T = 0.1$.

In this Example, $s = 2$, i.e., we refine H by a factor of 2, $h = \tau_n$ by a factor of 4. We keep $h = \tau = \sqrt{H}$, and compute the numerical convergence order $O(h^\alpha)$. For both models the theoretical $\alpha = 1$ and the results in Tables 5.12 and 5.11 show that the numerical $\alpha \approx 1$.

In Table 5.12, $\mathcal{E}_{wr}$ and η_{wr} are given by (4.187) and (4.189), respectively. In Table 5.13, $\mathcal{E}_{pp}$ and η_{pp} are given by (4.201) and (4.204), respectively.

In Tables 5.12 and 5.13 we see the robustness of the estimators η_{wr}, η_{pp} for the different values of r,h, and H. Note that the convergence order is pretty close to the value $\alpha = 1$ expected from Corollary 4.6.2.

In Examples 5.5.2 and 5.5.3 we confirmed the *a-priori* error estimates and verified the robustness of the *a-posteriori* error estimator with respect to the mesh size. Next, we verify the robustness of the estimator with respect to the parameters in $\mathcal{P}$.

Example 5.5.4. *We keep the same exact solution as in Examples 5.5.2 and 5.5.3. Fix $h = \tau = 2.5 \times 10^{-3}$ and $H = 5 \times 10^{-3}$, i.e., $r = 2$. We vary two parameters in $\mathcal{P}$ at a time. The parameters that are not varying are kept equal to one.*

Table 5.13: Example 5.5.3: Robustness of the estimator for the PP-model with $\mathcal{P} = \{0, 1, 1, 0, 1\}$, $T = 0.1$, $\tau = h$. The numerical experiment convergence order is $O(h^\alpha)$ given in the fifth column. From theory, we expect $\alpha = 1$.

h^{-1}	H^{-1}	r	$\mathcal{E}_{pp}$	α	η_{pp}	Θ
20	20	1	0.47674	-	3.5719	7.4923
80	40	2	0.12205	.09829	0.93246	7.6399
320	80	4	0.030663	0.9965	0.23457	7.6499
1280	160	8	0.0076747	0.9992	0.058717	7.6507

Table 5.14 analyses the robustness of the estimator as the LP-model "tends" to the PP-model. We observe the the estimator is robust and the only "bad" values for Θ are in the last column when $b = 10^4$. For finer meshes this last column also behaves well as one can see in Table 5.15 for $h = \tau = 1.25 \times 10^{-3}$, $H = 5 \times 10^{-3}$. Thus if the mesh is fine enough $\Theta \approx 7.7$.

In Table 5.16 we verify the robustness of the estimator with respect to the parameters a and c. Again we get bad values for Θ when $a = 10^4$. As mentioned before and illustrated in Table 5.15, it suffices to have the mesh fine enough to Θ to approach values around 7.7 as expected.

Now we test the *a-priori* error convergence and the *a-posteriori* error estimator in a 2-dimensional example. We verify the robustness of the estimator with respect to the h and τ and the ratio $r = H/h$.

Example 5.5.5. *Let $\Omega = (0, 1)$ and $(e^{-t}\sin(4\pi x)\sin(2\pi y), e^{-2t}(x^2 - x)(y^2 - y))$ be the exact solution of 3.32. We are going to test the estimator for:*

- *LP-model: $\mathcal{P} = 1^5$.*
- *$h^{-1} = 4\sqrt{2}, 8\sqrt{2}, 16\sqrt{2}$.*
- *$r = 1, 2, 4$.*

The time step is kept $\tau = \dfrac{h}{\sqrt{2}}$ and the errors are all analysed at $T = 1$. Based on the a-priori error estimate we know that the error convergence rate is $O(h + H + \tau)$. So we refine h, H, τ at the same rate.

Note in Table 5.17 the robustness of the estimator for the different values of r, h. As expected form the *a-priori* estimate (4.113), $\mathcal{E}_{lp}$ decays by a factor of 2 as we decrease

Table 5.14: Example 5.5.4: $\mathcal{P} = \{\lambda_1, 1, 1, b, 1\}$

b	10^{-8}	10^{-4}	1	10^4
λ_1	$\mathcal{E}_{lp}$			
10^{-8}	0.024538	0.024538	0.024557	0.098619
10^{-4}	0.024538	0.024538	0.024557	0.098619
1	0.024541	0.024541	0.024560	0.098619
10^4	0.024808	0.024808	0.024826	0.098686
λ_1	η_{lp}			
10^{-8}	0.18772	0.18772	0.18784	0.66808
10^{-4}	0.18772	0.18772	0.18784	0.66808
1	0.18772	0.18772	0.18784	0.66808
10^4	0.18773	0.18773	0.18785	0.66808
λ_1	Θ			
10^{-8}	7.6502	7.6502	7.6492	6.7744
10^{-4}	7.6502	7.6502	7.6492	6.7744
1	7.6494	7.6494	7.6484	6.7744
10^4	7.5676	7.5676	7.5667	6.7698

Table 5.15: Example 5.5.4: $\mathcal{P} = \{\lambda_1, 1, 1, 10^4, 1\}$, $h = \tau = 1.25 \times 10^{-3}$, $H = 5 \times 10^{-3}$

λ_1	$\mathcal{E}_{lp}$	η_{lp}	Θ
10^{-8}	0.012605	0.093927	7.4514
10^{-4}	0.012605	0.093927	7.4515
1	0.012635	0.094150	7.4517
10^4	0.087077	0.64724	7.4330

Table 5.16: Example 5.5.4: $\mathcal{P} = \{1, 1, a, 1, c\}$

a	10^{-8}	10^{-4}	1	10^4
c	$\mathcal{E}_{lp}$			
10^{-8}	0.00097025	0.00097026	0.0010284	0.034239
10^{-4}	0.0010008	0.0010008	0.0010573	0.034240
1	0.024557	0.024557	0.024560	0.042123
10^4	2.4536	2.4536	2.4536	2.4538
c	η_{lp}			
10^{-8}	0.0064095	0.0064098	0.0064440	0.035286
10^{-4}	0.0066815	0.0066817	0.0067165	0.035324
1	0.18783	0.18783	0.18784	0.19171
10^4	18.771	18.771	18.771	18.772
c	Θ			
10^{-8}	6.6060	6.6063	6.2659	1.0306
10^{-4}	6.6758	6.6761	6.3524	1.0317
1	7.6488	7.6488	7.6484	4.5512
10^4	7.6507	7.6507	7.6507	7.6502

h by a factor of 2. Also note that $\Theta \approx 4.4$, different from the value of $\Theta \approx 7.7$ for the 1-dimensional examples. However the constants that determine the value of Θ depend on the domain Ω, so for different domains we expect different values of Θ.

5.6 Numerical results for the NLP-model

In this section we consider the estimator η_{nlp} (4.211) and its performance for the NLP-model, for $\varphi(u) = \frac{\beta u}{1+\alpha u}$, the Langmuir isotherm. In this case the system is "almost" linear for small values of α. We use the parameters:

- $\beta = 1$, $\alpha = 0$: get back the linear system LP.
- $\beta = 2$, $\alpha = 0.05$.
- $\beta = 1$, $\alpha = 0.5$.
- $\beta = 1.5$, $\alpha = 0.1$.

Table 5.17: Example 5.5.5: Robustness of the estimator for the LP-model with $\mathcal{P} = 1^5$, $T = 1$, $\tau = h$

	$r = 1$				$r = 2$			
h^{-1}	$\mathcal{E}_{lp}$	α	η_{lp}	Θ	$\mathcal{E}_{lp}$	α	η_{lp}	Θ
$4\sqrt{2}$	2.3880	-	10.929	4.5768	2.3882	-	10.931	4.5770
$8\sqrt{2}$	1.2912	0.8871	5.5990	4.3363	1.2914	0.8870	5.6003	4.3364
$16\sqrt{2}$	0.66547	0.9563	2.8339	4.2586	0.66601	0.9555	2.8349	4.2565

	$r = 4$			
h^{-1}	$\mathcal{E}_{lp}$	α	η_{lp}	Θ
$4\sqrt{2}$	2.3889	-	10.934	4.5769
$8\sqrt{2}$	1.2914	0.8874	5.6023	4.3380
$16\sqrt{2}$	0.66556	0.9563	2.8363	4.2616

Recall that the NLP-model models the diffusion-adsorption application described in Section 2.4 if $b \equiv 0$. Thus, in this section we only consider the case $b \equiv 0$. We also only consider the case $h = H$.

In Section 5.6.1 we show simulations results that illustrate the dependence of the solutions in the parameters $\mathcal{P}$ and in the coefficients α, β of the Langmuir isotherm. In Section 5.6.2 we present numerical results to illustrate the robustness of the estimator η_{nlp} presented in Proposition 4.8.1.

5.6.1 Simulations for the diffusion-adsorption applications

Here we present simulations of a diffusion-adsorption process. We set $\mathcal{P} = \{1, 1, a, 0, c\}$. Recall that for the diffusion-adsorption application, u represents the concentration of the solute in the fluid flow and v represents the amount of the solute adsorbed by the porous media.

For the simulation examples we use the following setting:

- $\Omega = (0, 1)$.
- $h = H$, $h^{-1} = 10^3$,
- Uniform time-steps with $\tau = 10^{-2}$ and final time $T = 0.1$.
- Homogeneous Dirichlet boundary conditions.

- Initial conditions $u(x,0) = v(x,0) = 0$.
- $g \equiv 0$ and $f(x,t) = \begin{cases} 1, & |x-0.5| < 1 \text{ and } t < 0.05, \\ 0, & \text{otherwise.} \end{cases}$

Note that we start with $u(x,0) = v(x,0) = 0$ and we have the source $f(x,t)$ until $t = 0.05$. Thus we expect $u(x,t), v(x,t)$ to increase up to $t = 0.05$ and then to start to decrease for $t > 0.05$.

Example 5.6.1. *Let $\mathcal{P} = \{1, 1, a, 0, c\}$, we simulate the diffusion-adsorption process for:*

- $a = 1,\ 10^{-3}$.
- $c = 10^{-2},\ 10^{2}$.
- *Linear isotherm:* $\alpha = 1,\ \beta = 1$.
- *Langmuir isotherm:* $\alpha = 0.05,\ \beta = 2$.

We plot $u(x,t)$, $v(x,t)$ for:

- $t = 0.01$, *right after the beginning of the process.*
- $t = 0.05$, *at the time the source term f is shut off. Here $u(\cdot,t), v(\cdot,t)$ should achieve its maximum.*
- *At the final time* $t = 0.1$.

Recall that a represents the diffusivity of the porous media and that c is the inverse of the sorption time. This mean that the larger is the c, the smaller is the sorption time. Lower the sorption time faster the solute gets adsorbed to the media. Thus we expected the concentration adsorbed v to increase when c increases and the concentration of the solute in the fluid flow u to decrease as c increases.

To verify the effect of the sorption time c in the solutions compare the magnitude of the solutions between Figure 5.12 to Figure 5.13 for the linear isotherm. The two simulations presented in Figure 5.12 and Figure 5.13 only differ in the value of c. Note the difference especially in the amount adsorbed $v(x,t)$. For $t = 0.05$, $v(x, 0.05)$ ranges from $0 - 6 \times 10^{-6}$ for the high sorption time $1/c = 10^2$ in Figure 5.12 and $v(x, 0.05)$ ranges from $0 - 10^{-2}$ for the low sorption time $1/c = 10^{-2}$ in Figure 5.13. The same

Table 5.18: Example 5.6.2: Adsorption-Diffusion, $\mathcal{P} = \{1, 1, a, 0, 1\}$. Recall $\mathcal{E}_{nlp}$ is the error, η_{nlp} is the estimator, and Θ is the efficiency index

			$\beta = 1, \alpha = 0$ (Linear)			$\beta = 2, \alpha = 0.05$ (Langmuir)		
a	τ_n	h^{-1}	$\mathcal{E}_{nlp}$	η_{nlp}	Θ	$\mathcal{E}_{nlp}$	η_{nlp}	Θ
1	10^{-4}	10^3	$2.41.10^{-4}$	$1.87.10^{-3}$	7.74	$2.41.10^{-4}$	$1.87.10^{-3}$	7.74
	5.10^{-5}	2.10^3	$1.24.10^{-4}$	$9.61.10^{-4}$	7.74	$1.24.10^{-4}$	$9.61.10^{-4}$	7.74
10^{-3}	10^{-4}	10^3	$8.39.10^{-6}$	$5.92.10^{-5}$	7.06	$8.84.10^{-6}$	$5.93.10^{-5}$	6.70
	5.10^{-5}	2.10^3	$4.16.10^{-6}$	$3.04.10^{-5}$	7.31	$4.39.10^{-6}$	$3.04.10^{-5}$	6.92
			$\beta = 1, \alpha = 0.5$ (Langmuir)			$\beta = 1.5, \alpha = 0.1$ (Langmuir)		
a	τ_n	h^{-1}	$\mathcal{E}_{nlp}$	η_{nlp}	Θ	$\mathcal{E}_{nlp}$	η_{nlp}	Θ
1	10^{-4}	10^3	$2.42.10^{-4}$	$1.87.10^{-3}$	7.74	$2.42.10^{-4}$	$1.87.10^{-3}$	7.74
	5.10^{-3}	2.10^3	$1.24.10^{-4}$	$9.62.10^{-4}$	7.74	$1.24.10^{-4}$	$9.61.10^{-4}$	7.74
10^{-3}	10^{-4}	10^3	$9.08.10^{-6}$	$5.93.10^{-5}$	6.53	$8.63.10^{-6}$	$5.93.10^{-5}$	6.86
	5.10^{-5}	2.10^3	$4.34.10^{-6}$	$3.05.10^{-5}$	7.02	$4.28.10^{-6}$	$3.04.10^{-5}$	7.11

phenomenon is observed when comparing Figure 5.14 to Figure 5.15 for the Langmuir isotherm.

Comparing Figure 5.13 to Figure 5.16 and Figure 5.15 to Figure 5.17 we observe the effect of the permeability on the solutions.

5.6.2 Numerical results for the NLP-model

The next examples verify the robustness of the estimator η_{nlp} given in Proposition 4.8.1. The error is computed using the norm $\mathcal{E}_{nlp}$ (4.209).

Example 5.6.2. *Here we fix* $u = e^{-t}\sin(2\pi x)$, $b = g = 0$, *and* $c = 1$ *in* (3.45). *The final time is* $T = 10^{-3}$. *We then verify the robustness of the estimator* η_{nlp} *with respect to the parameter* a.

In Table 5.18 we see that the estimator is robust for both linear and Langmuir isotherms for various values of α.

The next example models the nonlinear pseudo-parabolic equation.

Example 5.6.3. *In this example we fix* $u = e^{-t}\sin(2\pi x)$, $b = g = 0$, *and* $c = 1$ *in* (3.45) *as in Example 5.6.2. The final time is* $T = 10^{-3}$. *Again, we verify the robustness of the estimator* η_{nlp} *given by* (4.211) *with respect to the parameter* a *and compare the results for the NLP-model for linear and the Langmuir isotherms.*

Figure 5.12: Example 5.6.1: simulation diffusion-adsorption for $\mathcal{P} = \{1, 1, 1, 0, 10^{-2}\}$ and linear isotherm.

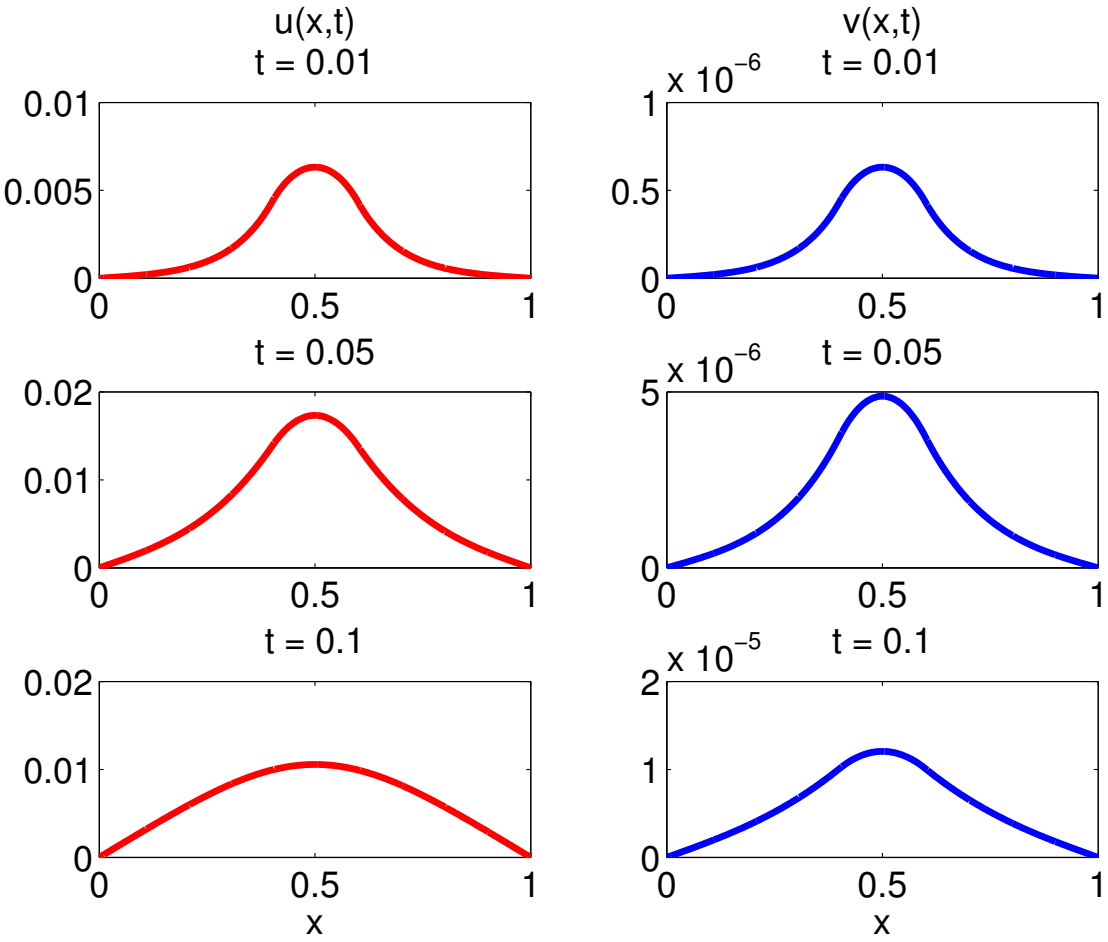

Figure 5.13: Example 5.6.1: simulation diffusion-adsorption for $\mathcal{P} = \{1, 1, 1, 0, 10^2\}$ and linear isotherm.

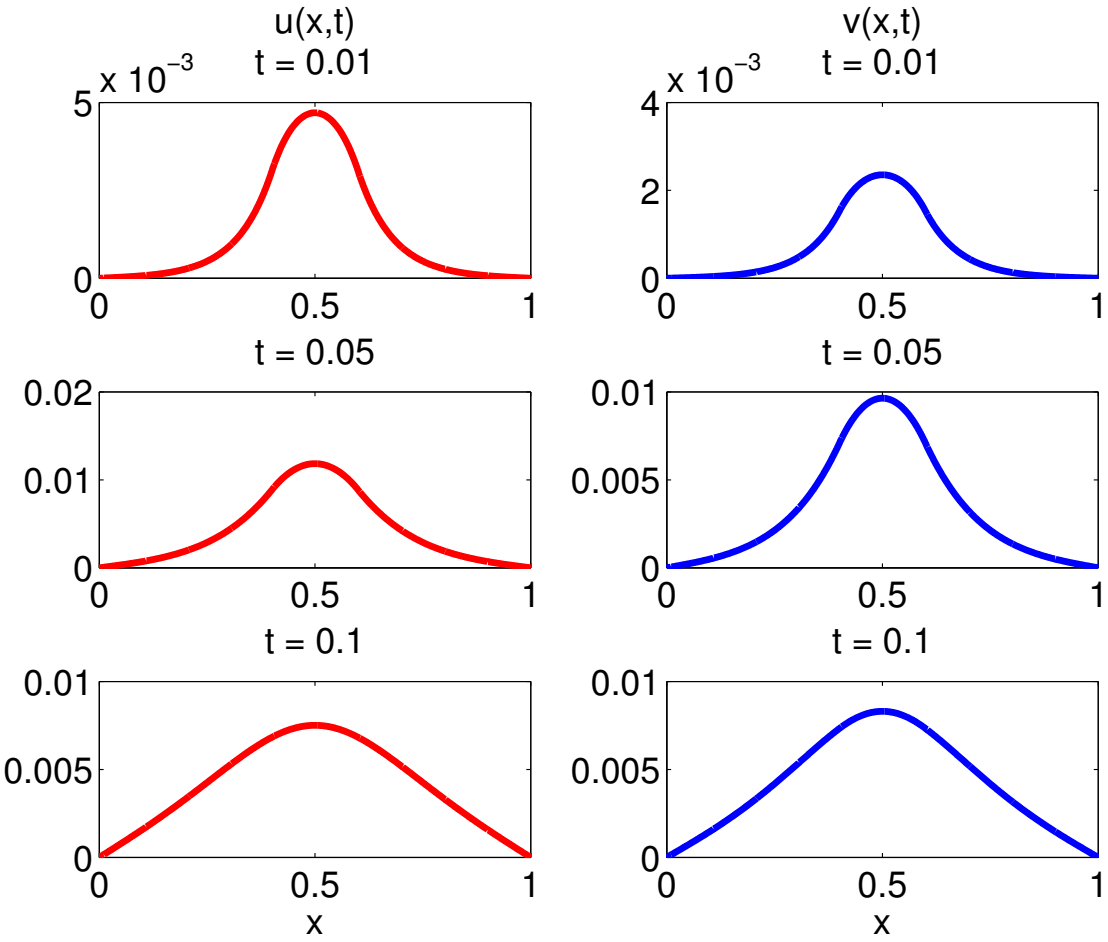

Figure 5.14: Example 5.6.1: simulation diffusion-adsorption for $\mathcal{P} = \{1, 1, 1, 0, 10^{-2}\}$ and Langmuir isotherm for $\alpha = 0.05$, $\beta = 2$.

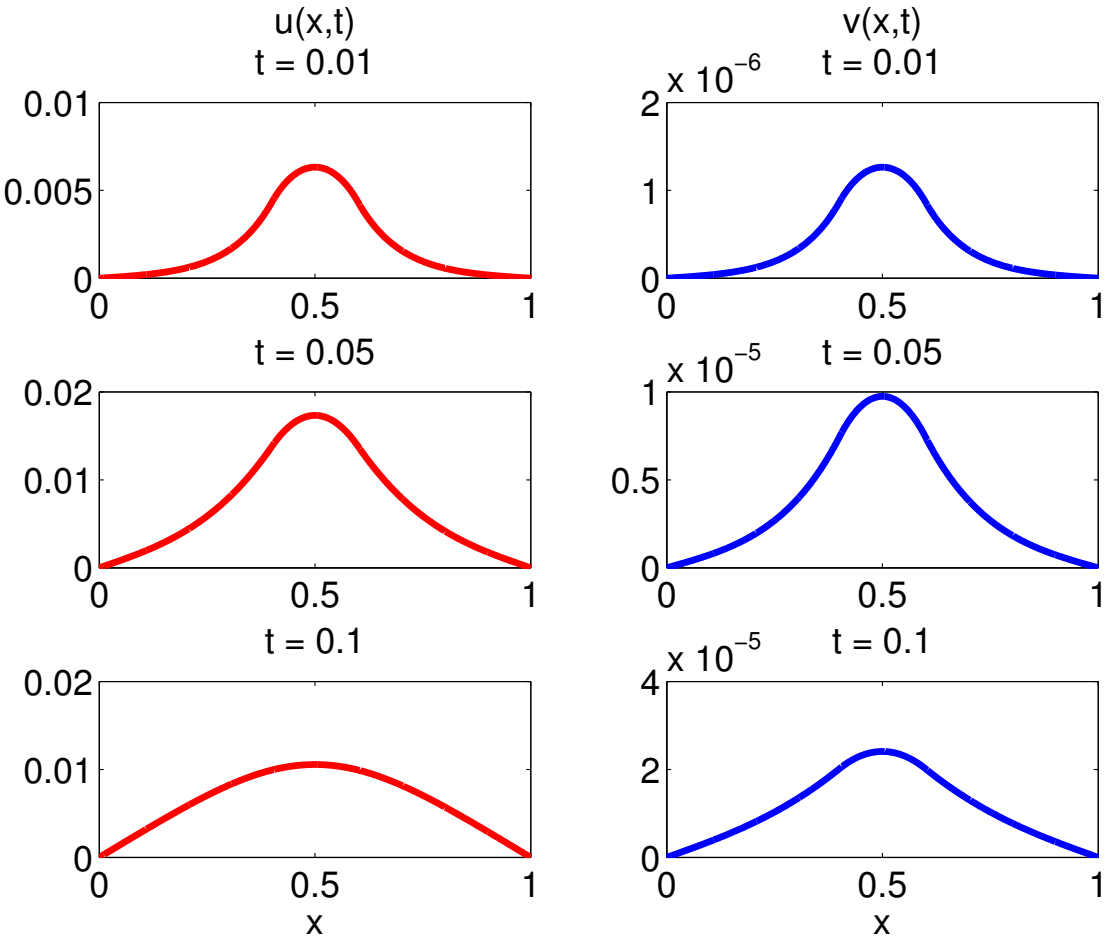

Figure 5.15: Example 5.6.1: simulation diffusion-adsorption for $\mathcal{P} = \{1, 1, 1, 0, 10^2\}$ and Langmuir isotherm for $\alpha = 0.05$, $\beta = 2$.

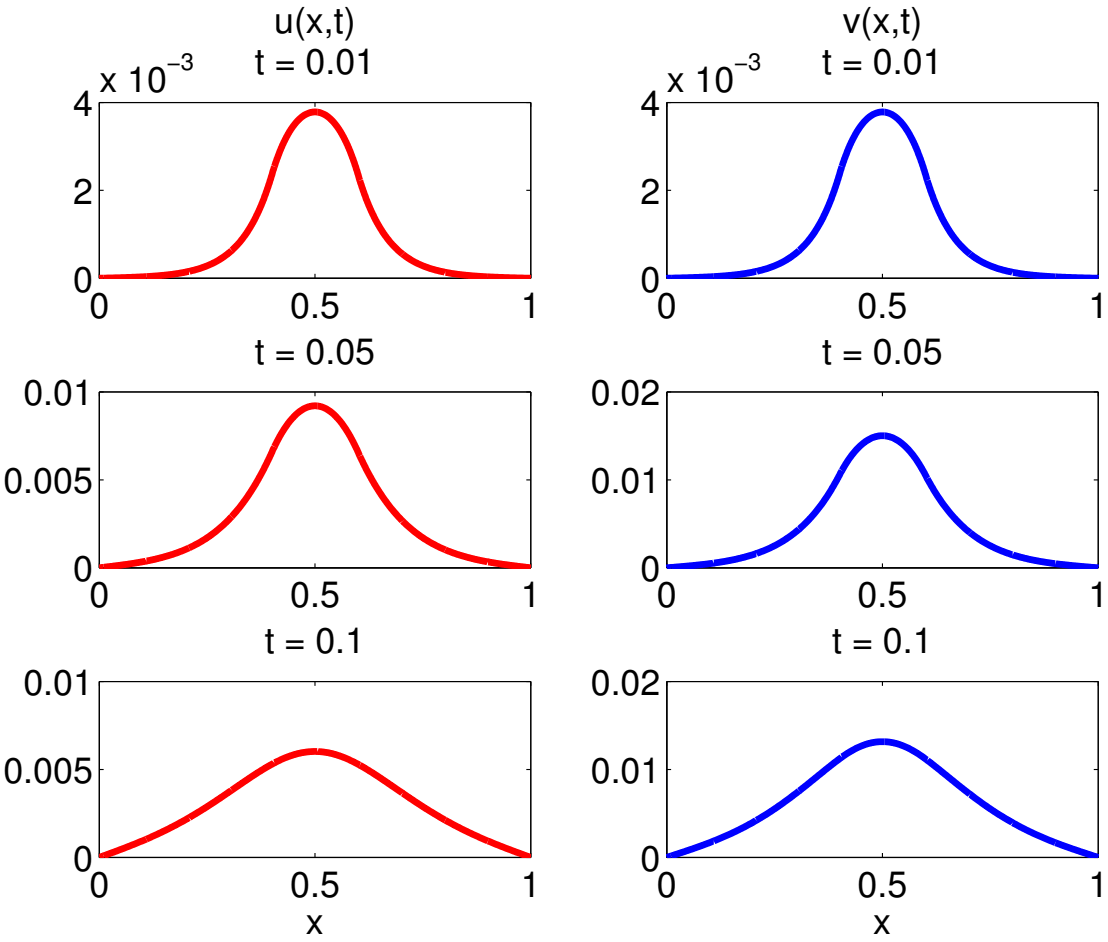

Figure 5.16: Example 5.6.1: simulation diffusion-adsorption for $\mathcal{P} = \{1, 1, 10^{-3}, 0, 10^2\}$ and linear isotherm.

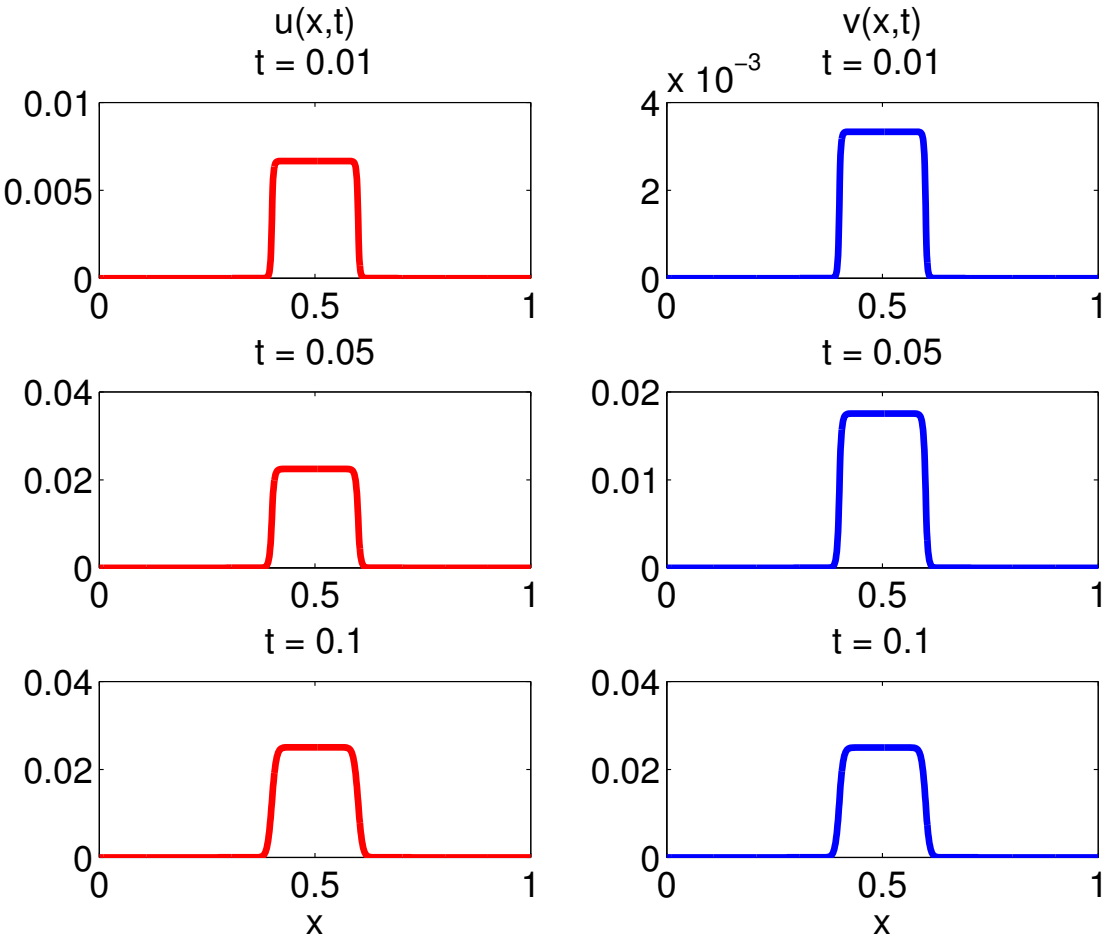

Figure 5.17: Example 5.6.1: simulation diffusion-adsorption for $\mathcal{P} = \{1, 1, 10^{-3}, 0, 10^{2}\}$ and Langmuir isotherm for $\alpha = 0.05$, $\beta = 2$.

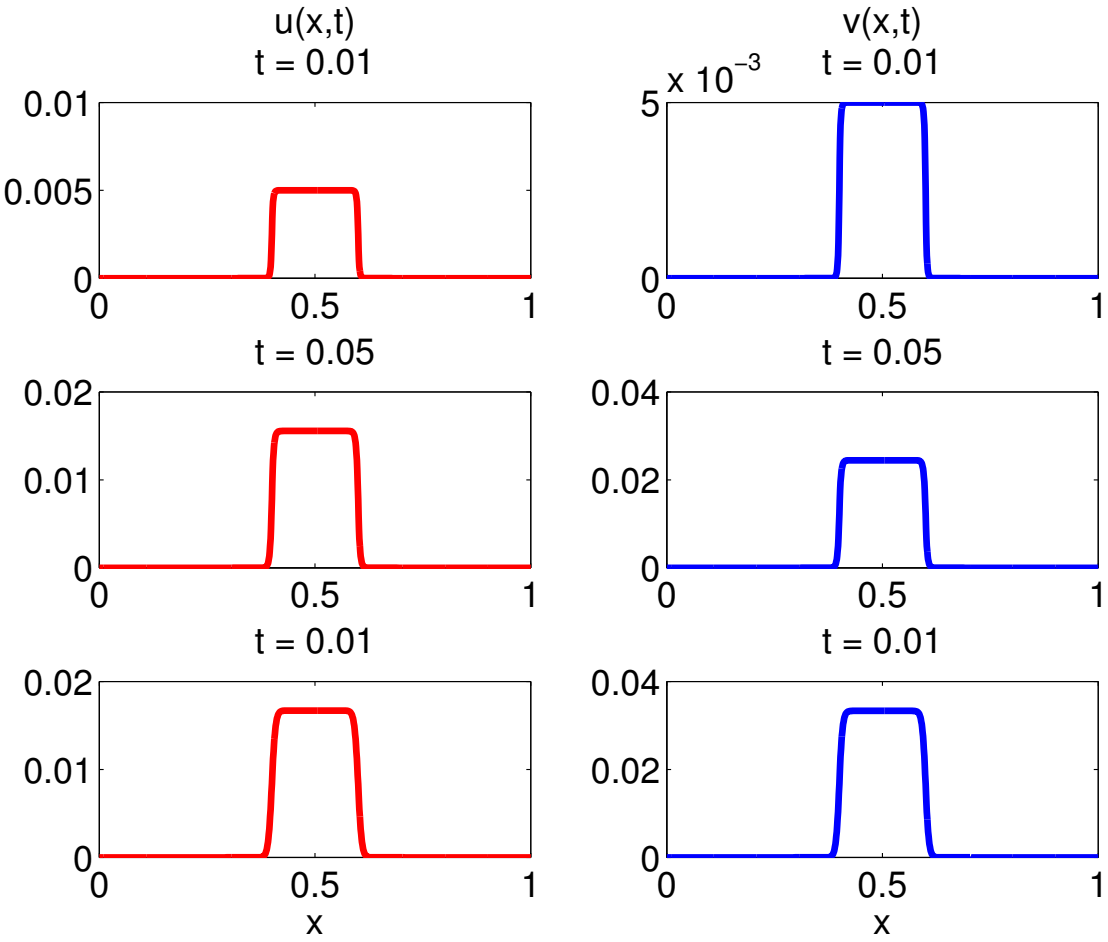

Table 5.19: Example 5.6.3: Nonlinear pseudo-parabolic, $\mathcal{P} = \{0, 1, a, 0, 1\}$. Recall $\mathcal{E}_{nlp}$ is the error, η_{nlp} is the estimator, and Θ is the efficiency index

			$\beta = 1, \alpha = 0$ (Linear)			$\beta = 2, \alpha = 0.05$ (Langmuir)		
a	τ_n	h^{-1}	$\mathcal{E}_{nlp}$	η_{nlp}	Θ	$\mathcal{E}_{nlp}$	η_{nlp}	Θ
1	10^{-4}	10^3	$2.41.10^{-4}$	$1.87.10^{-3}$	7.74	$2.41.10^{-4}$	$1.87.10^{-3}$	7.74
	5.10^{-5}	2.10^3	$1.24.10^{-4}$	$9.61.10^{-3}$	7.74	$1.24.10^{-4}$	$9.61.10^{-3}$	7.74
10^{-3}	10^{-4}	10^3	$8.02.10^{-6}$	$5.92.10^{-5}$	7.38	$8.50.10^{-6}$	$5.93.10^{-5}$	6.98
	5.10^{-3}	2.10^3	$4.12.10^{-6}$	$3.04.10^{-5}$	7.38	$4.36.10^{-6}$	$3.04.10^{-5}$	6.99
			$\beta = 1, \alpha = 0.5$ (Langmuir)			$\beta = 1.5, \alpha = 0.1$ (Langmuir)		
a	τ_n	h^{-1}	$\mathcal{E}_{nlp}$	η_{nlp}	Θ	$\mathcal{E}_{nlp}$	η_{nlp}	Θ
1	10^{-4}	10^3	$2.42.10^{-4}$	$1.87.10^{-3}$	7.74	$2.42.10^{-4}$	$1.87.10^{-3}$	7.74
	5.10^{-5}	2.10^3	$1.24.10^{-4}$	$9.62.10^{-4}$	7.74	$1.24.10^{-4}$	$9.62.10^{-4}$	7.74
10^{-3}	10^{-4}	10^3	$8.74.10^{-6}$	$5.93.10^{-5}$	6.78	$8.28.10^{-6}$	$5.93.10^{-5}$	7.16
	5.10^{-3}	2.10^3	$4.30.10^{-6}$	$3.04.10^{-5}$	7.08	$4.24.10^{-6}$	$3.04.10^{-5}$	7.18

In Table 5.19 we observe the robustness of the estimator for the linear and Langmuir isotherm.

5.7 Double-porosity, Barenblatt model

In this section we present simulations for the Warren-Root model, see Section 2.2. This model can be considered a macro–model, i.e., a homogenization limit of another micro–model. We discuss how to compute the coefficients of the macro-model from the micro–model and how to accurately and efficiently implement the macro-model. We consider the following questions:

Q1. How close are the numerical solutions of the micro and macro–model?

Q2. Since the macro-model is defined by averaging, how coarse can the grid for the macro-model be so we can still maintain a good approximation of the micro-model?

Q3. How accurately do we need to compute the coefficients of the macro-model?

Q4. How to estimate the error in the numerical solution of the macro-model?

Below we give details of numerical computations that address these questions.

5.7.1 Details of the model

Consider a porous media composed by three different materials layered periodically as in Figure 5.19(a). The media in divided in three disjoint regions $\Omega_1, \Omega_2, \Omega_3$. The region Ω_3 is called the interface region and it separates regions Ω_1 and Ω_2, usually called the fast and slow region, respectively. In each cell the regions are denoted by Y_1, Y_2, Y_3, as shown in Figure 5.19(b).

The fluid flow in the media is modelled by (2.9), which we recall here

$$\phi(x)\frac{\partial u}{\partial t} - \nabla \cdot (k(x)\nabla u) = 0. \tag{5.34}$$

The parameters ϕ and k represent the porosity and permeability of the medium, respectively. Because of the heterogeneity of the media

$$\begin{aligned} \phi(x) &= \phi_1\chi_1(x) + \phi_2\chi_2(x) + \phi_3\chi_3(x), \\ k(x) &= k_1\chi_1(x) + k_2\chi_2(x) + k_3\chi_3(x). \end{aligned}$$

Here χ_i, $i = 1, 2, 3$, is the characteristic function

$$\chi_i(x) = \begin{cases} 1, x \in \Omega_i, \\ 0, x \notin \Omega_i. \end{cases}$$

The ϕ_1, ϕ_2, ϕ_3 generally differ from each other by several orders of magnitude. The same with the coefficients k_1, k_2, k_3. As discussed in Section 2.2, solving the equation (5.34) directly, is very costly since it requires a very fine grid. Therefore an upscaled model is formulated in Ω for $\phi_3 = 0$ in [50].

Because the region Ω_2 is disconnected we have the WR-model proposed in [57], see Section 2.2.

$$\begin{cases} \tilde{\phi}_1\dfrac{\partial u_1}{\partial t} - \nabla \cdot (\tilde{K}_1\nabla u_1) + c(u_1 - u_2) = 0 \text{ in } \Omega, \\ \tilde{\phi}_2\dfrac{\partial u_2}{\partial t} + c(u_2 - u_1) = 0 \text{ in } \Omega. \end{cases} \tag{5.35}$$

Figure 5.18: Illustration of a periodic heterogeneous media. Figure (a): Ω_1 - white, Ω_2 - grey, and Ω_3 - dark grey. Figure (b): zoom of one cell.

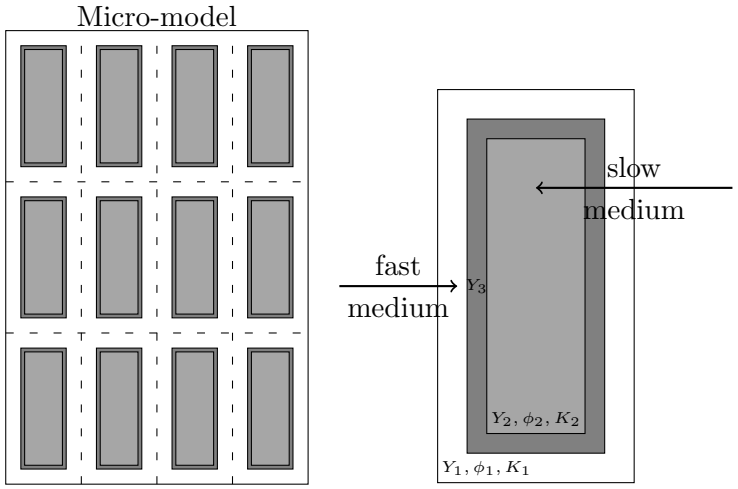

(a) Periodic media (b) One cell

The parameters $\tilde{\phi}_1, \tilde{\phi}_2$ are given by the average of the original porosities ϕ_1, ϕ_2 in a cell

$$\tilde{\phi}_i \quad = \quad \int_{Y_i} \phi_i(y)dy, i = 1, 2.$$

The parameters $\tilde{k}_1$ and c are more complicated to obtain. They require an auxiliary PDE equation to be numerically solved. Let us start with the parameter $\tilde{k}_1$. The parameter is given by a 2×2 matrix via

$$\tilde{k}_1(i,j) \quad = \quad \int_{Y_1} k_1(y)(\vec{e}_i + \nabla W_i(y)) \cdot (\vec{e}_j + \nabla W_j(y))dy, \ i, j = 1, 2.$$

Here W_i, $i = 1, 2$, is the solution of

$$\begin{cases} \nabla \cdot [k_1(\vec{e}_i + \nabla W_i(y))] = 0, \text{ in } Y_1, \\ k_1(\vec{e}_i + \nabla W_i(y)) \cdot \vec{n}_1 = 0, \text{ on } \Gamma_{1,3}, \\ W_i, k_1 \nabla W_i \cdot \vec{n}_1 \text{ are periodic.} \end{cases} \tag{5.36}$$

Figure 5.19: Illustration of Y_3 in grey

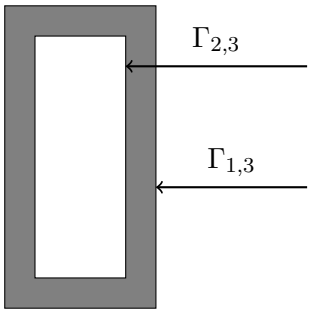

The parameter c is given by the solution of

$$c = \int_{\Gamma_{1,3}} \nabla_y U \cdot \nu_3 ds.$$

Here U is the solution of the following

$$\begin{cases} \nabla \cdot [k_3 \nabla U] = 0 \text{ in } Y_3, \\ U = 1, \text{ on } \Gamma_{1,3}, \\ U = 0, \text{ on } \Gamma_{2,3}. \end{cases} \tag{5.37}$$

See Figure 5.19 for an illustration of Y_3.

5.7.2 Computing coefficients of the macro-model

The parameters of this system $\tilde{k}_1, c$ have to be computed numerically. To this aim, we solve the PDEs (5.37), (5.36) using finite element spaces V_{h_c}, $V_{h_{k_1}}$, respectively. In Example 5.7.1 we show an example of the computation of the parameters c and k_1.

Example 5.7.1. *Let* $\Omega = (0,1)^2$, $Y_2 = (0.3, 0.7)^2$, $Y_3 = (0.2, 0.8)^2/Y_2$, *and* $Y_1 = (0,1)^2/Y_3$. *Let* $k = [1e-2, 1e-4, 1e-7]$ *and* $\phi = [1e-3, 1e-6, 0]$. *We discretize* Y_1 *and* Y_3 *in a mesh* $\mathcal{T}_h$ *with diameter* h, *for* $h^{-1} = 10, 40, 80$ *as listed below. We solve the PDEs* (5.37) *and* (5.36) *in the subspace generated by the meshes. The results are:*

- $h^{-1} = 10$*:* $\tilde{k}_1 = \begin{bmatrix} 4.6305 \times 10^{-3} & 0 \\ 0 & 4.6305 \times 10^{-3} \end{bmatrix}$ *and* $c = 1.9000 \times 10^{-6}$.

Figure 5.20: Illustration of numerical experiments for the double-porosity model with 9 cells

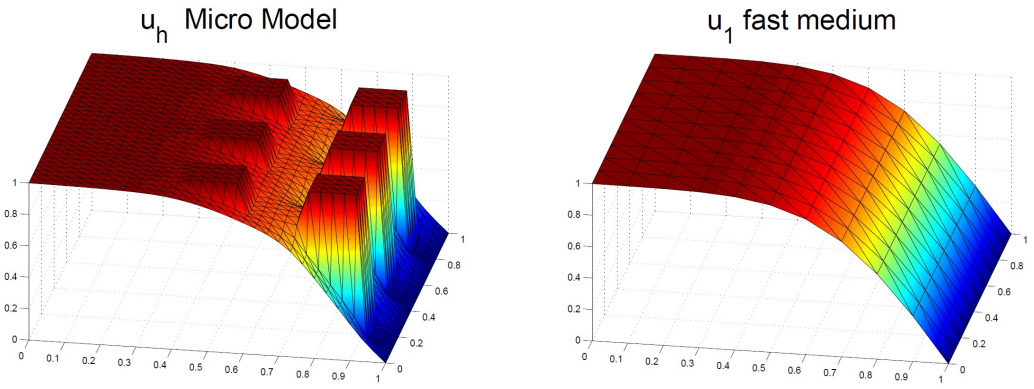

(a) Exact Model (b) Double-porosity model, u_1

- $h^{-1} = 40$: $\tilde{k}_1 = \begin{bmatrix} 4.5196 \times 10^{-3} & 0 \\ 0 & 4.5196 \times 10^{-3} \end{bmatrix}$ *and* $c = 1.8412 \times 10^{-6}$.
- $h^{-1} = 80$: $\tilde{k}_1 = \begin{bmatrix} 4.5086 \times 10^{-3} & 0 \\ 0 & 4.5086 \times 10^{-3} \end{bmatrix}$ *and* $c = 1.8310 \times 10^{-6}$.

5.7.3 Numerical solution of the macromodel

From now on we drop the superscript "˜" from the parameters $\tilde{\phi}_1, \tilde{\phi}_2, \tilde{k}_1$. Since the double porosity model (5.35) is an example of the WR-model, we know from the *a-priori* estimate (4.176) that the use of multilevel discretization is advantageous. The multilevel discrete form of (5.35) is given by:

$$\begin{cases} (\phi_1 \dfrac{u^n_{1,h} - u^{n-1}_{1,h}}{\tau_n}, \phi_h) + (k_1^{h_{k_1}} \nabla u^n_{1,h}, \nabla \phi_h) + (c^{h_c}(u^n_{1,h} - \Pi u^n_{2,H}), \phi_h) = 0, \\ (\phi_2 \dfrac{u^n_{2,H} - u^{n-1}_{2,H}}{\tau_n}, \psi_H) + (c^{h_c}(u^n_{2,H} - \Pi' u^n_{1,h}), \psi_H) = 0. \end{cases} \tag{5.38}$$

In Figure 5.20 we see an illustration of the numerical solution of the original model (5.34) and of the numerical solution for the fast medium u_1 of the double-porosity model (5.35).

With the notation introduced above we rephrase the question posed at the beginning of the section.

Q1. How well does $u_{1,h}$ approximate u_h in the fracture?

We want to compare the numerical approximation of the homogenized double-porosity system (5.35) with the numerical approximation of the exact model (5.34).

Q2. How well does $u_{1,\tilde{h}}$ approximate u_h in the fracture, with $\tilde{h} >> h$?

We want to compare the numerical approximation of the homogenized system using a coarser grid than the one to compute the micro-model. Since one of the goals in deriving the double-porosity model (5.35) is to be able to use a coarser mesh to compute the solution.

Q3. How small does h_c, h_{k_1} have to be?

We want to have an idea of the of how coarse the mesh to compute the parameters have to be in comparison with the mesh used to solve the double-porosity system (5.38).

Q4. How well does $u_{1,h}$ approximate u_1?

This is where our *a-posteriori* error estimator plays it role. We use the estimator to estimate the error and it also can be used for mesh adaptivity. See Example 5.5.5 for that.

From now on, we set for the problem (5.34):

- Domain $\Omega = (0,1)^2$.
- Boundary conditions: homogeneous Dirichlet-Neumann boundary given by

$$u(x,0;t) = 1, \quad u(x,1;t) = 0,$$
$$u(x,y;t) \cdot \vec{n} = 0 \ \text{ at } x = 0,1.$$

- Initial conditions: $u(x,y;0) = 1$.
- Parameters of the original problem (5.34):

$$\phi = [1, 10^{-4}, 0], \quad k = [1, 10^{-1}, 10^{-4}].$$

- Cells: $Y_2 = (0.3\varepsilon, 0.7\varepsilon)^2$, $Y_3 = (0.2\varepsilon, 0.8\varepsilon)^2/Y_2$ and $Y_1 = (0,\varepsilon)^2/Y_3$.

We compare the numerical approximations of the original model (5.34) and the numerical solution of the fast medium u_1 homogenized model (5.35) we use the following norms.

Definition 5.7.1. *Let T be the final time. For $u(x,y,T) \in V_h$*

$$\begin{aligned} \|u(x,y,T)\|_{*,1} &:= \int_0^1 |u(x,0.5,T)|dx, \\ \|u(x,y,T)\|_{*,2} &:= \left\{ \int_0^1 |u(x,0.5,T)|^2 dx \right\}^{1/2}. \end{aligned}$$

That is, we measure the L^1 and L^2 norm at the final time restricted to the strip $[0,1] \times \{0.5\}$.

Next we present examples concerning questions Q1, Q2, and Q3. All the examples use the settings described above.

Example 5.7.2. *Let $\Omega = (0,1)^2$ and fix the final time $T = 0.05$, $\tau = 10^{-4}$. Let $h = H$, $h^{-1} = 180$, $h_c^{-1} = 90$, $h_{k_1}^{-1} = 180$. We compare the solutions $u_{1,h}^N$ and u_h^N at the final time, T, for different number of cells in Ω.*

In Example 5.7.2 we address the question Q1. We compare the numerical solutions at the final time in the strip $[0,1] \times 0.5$, see in Figure 5.21 that bigger the number of cells, the closer the numerical solution of the micro-model is to the solution of the macro-model. In Table 5.20 we see that the smaller the size ε of the cells, the closer the solution of the two problem gets. We also note that the convergence seems to be of order $O(\varepsilon)$. This convergence was shown in [50] but no rate was given there.

In the next example we address Q2. We want to compare the numerical solution for fast component double-porosity solution u_1 in a coarser mesh than the one used to compute the numerical approximation u_h to the original model (5.34).

Example 5.7.3. *We use a mesh with 5×5 cells and $h^{-1} = 100$ for approximating the original model* (5.34)*. The run time for the simulation was 120 seconds.*

The double-porosity model solution $u_{1,\tilde{h}}$ is approximated is a mesh with diameter $\tilde{h}$ for the values:

- *$\tilde{h}^{-1}$: 10, 50, 100.*

Table 5.20: Example 5.7.2: "convergence" of the double-porosity model to the exact model

# cells N_c	size cells ε	$\|u_h^N - u_{1,h}^N\|_{*,1}$	$\|u_h^N - u_{1,h}^N\|_{*,2}$
3×3	0.3333	3.24×10^{-2}	1.19×10^{-2}
9×9	0.1111	1.05×10^{-2}	0.39×10^{-2}
5×5	0.2	7.4716×10^{-3}	0.039027
15×15	0.0667	2.3850×10^{-3}	0.011395
45×45	0.0222	0.80489×10^{-3}	0.0037118

Figure 5.21: Illustration of the part of the numerical solutions used to compute the error with different ε

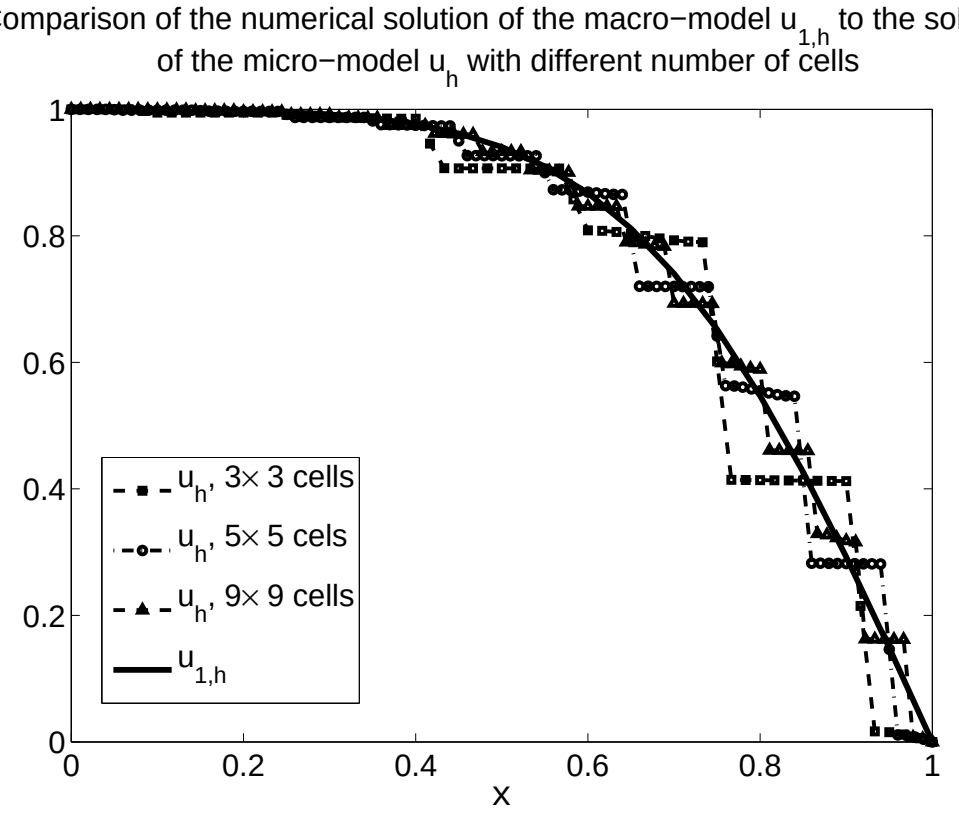

Table 5.21: Example 5.7.3: Comparison of the error between the numerical solution for the exact model and the double-porosity model with different mesh sizes

$\tilde{h}^{-1}$	$\|u_h^N - u_{1,\tilde{h}}^N\|_{*,1}$	$\|u_h^N - u_{1,\tilde{h}}^N\|_{*,2}$	run time(s)
100	7.0921×10^{-3}	1.9034×10^{-2}	511
50	7.0940×10^{-3}	1.9044×10^{-2}	56
10	7.1153×10^{-3}	1.9134×10^{-2}	3

- *We compute the parameters c, k_1 using the mesh diameters: $\tilde{h} = h_c = h_k$. The different values of c and k_1 can be see in Tables 5.22-5.23, respectively.*

We compare the solutions u_h and $u_{1,\tilde{h}}$ for the different values of $\tilde{h}$ in Table 5.21. The run time shown in Table 5.21 is referent for computing the solution of the double-porosity system and includes the run time of computing the parameters of the system.

In Table 5.21 we see that the error remains stable for approximating the system with a mesh much coarser than the one used for approximating the original model. Note also the difference in the computational time. We can decrease he computational time from 511 seconds to 3 seconds without significant changes in the error of the approximation. Also see in Figure 5.22 how close the solutions for different $\tilde{h}$ are from each other.

The next example address Q3, the issue of what mesh diameter to use to approximate the parameters of the double-porosity system.

Example 5.7.4. *Here we discuss the computation of the parameters c, k_1 of the double-porosity model with different mesh sizes. We fix 3×3 cells and $h^{-1} = 60$ to compute the numerical solution of the original model and of the double-porosity model,* (5.34), (5.35), *respectively. To compute the parameters we use:*

- *Keep $h_{k_1} = h$ and h_c^{-1}= 10, 50, 100, 200.*
- *Keep $h_c = h$ and $h_{k_1}^{-1}$= 10, 50, 100, 200.*

Because k_1 is a diagonal matrix with the diagonal entries equal to each other, only the entry $k_1(1,1)$ is show in Table 5.23.

From the results shown in Tables 5.22 and 5.23 we conclude that the problem is not very sensitive to c, thus we can use large h_c. We also see that the problem is more sensitive to the changes in the parameter k_1.

Figure 5.22: Example 5.7.3: Comparison of approximating the exact model with the double-porosity model with different mesh sizes

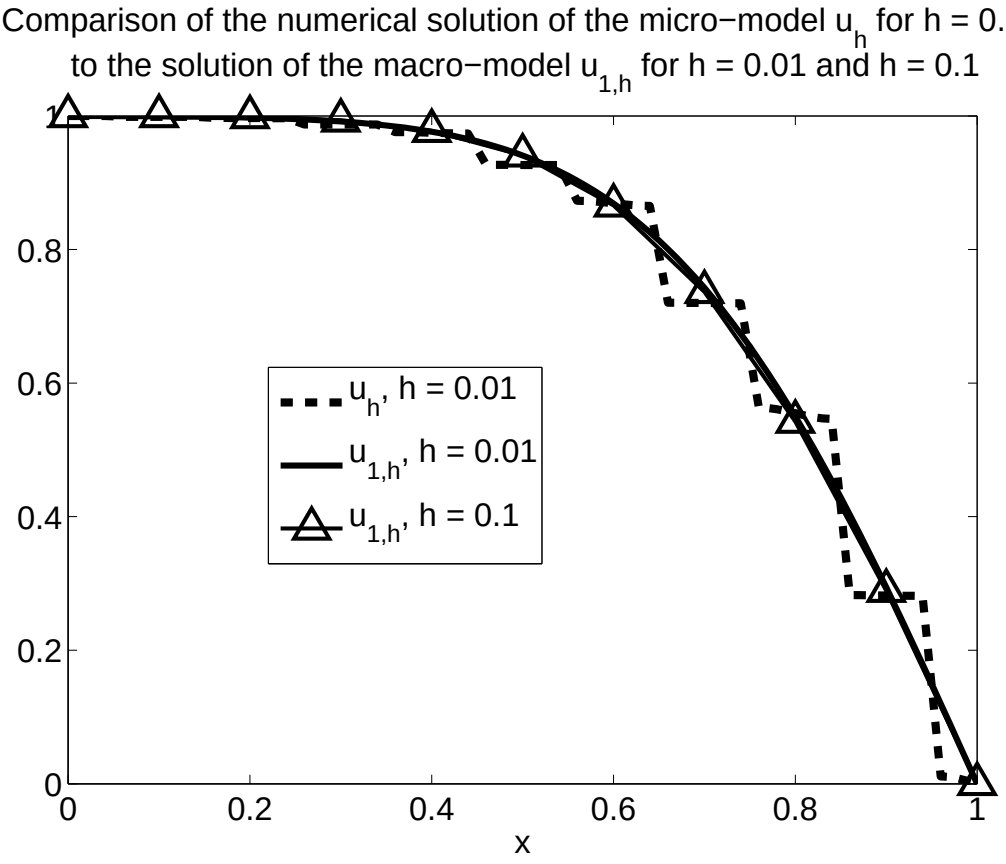

Table 5.22: Example 5.7.4: Sensitivity to c. The differences in the errors occur in the tenth decimal place.

h_c^{-1}	c	$\|u_h - u_{1,h}\|_{*,1}$	$\|u_h - u_{1,h}\|_{*,2}$
10	$1.9000 \times 10{-}3$	3.6251×10^{-2}	5.9026×10^{-2}
50	$1.8370 \times 10{-}3$	3.6251×10^{-2}	5.9026×10^{-2}
100	$1.8292 \times 10{-}3$	3.6251×10^{-2}	5.9026×10^{-2}
200	$1.8258 \times 10{-}3$	3.6251×10^{-2}	5.9026×10^{-2}

Table 5.23: Example 5.7.4: Sensitivity to k_1

$h_{k_1}^{-1}$	$k_1(1,1)$	$\|u_h - u_{1,h}\|_{*,1}$	$\|u_h - u_{1,h}\|_{*,2}$
10	4.6306×10^{-1}	3.5392×10^{-2}	5.7835×10^{-2}
50	4.5141×10^{-1}	$3.6222 \times 10{-}2$	5.8989×10^{-2}
100	4.5046×10^{-1}	3.6301×10^{-2}	5.9093×10^{-2}
200	4.5009×10^{-1}	3.6332×10^{-2}	5.9134×10^{-2}

5.8 Numerical results for the dependence of the solutions in the parameters

Here we present numerical experiments to illustrate the result in Proposition 4.9.1.

In all the examples, we use the following set up:

- $\Omega = (0, 1)$.
- $H = h$ and $\mathcal{T}_h$ a uniform grid with $h^{-1} = 200$. Except for Example 5.8.4 where $h^{-1} = 10,000$.
- Uniform time-stepping $\tau = \tau_n = 10^{-2}$ and final time $T = 1$.
- Right-hand side functions $f = e^{-t}x^2$, $g = x + t$.

We suppose that $\mathcal{P}$ is the exact set of parameters. Then, we compare the difference between the numerical solution of the LP-model (4.112) for $\mathcal{P} = \{\lambda_1, \lambda_2, a, b, c\}$ and for another set of parameters $\tilde{\mathcal{P}} = \{\lambda_1, \lambda_2, a, b, \tilde{c}\}$. We analyse this difference in the norm defined by equation (4.212). For simplicity we denote $\mathcal{E}_{\mathcal{P}} := \|(e_{u,c}, e_{v,c})\|_{**}$. From proposition 4.9.1 we expect $\mathcal{E}_{\mathcal{P}} = O(\|\epsilon\| = \|c - \tilde{c}\|)$.

Examples 5.8.1– 5.8.3 illustrate the case where both $c, \tilde{c}$ are constants. Example 5.8.4 consider the case where $c, \tilde{c}$ are both piecewise constants however the position of the jump is different.

Example 5.8.1. *Let* $\mathcal{P} = \{10^{-2}, 1, 1, 10^{-3}, 10^{-4}\}$ *and* $\tilde{\mathcal{P}} = \{10^{-2}, 1, 1, 10^{-3}, \tilde{c}\}$ *for:*

$$\tilde{c} = 10^{-4} + 1, 10^{-4} + 10^{-1}, 10^{-4} + 10^{-2}, 10^{-4} + 10^{-3}, 10^{-4} + 10^{-4}.$$

Thus

$$\|\epsilon\| = 1, 10^{-1}, 10^{-2}, 10^{-3}, 10^{-4}.$$

Table 5.24: Example 5.8.1: $\mathcal{E}_{\mathcal{P}} = O(\|\epsilon\|^{\alpha})$. From theory we expect $\alpha = 1$.

$\|\epsilon\|$	1	10^{-1}	10^{-2}	10^{-3}	10^{-4}
$\mathcal{E}_{\mathcal{P}}$	2.230×10^{-1}	2.775×10^{-2}	2.839×10^{-3}	2.846×10^{-4}	2.846×10^{-5}
α	–	0.9051	0.9900	0.9990	0.9999

Table 5.25: Example 5.8.2: we verify $\mathcal{E}_{\mathcal{P}} = O(\|\epsilon\|^{\alpha})$. From theory we expect $\alpha = 1$.

$\|\epsilon\|$	1	10^{-2}	10^{-4}	10^{-6}
$\mathcal{E}_{\mathcal{P}}$	2.2305×10^{-2}	2.8393×10^{-3}	2.8465×10^{-5}	2.8466×10^{-7}
α	–	0.9480	0.9994	1.000

In Table 5.24 we verify that $\mathcal{E}_{\mathcal{P}} = O(\|\epsilon\|)$. In the next example we let $c \equiv 0$.

Example 5.8.2. *Let* $\mathcal{P} = \{10^{-2}, 1, 1, 10^{-3}, 0\}$ *and* $\tilde{\mathcal{P}} = \{10^{-2}, 1, 1, 10^{-3}, \tilde{c}\}$ *for:*

$$\tilde{c} = 1, 10^{-2}, 10^{-4}, 10^{-6}.$$

Thus

$$\|\epsilon\| = 1, 10^{-2}, 10^{-4}, 10^{-6}.$$

Example 5.8.3. *Let* $\mathcal{P} = \{10^{-2}, 1, 1, 10^{-3}, 10^{4}\}$ *and* $\tilde{\mathcal{P}} = \{10^{-2}, 1, 1, 10^{-3}, \tilde{c}\}$ *for:*

$$\tilde{c} = 10^4 + 1, 10^4 + 10^{-2}, 10^4 + 10^{-4}, 10^4 - 1, 10^4 - 10^{-2}.$$

Thus

$$\epsilon = 1, 10^{-2}, 10^{-4}, -1, -10^{-2}.$$

Example 5.8.4. *Let* $\mathcal{P} = \{10^{-2}, 1, 1, 10^{-3}, c\}$ *and* $\tilde{\mathcal{P}} = \{10^{-2}, 1, 1, 10^{-3}, \tilde{c}\}$. *Here*

$$c(x) = \begin{cases} 0.01, & 0 \le x \le .5, \\ 1, & .5 < x \le 1, . \end{cases} \qquad \tilde{c}(x) = \begin{cases} 0.01, & 0 \le x \le d, \\ 1, & d < x \le 1. \end{cases}$$

Table 5.26: Example 5.8.3: we verify $\mathcal{E}_{\mathcal{P}} = O(\|\epsilon\|^{\alpha})$. From theory we expect $\alpha = 1$.

$\|\epsilon\|$	1	10^{-2}	10^{-4}	1	10^{-2}
$\mathcal{E}_{\mathcal{P}}$	2.035×10^{-8}	2.035×10^{-10}	2.079×10^{-12}	2.035×10^{-8}	2.035×10^{-10}
α	–	1.000	0.9954	–	1.000

Table 5.27: Example 5.8.4: $c, \tilde{c}$ piecewise constant functions. We verify $\mathcal{E}_{\mathcal{P}} = O(\|\epsilon\|^{\alpha})$. From theory we expect $\alpha = 1$.

d	0.6	0.51	0.501	0.5001
$\|\epsilon\|$	10^{-1}	10^{-2}	10^{-3}	10^{-4}
$\mathcal{E}_{\mathcal{P}}$	3.96×10^{-2}	3.89×10^{-3}	3.97×10^{-4}	3.98×10^{-5}
α	–	1.0077	0.9912	0.9989
d	0.4	0.49	0.499	0.4999
$\|\epsilon\|$	10^{-1}	10^{-2}	10^{-3}	10^{-4}
$\mathcal{E}_{\mathcal{P}}$	3.81×10^{-2}	3.82×10^{-3}	3.97×10^{-4}	3.98×10^{-5}
α	–	0.9987	0.9832	0.9989

for $d \in (0, 1)$. We test the convergence of $\mathcal{E}_{\mathcal{P}}$ for

$$d = 0.6, 0.51, 0.501, 0.5001, 0.4, 0.49, 0.499, 0.4999.$$

It is easy to see that $\|\epsilon\| = (0.99)^2 |d - 0.5|$.

6 Conclusions

In this thesis, we developed several *a-priori* and *a-posteriori* error estimates applicable to elliptic and parabolic systems. The main theoretical results are in Theorems 4.3.4 and 4.5.6 and in Corollaries 4.6.5, 4.7.4. The numerical experiments presented in Chapter 5 confirm that the estimators have the desired properties, and that the schemes converge at the predicted rate. The estimators are robust with respect to the parameters of the problem $\mathcal{P}$. Moreover, the estimators are robust with respect to the multilevel discretization of the system studied here.

The theoretical and numerical results in this thesis apply to models of many important phenomena in fluid flow and transport in porous media. We demonstrated some applications with numerical simulations.

Our current work includes extensions of the theory to various nonlinear models. We are also working on extending the results for time-dependent problems to allow for multilevel time-stepping. Another extension is to apply the estimator developed to the LP-model for the ECBM process. Other important but non-trivial extensions include first order, i.e., advection terms.

We would like to acknowledge that this thesis research was partially supported by the grants NSF 0511190 and DOE 98089.

Bibliography

[1] R. A. Adams and J. J. F. Fournier. *Sobolev spaces*, volume 140 of *Pure and Applied Mathematics (Amsterdam)*. Elsevier/Academic Press, Amsterdam, second edition, 2003.

[2] M. Ainsworth and J. T. Oden. A posteriori error estimators for second order elliptic systems. I. Theoretical foundations and a posteriori error analysis. *Comput. Math. Appl.*, 25(2):101–113, 1993.

[3] M. Ainsworth and J. T. Oden. A posteriori error estimators for second order elliptic systems. II. An optimal order process for calculating self-equilibrating fluxes. *Comput. Math. Appl.*, 26(9):75–87, 1993.

[4] M. Ainsworth and J. T. Oden. *A posteriori error estimation in finite element analysis*. Pure and Applied Mathematics (New York). Wiley-Interscience [John Wiley & Sons], New York, 2000.

[5] J. Alberty, C. Carstensen, and S. A. Funken. Remarks around 50 lines of Matlab: short finite element implementation. *Numer. Algorithms*, 20(2-3):117–137, 1999.

[6] T. Arbogast, J. Douglas Jr., and U. Hornung. Derivation of the double porosity model of single phase flow via homogenization theory. *SIAM J. Math. Anal.*, 21(4):823–836, 1990.

[7] R. Aris. *The mathematical theory of diffusion and reaction in permeable catalysts*. Oxford University Press, 1975.

[8] K. Atkinson and W. Han. *Theoretical numerical analysis*, volume 39 of *Texts in Applied Mathematics*. Springer, Dordrecht, Third edition, 2009. A functional analysis framework.

[9] I. Babuska and W. C. Rheinboldt. Error estimates for adaptive finite element computations. *SIAM J. Numer. Anal.*, 15(4):736–754, 1978.

[10] R. E. Bank and R. K. Smith. A posteriori error estimates based on hierarchical bases. *SIAM J. Numer. Anal.*, 30(4):921–935, 1993.

[11] R. E. Bank and A. Weiser. Some a posteriori error estimators for elliptic partial differential equations. *Math. Comp.*, 44(170):283–301, 1985.

[12] G. Barenblatt, I. Zheltov, and I. Kochina. Basic concepts in the theory of seepage homogeneous liquids in fissured rock (strata). *Appl. Math. Mech.*, 24(1):1286–1303, 1960.

[13] J. W. Barrett and P. Knabner. Finite element approximation of the transport of reactive solutes in porous media. I. Error estimates for nonequilibrium adsorption processes. *SIAM J. Numer. Anal.*, 34(1):201–227, 1997.

[14] J. W. Barrett and P. Knabner. Finite element approximation of the transport of reactive solutes in porous media. II. Error estimates for equilibrium adsorption processes. *SIAM J. Numer. Anal.*, 34(2):455–479, 1997.

[15] A. Bergam, C. Bernardi, and Z. Mghazli. A posteriori analysis of the finite element discretization of some parabolic equations. *Math. Comp.*, 74(251):1117–1138 (electronic), 2005.

[16] C. Bernardi and R. Verfürth. Adaptive finite element methods for elliptic equations with non-smooth coefficients. *Numer. Math.*, 85(4):579–608, 2000.

[17] M. Bohm and R. E. Showalter. Diffusion in fissured media. *SIAM J. Math. Anal.*, 16(3):500–509, 1985.

[18] M. Bohm and R. E. Showalter. A nonlinear pseudoparabolic diffusion equation. *SIAM J. Math. Anal.*, 16(5):980–999, 1985.

[19] D. Braess. *Finite elements*. Cambridge University Press, Cambridge, third edition, 2007. Theory, fast solvers, and applications in elasticity theory, Translated from the German by Larry L. Schumaker.

[20] W. L. Briggs, V. E. Henson, and S. F. McCormick. *A multigrid tutorial*. Society for Industrial and Applied Mathematics (SIAM), Philadelphia, PA, second edition, 2000.

[21] C. Carstensen. Some remarks on the history and future of averaging techniques in a posteriori finite element error analysis. *ZAMM Z. Angew. Math. Mech.*, 84(1):3–21, 2004.

[22] P. G. Ciarlet. *The finite element method for elliptic problems*, volume 40 of *Classics in Applied Mathematics*. Society for Industrial and Applied Mathematics (SIAM), Philadelphia, PA, 2002. Reprint of the 1978 original [North-Holland, Amsterdam; MR0520174 (58 #25001)].

[23] P. Clément. Approximation by finite element functions using local regularization. *Rev. Française Automat. Informat. Recherche Opérationnelle Sér. RAIRO Analyse Numérique*, 9(R-2):77–84, 1975.

[24] A. W. Craig, J. Z. Zhu, and O. C. Zienkiewicz. A posteriori error estimation, adaptive mesh refinement and multigrid methods using hierarchical finite element bases. In *The mathematics of finite elements and applications, V (Uxbridge, 1984)*, pages 587–594. Academic Press, London, 1985.

[25] K. Eriksson and C. Johnson. Adaptive finite element methods for parabolic problems. I. A linear model problem. *SIAM J. Numer. Anal.*, 28(1):43–77, 1991.

[26] L. C. Evans. *Partial differential equations*, volume 19 of *Graduate Studies in Mathematics*. American Mathematical Society, Providence, RI, 1998.

[27] W. Hackbusch. *Multigrid methods and applications*, volume 4 of *Springer Series in Computational Mathematics*. Springer-Verlag, Berlin, 1985.

[28] C. T. Kelley. *Iterative methods for linear and nonlinear equations*, volume 16 of *Frontiers in Applied Mathematics*. Society for Industrial and Applied Mathematics (SIAM), Philadelphia, PA, 1995. With separately available software.

[29] V. Klein and M. Peszynska. Adaptive multi-level modeling of coupled multiscale phenomena with applications to methane evolution in subsurface. In *Proceedings of CMWR XVIII, Barcelona, June 21-24*.

[30] V. Klein and M. Peszynska. Robust a-posteriori estimators for multilevel discretizations of reaction- diffusion systems. *IJNAM*, 8(1):1–27, 2011.

[31] P. Ladeveze and D. Leguillon. Error estimate procedure in the finite element method and applications. *SIAM J. Numer. Anal.*, 20(3):485–509, 1983.

[32] L. W. Lake. *Enhanced Oil Recovery*. Prentice Hall, INC., 1989.

[33] M. G. Larson and A. J. Niklasson. Adaptive multilevel finite element approximations of semilinear elliptic boundary value problems. *Numer. Math.*, 84(2):249–274, 1999.

[34] A. I. Lee and J. M. Hill. On the general linear coupled system for diffusion in media with two diffusivities. *J. Math. Anal. Appl.*, 89(2):530–557, 1982.

[35] M. Lees. A priori estimates for the solutions of difference approximations to parabolic partial differential equations. *Duke Math. J.*, 27:297–311, 1960.

[36] N. Madden and M. Stynes. A uniformly convergent numerical method for a coupled system of two singularly perturbed linear reaction-diffusion problems. *IMA J. Numer. Anal.*, 23(4):627–644, 2003.

[37] G. Marsily. *Quantitative Hydrology*. Academic Press, INC., 1986.

[38] D. Pascali and S. Sburlan. *Nonlinear mappings of monotone type*. Martinus Nijhoff Publishers, The Hague, 1978.

[39] M. Peszynska, R. Showalter, and S.-Y. Yi. Homogenization of a pseudoparabolic system. *Appl. Anal.*, 88(9):1265–1282, 2009.

[40] M. Picasso. Adaptive finite elements for a linear parabolic problem. *Comput. Methods Appl. Mech. Engrg.*, 167(3-4):223–237, 1998.

[41] L. I. Rubinstein. On a question about the propagation of heat in heterogeneous media. *Izvestiya Akad. Nauk SSSR. Ser. Geograf. Geofiz.*, 12:27–45, 1948.

[42] D. Ruthven. *Principles of adsorption and adsorption processes*. Wiley, 1984.

[43] G. Sangalli. Numerical evaluation of FEM with application to the 1D advection-diffusion problem. In *Numerical mathematics and advanced applications*, pages 165–172. Springer Italia, Milan, 2003.

[44] G. Sangalli. Robust a-posteriori estimator for advection-diffusion-reaction problems. *Math. Comp.*, 77(261):41–70 (electronic), 2008.

[45] J.-Q. Shi, S. Mazumder, K.-H. Wolf, and S. Durucan. Competitive methane desorption by supercritical CO_2 injection in coal. *TiPM*, 75:35–54, 2008.

[46] R. E. Showalter. *Hilbert space methods for partial differential equations*. Pitman, London, 1977. Monographs and Studies in Mathematics, Vol. 1.

[47] R. E. Showalter. *Monotone operators in Banach space and nonlinear partial differential equations*, volume 49 of *Mathematical Surveys and Monographs*. American Mathematical Society, Providence, RI, 1997.

[48] R. E. Showalter, T. D. Little, and U. Hornung. Parabolic PDE with hysteresis. *Control Cybernet.*, 25(3):631–643, 1996. Distributed parameter systems: modelling and control (Warsaw, 1995).

[49] R. E. Showalter and T. W. Ting. Pseudoparabolic partial differential equations. *SIAM J. Math. Anal.*, 1:1–26, 1970.

[50] R. E. Showalter and D. Visarraga. Double-diffusion models from a highly-heterogeneous medium. *J. Math. Anal. Appl.*, 295(1):191–210, 2004.

[51] J. Smoller. *Shock waves and reaction-diffusion equations*, volume 258 of *Grundlehren der Mathematischen Wissenschaften [Fundamental Principles of Mathematical Sciences]*. Springer-Verlag, New York, second edition, 1994.

[52] V. Thomee. *Galerkin finite element methods for parabolic problems*, volume 25 of *Springer Series in Computational Mathematics*. Springer-Verlag, Berlin, second edition, 2006.

[53] R. Verfürth. *A review of a posteriori error estimation and adaptive mesh-refinement techniques*. Wiley & Teubner, 1996.

[54] R. Verfürth. A posteriori error estimators for convection-diffusion equations. *Numer. Math.*, 80(4):641–663, 1998.

[55] R. Verfürth. Robust a posteriori error estimators for a singularly perturbed reaction-diffusion equation. *Numer. Math.*, 78(3):479–493, 1998.

[56] R. Verfurth. A posteriori error estimates for finite element discretizations of the heat equation. *Calcolo*, 40(3):195–212, 2003.

[57] J. E. Warren and P. J. Root. The behavior of naturally fractured resevoirs. *Soc. Petroleum Engr. J.*, 3:245–255, 1963.

[58] M. F. Wheeler. A priori L_2 error estimates for Galerkin approximations to parabolic partial differential equations. *SIAM J. Numer. Anal.*, 10:723–759, 1973.

[59] J. Xu. Two-grid discretization techniques for linear and nonlinear PDEs. *SIAM J. Numer. Anal.*, 33(5):1759–1777, 1996.

[60] O. C. Zienkiewicz and J. Z. Zhu. A simple error estimator and adaptive procedure for practical engineering analysis. *Internat. J. Numer. Methods Engrg.*, 24(2):337–357, 1987.

APPENDIX

.1 Codes for computing I_H^h

.1.1 Dimension 1

```
function [Int] = interpolationmatrix(xnelH,h,nodH,r,nnodesh,nnodesH)
%% computes the interpolation matrix Int = N-by-n
%matrices computed by hand for r=2 and r=4 to test the code
 %inin = [5/12 1/2 1/12 ; 1/12 1/2 5/12]*hel/2; % for r=2
 %inin = 1/4*[ 11/12 3/2 1 1/2 1/12;1/12 1/2 1 3/2 11/12]*hel/2; % for r=4

%%%%%%%%%%%%%%%%%%%%%%%% set up numerical integration

%% set up quadrature parameters on the reference element (-1,1)
%% set up number of integration points nw, nodes xw, and weights w
maxord = 2;
if maxord == 1      %% exact for linears
      nw = 1;
      xw(1) = 0.;
      w(1) = 2.;
elseif maxord == 2  %% exact for cubics
      nw = 2;
      xw(1) = -1/sqrt(3); xw(2) = -xw(1);
      w(1) = 1; w(2) = 1;
elseif maxord == 3  %% exact for polynomials of degree 5
      nw = 3;
      xw(1) = -sqrt(3./5.); xw(2)=0.; xw(3) =- xw(1);
      w(1) = 5./9.; w(2)=8./9.; w(3)=w(1);
end;

%% Matching Elements
 % says which intervals of the refined grid are inside the coarse interval
Match = zeros(xnelH,r+1);
for el = 1:xnelH
    Match(el,:) = [1:r+1] + (el-1)*r;
end

%% Interpolation Matrix
%interpolation matrix for prolongation (VH to Vh), use Int' for restriction
Int = sparse(nnodesh,nnodesH);
Element = zeros(2,r+1);
dx = h/2;
for j = 1:r
    cell = zeros(2,2);
    for l = 1:nw
        [psi,phi] = shape(xw(l),r,j);
        cell = cell + phi*psi'*w(l)*dx;
    end
```

```
    vec = [1:2] + (j-1);
    Element(:,vec) = Element(:,vec) + cell;
end

for el = 1:xnelH %assembling by element in Vh
    Int(Match(el,:),nodH(el,:)) =  Int(Match(el,:),nodH(el,:))  + Element';
end
%%%%%%%%%%%%%%%%%%%%%%%%%%%%%%%%%%%%%%%%%%%%%%%%%%%%%%%%%%%%%%%%%%%%%%%%%%%
%% end of algorithm
%%%%%%%%%%%%%%%%%%%%%%%%%%%%%%%%%%%%%%%%%%%%%%%%%%%%%%%%%%%%%%%%%%%%%%%%%%%
function [y,z] = shape(x,r,j)
%% shape function on reference element (-1,1)
   y  (1,:) = .5.*(1.-x);
   y  (2,:) = .5.*(1.+x);

   z(1,:) = -1/(2*r) .*x + (1 - (2*j-1)/(2*r));
   z(2,:) = 1/(2*r) .*x + (2*j-1)/(2*r);
```

.1.2 Dimension 2

1. elementmatching.m

```
function M = elementmatching(n,N)
%% Input:
%% n = number of elements in the finer mesh in the x-direction;
%% N = number of elementes in the coarser mesh in the x-direction
%% Note that n>= N;
%% Gives the cells in the refined grid inside the Elements in the coarse
%% grid, the even numbered cells are the flipped cells
%% Output:
%% M =  # of the cells of refined grid inside each element in the coarse one)
r = n/N;
M = zeros(1,r^2);
last = 0; %flag for vec
        for k = 1:r
            vec = [last + 1 : last + 2*r - 1 - 2*(k-1) ];
            last = vec(end);
            vecodd = [1:2*r-1 - 2*(k-1)]+2*n*(k-1);
            M(vec) = vecodd;
        end
```

2. assemblingcells.m

```
function Matching = assemblingcells(n,N)
%% Input:
```

```
%% n = number of elements in the finer mesh in the x-direction;
%% N = number of elementes in the coarser mesh in the x-direction
%% Note that n>= N;
%% Gives the information needed to assemble the integration
%% inside an element for the r^2 cells
%% Output:
%% Matching = r^2 - by 3 matrix containing the nodes of each cell inside an element
r = n/N;
Matching = [];
z = 0;%flags for the jumps in each level
w = 0;
for i = 1:r
    M = zeros(2*(r - i) + 1,3);
    P = zeros(r-i+1,3);
    P(:,1) = [1:r-i+1] + z;
    P(:,2) = P(:,1) + 1;
    P(:,3) = P(:,2) + r - i + 1;
      if r-i > 0
       F = zeros(r-i,3);
       F(:,1) = [r+3:2*r+2-i] + w;
       F(:,2) = F(:,1) - 1;
      F(:,3) = F(:,2) - r + i - 1;
       M(1:2:2*(r-i) + 1,:) = P;
       M(2:2:2*(r-i),:) = F;
     else
       M = P;
     end
      Matching = [Matching;M];
     z = z + r - i + 2; %update the flags
     w = w + r - i + 1;
    end
```

3. matching.m

```
function M = matching(n,N)
%% Input:
%% n = number of elements in the finer mesh in the x-direction;
%% N = number of elementes in the coarser mesh in the x-direction
%% Note that n>= N;
%% Gives back the matrix relating the nodes in the refined grid with the
%% elements in the coarse one. The matrix is oriented in the way that
%% matchs the order of the nodes in the reference element.
r = n/N;
M = zeros(2*N^2 , (r+1)*(r+2)/2);
%% Assembling
for i = 1:N
     for j = 1:N
```

```
        last = 0; %flag for vec
        for k = 1:r+1
             vec = [last + 1 : last + 1 + r + 1 - k ] ;
             last = vec(end);
             vecodd = [1:r+1 - k + 1] + r*(j-1) + (k-1)*(n+1);
             M(2*j-1 +2*N*(i-1),vec) = vecodd + (i-1)*r*(n+1);
             veceven = (r+1) + (n+1)*r - [0:r - k + 1] + r*(j-1) - (k-1)*(n+1);
             M(2*j + 2*N*(i-1),vec) = veceven + (i-1)*r*(n+1);
        end
    end
end
```

4. interpolation2D.m

```
function I = interpolation2D(n,N)
%%%%%%%%%%%%%%%%%%%%%%%%%%%%%%%%%%%%%%%%%%%%%%%%%
%% Interpolation in 2D
%% Remarks:
%% 1)only uses uniform grids,with triangles
%% 2)the grid is square
%% 3)n >= N
%% Input:
%% N = number of elements in coarse grid
%% n = number of elements in the refined grid
%% Output
%% I = interpolation matrix I_H^h
r = n/N;
h=1/N;
x=0:h:1;
[coordinates,en]=feval(@fegrid2,N,x); %generates the coarser grid

%% Set up numerical integration
%% Gaussian points (xq,yq) and weights wq for integrating in a triangle
wq = [ 0.1125    0.0662    0.0662    0.0662    0.0630    0.0630    0.0630 ];
xq = [ 0.3333    0.4701    0.0597    0.4701    0.1013    0.7974    0.1013 ];
yq = [ 0.3333    0.4701    0.4701    0.0597    0.1013    0.1013    0.7974 ];

%% Set up the vectors J for the flipped and non-flipped cells
J_flipped = zeros( r*(r-1)/2,3);
J = zeros(r*(r+1)/2,3);

last = 0; %flag for vec
for i = 1:r
      vec = [last + 1 : last + r - i + 1 ];
      last = vec(end);
      J(vec,1) = [i:r];
     J(vec,2) = r - [0:r-i];
```

```
      J(vec,3) = r-i+1;
end
last_f = 0;
for i = 1:r-1
      vec = [last_f + 1 : last_f + r - i  ];
      last_f = vec(end);
      J_flipped(vec,1) = [i:r-1];
      J_flipper(vec,2) = r-1 - [0:r-i-1];
      J_flipper(vec,3) = r-i;
end
%% Integrating in a reference element
%% Divide every element in the coarse grid into r^2 cells and integrate in
%% each cell, then assemble the results for the element
Match = elementmatching(N,n);% used to find the flippers
Matcell = assemblingcells(N,n); %find the nodes inside the reference element
flagf = 0;
flag = 0;
    Element = zeros(3,(r+2)*(r+1)/2);
jac = 1/n^2; %jacobian of the change of variables for the numerical integration

for j = 1 : r^2
        cell = zeros(3,3);
        if mod(Match(1,j),2) == 0 %the cell is flipped
            flagf = flagf + 1; %count the flippers
            w = J_flipped(flagf,:);%find the behavior of the basis functions
            phi = basisflipped(xq,yq,w,r);
        else
            flag = flag + 1; %count the non-flippers
            w = J(flag,:);%find the behavior of the basis functions
            phi = basisnonflipped(xq,yq,w,r);
        end
         psi = basisfunction(xq,yq,wq);
         cell = phi*psi'*jac;
        Element(:,Matcell(j,:)) = Element(:,Matcell(j,:)) + cell;
end
%% Assembling the interpolation matrix
I = sparse((n+1)^2,(N+1)^2);
Matelement = matching(n,N);
for i = 1: size(en,2)
     I(en(:,i),Matelement(i,:)) = I(en(:,i),Matelement(i,:)) + Element;
   end
%%%%%%%%%%%%%%%%%%%%%%%%%%%%%%%%%%%%%%%%%%%%%%%END OF THE CODE%%%%%%%%%%%%%%%%%%%%%%
function [psi] = basisfunction(x,y,wq)
psi(1,:) = (1 - x - y).*wq;
psi(2,:) = x.*wq;
psi(3,:) = y.*wq;
```

```
function [phi] = basisnonflipped(x,y,j,r)
phi(1,:) = (r - j(1) + 1)/r - x/r - y/r;
phi(2,:) = (r - j(2))/r + x/r;
phi(3,:) = (r - j(3))/r + y/r;


function [phi] = basisflipped(x,y,j,r)
phi(1,:) = (r - j(1) - 1)/r + x/r + y/r;
phi(2,:) = (r - j(2))/r - x/r;
phi(3,:) = (r - j(3))/r - y/r;
```

.2 Code for computing E-model in 1D

```
function [error,estimator,efficiency_index] = two_grid_FEM1d (xnel_u,xnel_v,coef,a,b);
%%%%%%%%%%%%%%%%%%%%%%%%%%%%%%%%%%%%%%%%%%%%%%%%%%%%%%%%%%%%%%%%%%%
%% This function shows how to set up a finite element solution
%% of a two-point BVP in the interval (a,b)
%% lambda1*u- div(alpha*grad u) + c*(u - v) =f,
%% lambda2*v- div(beta*grad v) + c*(v - u) =g, u(a)=ua, u(b)=ub
%% using Galerkin linear Finite Elements
%% coef = [lambda1,lambda2,a,b,c]
%% xnel_u >= xnel_v later one can develop a more complete code
%% that can alternate which solution is in a finer mesh
%% The code use the exact solution that can be modified
%% together wit the right-hand side to compute the error
%% and get the boundary conditions
%% Output:
%% -Error in the energy norm
%% -Estimator
%% - Efficiency index of the estimator
%% Example to run:
%% two_grid_FEM1d(100,50,[ 1 2 1 2 1],0,1);
%%%%%%%%%%%%%%%%%%%%%%%%%%%%%%%%%%%%%%%%%%%%%%%%%%%%%%%%%%%%%%%%%%%

clf;
set(0,'DefaultLineLineWidth',3);
%%%%%%%%%%%%%%%%%%%%%%%% set up the two grids
r = xnel_u/xnel_v;
[nnodes_v,nnodes_u,nels_v, nels_u,xnel_v,xnel_u,nod_v,nod_u,xnod_v,...
    xnod_u,maxord,ord_v,ord,hel_v,hel_u] = setupgrid(xnel_v,xnel_u,a,b);
%%%%%%%%%%%%%%%%%%% separate the free nodes
freenodes = [2:nnodes_u-1, nnodes_u+2:(nnodes_u + nnodes_v-1)];
%% set up quadrature parameters on the reference element (-1,1)
%% set up number of integration points nw, nodes xw, and weights w
if maxord == 1      %% exact for linears
      nw = 1;
```

```
      xw(1) = 0.;
      w(1) = 2.;
elseif maxord == 2  %% exact for cubics
      nw = 2;
      xw(1) = -1/sqrt(3); xw(2) = -xw(1);
      w(1) = 1; w(2) = 1;
end
%%%%%%%%%%% matrix and rhs of linear system %%%%%%%%%%%%%%%%%%%%%%%%%
%% set up can be easily modified to include higher order elements
%% as well as
S_u = sparse(nnodes_u,nnodes_u); %stiffness matrix for Vh
S_v = sparse(nnodes_v,nnodes_v);
RHS_u = sparse(nnodes_u,1);
RHS_v = sparse(nnodes_v,1);
M_v = sparse(nnodes_v,nnodes_v);%mass matrix for VH
M_u = sparse(nnodes_u,nnodes_u);
%% assemble mass and stiffness matrix for Vh
for el = 1:nels_u
    x1 = xnod_u(nod_u(el,1)); x2 = xnod_u(nod_u(el,2)); %% left and right endpoint
    dx = (x2-x1)/2.;                            %% Jacobian of transformation
    %% compute element stiffness matrix and load vector
    aa = zeros(ord(el),ord(el));                %% element stiffness matrix for b
    bb = zeros(ord(el),ord(el));
    f = zeros(ord(el),1);
    for l = 1:nw
        x = x1 + (1 + xw(l))*dx;                %% x runs in true element,
                                                %% xw runs in reference element
        [psi,dpsi] = shape(xw(l),ord);          %% calculations on ref.element
        aa = aa + dpsi*dpsi'/dx/dx * w(l)*dx;
        bb = bb + psi*psi' * w(l)*dx;
        [fval] = feval(@rhsfun,x,coef);
        f = f + fval * psi * w(l)*dx;
    end
    RHS_u(nod_u(el,:)) = RHS_u(nod_u(el,:)) + f(:);
    S_u (nod_u(el,:),nod_u(el,:)) = S_u(nod_u(el,:),nod_u(el,:)) + aa;
    M_u(nod_u(el,:),nod_u(el,:)) = M_u(nod_u(el,:),nod_u(el,:)) + bb;
end;
%% assemble mass and stiffness matrix for VH
for el = 1:nels_v
    x1 = xnod_v(nod_v(el,1)); x2 = xnod_v(nod_v(el,2)); %% left and right endpoint
    dx = (x2-x1)/2.;                            %% Jacobian of transformation
    %% compute element stiffness matrix and load vector
    aa = zeros(ord(el),ord(el));                %% element stiffness matrix for b
    bb = zeros(ord(el),ord(el));
    g = zeros(ord(el),1);
    for l = 1:nw
        x = x1 + (1 + xw(l))*dx;                %% x runs in true element,
```

```
                                          %% xw runs in reference element
        [psi,dpsi] = shape(xw(l),ord);    %% calculations on ref.element

        aa = aa + dpsi*dpsi'/dx/dx * w(l)*dx;
        bb = bb + psi*psi' * w(l)*dx;
        [fval,gval] = feval(@rhsfun,x,coef);
        g = g + gval * psi * w(l)*dx;
    end
    RHS_v(nod_v(el,:)) = RHS_v(nod_v(el,:)) + g(:);
    S_v (nod_v(el,:),nod_v(el,:)) = S_v(nod_v(el,:),nod_v(el,:)) + aa;
    M_v(nod_v(el,:),nod_v(el,:)) = M_v(nod_v(el,:),nod_v(el,:)) + bb;
end;

%% interpolation matrix I_Hh
Int = interpolationmatrix(xnel_v,hel_u,nod_v,r,nnodes_u,nnodes_v);

Mat = [(coef(1) + coef(5))*M_u + coef(3)*S_u -coef(5)*Int ;...
    -coef(5)*Int' (coef(2) + coef(5))*M_v + coef(4)*S_v];

RHS = [RHS_u;RHS_v];
sol = zeros(nnodes_u+nnodes_v,1);

%% impose Dirichlet boundary conditions
[b1u,b1v] = feval(@exfun,a);   sol(1)=b1u;  sol(1+nnodes_u)=b1v;
[b2u,b2v] = feval(@exfun,b);   sol(nnodes_u) = b2u; sol(nnodes_u + nnodes_v)=b2v;

%% eliminate known values from the system
RHS = RHS - Mat*sol;
sol(freenodes) = Mat(freenodes,freenodes)\RHS(freenodes);

solu = sol(1:nnodes_u);
solv = sol(nnodes_u+1:nnodes_u + nnodes_v);


%% set up the interpolation of the solution to compute the error in the
%% finer mesh Vh
solvi = M_u\Int*solv;
solui = M_v\Int'*solu;

%% set up numerical integration
  %quadrature points
 exw(1)=-.9491079123; exw(2)=-.7415311856;
 exw(3)=-.4058451514;exw(4)=0;exw(5)=-exw(3);exw(6)=-exw(2);exw(7)=-exw(1);

 %weights
 ew(1)=0.1294849662;ew(2)=0.2797053915;ew(3)=0.3818300505;ew(4)=0.4179591837;
 ew(5)=ew(3);ew(6)=ew(2);ew(7)=ew(1);
```

```
%% Error computation by element in Vh
jacobian=.5*hel_u;
en = 0;
for i=1:nels_u
    t=xnod_u(i)+.5*hel_u*(xw+1);
    [uex,vex]=exfun(t);
    [duex,dvex]=diffexfun(t);

    du = 1/hel_u*(solu(i+1)-solu(i))*ones(1,length(w));
    u=interp1([xnod_u(i) xnod_u(i+1)],[solu(i) solu(i+1)],t);

    dv = 1/hel_u*(solvi(i+1)-solvi(i))*ones(1,length(w));
    v=interp1([xnod_u(i) xnod_u(i+1)],[solvi(i) solvi(i+1)],t);

   en = en + jacobian*( coef(1)*(uex-u).^2 + coef(2)*(vex-v).^2 ...
        +coef(3)*(duex-du).^2 + coef(4)*(dvex-dv).^2 ...
       + coef(5)*((uex-u)-(vex-v)).^2)*w';
end
error = sqrt(en);

%% Estimator computation

%% compute the jumps on the edges
edgejumpu = zeros(1,2*nels_u);
for i = 1 : nels_u
    edgejumpu(2*i-1) = (solu(i + 1) - solu(i))/hel_u;
    edgejumpu(2*i) = edgejumpu(2*i-1);
end
edgejumpv = zeros(1,2*nels_v);
for i = 1 : nels_v
    edgejumpv(2*i-1) = (solv(i + 1) - solv(i))/hel_v;
    edgejumpv(2*i) = edgejumpv(2*i-1);
end

Reu = zeros(1,nnodes_u);
% Reu(1) = 0; % Reu(end) = 0;
Rev = zeros(1,nnodes_v);
% Rev(1) =0; % Rev(end) = 0 ;
for  i = 2 : nnodes_u-1
    Reu(i) = coef(3)^2*(edgejumpu(2*i-1) - edgejumpu(2*i-2))^2;
end
for  i = 2 : nnodes_v-1
    Rev(i) = coef(4)^2*(edgejumpv(2*i-1) - edgejumpv(2*i-2))^2;
end

%% compute the residuals
```

```
Rtu = zeros(1,nels_u);
Rtv = zeros(1,nels_v);

jac_u = 0.5*hel_u;
for i=1:nels_u
         t=xnod_u(i)+.5*hel_u*(xw+1);
         [f]=rhsfun(t,coef);
         uinterp=interp1([xnod_u(i) xnod_u(i+1)],[solu(i) solu(i+1)],t);
         vinterp=interp1([xnod_u(i) xnod_u(i+1)],[solvi(i) solvi(i+1)],t);

         fgu = f   + coef(5).*(vinterp - uinterp) - coef(1)*uinterp;
         fgu = fgu.^2;
         Rtu(i) = jac_u*((fgu)*w');

end
jac_v = 0.5*hel_v;
for i=1:nels_v
         t=xnod_v(i)+.5*hel_v*(xw+1);
         [f,g]=rhsfun(t,coef);
         uinterp=interp1([xnod_v(i) xnod_v(i+1)],[solui(i) solui(i+1)],t);
         vinterp=interp1([xnod_v(i) xnod_v(i+1)],[solv(i) solv(i+1)],t);
         fgv = g   + coef(5).*(uinterp - vinterp) - coef(2)*vinterp;
         fgv = fgv.^2;
         Rtv(i) = jac_v*((fgv)*w');
end

%% set up the scaling coefficients
thetau = zeros(1,nels_u);
thetav = zeros(1,nels_v);
gammau = zeros(1,nels_u);
gammav = zeros(1,nels_v);
for i = 1:nels_u
     thetau(i) = min(hel_u/sqrt(coef(3)),1/sqrt(coef(1)));
     gammau(i) = 2*sqrt(thetau(i))*(coef(3))^(-.25);
end
for i = 1:nels_v
     thetav(i) = min(hel_v/sqrt(coef(4)), 1/sqrt(coef(2)));
     gammav(i) = 2*sqrt(thetav(i))*(coef(4))^(-.25);
end

%% add the estimator over the elements
etau = zeros(1,nels_u);
etav = zeros(1,nels_v);
for i =1:nels_u
    etau(i) = thetau(i)^2 * Rtu(i) + 0.5*(gammau(i)^2*Reu(i) + gammau(i)^2*Reu(i+1));
end
for i =1:nels_v
```

```
   etav(i) = thetav(i)^2 * Rtv(i) + 0.5*(gammav(i)^2*Rev(i) + gammav(i)^2*Rev(i+1));
end
estimator = sqrt(sum(etau) +sum(etav));

efficiency_index = estimator/error;

%% Graphic representation
xplot = a:0.01*hel_u:b;
[exactu,exactv ] = exfun(xplot);
subplot(1,2,1)
plot(xplot,exactu,'r',xnod_u,solu','o-');
subplot(1,2,2)
plot(xplot,exactv,'r',xnod_v,solv','o-');
%%%%%%%%%%%%%%%%%%%%%%%%%%%%%%%%%%%%%%%%%%%%%%%%%%%%%%%%%%%%%%%%%%%%%%%%%%%
%% end of algorithm
%%%%%%%%%%%%%%%%%%%%%%%%%%%%%%%%%%%%%%%%%%%%%%%%%%%%%%%%%%%%%%%%%%%%%%%%%%%
function [y,dy] = shape(x,n)
%% shape function on reference element (-1,1)
%% n = 2: linear
%% n = 3: quadratic (must be coded)

if n == 2

   y  (1,:) = .5.*(1.-x);
   y  (2,:) = .5.*(1.+x);
   dy (1,:) = -.5;
   dy (2,:) = .5;

end


function [f,g] = rhsfun(x,coef)  %%%%%%%%%%%%% rhs function
f = coef(1)*x.^2.*sin(pi*x) - coef(3)*(2*x.*pi.*cos(pi*x)-x.^2*pi^2.*sin(pi*x)...
    + 2*sin(pi*x) +2*x.*pi.*cos(pi*x)) + coef(5)*(x.^2.*sin(pi*x) - (x - x.^3));
g = coef(2)*(x - x.^3) + coef(4)*6*x + coef(5)*((x - x.^3) - x.^2.*sin(pi*x));

function [u,v] = exfun(x)   %%%%%%%%%%%%% exact solution: provides ua,ub
u = x.^2.*sin(pi*x);
v = (x - x.^3);

function [u,v] = diffexfun(x)
u = x.^2.*pi.*cos(pi*x) + 2*x.*sin(pi*x);
v = 1 - 3*x.^2;

function[nnodes,nnodes2,nels, nels2,xnel,xnel2,nod,nod2,...
xnod,xnod2,maxord,ord,ord2,hel,hel2] = setupgrid(xnel,xnel2,a,b);
%% uniform grid
```

```
   nels = xnel;
   hel = (b-a)./nels;
   xel = a : hel : b-hel;

   nels2 = xnel2;
   hel2 = (b-a)./nels2;
   xel2 = a : hel2 : b-hel2;
%% set up uniform order of elements = 1 + degree of polynomial =
%% = number of degrees of freedom

ord = zeros(nels,1) + 2;  %% type of elements: linear
maxord = max(ord);
ord2 = zeros(nels2,1) + 2;  %% type of elements: linear
maxord2 = max(ord2);

%% number  of nodes
nnodes = sum(ord-1)+1;
nnodes2 = sum(ord2-1)+1;

%% derive global indexing of nodes:
%% nod(i,1) is the global number of j'th node in element i
nod = zeros(nels,maxord); myel = zeros(nnodes,2);
n = 1;
for i = 1:nels
    for j = 1:ord(i)
        nod(i,j) = n;
        if j == 1
            myel(n,2) = i;
        elseif j == ord(i)
            myel(n,1) = i;
        else myel(n,1) = i;
            myel(n,2) = i;
        end;
        if j ~= ord(i)
            n = n+1;
        end
    end;
end;
nod2 = zeros(nels2,maxord2); myel = zeros(nnodes2,2);
n = 1;
for i = 1:nels2
    for j = 1:ord2(i)
        nod2(i,j) = n;
        if j == 1
            myel(n,2) = i;
        elseif j == ord2(i)
            myel(n,1) = i;
```

```
        else myel(n,1) = i;
            myel(n,2) = i;
        end;
        if j ~= ord2(i)
            n = n+1;
        end
    end;
end;
%% xnod (i=1..nnodes): coordinates of node i
xnod = zeros(nnodes,1);
for i=1:nels-1
    h = xel(i+1)-xel(i);
    hi = h/(ord(i)-1);
    for j=1:ord(i)
        xnod (nod(i,j)) = xel(i) + hi*(j-1);
    end;
end;
i = nels; h = b-xel(i); hi=h/(ord(i)-1);
for j=1:ord(i)
    xnod (nod(i,j)) = xel(i) + hi*(j-1);
end;


xnod2 = zeros(nnodes2,1);
for i=1:nels2-1
    h = xel2(i+1)-xel2(i);
    hi = h/(ord2(i)-1);
    for j=1:ord2(i)
        xnod2 (nod2(i,j)) = xel2(i) + hi*(j-1);
    end;
end;
i = nels2; h = b-xel2(i); hi=h/(ord2(i)-1);
for j=1:ord2(i)
    xnod2 (nod2(i,j)) = xel2(i) + hi*(j-1);
end;
```